Cover Page

APPLICATION OF ZEOLITE 4A – METAKAOLIN MATRIX FOR THE REMOVAL OF SOME HEAVY METALS FROM CRUDE OIL TANK FARM WASTEWATER

By

FRANCISCA UNOMA NWAFULUGO

DEPARTMENT OF CHEMICAL ENGINEERING

AHMADU BELLO UNIVERSITY

ZARIA – NIGERIA

AUGUST, 2014

Title Page

APPLICATION OF ZEOLITE 4A – METAKAOLIN MATRIX FOR THE REMOVAL OF SOME HEAVY METALS FROM CRUDE OIL TANK FARM WASTEWATER

By

Francisca Unoma NWAFULUGO (M. ENG. FUT MINNA) 2002
PhD/ENG/13494/2007-08

A PROJECT DISSERTATION SUBMITTED TO THE SCHOOL OF POSTGRADUATE STUDIES,

AHMADU BELLO UNIVERSITY, ZARIA

IN PARTIAL FULFILMENT OF THE REQUIREMENTS FOR THE AWARD OF DOCTOR OF PHILOSOPHY DEGREE IN CHEMICAL ENGINEERING

DEPARTMENT OF CHEMICAL ENGINEERING,

FACULTY OF ENGINEERING

AHMADU BELLO UNIVERSITY, ZARIA

NIGERIA

AUGUST, 2014

DECLARATION

I declare that the work in this Dissertation entitled Application of Zeolite 4A-Metakaolin Matrix for the Removal of some Heavy Metals from Crude Oil Tank Farm Wastewater has been carried out by me in the Department of Chemical Engineering. The information derived from the literature has been duly acknowledged in the text and a list of references provided. No part of this dissertation was previously presented for another degree or diploma at this or any other Institution.

NWAFULUGO Francisca Unoma _____ _____

Signature Date

CERTIFICATION

This dissertation entitled APPLICATION OF ZEOLITE 4A – METAKAOLIN MATRIX FOR THE REMOVAL OF SOME HEAVY METALS FROM CRUDE OIL TANK FARM WASTEWATER by Francisca Unoma NWAFULUGO meets the regulations governing the award of the degree of Doctor of Philosophy of the Ahmadu Bello University, and is approved for its contribution to knowledge and literary presentation.

Prof. S.S. Adefila Chairman Supervisory Committee	_____ Signature	_____ Date
Dr. A.S. Olawale Member Supervisory Committee	_____ Signature	_____ Date
Dr. O.A. Ajayi Member Supervisory Committee	_____ Signature	_____ Date
Dr. I.A Mohammed-Dabo Head, Department of Chemical Engineering, A.B.U Zaria	_____ Signature	_____ Date
Professor A.A. Joshua Dean, Postgraduate School, A.B.U Zaria	_____ Signature	_____ Date

ACKNOWLEDGEMENT

I give all the glory to Almighty God for His sufficient grace; indeed it is His grace that led to the success of this dissertation. My profound gratitude goes to my team of supervisors in the persons of Prof. S.S. Adefila, Dr A.S.Olawale and Dr O.A. Ajayi for their tireless supervision, encouragement and consistent efforts to adding value to the work; God bless you all Sirs. My thanks also go to the Head of Department for all his encouraging words and assistance and infact, to all staff of Chemical Engineering Department, Ahmadu Bello University, ABU Zaria, especially the staff in the laboratories, in the persons of Mr M. A. Muhammad and Mr A. Abdullahi.

I will not fail to acknowledge my colleagues in Chemical Engineering Department, Kaduna Polytechnic: like Engr. Hassan Funsho, Engr. P. N. Okolie, Mudi Kehinde and Mudi Taiye., Hamzatt Aderemi, Sunday Igoche, Pastor S.O. Omale, Muazu Ibrahim, Patrick Nwoseibe, Abubakar Ali, Sanni Shehu, Waziri Jibrin, John Goji and all staff in the Laboratory like Mr. Haruna, Kabiru and Nura, Dr. Lawal, HOD Applied Science Department. Engr. Johnson Fatuase of Ahmadu Bello University, Zaria, Mr. Wakasi of Water Laboratory, Civil Engineering Department, Kaduna Polytechnic. My thanks also goes to Mr. Collins and Mrs. Ego of National Geoscience Research Laboratory, Kaduna, Mr. Ohworuka of Chemistry Laboratory, Nigerian Defence Academy (NDA), Kaduna. Miss Rachael Ovbiagheli and Mr. A. Mohammed of Defence Industrial Corporation of Nigeria (DICON) Kaduna. My heart felt gratitude goes to my lovely husband, Mr. P. M. Nwafulugo, my children, sisters and brothers, thank you all for being there for me, it is indeed a time to remember and a big story to tell. Finally, I will like to appreciate the following establishments for their immense contributions to the success of this research:

Ahmadu Bello University, Zaria

Kaduna Polytechnic, Kaduna, Nigeria

Kaduna Refinery and Petrochemical Company (KRPC)

National Geological Science Laboratories, Kaduna, Nigeria.

Chemistry laboratory, National Defense Academy, Kaduna, Nigeria

Research and Development Laboratory, Defence Industrial Corporation of Nigeria (DICON), Kaduna, Nigeria

Kaduna State Water Board, Kaduna, Nigeria

University of Johannesburg, South Africa.

Mount Castle Zeolite, Australia and

UOP, Honeywell group of Companies, New Jersey, USA.

ABSTRACT

Pollution of water, especially in communities close to crude oil deposits and refineries, has created worldwide concerns because of the associated heavy metals, *inter-alia*, released to the environment which have adverse effects on the environment - human and aquatic life. Despite all the efforts of the refineries to curtail this, the inorganic pollutants were not sufficiently catered for. Analysis of the pollution loading of wastewater samples collected from the dewatering tanks in the tank farm of Kaduna Refining and Petrochemicals Company (KRPC) and at the point of discharge to the receiving river indicated concentrations of 0.04 mg/l of Ni, 0.225 mg/l Pb, 0.022 mg/l Cd and 1.823 mg/l Mn as against 0.01 mg/l, 0.01 mg/l, 0.003 mg/l and 0.2 mg/l standards, respectively, set by the National Environmental standard Regulatory and Enforcement Agency (NESREA). There was a consideration to use commercial Zeolite 4A, deriving from its high pore volume and adsorptive sites, but in order to reduce the cost of importation of the Zeolite 4A, a cheap and available local kaolin from Kankara village in Katsina State was used as a blend. The kaolin was processed to sodium base metakaolin using ion exchange techniques to insert sodium ion in the metakaolin structure. The sodium based metakaolin was blended in various proportions with Zeolite 4A to form matrices of Zeolites 4A and metakaolin. The mineralogical and chemical compositions of Zeolites 4A, metakaolin and Zeolites 4A–metakaolin matrices were investigated and analysed using X-ray Florescence (XRF), X-ray Diffraction (XRD), Scanning Electron Microscopy (SEM)-Energy Dispersive X - ray (EDX) and Brunauer, Emmett and Teller (BET). The metakaolinization was achieved under controlled calcination at the temperature of 750 ^{o}C for 3 hours and the blend of Zeolites 4A and metakaolin in the ratio of 25 to 75 % respectively gave a unique matrix. The batch adsorption process was used to investigate the effect of variables such as contact

time, matrix dose and pH, on the response. The aggregate removal of the specified heavy metals (nickel, lead, cadmium and manganese) from crude oil tank farm wastewater was achieved in one batch process. This could be attributed to the adsorbent's high surface area per unit mass, numerous ionic sites per unit mass and their corresponding affinity to the metals. Isotherm and Kinetic studies were carried out. The correlation coefficient (R^2) for the adsorption isotherm models showed that the experimental data fitted well with the Freundlich, Langmuir, Temkin, and pseudo – second – order models. A statistical analysis was also carried out for factorial and Response Surface methodology (RSM). The results indicated that the main effects and the 2-way-interactions of the three variables has the highest effect on the response and should be more carefully controlled during routine experiment. The RSM results indicated that at optimum condition of 1.28 g/50 ml of Matrix 4 dose, 20 minutes contact time and pH of 10.35, that the adsorption of 97.991 % nickel, 94.234 % lead, 99.239 % cadmium and 99.919 % manganese could be achieved which is commensurate to the one factor at a time laboratory result of 1 g/50 ml, contact time of 10 minutes and pH range of 8 - 10. The crude oil tank farm wastewater treated at this condition was compared to the untreated sample and it showed a marked decrease in the concentration of the specified metals far below the standard limits set by NESREA.

TABLE OF CONTENTS

Cover Page 1

Title Page 2

Declaration 3

Certification 4

Acknowledgement 5

Abstract 6

Table of Contents 8

List of Figures 14

List of Tables 18

List of Plates 20

List of Abbreviations/Acronyms 21

CHAPTER ONE: INTRODUCTION 23

1.1 Preamble 23

1.2 Statement of the Research Problem 25

1.3 Justification of the Study 25

1.4 Aim and Objectives 26

1.5 Research Questions 26

1.6 Scope 26

1.7 Research Limitations 27

1.8 Research Challenges 27

CHAPTER TWO: LITERATURE REVIEW 28

2.1 The Petroleum Industry 28

2.1.1 Overview of refinery wastewaters 29

2.2 Zeolites 32

2.2.1 Definition of zeolite 32

2.2.2 Framework of zeolite Linde Type A 34

2.2.3 Porosity, surface area and molecular sieve effect of zeolite Linde type A 35

2.2.4 Shape selectivity 37

2.2.5 Synthesis 39

2.2.6 Applications 39

2.3 Clay 40

2.3.1 Classification of clay 40

2.3.2 Definition of kaolin 41

2.3.3 Structure of kaolinite 42

2.3.4 Kaolinite clay deposits in Nigeria 43

2.3.5 Metakaolinization of kaolin 43

2.3.6 Structure of metakaolin 44

2.4 Characterization Techniques 45

2.4.1 X-ray diffraction (XRD) analysis 45

2.4.2 BET Isotherm analysis 46

2.4.3 Scanning electron microscopy (SEM) analysis.....46

2.4.4 Energy dispersive X-ray (EDX) analysis.....46

2.4.5 Atomic absorption spectroscopy (AAS).....46

2.5 Adsorption Isotherm/Kinetic Studies.....47

2.5.1 Freundlich isotherm.....47

2.5.2 The Langmuir isotherm.....48

2.5.3 Temkin isotherm.....48

2.5.4 Adsorption kinetics.....49

2.6 Environmental and Health Risks of Heavy Metals.....51

2.6.1 Nickel (Ni).....51

2.6.2 Lead (Pb).....52

2.6.3 Cadmium (Cd).....52

2.6.4 Manganese (Mn).....52

2.6.5 Remediation of heavy metals.....53

CHAPTER THREE: MATERIALS AND METHODS.....57

3.1 Materials.....57

3.2 Methods.....59

3.2.1 Zeolite and kaolin (materials).....60

3.2.2 Wastewater collection and preparation.....63

3.2.3 Removal of heavy metals from simulated wastewater.....65

3.2.4 Adsorption of heavy metals from crude oil tank farm wastewater.....67

3.2.5 Analysis of samples 68

3.2.6 Experimental analysis using computer software 72

CHAPTER FOUR: RESULTS 77

4.1 Determination of Level of Heavy Metals in Crude Oil Tank Farm Wastewater 77

4.2 Characteristics of the Adsorbents 78

4.2.1 Ion exchange capability of the matrices....80

4.3 Heavy Metal Removal from Simulated Wastewater by the Matrices....81

4.3.1 Effect of pH on heavy metal removal 81

4.3.2 Effect of matrix dose on heavy metal removal....81

4.3.3 Effect of contact time on heavy metal removal....84

4.3.4 Effect of initial concentration of heavy metals on adsorption 86

4.4 Determination of Best Matrix and Selectivity....87

4.4.1 Selection of the best matrix based on adsorption capacity 87

4.4.2 Determination of the selectivity for heavy metals removal 88

4.5 Analysis on Interferences of the Individual Heavy Metals in the Simulated Wastewater 88

4.6 Characterization of the Best Matrix (Matrix 4) 90

4.6.1 Morphology and surface conditions of the Fresh and Spent matrices....90

4.7 Determination of Heavy Metal Removal from Crude Oil Tank Farm Wastewater 93

4.8 Adsorption Isotherms and Kinetic 96

4.8.1 Adsorption isotherms 96

4.8.2 Adsorption kinetic studies 100

4.9 Statistical Analysis of Data using Computer Software 105

4.9.1 Full factorial analysis 105

4.9.2 Optimisation by Response Surface Method (RSM) i

CHAPTER FIVE: DISCUSSION OF RESULTS xviii

5.1 Determination of Level of Heavy Metals in Crude Oil Tank Farm Wastewater xviii

5.2 Characteristics of the Adsorbents xviii

5.2.1 Composition and structure of adsorbents xviii

5.2.2 Ion Exchange Capability of the Matrices xx

5.3 Heavy Metal Removal from Simulated Wastewater by the Matrices xxi

5.3.1 Effect of pH on Heavy Metal Removal xxi

5.3.2 Effect of matrix dose on heavy metal removal xxii

5.3.3 Effect of contact time on heavy metal removal xxii

5.3.4 Effect of initial concentration of heavy metals on adsorption xxiii

5.4 Determination of Best Matrix and its Selectivity xxiv

5.4.1 Selection of the best matrix based on adsorption capacity xxiv

5.4.2 Determination of the Selectivity for Metal Removal xxiv

5.5 Analysis on Interferences of the Individual Heavy Metals in the Simulated Wastewater xxv

5.6 Charactrization of the Best Matrix (Matrix 4) xxv

5.6.1 Morphology and surface conditions of the matrices xxvi

5.7 Determination of Heavy Metal Removal from Crude Oil Tank Farm Wastewater xxviii

5.8 Adsorption Isotherms and Kinetic Studies xxix

5.8.1 Adsorption isotherms studies xxix

5.8.2 Adsorption kinetics xxxi

5.9 Statistical Analysis of Data using Computer Software xxxii

5.9.1 Full factorial analysis xxxii

5.9.2 Optimisation by Response Surface Method (RSM) xxxiv

CHAPTER SIX: CONCLUSION AND RECOMMENDATIONS xxxviii

6.1 Conclusion xxxviii

6.2 Recommendations xxxix

6.2.1 Contributions to knowledge xxxix

REFERENCES xl

APPENDICES liii

LIST OF FIGURES

Figure 2.1. Refining Percentage Capacity Utilization: Second Quarter, 2012 28

Figure 2.2. Refinery water balance 30

Figure 2.3. Representation of the Structure of Zeolite LTA and Hydroxysodalite 35

Figure 2.4. Molecular Sieve Action 36

Figure 2.5. (a) Molecular Sieve Type A (b) Molecular sieve 4A 37

Figure 2.6. Shape Seectivity 38

Figure 2.7. Classification of silicates 41

Figure 2.8. Crystallochemical structure of kaolinite 42

Figure 2.9. The change of the tetrahedrical (light) and octahedral (dark) sheets 43

Figure 3.1. Flow Diagram of the Research Methodology 60

Figure 4.1. XRD pattern for (a) Zeolite 4A (b) Kaolin (c) Metakaolin 78

Figure 4.2. SEM images of (a) Matrix 1; (b) Matrix 2; (c) Matrix 3; (d) Matrix 4; (e) Matrix 5 80

Figure 4.3. Effect of pH on Heavy Metal Removal by Zeolite 4A (Matrix 1) 81

Figure 4.4. Effect of pH on Heavy Metal Removal for Metakaolin (Matrix 5) 81

Figure 4.5. Effect of Matrix 1 dose on heavy metal removal 82

Figure 4.6. Effects of Matrix 2 dose on Heavy Metal Removal 82

Figure 4.7. Effects of Matrix 3 dose on Heavy Metal Removal 83

Figure 4.8. Effects of Matrix 4 dose on Heavy Metal Removal 83

Figure 4.9. Effect of Matrix 5 dose on Heavy Metal Removal 84

Figure 4.10. Effect of Contact time on Heavy Metal Removal by Matrix 1 84

Figure 4.11. Effects of Contact time on Heavy Metal Removal by Matrix 2 85

Figure 4.12. Effect of Contact time on Heavy Metal Removal by Matrix 3 85

Figure 4.13. Effect of Contact time on Heavy Metal Removal by Matrix 4 86

Figure 4.14. Effect of Contact Time on Metal Removal by Matrix 5 86

Figure 4.15. Effect of Initial Metal Concentration on Heavy Metal Removal by Zeolite 4A (Matrix 1) 87

Figure 4.16. Relative Heavy Metal Removal by the Adsorbents..... 88

Figure 4.17. Removal order (selectivity) of Heavy Metals by Matrix 4 88

Figure 4.18. Effect of Matrix 4 dose on Single Heavy Metal in Solution..... 89

Figure 4.19. Effect of Matrix 4 dose on two Metals in Solution (binary mixture)..... 89

Figure 4.20. Effect of Matrix 4 on Four Metals mixed together (composite mixture) ... 90

Figure 4.21. XRD Pattern of Matrix 4..... 90

Figure 4.22. SEM images of Matrix 1 (a) Fresh and (b) Spent 91

Figure 4.23. (a) SEM images of Matrix 4 (a) Fresh and (b) Spent 91

Figure 4.24. SEM images of Matrix 5 (a) Fresh and (b) Spent 92

Figure 4.25. Effect of pH on Crude Oil Tank Farm Wastewater 93

Figure 4.26. Effect of Matrix 4 dose on Crude Oil Tank Farm Wastewater 94

Figure 4.27. Effect of Contact time on Crude Oil Tank Farm Wastewater..... 94

Figure 4.28. Comparison of Effect of Best Matrix on Simulated Wastewater and Crude Oil Tank Farm Wastewater..... 95

Figure 4.29a. Freundlich plot Ni ions..... 96

Figure 4.29b. Freundlich plot Pb ions 96

Figure 4.29c. Freundlich plot Cd ions..... 97

Figure 4.30a. Langmuir Isotherm for Ni ions..... 97

Figure 4.30b. Langmuir Isotherm for Pb ions 98

Figure 4.30c. Langmuir Isotherm for Cd ions 98

Figure 4.31a. Temkin plot Ni ions 99

Figure 4.31b. Temkin plot Pb ions..... 99

Figure 4.31c. Temkin plot Cd ions..... 100

Figure 4.32a. First order kinetics Ni 100

Figure 4.32b. First order kinetics Pb 101

Figure 4.32c. First order kinetics Cd 101

Figure 4.33a. Second order kinetics Ni 102

Figure 4.33b. Second order kinetics Pb 102

Figure 4.33c. Second order kinetics Cd 103

Figure 4.34a. Intra particle Ni 103

Figure 4.34b. Intra particle Pb 104

Figure 4.34c. Intra particle Cd 104

Figure 4.35. Normal Probability plot of the Standardized Effects for nickel 108

Figure 4.36. Normal Probability plot of the Residual Effects for nickel 108

Figure 4.37. Pareto Chart of the standardized Effects for Nickel 108

Figure 4.38. Residual Versus the Order of the data for Nickel 108

Figure 4.39. Normal Probability Plot of the Standardized effects for Lead 109

Figure 4.40. Normal Probability of the Residuals for Lead 109

Figure 4.41. Pareto Chart of the Standardized Effects for Lead 109

Figure 4.42. Residuals versus the Order of the Data for Lead 109

Figure 4.43. Normal Probability Plot of the Standardized Effects for Cadmium 110

Figure 4.44. Normal Probability of the Residuals for Cadmium 110

Figure 4.45. Pareto chart of the Standardized Effects for Cadmium 110

Figure 4.46. Residuals Versus order of the Data for cadmium 110

Figure 4.47. Normal Probability Plot of the Standardized effects for Manganese 111

Figure 4.48. Normal probability Plot of the residuals for Manganese 111

Figure 4.49. Pareto Chart of the Standardized Effects for Manganese 111

Figure 4.50. Residuals versus the order of the Data for manganese 111

Figure. 4.51. The contour diagram for (a) Nickel (b) Lead (c) Cadmium and (d) Manganese ix

Figure 4.52. Three- dimentional Response Surface Plots for (a) nickel (b) lead (c) cadmium and (d) manganese xv

Figure. 4.53. Residual plot for (a) nickel (b) lead (c) cadmium and (d) manganese xvii

LIST OF TABLES

Table 2.1. Sources of Wastewater during Refining Processes 31

Table 2.2. Property Relations and Potential Applications of Features Presented by Zeolites. 33

Table 2.3. Properties of Selected Heavy Metals 56

Table 2.4. Permissible Limits of some Metals with the Health Impacts 56

Table 3.1. List of analytical equipment used and their domiciliation 59

Table 3.2. Formulated Matrices of Zeolite 4A and Metakaolin 63

Table 3.3. Design of Experiment for Factorial Analysis for Parameters Matrix 4 dose (X_1), Contact time (X_2), pH (X_3).....74

Table 3.4. RSM design of experiment (Box–Behnken design) 76

Table 4.1. Heavy Metals Content of Wastewater Collected from the Crude oil Tank Farm.....77

Table 4.2. XRF Result of Chemical Composition of Zeolite 4A, Beneficiated Kankara Kaolin and Metakaolin 79

Table 4.3. Ion Exchange Capacity for Matrix 1, 2, 3, 4 and 5.....80

Table 4.4. Comparative Coposition of the Matrices Before and After Adsorption (EDX Results).....92

Table 4.5. BET Surface Characteristics of the Adsorbents Matrices.....93

Table 4.6. Quality of the Untreated and Treated Crude Oil Tank Farm wastewater 95

Table 4.7. Parameters for Adsorption Isotherm Models using Matrix 4 for Heavy Metal Removal from Simulated Wastewater.....105

Table 4.8. Parameters for Adsorption Kinetic Models using Matrix 4 for Heavy Metal Removal from Simulated Wastewater.....105

Table 4.9. Factorial Design of Experiments and Percentage Heavy Metal Removal (Response) at the Specified Conditions of Matrix 4 dose, Contact time and pH 105

Table 4.10. Estimated Effects and Coefficients for yNi, yPb, yCd & yMn (coded units) 107

Table 4.11. Analysis of Variance (coded units).....112

Table 4.12. Factorial Statistics for Nickel, Lead, Cadmium and Manganese 113

Table 4.13. Design of Experiment (DOE) for Optimisation by Response Surface methodology (RSM) and Percentage heavy metal removal i

Table 4.14. Sequential Model Sum of Squares: Response: Ni, Pb, Cd, & Mn Removal. ii

Table 4.15. The model fit summary iii

Table 4.16. Lack of Fit Tests iv

Table 4.17. ANOVA of Response Surface Quadratic Model for Ni, Pb, Cd and Mn vi

Table 4.18. Diagnostic case statistics for Nickel, Lead, Cadmium and Manganese.....x

Table 4.19. The optimized RSM values xvi

LIST OF PLATES

Plate I Picture of (a) Zeolite 4A and (b) Raw Kaolin.....61

Plate II Atomic Absorption Spectrometer [AA240FS (Fast sequential absorption spectrometer (VARIAN)].....69

Plate III XRF Machine 69

Plate IV Phillip X-Pert X- ray Diffractometer.....71

LIST OF ABBREVIATIONS/ACRONYMS

Matrix 1 = 100 % Zeolite 4A & 0 % metakaolin

Matrix 2 = 75 % Zeolite 4A & 25 % metakaolin

Matrix 3 = 50 % Zeolite 4A & 50 % metakaolin

Matrix 4 = 25 % Zeolite 4A & 75 % metakaolin

Matrix 5 = 0 % Zeolite 4A & 100 % metakaolin

CEC = Cation Exchange Capacity

CMK100 = Matrix 5

CMK100T = Spent Matrix 5

CZ100 = Matrix 1

CZ100T = Spent Matrix 1

ZKM75/25 = Matrix 4 (25 % Zeolite 4A /75 % metakaolin)

ZKM75/25T = Spent Matrix 4 (25 % Zeolite 4A/ 75 % metakaolin)

AAS= Atomic Absorption Spectroscopy

ABU = Ahmadu Bello University Zaria

AGO = Automotive Gas Oil

ANOVA = Analysis of Variance

BET = Braunner-Emmett-Teller

DICON= Defence Industry Corporation of Nigeria

EDX = Energy dispersive X-ray

KRPC = Kaduna Refinery and Petrochemical Company

LAB = Linear Alkyl Benzene

LPG = Liquefied Petroleum Gas

NAGRL= National Geoscience Research Laboratory

NESREA = National Environmental Standard and Regulation Enforcement Agency

NNPC = Nigerian National Petroleum Corporation

OFAT = One Factor at Time

PHRC = Port Harcourt Refining Company

PMS = Premium Motor Spirit

QPI = Quarterly Petroleum Information

RSM = Response Surface Method

SEM = Scanning Electron Microscope

SON = Standard Organization of Nigeria

WHO = World Health Organization

WRPC = Warri Refinery and Petrochemical Company

WWT = Waste Water Treatment

XRD = X-ray Diffraction

XRF = X–ray Fluorescence

CHAPTER ONE

INTRODUCTION

1.1 Preamble

One of the major industries that poses danger to man and its environment is the petroleum industry. Many of its production and processing activities, including the transformation of crude oil to its final consumable products such as liquefied petroleum gas (LPG), premium motor spirit (PMS), automotive gas oil (AGO), dual purpose kerosene (DPK), etc., result to the release of heavy metals, *inter-alia* to the receiving waters. As a result, many ground waters within such catchment areas have been found to contain relatively high concentration of these toxic metals. According to Lars-Jarup (2011) British Medical Bulletin, exposure to heavy metals is a main threat to human health. Accumulation of these heavy metals within the soft tissues of the human body can lead to cancer, damage or reduced mental activity and central nervous function, reduced learning ability and damage to blood composition, lungs, kidneys and other vital organs, hence immediate attention is needed to address this challenge (Mudi, 2011). To address the primary challenges of water contamination, wastewater treatment (WWT) plants are designed and constructed to treat all wastewaters so that discharged wastewaters from refineries are brought to acceptable quality level (Bashir, 2008). The Refinery wastewater streams being discharged to the environment come from the crude oil tank (dewatering tanks), desalter, sour water stripper, lube (base oil and asphalt) plants, spent caustic treated, and sanitary waste (Inelo, 2010). The major wastewater comes from the crude oil tank farm where they have the crude oil dewatering tanks discharging wastewater with high proportion of salts and dissolved solids (TDS). During the dewatering process, crude is allowed to settle and water drained off with its accumulated pollutants being sent to the wastewater treatment unit. Akor, (2009) stated

that most of these crude's associated heavy metals are hardly diluted or adsorbed. Osuji and Uwakwe (2006) further reported that these metals can easily be dispersed to soil and rivers by flood and intense rainfall.

To curtail this pollution challenge, Babel and Kurniawan, (2004) had earlier stated that, conventional treatment processes such as chemical precipitation, electrochemical removal etc. have significant disadvantages. Some of the disadvantages are incomplete removal, high-energy requirements, and production of toxic sludge (Eccles, 1999). According to Leung *et al.,* (2000), the search for low cost adsorbents which could be of mineral origin or organic resins has really intensified (Kurniawan *et al.*, 2005, Aderemi 2004). A consideration to use Zeolite 4A was based on earlier findings of previous researchers, thus El-Nafaty and Jibril (2008) reported that zeolites have been found to be one of the effective materials for removal of both organic and inorganic contaminants from the environment. Some researchers also have noted that zeolites' chemical inertness, modifications, unique properties and selectivity distinguished them as effective materials for solving environmental pollution (Ismail *et al.,* 2013*,* Inglezakis *et al.,* 2000). Literature search has shown that many previous researchers premised their investigations on these inherent and derived properties of zeolites. Others have employed biological and chemical bases to attempt to remediate the prevalence of heavy metals as pollutants in the environment (Aderemi 2000, Mudi, 2011, and Uwakwe, 2006).

Referring to the use of zeolites for heavy metal remediation, insufficient emphasis was also not laid on process improvement and adsorbent's matrix formation.

This research intends to carry out an aggregate removal of some selected predominant heavy metals from petroleum wastewater using Zeolite 4A – metakaolin matrix and also

to conduct an optimization study and to generate model equations using MINITAB and DESIGN – EXPERT software.

1.2 Statement of the Research Problem

i. Environmental Concern:

Crude oil tank farm wastewater are source of environmental pollutants with adverse effect on man and its environment. The current treatment processes in the refineries are inadequate to meet prescribed environmental standard. Thus the receiving waters which are sources of both domestic and industrial water become overloaded with toxic heavy metals.

ii. Previous attempts by researchers to mitigate this environmental challenge came with their side effects:

a. Unacceptable high cost of resins/adsorbents being currently used.

b. Selective removal of heavy metals; and

1.3 Justification of the Study

i. There is availability of local kaolin clay which could be processed to Zeolite 4A and metakaolin matrix for treatment of crude oil tank farm wastewater.

ii. There are also availability and environmental impact of crude oil tank farm wastewater.

iii. There will be reduction of cost of treatment through the use of matrices of Zeolite 4A and metakaolin.

iv. Mathematical models for for this process will be developed for future application in environmental pollution management.

v. Optimal conditions for wastewater treatment will be established.

vi. Job will be created for the teeming unemployed and

vii. There will be assurance of eco-friendly environmental sustainability.

1.4 Aim and Objectives

The aim of this work is to establish the appropriateness of Zeolite 4A, metakaolin and their matrices for removal of nickel, lead, cadmium and manganese from crude oil tank farm wastewater.

To reach the aforementioned aim, the following objectives will be achieved:

i. To determine heavy metals pollution loadings of crude oil tank farm wastewater
ii. To characterize Zeolite 4A, metakaolin and their matrices (using XRD, XRF, SEM-EDX, BET and AAS)
iii. To apply Zeolite 4A and metakaolin and their matrices for aggregate removal of heavy metals in crude oil tank farm wastewater.
iv. To establish the mathematical models and optimal conditions for removal of the four heavy metals predominant in crude oil tank farm wastewater.

1.5 Research Questions

i. What are the pollution loadings of nickel, lead, cadmium and manganese in the crude oil tank farm wastewater?
ii. What can be used to remove or reduce the heavy metal loadings in the crude oil tank farm wastewater sample?
iii. What best conditions can be used to achieve a maximum removal?

1.6 Scope

i. Both simulated and real crude oil tank farm wastewater were investigated.

ii. Zeolite 4A, metakaolin and their matrices were evaluated and the adsorbate/adsorbent characterized using XRD, XRF, SEM-EDX BET and AAS.

iii. Factorial analysis and response surface methodology were applied to the data collected.

1.7 Research Limitations

This research work is limited to the application of Zeolite 4A, metakaolin and Zeolite 4A – Metakaolin matrices for treatment of crude oil tank farm wastewater.

1.8 Research Challenges

i. Unavailability of research grant.

ii. Scarcity of analytical equipment/apparatus.

iii. Interruptive power supply.

CHAPTER TWO

LITERATURE REVIEW

2.1 The Petroleum Industry

The petroleum industry covers the processes of bringing crude oil from its raw form to the final consumable products. Reports from the Nigerian National Petroleum Corporation (NNPC) quarterly petroleum information (QPI, 2012) stated that the three local refineries in Nigeria, namely Kaduna Refinery and Petrochemical Company (KRPC), Port Harcourt Refinery (PHRC) and Warri Refinery and Petrochemical Company (WRPC) received a total of 1,385 thousand metric tonnes (MT) of crude oil in the second quarter of 2012 and about 1,355 thousand MT was processed with KRPC processing about 36.46 % of the crude oil as presented in Figure 2.1

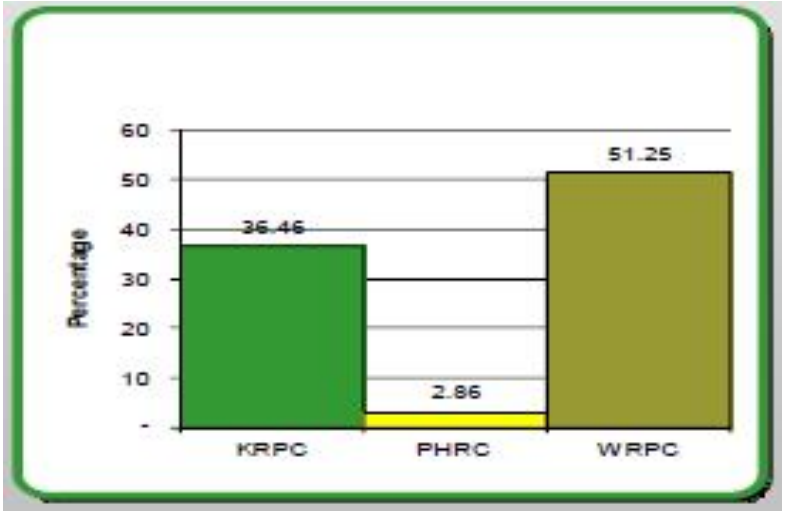


Figure 2.1 Refining Percentage Capacity Utilization: Second Quarter, 2012

The petroleum industry classifies and characterizes crude according to their geographical and geological formation such as Nigerian crude, Iraq, Kuwait and Venezuela etc., but this provides only little information on the state and toxicity of the

crude and thus it is not a useful classification scheme when considering petroleum wastewater analysis.

Thus, Umudi (2011) carried out analysis on produced water from different areas in the Niger Delta. He reported that the concentration of the crude associated metals were higher than the accepted limits by World Health Organization (WHO) and the National Environmental Standard and Regulation Enforcement Agency (NESREA).

According to Jacque and Barboza (2008), oil refineries release high pollutants, consume large energy and water thereby producing large quantities of wastewater. Nweke and Okpokwasili (2010) reported that though the concentration of toxic heavy metals generated from the wastewaters per unit of crude oil processed may not be too high, they accumulate in the receiving water bodies due to their non-biodegradable nature; thus the need to effectively and economically handle these wastewaters must be critical to the success in the oil processing business.

2.1.1 Overview of refinery wastewaters

The refinery operations are determined by the quantity and composition of crude oil received and commodities produced, implying that refineries vary in size based on the complexity of their separation, crude oil capacity and treatment processes. (www.ladco.org/reports/control/whitepappers/petroleum) leading to corresponding volumes of wastewater generated. Figure 2.2 shows the water network in a refinery which may be said to be as unique as the production processes. Thus water used in the refinery processes could be treated and recycled continually or discharged to the environment (www.ipieca.org). Typical wastewater streams due to refining processes are presented in Table 2.1.

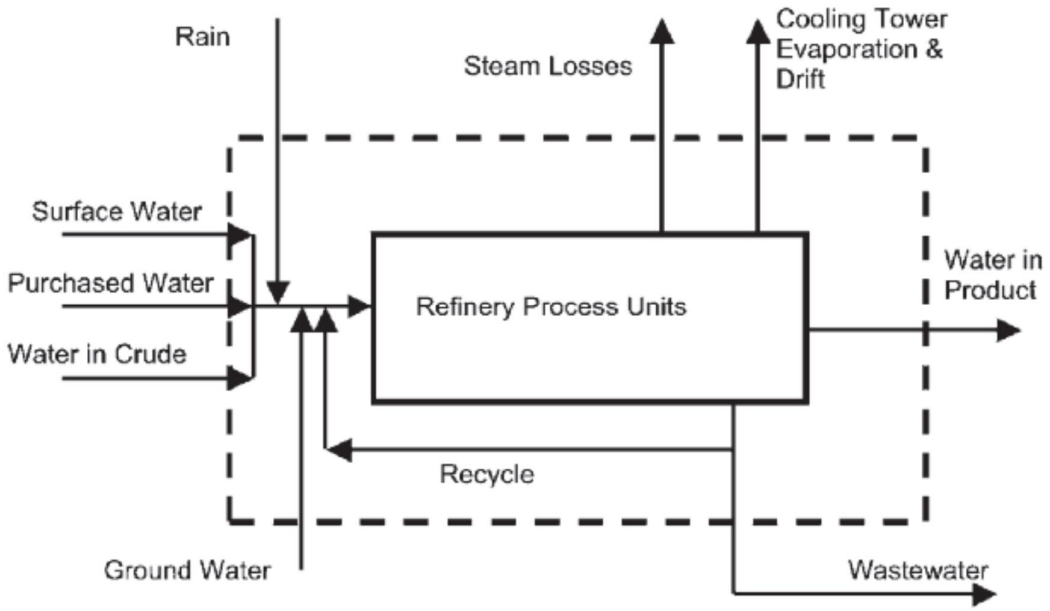


Figure 2.2. Refinery water balance (www.ipieca.org)

Table 2.1. Sources of Wastewater during Refining Processes

Refinery process	Wastewater description	Waste by-products
Storage tanks	Crude oil comes with a considerable amount of water, during storage, this water settles in the storage tanks and is periodically drained off.	Sulphides, salts, TDS, and oil
Desalting unit	The desalting process produces salt water from the washing of the crude oil. The undercarry from the desalter contains residual produced water that came with the crude as well as wash water which is added prior to desalting to dilute and remove contaminants.	Mineral salts, heavy metals
Distillation	Oily sour water is drained from the "knock down" sump vessels of the fractionator.	Sulphur and Ammonia
LPG caustic washing	In the liquefied petroleum gas caustic soda wash unit, caustic is added to convert sulphur (H_2S) to sodium D –sulphide (NaS_2).	High sulphides
Cooling Tower blow - down	Water used for cooling is recirculated in closed loop. Water drained as "blow down" to maintain acceptable temperature and dissolved solids levels.	Corrosion inhibitors, TDS
Miscellaneous	Other wastewaters are produced from wash down of operations, boiler blow down, MEK de – waxing and propane De–asphalting.	Propane, methyl, ethyl, ketone, TDS, oil and others.

Source: New Logic Research, 2003 (www.vsep.com/pdf/desaltercasestudy)

Considering the waste by-products in Table 2.1, the principle of operational technics carried out by the wastewater treatment of the refineries may not in any case cater for the toxic heavy metals *(NNPC Kaduna Refinery Operational Manual, 1980, Inelo, 2010).*

2.2 Zeolites

2.2.1 Definition of zeolite

Bell, in 2001, defined zeolites as microporous crystalline solids with well-defined structures. Generally, they contain silicon, aluminium and oxygen in their framework and metal cations, water and / or other molecules within their pores. Also the commission on new minerals and mineral names stated that "A zeolitic mineral is a crystalline substance with a structure characterized by a framework of linked tetrahedral, each consisting of four oxygen atoms surrounding a metal cation. This framework contains open channels and cages, and as aforementioned, are usually occupied by H_2O molecules and extra-framework cations that are commonly exchangeable.

By the conventional definition, zeolites are microporous aluminosilicates. This definition, according to Ajayi (2012) has been modified within the past years and currently isomorphously substituted materials, like for example gallosilicates, titanosilicates or aluminophosphates, are also called zeolites or zeolitic materials.

Conventional definition: "Microporous Framework Aluminosilicates"

$$M^{x+}_{m/x}\,[Al_mSi_nO_{2(m+n)}]\cdot p\,H_2O$$

Nowadays also: Microporous Framework Titanosilicates, Gallosilicates, Aluminophosphates, etc.

$$M_x\,M_y'\,N_z\,[T_m\,T_n'\,\ldots O_{2(m+n+..)-e}\,(OH)_{2e}]\,(OH)_{br}\,(aq)_p\;qQ$$

Microporosity (pores with diameters below 2 nm) is an intrinsic feature of all these materials and is caused by channels and cavities within the crystal structures of zeolites. The wide application of zeolites on environmental management is based on its unique

properties. Thus zeolites contains cations like Na^+, K^+, or NH_4^+ after synthesis. The negative net–charge caused by the trivalent aluminium cations are balanced by the aforementioned cations which are coordinated tetrahedrally by oxygen ions. When solutions containing other metal cations are in contact with zeolite containing sodium ions (Zeolite 4A), the sodium ions can be exchanged with the other ion provided the ions are within the zeolite pore size (molecular sieve).

In another presentation, Adefila (2012) averred that "Zeolites are traditionally known as advanced materials resulting from crystalline silicates and aluminosilicates linked through oxygen atoms, producing a three-dimensional network containing channels and cavities of molecular dimensions. However, some relatively recent discoveries of materials virtually identical to the classical zeolite, but consisting of oxide structures with elements replacing silicon and aluminium from their corresponding columns in the Periodic Table of Elements have stretched the definition. Most researchers now include in their definition of a zeolite virtually all types of these tailorable micro porous oxide structures that have well-defined pore structures due to a high degree of crystallinity. These oxides are of titanium, gallium, iridium, thallium and phosphates, e.g. AIPOs SAIPOs, GaPOs, etc. The original elements – silicon and aluminium – can similarly be substituted to extend the formation of zeolites, beyond linking the Columns Three and Four elements, to other contiguous elements, to produce novel advanced materials; the elements can also be replaced with organic functional groups to form organometallic zeolites. Further extension can, yet, be effected by replacing the nodal oxygen in zeolites with any of the other Column Six element." Adefila (2013) also crystalized the feature-property-application of zeolites as presented in Table 2.2.

Table 2.2: Property Relations and Potential Applications of Features Presented by Zeolites.

Feature	Conferred Property	Potential Applications/Advantages
Porosity	Low density solid	Ease of fluidisation arising from low required lift energy per unit mass
Regular pore with molecular dimension	Specific pore dimension	Sieving effect, selectivity/controlled reaction and size/product distribution, subsequent separation requirement
High pore volume per unit mass	Thermodynamic suction pump effect*	Reduction of diffusion resistance per unit length of pore and higher materials, such as introduced conventional catalysts, in catalysis and as impurities from environment of zeolite
Entrained cations	Controlled acidity and free passage	Controlled catalytic reactions
High available internal and ionised surface area per unit mass	Enhanced surface area phenomena	High/catalytic reactivity or/and adsorption of material and relatively transfer, for controlled reaction
Liable entrained charged cations	Ion exchangeability	Selective removal or introduction of cations such as water softening

* The suction pump effect is effective in the liquid transport.
Source; Adefila, S. S, (2013) *Production of Zeolites from Local Minerals for Petroleum Refining Processes. APWEN public lecture, 25 June, 2013.*

2.2.2 Framework of zeolite Linde Type A

In a research carried out by Janjira, (2002), he stated that pseudo unit cell of zeolite Na-A consists of 12 SiO_2 and $12Al_2O_3$ unit. The chemical composition of pseudo unit cell is Na_{12} $[Al_{12}SiO_{12}O_{48}]$ $\cdot 27H_2O$. It is 1/8 of the true unit cell. Zeolite A exhibits a Linde type A structure with a 3 – dimensional pores running perpendicular to the x, y, z planes which comprises of 4,6, 8 and 4 – 4 secondary building units as indicated in Figure 2.3. It has a structured cavity caged with eight sodalite cages connected by their faces in cubic structure with a minimum free diameter 11.4Å (http://www.personal.utusa.edu/geoffery-price/zeolite/ita.htm). Zeolite 4A has a void volume fraction of 0.47 with Si/Al ratio of 1.0 and a decomposition temperature of 700 ºC (Adel *et al.*, 2010). Figure 2.3 presents Janjira's model.

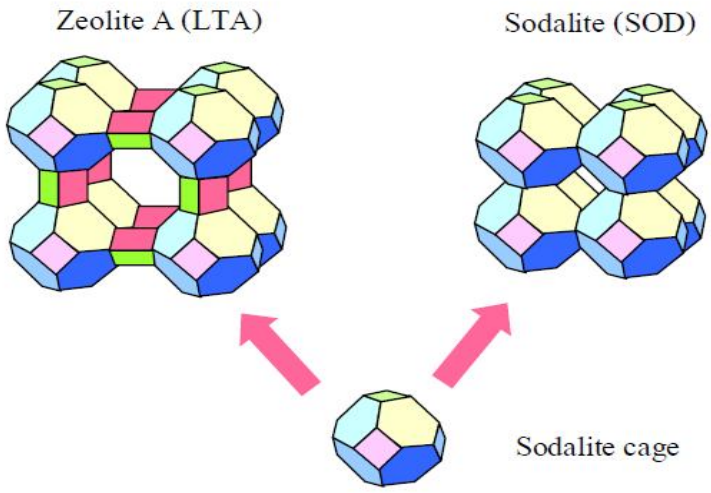


Figure 2.3. Representation of the Structure of Zeolite LTA and Hydroxysodalite (Janjira, 2002)

2.2.3 Porosity, surface area and molecular sieve effect of zeolite Linde type A

Generally the high porosity of zeolites confer on them low density, high pore volume and surface area per unit mass. Pore sizes of zeolites are highly dependent on their structure and can be varied depending on the ion exchanging the zeolite (Kovo, 2011). Metal cations can be deposited on the windows thereby making it wider, thus the windows determine the accessibility of the zeolite pore system for other molecules (Adel, et al., 2010). Molecular sieves or desiccants are so called because of their property of screening molecules at the activated alumina which have very wide pore distributions. Zeolites type A have regular pore sizes, based on the pore sizes- they are called 3, 4, 5, or 10 Angstroms. According to Database of zeolite structure (2002), Zeolites type A classified as different cation grades, 3A, 4A and 5A, all of which possess the same general formula but have different cation type. When 75 % of its sodium is replaced by potassium, it is referred to as Zeolite (3A). Alternatively, replacement of sodium by calcium gives rise to (5A) type (Ugal *et al.,* 2010; www.decimpinti.com/DEC/TEXT/ENGLISH/dec.zeolite.uk.html).

According to Ajayi (2012), the modification of the pores to precisely determine the uniform openings allows molecules smaller than the zeolite pore diameter to pass through while excluding larger molecules as represented in Figure 2.4, hence the name “molecular sieve”. The different pore sizes of synthetic zeolites open up a wide range of possibilities in terms of "sieving" molecules of different size or shape from gases and liquids.

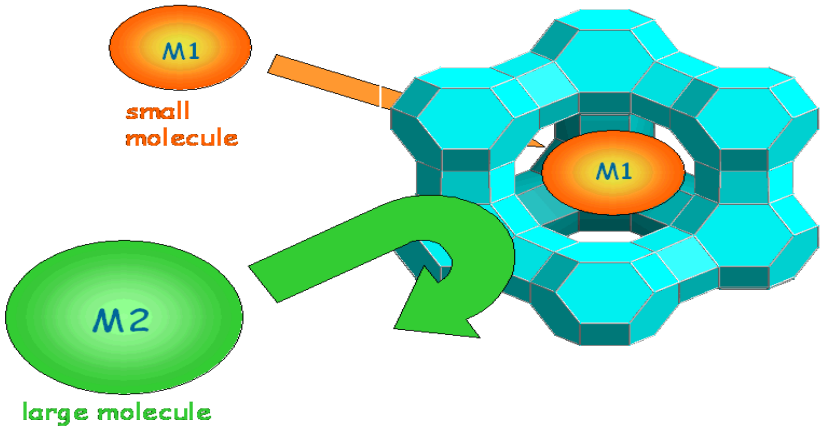
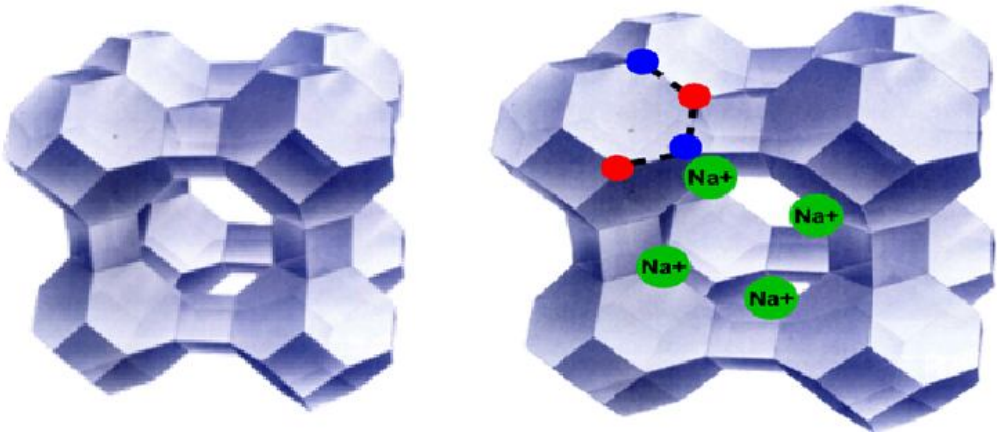


Figure 2.4. Molecular Sieve Action

Source: Gregg and Sing (1982) Adsorption, Surface Area and porosity, Academic Press.



(a) (b)

Figure 2.5 (a) Molecular Sieve Type A (b) Molecular sieve 4A

The pore size plays a significant role as depicted in Figure 2.5 (a&b), controlling the entrance of the molecules in and out of the pore system. In fact, the adsorption of molecules on the adsorbents is based on the following physical molecular properties:

i. Size and shape, and
ii. Molecular polarity and ionic strength.

Molecules larger than the pore opening will be excluded while smaller molecules will pass through, thus Hazard (2010) studied the adsorption behaviour of Zeolite A and Zeolite X on the removal of Cu, Cd, Cr, Ni and Zn. He discovered that the uptake depends on hydrated ion diameter. Polar molecules can be adsorbed preferentially under identical conditions (http://www.molelarsieve.org/zeolitemolecularsieve.htm). Further, ionic strength, which reduces directly with increasing density per unit atomic/molecular polarity, influences corresponding adhesive strength.

2.2.4 Shape selectivity

Due to the existence of trivalent aluminium to tetravalent silicon in the crystal structure, natural zeolites have net negative charge per primary building unit and thus function well as cation exchange materials. It has virtually no affinity for anions or non – polar organics. However, when treated with cationic surfactants, their surface chemistry become dramatically altered. These large organic cations exchange selectively with inorganic cations to form a stable organic rich coating on the external surface of zeolite. Figure 2.6 presents the selectivity of zeolites. This selectivity of zeolites is led by the limited pore size which only allows specific molecules either to enter the pores (reactant selectivity) or to leave the pores (product selectivity) depending on their sizes as noted before (see Figures 2.6(a & b). Furthermore, not every transition state during reaction

might be possible, thus forcing a reaction only into one direction (restricted transition – state selectivity) as indicated in Figure 2.6c and sometimes, during the process of utilization of zeolites, coke is characteristically formed on their exterior surfaces (Exterior coke formation) as depicted in Figure 2.6d.

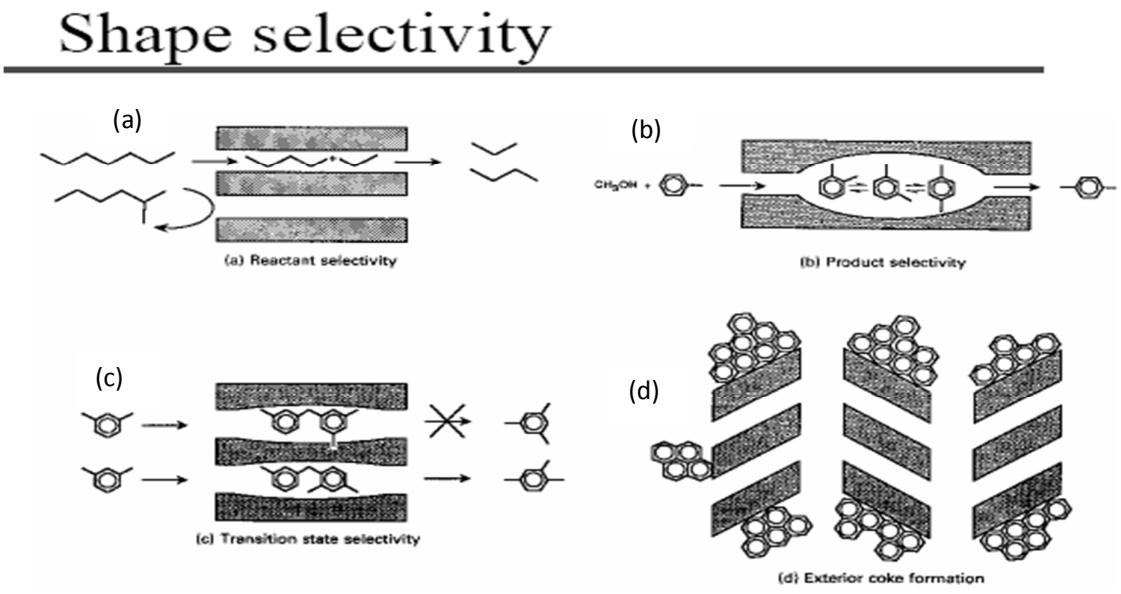


Figure 2.6. Shape Seectivity (Ajayi, 2012)

Thus the ion exchange property has been used to study the exchange behaviour between a zeolitic system containing Na, Ca and K and Cr ions initially in solution. For this purpose, natural and synthetic zeolites could be used. Ozge *et al.,* (2010) applied copper model for solid diffusion controlled process to the system in order to investigate the dynamic behaviour of the system. As a result of this simulation, breakthrough was well predicted. The study concluded that the local zeolites tuff can be used for the removal of copper, nickel and cobalt ion from aqueous solutions.

Zeolite Na-A is the simplest synthetic zeolite with a molecular formulation of one silicon to one aluminum to one sodium cation.

2.2.5 Synthesis

Zeolites are generally synthesized by gelling process. In principle alumina is sourced from sodium aluminate while silica is from sodium silicate: - both are mixed in basic aqueous solution to produce a gel. Sodium hydroxide, ammonium salt or any other polar organic can be used as requisite alkali agent. The gel crystallizes within the range 70 to 300 ºC, in the sodium form (http://www.chemistry-of-zeolites-and-related-porous-material-synthesis-and-structure).

2.2.6 Applications

Due to its unique and special properties which are suitable for various kinds of chemical reactions, Zeolite A has been widely used in many applications such as in ion exchange separation. Both natural and synthetic zeolites have become important and integral part of many process industries (Kovo, 2011). Inglezakis *et al.* (2000) reported that pre-treatment leads to a high effective capacity of a zeolitic material. Inglezakis *et al.* (2004) observed in his work that modification of a natural zeolite sample is favourable, leading to an increase of removal efficiency by 32 to 100 %.

Therefore, in this research, metakaolin is to be synthesized from a local kaolin to form matrices with a commercial Zeolite 4A (Zeolite 4A-metakaolin matrices) for aggregate removal of the predominant toxic metals in petroleum wastewater. It then becomes necessary to have good understanding of the kaolin clay formation, structure and properties.

2.3 Clay

Clay refers to sediment or fine-grained mineral fraction of the earth material. According to clay mineralogist, clay is a layered silicate mineral or other mineral which impacts plasticity and hardens upon drying and firing (Guggenheim et al., 1998).

2.3.1 Classification of clay

Two main classes of clay are recognized as residual and sedimentary (transported) clays. Ajayi (2012) averred that residual clays are those clays that are located at their points of origin. They are found side-by-side with the altered igneous rocks from which they are formed. They are usually extracted from the parent rock and obtained in comparatively pure state. Example of such clay is China clay in Cornwall, United Kingdom. On the other hand, the sedimentary clay, are those which have been removed from their origin by natural agencies, as a result of this transit, inherent impurities are attracted resulting to impure fine grain type of clay (*Worrall, 1986*). Kankara kaolin is believed to belong to this class, i.e. sedimentary, resulting to its high level of impurities (Ajayi, 2012). Rasheed (2001) used kaolin in its natural ore for wastewater treatment and achieved a commendable result.

Clay minerals are part of the silicate family called phyllosilicates. There are five common and important types of clay found in nature, namely kaolinite, montmorillonite, hydrous mica, vermiculite and allophone. The first four are crystalline and can be regarded as small sheet-like particles as presented in Table 2.7.

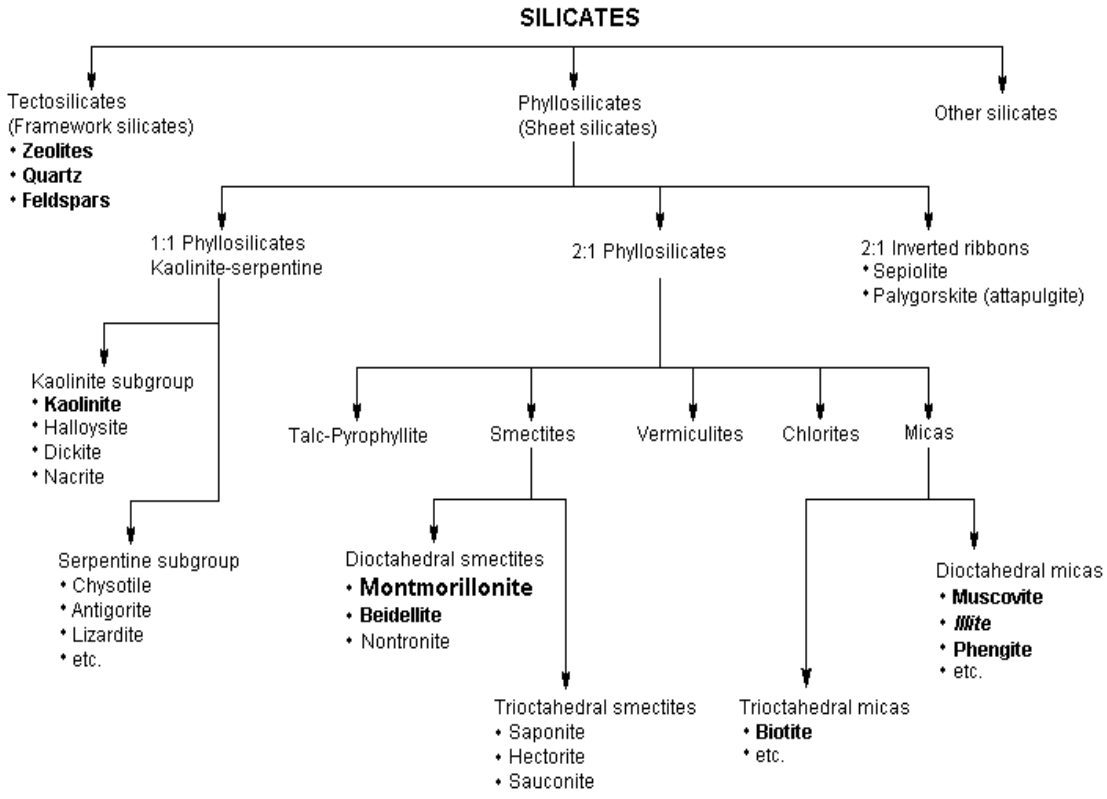


Figure 2.7. Classification of silicates (adopted from Bailey, 1980 and Rieder et al., 1998)

2.3.2 Definition of kaolin

Kaolin as a soft, lightweight, often chalk- like sedimentary rock that has an earthly odor. Kaolin has been widely used in the ceramic industry because of its fine structure and its plastic nature. Kaolin may have a color of white, pink and grey depending on its geological formation and composition. It is very soft with hardness of 2-2.5 (Grim 1968, Velde 1992). Rocks that are rich in kaolinite are known as kaolin thus the chemical formula of kaolinite is $Al_2O_3 \cdot 2SiO_2 \cdot 2H_2O$ and the composition expressed in oxides is 46.54 % SiO_2, 39.50 % Al_2O_3 and 13.96 % H_2O (Ajayi, 2012). Kaolinites are aluminosilicates, with a 1:1 uncharged dioctahedral layered structure. Each layer consists of a sheet of SiO_4 tetrahedral forming six-membered silicate rings connected

via common oxygen atoms to a sheet of Al_4O_6 octahedral building four membered aluminate rings as shown in Figure 2.8 (Bongeard, 2000).

2.3.3 Structure of kaolinite

The 1:1 structure of kaolinite is composed of SiO_4 tetrahedral sheets and $Al_2 (O_5OH)_6$ octahedral sheets with pseudo-hexagonal symmetry occupied as follows:

O_6–Si_4–O_4–$(OH)_2$–Al_4–$(OH)_6$. (*Ajayi, 2012*). The report of Hazard (2010) that the uptake of metals depends on hydrated ion diameter of kaolin explains it's shrinking and swelling when mixed with water. It has a plastic property and it is easy to mould. The structure and lattice layers of kaolinite in Figures 2.8 and 2.9 (Ajayi, 2012) depicts the closeness in layers, thereby disallowing water molecules from getting between the sheets.

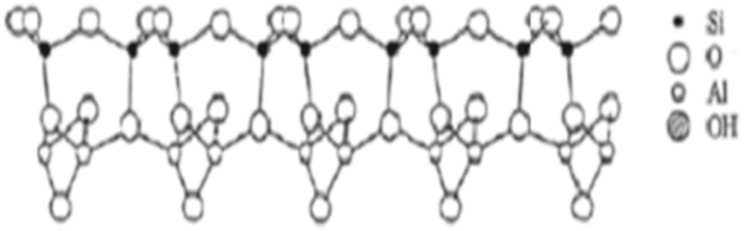


Figure 2.8 Crystallochemical structure of kaolinite

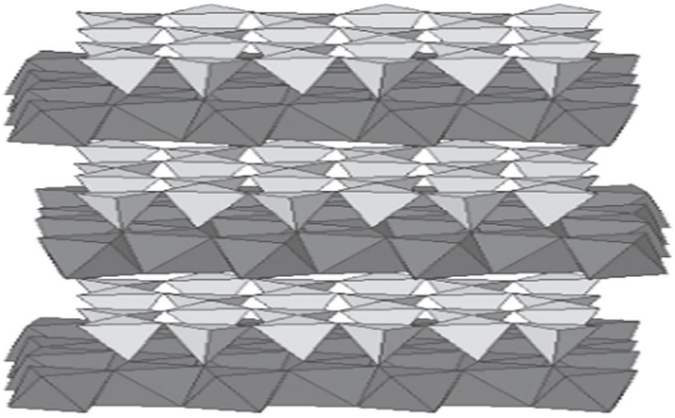


Figure 2.9. The change of the tetrahedrical (light) and octahedral (dark) sheets

2.3.4 Kaolinite clay deposits in Nigeria

Farriconsulting blogspot.com reported that apart from the crude oil potentials in Nigeria, Nigeria has comparative advantage in solid minerals sector due to the abundance deposits of kaolin scattered in different parts of the country (http://farriconsulting.blogspot.com/2010/07/kaolin-deposits-in-nigeria-08.html).

There is an estimated reserve of about three (3) billion metric tonnes of kaolin deposit scattered in different parts of the country like Ogun, Edo, Plateau, Nasarawa and Katsina State (Bamidele, 2012). The industrial prospects for kaolin are high and sustainable because of its wide applications. As a measure to improve industrial dependence on local kaolin, a ban was placed on importation of kaolin into the country (http://www.foramfera.com/index.php/investment-oppurtunities-nigeria/item/deposits-and-mimningin-nigeria-oppuortunities).

2.3.5 Metakaolinization of kaolin

The raw form of kaolin is less reactive and forms hydrosodalite when reacted with sodium hydroxide. The process of metakaolinization involves beneficiation and calcination. Metakaolinization occurs within the temperatures of 550 to 900 ^{o}C (Tarek *et al.,* 2010). This process involves the loss of hydroxyl group, followed by

rearrangement of the octahedral layer to tetrahedral shape in the calcined clay (Kovo, 2011).

$$Al_2O_3 \cdot 2SiO_2 \cdot 2H_2O \xrightarrow{550-900\ ^oC} Al_2O_3 \cdot 2SiO_2 \cdot 2H_2O(g)$$

$$2Al_2Si_2O_5(OH)_4 \xrightarrow{550-900\ ^oC} 2Al_2Si_2O_7 + 4H_2O(g)$$

(2.1)

$Kaolin$ $Metakaolin$

2.3.6 Structure of metakaolin

The thermal decomposition of kaolinite crystal to partially disordered metakaolin is known as dehydroxylation. The new phase less amorphous metakaolinite, does not collapse but, rather, retains a layered structure. This enhances its application for water treatment, hence Lawrence et al. (2013) studied the kinetic adsorption of nickel ion on Kankara kaolinite and achieved 97.68 % adsorption capacity at a temperature of 50 ^oC. The first compilation of crystallographic model of metakaolinite was made by *Brindley and Nakahira (1957 and 1959).* They proposed an ideal well-ordered lattice presented in Figure 2.10

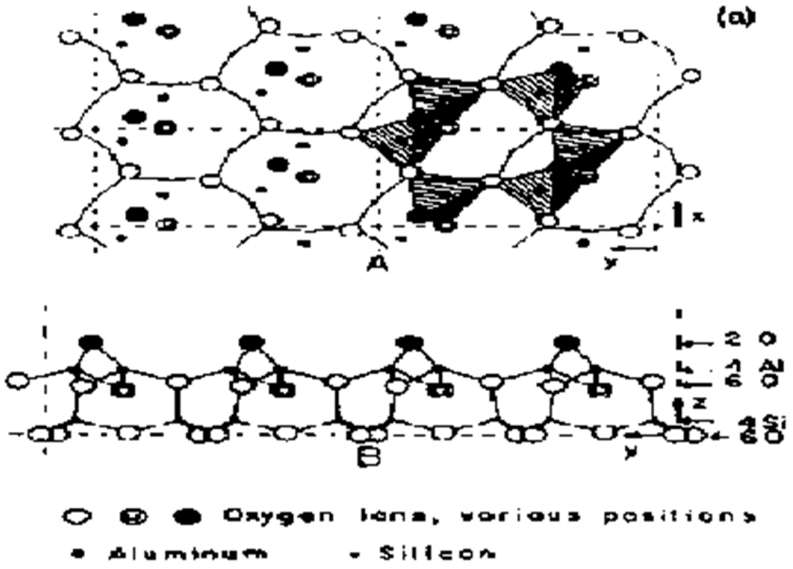


Figure 2.10. Lattice of metakaolinite proposed by Brindley and Nakahira (1957)

2.4 Characterization Techniques

2.4.1 X-ray diffraction (XRD) analysis

XRD is a good characterization tool used in solid state chemistry and material science, to determine the crystallinity of a solid sample by measuring the diffraction pattern and providing information about the electronic distribution of atoms throughout the solid structure. According to Cullity (2012), amorphous materials are materials that have no definite form or shape. Its shape can be easily altered while crystalline solid matter are arranged in regular, repeating patterns. The diffracted x-rays have elevated scattering intensities also known as the diffraction counts at certain diffraction angles. When there is perodic arrangement as in crystalline structure, the x-rays will be scattered only in certain directions as they hit the formed lattice planes and this will cause high intensity peaks. For the amorphous structure, the x-rays will be scattered in many directions leading to a diffuse peaks distributed in a wide 2 theta range. Thus, this analysis can be applied to investigate whether the solid sample has an amorphous or crystalline phases,

to make available the knowledge of lower crystallinity leading to an increase of amorphous materials within as reported by Janjira, (2002).

2.4.2 BET isotherm analysis

BET-surface area measurements are generally based on the phenomenon of gas adsorption-desorption isotherm. Brunauer, Emmett and Teller (Brunauer *et al.,* 1938) modified and optimized Langmuir's theory by using the hypothesis of multilayer gas adsorption. Thus, a new theory was evolved, which was called BET-isotherm. The pore structure and the total surface area, which includes all the internal structure of a solid sample, can be calculated using BET-method (Bashir, 2011, Adefila, 2003).

2.4.3 Scanning electron microscopy (SEM) analysis

Scanning electron microscope (SEM) is a type of microscope that uses electrons to form an image. SEM allows huge amount of sample to be focused at a time due to its large depth of field (http://www.scanning-electron-microscopy). It produces images of high resolution; thus the combination of higher magnification, larger focus, greater resolution, and ease of observation makes SEM one of the most used instruments in current researches (Bashir, 2011)

2.4.4 Energy dispersive X-ray (EDX) analysis

EDX analysis provides the chemical composition on the selected spots located on the external surface of a solid crystal. Its spectrum displays peaks corresponding to the energy levels and each of these peaks is unique to a single element. The peaks depict how concentrated the element are in the specimen, thus the higher the peak, the more the concentration (http://www.scanning-electron-microscopy).

2.4.5 Atomic absorption spectroscopy (AAS)

Atomic absorption spectroscopy (AAS) is described as one of the analytical techniques that gives reliable result for the metal concentration of a sample (Bashir, 2011). AAS makes use of the amount of light that passes through a cloud of atoms (absorbance). This gives a quantitative determination of the amount of element present as each element has its own unique pattern of wavelength.

2.5 Adsorption Isotherm/Kinetic Studies

Boparai (2010) reported that adsorption isotherm could be described as the amount of sorbate that is distributed between the liquid and solid phases at equilibrium (http://www.researchgate.net/publication/kinetics-and-thermodynamics-of-cadmium-ion-removal). Mohammed *et al.* (2010) stated that when adsorbent and ion solutions are in contact, the concentration of ions on the absorbent will increase until a dynamic equilibrium is reached. Adsorption isotherms are widely applied in the optimum use of adsorbents (Edison *et al.*, 2011). However there are varieties of widely accepted surface adsorption models among which are Freundlich, Langmuir and Temkin models. Thus equilibrium isotherms on this study were analysed from the highlighted models.

2.5.1 Freundlich isotherm

The Freundlich isotherm describes both monolayer and multilayer adsorption and is based on the assumption that adsorption process takes place on heterogeneous surface (Yang, 1998). The linear form of the Freudlich isotherm is as follows:

$$q_e = K_F C_e^{1/n} \tag{2.2}$$

$$logq_e = logK_F + \frac{1}{n} logC_e \tag{2.3}$$

where C_e is the equilibrium concentration of the adsorbate (mg/l); q_e is the amount of the metal adsorbed per unit mass of adsorbent (mg/g); K_F and n are Freundlich

constants with *n* indicating the favourability of the adsorption process. K_F (mg/g). *1/n* is roughly an indicator of the adsorption capacity of the adsorbent.

2.5.2 The Langmuir isotherm

The theoretical Langmuir isotherm is valid for adsorption of a solute from a liquid solution as a monolayer adsorption on a surface containing a finite number of identical sites (Yabba *et al*, 2003). The Langmuir isotherm has an assumption that fixed individual sites exist on the surface of the adsorbent, each of these sites being capable of adsorbing one molecule. Once a particular site is filled, there will be no deposit of ions at that site. The surface will eventually attain saturation where maximum adsorption of the surface will be achieved. At this point, the rate of adsorption is proportional to the driving force which is the difference between amount adsorbed and amount that can be adsorbed at that concentration (Chngombe, 2006). At equilibrium concentration, the driving force is zero (Metcalf, 2003). Thus the Langmuir isotherm model assumes that the surface is homogeneous and the energy of adsorption is equal for all adsorption sites and is expressed as:

$$\frac{1}{q_e} = \frac{1}{QbC_e} + \frac{1}{Q} \qquad (2.4)$$

where C_e is the equilibrium concentration of the adsorbate (mg/l); q_e is the amount of adsorbate per unit mass of adsorbent (mg/g); Q (mg/g) and b (l/mg) are the Langmuir constants related to adsorption capacity and rate of adsorption, respectively. When 1/qe is plotted against $1/C_e$, a straight line is obtained. Q is calculated from the slope, while b is determined from the intercept. Equilibrium data are then fitted with the Langmuir isotherm.

2.5.3 Temkin isotherm

The Temkin isotherm model assumes that the heat of adsorption of all molecules will decrease linearly with the surface coverage due to adsorbent–adsorbate interactions. The model is given by the following expression;

$$q_e = \frac{RT}{b} lnKT + \frac{RT}{b} lnC_e \quad (2.5)$$

Where R is the universal gas constant, b is the constant related to the heat of adsorption (J mol^{-1}) and *KT* is the Temkin equilibrium constant (Lg^{-1}).

2.5.4 Adsorption kinetics

This explains the adsorption kinetics in terms of rate constants (Lawrence *et al.*, 2013). This could be evaluated by applying the three common kinetic models; - pseudo-first-order model, pseudo-second-order model and intra-particle diffusion model.

Pseudo-First-Order Kinetic Model

According to Ho and Mckay (1998), this model describes the adsorption rate based on the solid uptake capacity with the assumption that rate of uptake is directly proportional to the equilibrium concentration. The differential equation is generally expressed as

$$\frac{dq_t}{dt} = K_1(q_e - q_{t)} \quad (2.6)$$

$$\log((q_e - q) = logq_e - \frac{K_1}{2.303} t \quad (2.7)$$

where q_e is the equilibrium concentration of the adsorbate (mg/g); q is the amount of the metal adsorbed per unit mass of adsorbent (mg/g) at time t; K_1 is the rate constant (min^{-1})

Pseudo-second-order kinetic model

The pseudo-second-order kinetic model also known as the Ho model assumes that the rate of adsorption is proportional to the square of the number remaining free surface sites (Aleksandra *et al.*, 2013). This is based on chemisorption involving valence forces through sharing or exchange of electrons between adsorbent and adsorbate. The equation according to Li *et al.* (1999) is:

$$\frac{dq_t}{dt} = K_2(q_e - q_t)^2 \tag{2.8}$$

$$\frac{t}{q} = \frac{1}{K_2 {q_e}^2} + \frac{1}{q_e} t \tag{2.9}$$

where K_2 is the second – order adsorption rate constant (g mg^{-1} min^{-1})

Intra-particle Diffusion Model

Intra-particle diffusion is the rate controlling the mechanism of diffusion. Metals could be transported from the solution phase to the surface of the adsorbent, and if the adsorbent is porous according to Silvio *et al* (2008), diffusion could subsequently proceed into the interior, thus the transport of the adsorbate from the liquid phase to the solid boundary is described by liquid film diffusion model and it also plays significant role in adsorption. The intra-particle diffusion model is given as

$$q = K_i t^{0.5} + \mathrm{C} \tag{2.10}$$

2.6 Environmental and Health Risks of Heavy Metals

Heavy metals could be defined as those metallic chemicals that are poisonous at high concentrations. They are natural components of the earth's crust which cannot be destroyed or degraded (Mudi, 2011). Heavy metals are very dangerous because they tend to bio-accumulate rather than break down or get excreted; they get stored up in the body. These metals that are emitted from industries are released into the stream, lakes, rivers and ground water. Heavy metal contamination is a worldwide problem and due to their toxic effect they are major pollutants in ground, marine, industrial and untreated wastewater (Rasheed, 2001). (http://www.lenntech.com/periodic/elements/htm) gave a detailed theory on most common heavy metals, stressing on the health and environmental impacts as discussed in this work.

2.6.1 Nickel (Ni)

Nickel is silvery-white metal which belongs to the iron group. It is a bivalent naturally occurring element that exist in nature although it assumes other valences; it also forms a number of complex compounds. Most nickel compounds are blue or green and dissolve slowly in dilute acids but, like iron, becomes passive when treated with nitric acid (http://www.lenntech.com/periodic/elements/htm). Nickel is essential to the human in small quantities but in high concentration it can be dangerous to the health. Uptake of nickel in large quantities has the consequence of increasing chances of the development of cancer in body tissues like lung, larynx and prostate in aging humans; could also cause illness, dizziness after long exposure in gaseous form, birth defects, asthma, respiratory failure and chronic bronchitis (http;//www.lenntech.com/periodic/elements/.htm).

2.6.2 Lead (Pb)

Lead is a bluish-white soft metal which tarnishes on exposure to air but very resistant to water and its isotopes are the end products of each of the three series of naturally occurring radioactive elements. Corroded pipes could cause lead contamination in water especially in acidic water. It enhances pH adjustment in water for drinking purposes. Lead has no significant benefit in human system but could cause severe damages to the body organs like kidney and brain disruptive nervous systems. It particularly reduces learning ability of children (http://www.lenntech.com/periodic/elements/ni.htm) etc. Although lead could occur naturally in the environment, most of lead contaminants are mainly from human activities especially from industrial processes.

2.6.3 Cadmium (Cd)

Cadmium is a very malleable metal, with a bluish tinge on the surface. Cadmium is soluble in acids but insoluble in alkali medium. People living near hazardous waste sites, especially near metal refining industries are highly exposed to cadmium poisoning. It takes a long time for accumulated cadmium to be excreted from the body. Other health effects caused by cadmium are damage to the central nervous system, damage to the immune system, psychological disorders and cancer development (http://www.lenntech.com/periodic/elements/htm).

2.6.4 Manganese (Mn)

Manganese is a pinkish-grey, hard and chemically active element. Manganese is very reactive, easily oxidized and hardly melts when found in its pure state. Manganese powder reacts with water, burns in oxygen and also dissolves in dilute acids. Manganese is one of the essential elements in human, commonly found on earth, but can be toxic and dangerous for humans when it accumulates in high quantity in human tissues.

Poisoning effects of manganese are weak muscles, acute headaches, dullness etc. A high incidence of pneumonia and other upper respiratory infections has been found in

workers exposed to dust or fume of manganese compounds (http://www.lenntech.com/periodic/elements/.htm).

2.6.5 Remediation of heavy metals

Based on the established harmful effects of heavy metals like nickel, lead, cadmium, manganese, treatments are designed by researchers to remove/reduce these pollutants to meet the discharge requirements, and/or to achieve reuse/recycle water quality (www.water.siemens.com/application/wastewater/treatment/metal)

Observations made on past reviews show that most of the methods employed emphasized on selective removal of metals by different adsorbents, production of pathogens and sludge. For example Settle *et al.* (1998) studied the potential use of halophytic species to reduce the volume of wastewater and concentration of salt by accumulating salt in high level plant tissues. It was observed that accumulation of such high levels of heavy metals is highly toxic and would certainly kill the common non-accumulator plant. However, the extent of metal removal is ultimately limited by plant ability to extract and tolerate only a finite amount of metals, not exceeding their metabolic needs.

The other biological parameter which limits the potential for metal phytoextraction is biomass production. Metal hyperaccumulator plants which can accumulate exceptionally high amounts of metals (in 1000s ppm) are slow growing and produce little biomass. These characteristics severely limit the use of hyperaccumulator plants for environment clean-up. (Mudi, 2011). Mudi (2011) also worked on the modelling of heavy metal removal from polluted water by phytoextraction. He carried out batch equilibrium metal uptake experiments on the removal of four heavy metal ions (copper, nickel, lead, and zinc) from polluted site by Spinach and Lettuce in the presence of Dissolved Organic Matter (DOM). Results showed that under acidic and neutral pH

conditions, the uptake of all heavy metals by the leaves increased. However, in the alkaline pH region, the uptake decreased, primarily due to the high DOM concentration.

Also Siddhesh *et al*. (2004) examined the extent of arsenic removal as a function of pH. The adsorbent showed a significant removal over a pH range of 2 to 12. Chandra *et al.* (2007) studied a column performance for lead removal from wastewater and recorded an encouraging performance for lead. Sameer *et al.* (2002) investigated the main and interaction effects of some parameters on sorption of copper using spent animal bones. He reported that though the effects of the influent flowrate and metal concentration were marginal but their interaction is significant. Uwakwe *et al.* (2006) studied the application of simple chemistry i.e. the waste can be reduced particularly in natural bodies of water by direct oxidation–reduction processes or simple chemical combinations, acid – base reactions and solubility equilibra. Also Nermen *et al*. (2010) investigated the removal efficiency of heavy metals using the newly synthesized metal oxides. Though commendable results were recorded but there are threats of sludge accumulation. The chemical methods have limitations and are neither practical nor implementable at every site. Furthermore, the chemical methods may be incompatible with other treatment technologies because of native geochemical processes that may have been underway on the site prior to remedial intervention. As a result, insufficient chemical treatments may temporarily cause site conditions to worsen. Another drawback of this method is that the oxidants are not chemically specific for some compounds but instead react non-selectively with a wide range of naturally occurring organic and inorganic compounds. (Oledibe, 2011). Barakat *et al* (2011) carried out a study on new trend in removing these heavy metals from industrial wastewater. The research focused on the removal processes like adsorption, membrane filtration,

electrolysis and photocatalysis. He reported that the key elements in selecting suitable treatment methods are technical acceptability, plant simplicity and cost effectiveness.

Badmus *et al.* (2006) studied the batch removal of some selected metals from brewing industry wastewater using hydrogen peroxide under different experimental conditions. This was achieved by pre-treating hydrogen peroxide with copper, thereby breaking it down to water and oxygen. Although the removal efficiency was found to be effective, field application of this technology would be capital intensive. Nhapi *et al.* (2011) investigated used carbonized rice husk (CRH) and activated rice husk (ARH) for treatment of industrial wastewater at a controlled pH. He observed that both CRH and ARH have high ability to remove all selected heavy metals but the tendency to accumulate sludge is very high which is still detrimental to the environment. Jelena *et al.* (2010) engaged a cascade line reactor with a precipitating agent, for the treatment of synthetic metal bearing effluent with chemical composition similar to the effluent from copper mining and smelting complex. The technology is viable for selective removal of heavy metal from industrial effluents but the huge precipitates generated would definitely cause environmental pollution except where recovery and recycling of the secondary raw materials are necessary. Zaida and Piakong (2011) studied the use of plant for remediation of soil and water contaminated with heavy metals (phytoremediation); the technology was reported to be cost effective and non-invasive but the plants would not accumulate to exceed their metabolic needs and the hyperaccumulator plants are slow growing. Saifuddi and Kumaran (2005) studied a biosorption process by coating chitosan onto oil palm shell charcoal for removal of heavy metal contaminated industrial wastewater. The biosorption process was reported to be effective but regeneration of the adsorbent and recovery of the metals might not be viable. Mohammed and Nwadozie (2011) worked on a batch adsorption experiment

using algae-seaweed in its natural form for the removal of heavy metals from simulated wastewater samples. The preferential order of the metal uptake indicates strong contribution of the ionic radius. Ajay *et al.* (2005) used commercial carbon aerogels without any pre-treatment on synthetic stock solution of some selected heavy metals to determine the efficiency of the metal uptake by the absorbent. The metals removal was found to be dependent on *p*H, contact time, and adsorbent dose.

The properties and health impact of the aforementioned heavy metals which might be of great value for the removal processes are listed in Tables 2.3 and 2.4.

Table 2.3. Properties of Selected Heavy Metals

Metal	Atomic no.	Ionic charge	Ionic radius (nm)	Relative atomic radius
Nickel	28	+2	0.069	405.797
Lead	82	+2	0.132	621.212
Cadmium	48	+2	0.097	494.840
Manganese	25	+2	0.080	312.500

Source: (http://lenntech.com/priodic/element/htm)

Table 2.4. Permissible Limits of some Metals with the Health Impacts

Metals	WHO	*Drinking water Quality standard	**Maximum Permitted Limit	Health Impact
Ni (mg/l)	0.010	0.010	0.020	Carcinogenic
Pb (mg/l)	0.010	0.010	0.010	Carcinogenic
Cd (mg/l)	0.003	0.003	0.003	Toxic to the kidney
Mn (mg/l)	0.040	0.200	0.200	Neurological disorder

* National Environmental Standards and Regulations Enforcement Agency (NESREA, 2010) .
**The Maximum Permitted Limit (SON, 2007)

CHAPTER THREE

MATERIALS AND METHODS

3.1 Materials

The following instruments and equipment were used in the course of the research:

1. Commercial Zeolite 4A from UOP, a subsidiary of Honeywell Companies, New Jersey, USA.
2. Raw clay sample from Kankara, Katsina State
3. Ball mill (Armfield Technical Education company Limited, Ringwood Hampshire, England)
4. Sieve (150 μm)(Voss Maldon Essex)
5. Plastic drums and buckets (100 L and 10 L, polypropylene
6. Deionized water (Druckloser Mischbett, Wasservollent salzer pressureless ion exchanger)
7. Tapwater (Water Board Kaduna)
8. Locally fabricated ceramic crucibles
9. Electric furnace (Voss Maldon Essex, Model No.LH 120/4, Max. Temp. =1400 ^{o}C)
10. Desiccator with silica gel (Voss Maldon Essex)
11. Electrically powered shaker (Stuart Scientific Shaker SFI, manufactured in Great Britain)
12. Domestic blender (Nakai, Japan, Model no. 462)
13. Sample bottles (polyethylene)
14. Filter paper (Whatman, 110 mm, No 2 medium crystalline, SANS CENDRES, Model no. 6548)

15. Electric Stirrer (100 rpm,Voss Maldon Essex)

16. Fume cupboard

17. Electronic weighing machine (PW 184, M: 180 g Accuracy (10^{-4} g)

18. Vacuum pump (Edward High vacuum pump, model No: E500, England)

19. 7.0 Buchner funnel

20. pH meter (Pocket-sized pH meter, HANNA Instruments)

21. Laboratory Oven (Model No:MD6C-64, Michem Instrument)

22. 1 L conical flasks (Pyrex – England)

23. 250 ml beakers (Pyrex – England)

24. Measuring cylinders (1 L and 250 ml, Model no. 01TX)

25. Analytical grade lead nitrate [$Pb(NO_3)_2.4H_2O$], nickel nitrate [$Ni(NO_3)2.6H_2O$], cadmium nitrate [$Cd(NO_3)_2$.4H2O], manganese powder (Mn), Sodium hydroxide pellets (98.6 % NaOH), concentrated hydrochloric acid and nitric acid (BDH Chemicals Ltd Poole – England, May & Baker Dagenham, England). The list of the analytical equipment and their locations are presented in Table 3.1.

Table 3.1 List of analytical equipment used and their domiciliation

S/No.	Name of Equipment	Location
1.	Atomic Absorption Spectrometer (AAS) (AA240FS, Fast sequential absorption spectrometer (VARIAN)	Applied Science Department, Kaduna Polytechnic, Defence Industry Corporation of Nigeria (DICON), and Multi user laboratory at Chemistry Department, Ahmadu Bello University Zaria (ABU)
2.	X-ray Fluorescence Machine (XRF – PANalytical)	Defence Industry Corporation of Nigeria (DICON) and Multi-User Laboratory Chemistry Department, Ahmadu Bello University (ABU) Zaria
3.	X-ray Diffractometer (XRD – PANalytical, Philips X" Pert)	National Geoscience Research laboratory (NAGRL) Kaduna and University of Johannesburg, South Africa.
4.	Scanning Electron Microscope (JEOL JSM–5600)	Energy Dispersive Spectrometer (SEM–EDS), University of Johannesburg, South Africa
5.	Braunner-Emmett-Teller Surface Area Measurement (BET) (Barret – Joyner – Halends model)	University of Johannesburg, South Africa.

3.2 Methods

This section gives a fairly detailed description (of the process) of sampling of petroleum wastewater; procuring and processing of commercial Zeolites 4A and Kankara kaolin, modification of kaolin to sodium base metakaolin, preparation of matrices of Zeolite 4A and metakaolin. This is subsequently followed by the adsorption and ion exchange experiment, as summarized in Figure 3.1.

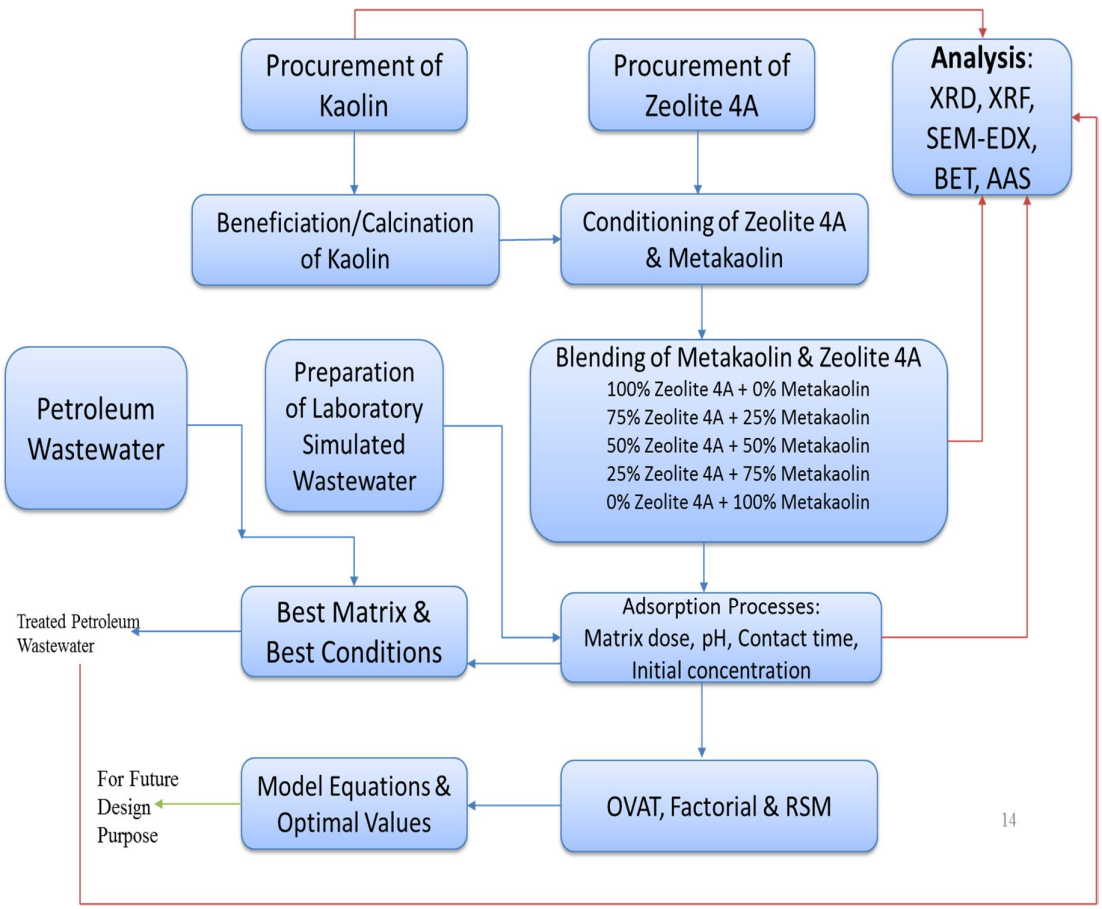


Figure 3.1. Flow Diagram of the Research Methodology

3.2.1 Zeolite and kaolin

i. Processing of zeolite and kaolin

The commercial Zeolite 4A was purchased from UOP, a subsidiary of Honeywell group of companies New Jersey, U.S.A while the kaolin was procured from Kankara Village in Katsina State. Plate I a & b clearly depict both materials.

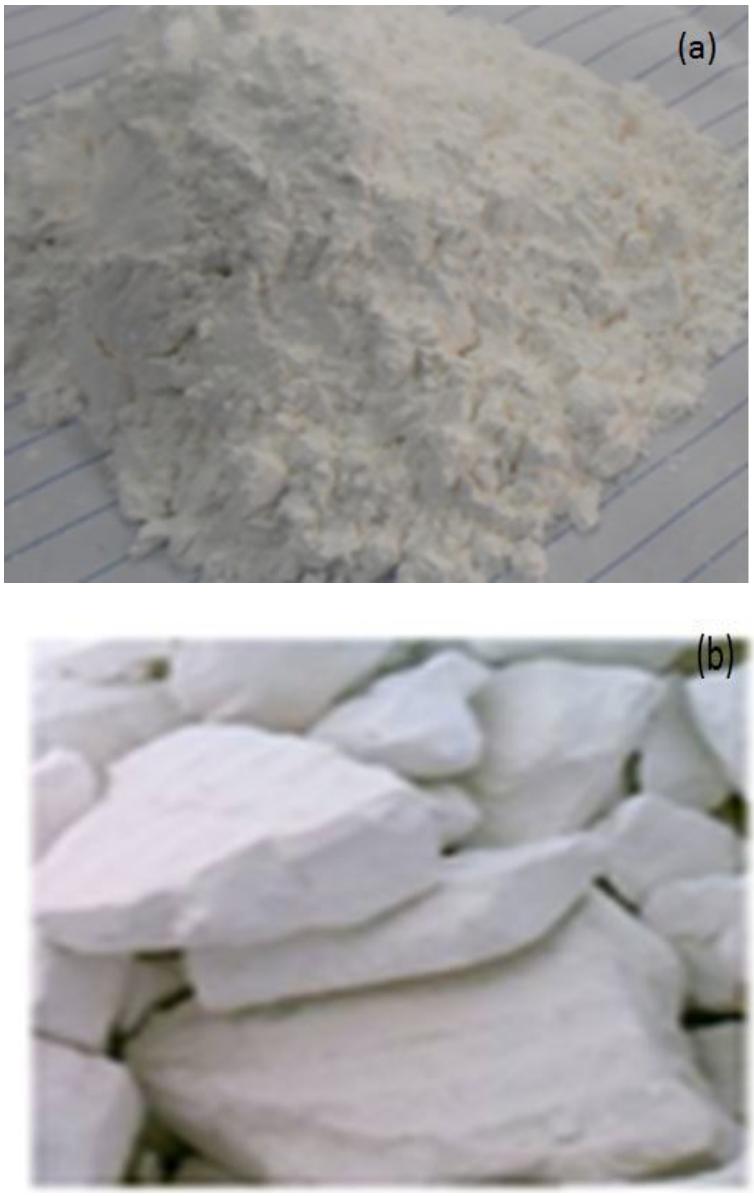


Plate I Picture of (a) Zeolite 4A and (b) Raw Kaolin

ii. Beneficiation of kaolin

About 2 kg of white kaolinite clay was procured from Kankara Village in Katsina State of Nigeria. This was mixed with 10 L of tap water to form slurry and was allowed to age for four days. Sedimentation, decantation of the overflow and replenishing of fresh water at one day intervals was done until the last day, when the overflow had become clear and free from suspended particles. The resulting thick slurry was sieved with muslin cloth and carefully spread out to dry at atmospheric conditions. The beneficiated kaolin was gathered and stored. The lumped kaolin clay (cake) was milled with a ball mill and passed through a 150 μm mesh sieve.

iii. Calcination of Kaolin

The dried kaolin powder was placed in locally fabricated crucibles and charged into a calibrated, heated furnace at 750 ^{o}C for 3 hours where decomposition occurred leading to the destruction of the original structure and removal of the undesirable volatile matter (Ajayi 2012, Ahmed and Onaji (1998) and Aderemi 2004). By this process, kaolin was converted to metakaolin.

iv. Conditioning of metakaolin to sodium base

The conditioning was done with about 8 M NaOH solution which was prepared by dissolving 400 g of sodium hydroxide pellets in 1250 ml of deionized water. 300 g of metakaolin was added to 1.5 L of the 8 M NaOH and mixed thoroughly to form slurry. The mixture was then heated up to 90 ^{o}C with continuous vigorous stirring for 4 hours. The slurry was thereafter allowed to cool for several hours, washed several times, allowed to settle for several hours, and then dried in an oven at 110 ^{o}C, to a moisture content of about 5 %. The sodium based metakaolin was packed and stored in a nylon bag

v. Particle size analysis and blending

Particle size analysis for both the commercial Zeolite 4A and sodium based metakaolin was carried out by ball milling and sieving with a sieve of 150 μm aperture to ensure even particle size distribution.

The specified weight ratios given in Table 3.2 were measured, mixed and properly blended with a domestic blender (Nakai, Japan, Model no. 462) Matrix Nos 2, 3 and 4 to ensure homogeneity of the resulting Zeolite 4A – metakaolin matrix.

Table 3.2. Formulated Matrices of Zeolite 4A and Metakaolin

Description	**Matrix\Identity**
100 % Zeolite 4A + 0 % metakaolin	Matrix 1
75 % Zeolite 4A + 25 % metakaolin	Matrix 2
50 % Zeolite 4A + 50 % metakaolin	Matrix 3
25 % Zeolite 4A + 75 % metakaolin	Matrix 4
0 % Zeolite 4A + 100 % metakaolin	Matrix 5

3.2.2 Wastewater collection and preparation

i. Preparation of standard solution of heavy metals

The procedure from Delloyd's laboratory technological resource (2000) was adopted. This provides a method of preparing 1000 ppm atomic absorption standard of a metal from its pure element or from its salt, using deionized water.

Nickel

To prepare a 5 ppm of nickel metal from nickel nitrate, according to the aforementioned procedure, 4.9530 g of nickel nitrate [$Ni(NO_3)_2.6H_2O$] was dissolved in 1 L of deionized water in a volumetric flask stock solution so

prepared was then diluted to give 5 ppm nickel solution according to Equation 3.1.

$$C_1V_1 = C_2V_2 \quad (3.1)$$

where C_1 and C_2 are the initial and final concentration and, $V_1 and\ V_2$ are initial and final volumes respectively. Similar method was used for lead, nickel and cadmium.

Lead

An accurate measurement of 1.5980 g of lead nitrate [$Pb(NO_3)_2.4H_2O$] was dissolved in 100 ml of deionized water and diluted to 1 L in a volumetric flask and further diluted to give 5 ppm solution.

Cadmium

Exact measurement of 2.1032 g of cadmium [$Cd\ (NO_3)_2.4H_2O$] was dissolved in 250 ml deionized water and vigorously stirred then diluted to 1 L in a volumetric flask and further diluted to obtain 5 ppm solution.

Manganese

Precise measurement of 1.000 g of manganese powder was dissolved in 50 ml of concentrated hydrochloric acid. The solution was diluted to 1 L in a volumetric flask with deionized water and was further diluted to obtain 5 ppm solution.

ii. Crude oil tank farm wastewater collection and preservation

The wastewater sample was collected from the dewatering tanks in the Oil Movement farm of Kaduna Refining and Petrochemical Company (KRPC) Kaduna, Nigeria. A composite sampling method was used whereby wastewater samples from various dewatering tanks in the farm were collected and then mixed together. The crude oil being processed at the facility is the Escravos crude (Quarterly Petroleum Information, 2012). Sample preservation was carried

out using nitric acid solution to keep the wastewater sample in acidic medium. (pH < 2) to avoid condition deterioration.

Treatment of the sample bottles

Plastic bottles were used for water collection for the determination of metals. The sample bottles were washed with non-ionic detergent, rinsed with tap water and later soaked in 10 % nitric acid for 24 hours and finally rinsed with deionised water prior to usage.

Digestion Procedures

The crude oil tank farm wastewater sample was digested using the following method:

100 ml of the sample was transferred into a beaker and 5 ml concentrated HNO_3 added. The beaker was covered with a wet glass and then placed on a hot plate and evaporated down to about 20 ml. The beaker was thereafter allowed to cool and additional 5 ml concentrated nitric was added, covered with a watch glass and returned to the hot plate. The heating continued until the solution appeared light coloured and clear. The beaker was rinsed with distilled water and the sample filtered to remove all insoluble materials that could clog the atomizer. The volume was then adjusted to 100 ml with distilled water.

3.2.3 Removal of heavy metals from simulated wastewater

3.2.3.1 Assessment of heavy metals removal from simulated wastewater by adsorbents.

The optimal conditions were determined by using five different matrices for the removal of nickel, lead, cadmium and manganese from simulated wastewater. The simulated wastewater was prepared with the standard solutions in accordance to the procedure presented in Section 3.2.2. Samples of the simulated wastewater were prepared by mixing the four metal solutions ultimately

together, then two metal solutions at a time. And finally, each metal solution was treated selectively. The rate of removal of individual metals from the wastewater samples was determined using different contact time, adsorbent matrices dose and *p*H.

The adsorption of the four heavy metal ions were carried out in 50 ml stoppered conical flask by taking appropriate amounts of the simulated wastewater sample and adsorbent (Zeolites 4A/metakaolin). The pH values of the solutions were adjusted from 2 to 12 with 0.5 M NaOH and 0.5 M HCl, and measured with a pH meter.

3.2.3.2 Determination of effect of adsorbent dose on adsorption capacity

Precise measurements of 0.10, 0.25, 0.50, 1.00, 1.50, 2.00 and 2.50 g of Zeolite 4A-metakaolin matrices were dispensed separately into each of seven 250 ml Pyrex flasks and the eighth flask was adsorbent free. Then, 50 ml of the simulated wastewater samples were added to the contents of the eight flasks in turn and stoppered. This was followed by agitation at constant speed, for a contact time of 60 minutes and pH of 8 against literature range of 30 to 60 minutes and pH of 7 to 8. The mixtures in each flask was filtered by suction pump through a sintered glass crucible and the different filtrates were collected and analysed using the atomic absorption spectrophotometer (AAS). The spent adsorbents were collected, dried at atmospheric condition and analysed using XRF, XRD, BET, and SEM-EDX.

3.2.3.3 Determination of effect of contact time on adsorption capacity

Samples of 50 ml simulated wastewater were added to eight different 1.0 g of the matrices (best matrix dose from Section 3.2.3 (ii)) in 250 ml Pyrex flasks. The contents were then agitated at a constant speed and pH of 8 from literature

for different contact times of 0, 1, 2.5, 5, 10, 20, 40 and 60 minutes. The different filtrates were collected and analysed using atomic absorption spectrophotometer (AAS). The spent adsorbents were also collected, dried at atmospheric condition and analysed with XRF, XRD, BET and SEM-EDX.

3.2.3.4 Determination of effect of pH on adsorption capacity

Samples of 50 ml of simulated wastewater containing 5 ppm heavy metals were maintained at different pH of 2, 4, 6, 8, 10, and 12. To each sample was added dose of 1.0 g adsorbent matrices in 250 ml Pyrex flasks and stoppered. The content of each flask was subjected to agitation at constant speed of 100 rpm for 10 minutes. Thereafter, the filtrates were individually collected and analysed using atomic absorption spectrophotometer (AAS). Standard solutions of the metals were used for calibration. The spent adsorbents were also collected, individually dried at atmospheric condition and analyzed using XRF, XRD, BET, and SEM-EDX.

3.2.3.5 Determination of effect of initial concentration on adsorption capacity

About 50 ml simulated wastewater (50 ml) of concentrations 5, 25, 50, 75 and 100 ppm were separately added to 1.0 g of the Zeolite 4A in 250 ml Pyrex flasks and stoppered. The contents were then subjected to constant agitation for 10 minutes and at a pH of 8. The different filtrates were thereafter collected and analysed using atomic absorption spectrophotometer (AAS). The spent adsorbents were also collected, dried at atmospheric condition and analysed using XRF, XRD, BET, SEM and EDX.

3.2.4 Adsorption of heavy metals from crude oil tank farm wastewater

The crude oil tank farm wastewater sample collected from KRPC (see Section 3.2.2 (ii)) was treated with Matrix 4 investigated in Section 3.2.3 at the best identified conditions of 10 minutes, 1.0 g Matrix 4 in 50 ml crude oil tank farm wastewater, at pH of 8. The filtrate obtained was analysed using AAS and compared with standard. Further analysis was carried out by varying matrix doses, contact times and pH and the trend compared to that of the simulated wastewater.

3.2.5 Analysis of samples

Various analytical techniques were used to assess the properties and structure of the raw and modified materials used in this research. This section gives the experimental procedures for AAS, XRF, XRD, SEM–EDS and BET.

i. Atomic absorption spectrometer (AAS) Analysis

The digested sample solutions were diluted to a proper level according to the calibration curves prepared from series of similar reference solutions. The concentrations of nickel, lead, cadmium and manganese were measured by Fast sequential absorption spectrometer (VARIAN, AA240FS) presented in Plate II. The results obtained were reported in the form of weight percentage (ppm).

ii. X – Ray Flurescence (XRF)

The XRF–PANalytical spectrometer was used for this analysis. The samples of Zeolites 4A and beneficiated kaolin were air dried properly, homogenized and placed on the sample holder of the machine for scanning and documentation of the results by the attached computer, as indicated in Plate III.



Plate II Atomic Absorption Spectrometer [AA240FS (Fast sequential absorption spectrometer (VARIAN)]



Plate III XRF Machine

iii. X–Ray Diffraction (XRD) analysis

The XRD equipment used, presented in Plate IV is the Philips X" Pert X-ray Diffractometer with a copper X-ray tube (Cu Kα 1 and Cu Kα 2) as radiation sources; the (Kα) is the desired radiation that will pass through to the specimen. The instrument settings for each test at room temperature were: Tension = 40 kV, Current = 30 mA, Scan speed =1.0000 deg. /min, Number of steps = 4368, Total run time (h:m:s) = 00:30:45, and 2θ interval between 2° to 50° (with a standard error of the peak position, 2θ). This was used to determine the crystallinity and electronic distribution of atom of the kaolin, sodium base metakaolin and Zeolites 4A – metakaolin matrices. Each crystalline solid was identified by its unique characteristics x–ray pattern, typically utilized as finger print for the purpose of identification and classification (Bashir, 2011).

iv. Scanning Electron Microscopy (SEM)

A JEOL JSM–5600 SEM with Si (Li) EDU detector (with vantage software from Noran Instruments Inc.) was used in this study. The SEM was coupled to EDX (energy dispersive X–ray) at 30 keV, a type of semi–quantitative analysis which uses standardless EDX reference spectra, supplied by the manufacturer with +/- 5 % confidence interval (Frank, 2009). The SEM gives the images of the sample and thus the crystal shape and size were identified from the micrograph (Janjira, 2002).



Plate IV Phillip X-Pert X-ray Diffractometer (Frank, 2009)

v. BET-experimental operating conditions

The Barret-Joyner-Halends BET machine model was used to determine the surface characteristics of the samples of Zeolites 4A–metakaolin matrices before and after treatment (Palesa *et. al.,* (2011). The sample in the form of powder was loaded in a bulb ended quartz tube and heated in the furnace to about 350 ^{o}C for outgassing for about 480 minutes (8 hours) to remove moisture and contaminants (Bashir, 2011). The corrected weights were then taken for BET analysis.

vi. Determination of the exchange capacity of Zeolites 4A and metakaolin matrices.

Cation exchange capability for all the Matrices: 1 g of the air dried Matrix 1 (100 % zeolites 4A / 0 % metakaolin) sample was placed into a 250 ml beaker. Thereafter 100 ml of potassium chloride solution of concentrations 600, 1000, 1400 and 2000 ppm were added to the samples. The mixtures were vigorously shaken at 100 rpm by an electrically powered shaker (Stuart scientific shaker SFI) for 8 hours. At the end of the stipulated contact time, the slurries were individually filtered and the filtrates sent for AAS analysis.

3.2.6 Experimental analysis using computer software

i. Analysis of data using Factorial Minitab 14.0 software

An experimental design was generated for factorial analysis using Minitab 14.0 software. The 3 factors under consideration were Matrix 4 dose (X_1), contact time (X_2) and pH (X_3), at 2 levels resulting to 8 runs and 2 replicates which led to 16 runs as depicted in Figure 3.2. This is preferable for minimizing errors and sample size calculations. A batch adsorption experiment was carried out at the specified conditions indicated in Minitab 14.0 design of experiment presented in Table 3.3 by weighing the specified quantities of Matrix 4 adsorbent dose in 50

ml of simulated wastewater sample at the specified pH and letting it to equilibrate at the specified contact time. The slurry was filtered and the solution digested and analyzed for metal ion content. The cation content in the filtrate was determined by AAS. A total of 16 runs as generated by Minitab 14.0 were carried out as presented in Table 3.3.

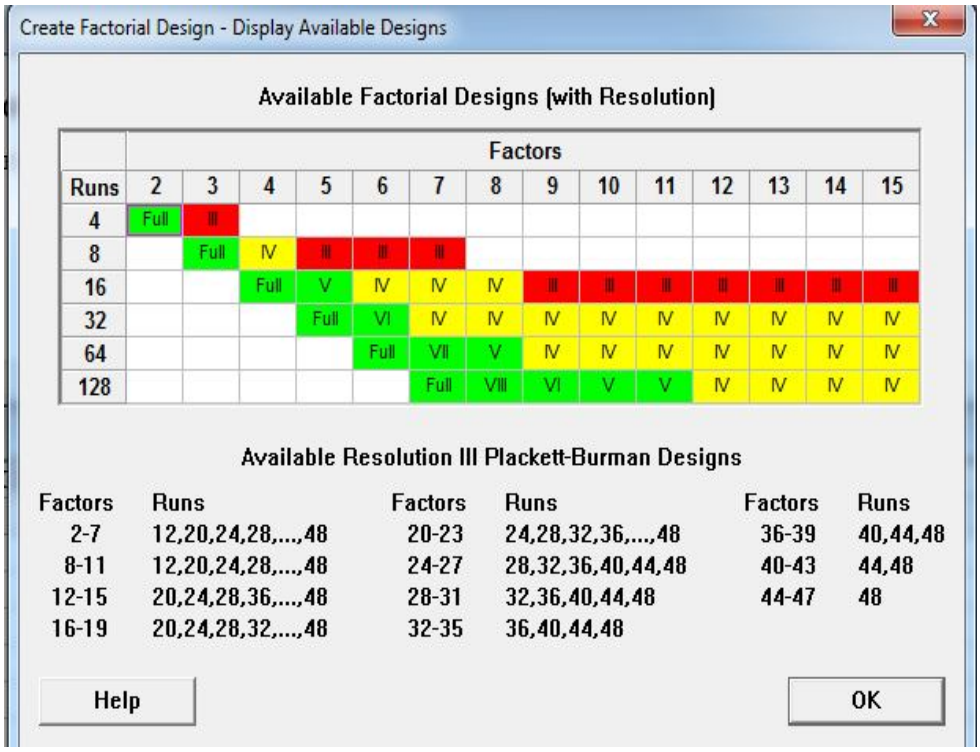


Figure 3.2. Minitab 14.0 Design of Experiment (DOE) Display

Table 3.3: Design of Experiment for Factorial Analysis for Parameters Matrix 4 dose (X_1), Contact time (X_2), pH (X_3)

Run/Order	Centre Pt	Blocks	X_1	X_2	X_3
1	1	1	1.5	20	12
2	1	1	0.5	5	4
3	1	1	1.5	20	4
4	1	1	0.5	20	12
5	1	1	0.5	20	4
6	1	1	1.5	5	4
7	1	1	0.5	20	12
8	1	1	1.5	20	4
9	1	1	1.5	20	12
10	1	1	0.5	5	12
11	1	1	0.5	20	4
12	1	1	1.5	5	12
13	1	1	0.5	5	12
14	1	1	1.5	5	12
15	1	1	1.5	5	4
16	1	1	0.5	5	4

Notation:

Centre Pt = Centre point

X_1=Matrix 4 dose, g/50 ml

X_2=Contact time, min

X_3=*p*H

ii. Analysis of data using Response Surface Methodology (RSM)

The RSM was applied using Design-Expert 6.0.8 Program design in Figure 3.3. Box-Behnken response surface was adopted because it required fewer treatment combinations than central composite design in cases involving 3 or 4 factors. The Box-Behnken design is rotatable and this property prevents a potential loss of data and it requires 3 levels for each factor by producing a centre point (Montgomery, 2005).

This involves designing of experiment to provide adequate and reliable measurement of the response, development of mathematical models having best

fit to the data obtained from the experimental design and determining the optimal values of the independent variables that gives maximum response. (Liu *et al.,* 2011, Gokhale *et al.,* 2009).

Here, the parameters affecting the removal of nickel, lead, cadmium and manganese from simulated wastewater sample were studied. The three independent variables considered were coded as follows: Matrix 4 dose (X_1) contact time (X_2), and pH (X_3). A total of 17 experimental runs were carried out according to the experimental design matrix shown in Table 3.4. This was carried out in the laboratory as described in Section 3.2.6 (ii) using the specified conditions in Table 3.4. Analysis of the data generated was done using coefficient of determination (R^2). Other fit statistics, Mathematical models and response plots were obtained for the systems.

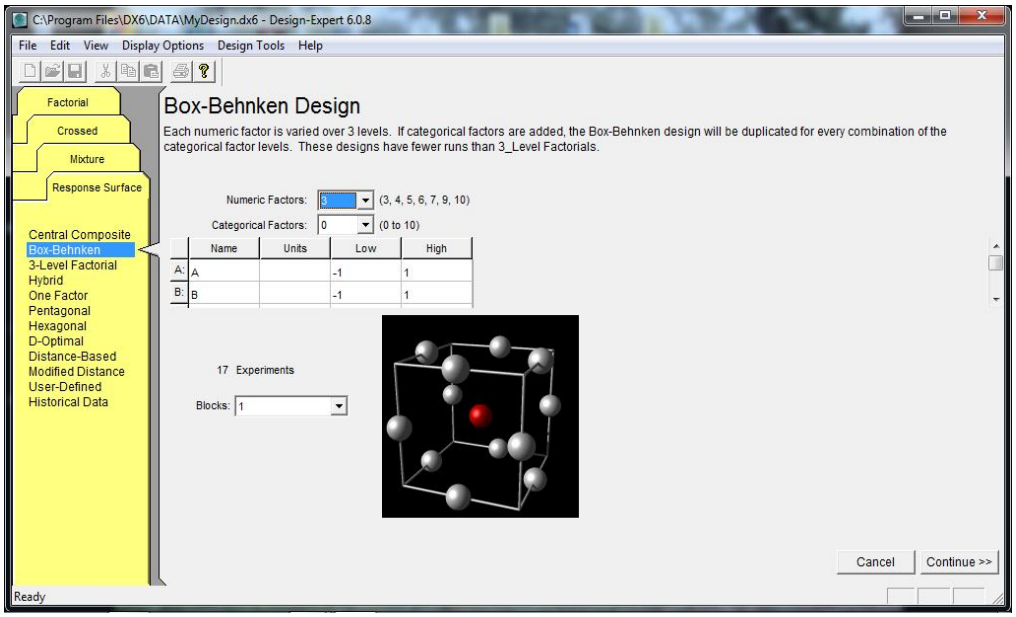


Figure 3.3 Design Expert 6.0.8 program design

Table 3.4 RSM design of experiment (Box–Behnken design)

Run	Block	Matrix 4 dose (g/50 ml)	Contact time (min)	pH
1	1	0.5	5	8
2	1	0.5	5	8
3	1	1	20	12
4	1	1	5	12
5	1	1.5	12.5	4
6	1	1	12.5	8
7	1	1.5	20	8
8	1	0.5	20	8
9	1	1	5	4
10	1	1	20	4
11	1	1	12.5	8
12	1	1	12.5	8
13	1	1	12.5	8
14	1	0.5	12.5	12
15	1	0.5	12.5	4
16	1	1	12.5	8
17	1	1.5	12.5	12

CHAPTER FOUR

RESULTS

4.1 Determination of Level of Heavy Metals in Crude Oil Tank Farm Wastewater

Table 4.1 Heavy Metals Content of Wastewater Collected from the Crude oil Tank Farm (Before treatment) and from Wastewater Treatment Unit (After Refinery Treatment) (KRPC, Kaduna)

Metals	Wastewater from crude oil tank farm (before treatment)	Wastewater from wastewater treatment unit (after treatment)	*Drinking water quality standard
Ni (mg/l)	0.040	0.044	0.010
Pb (mg/l)	0.225	0.220	0.010
Cd(mg/l)	0.022	0.022	0.003
Mn (mg/l)	1.858	1.823	0.200

*National Environmental Standards and Regulations Enforcement Agency (NESREA, 2010)

4.2 Characteristics of the Adsorbents

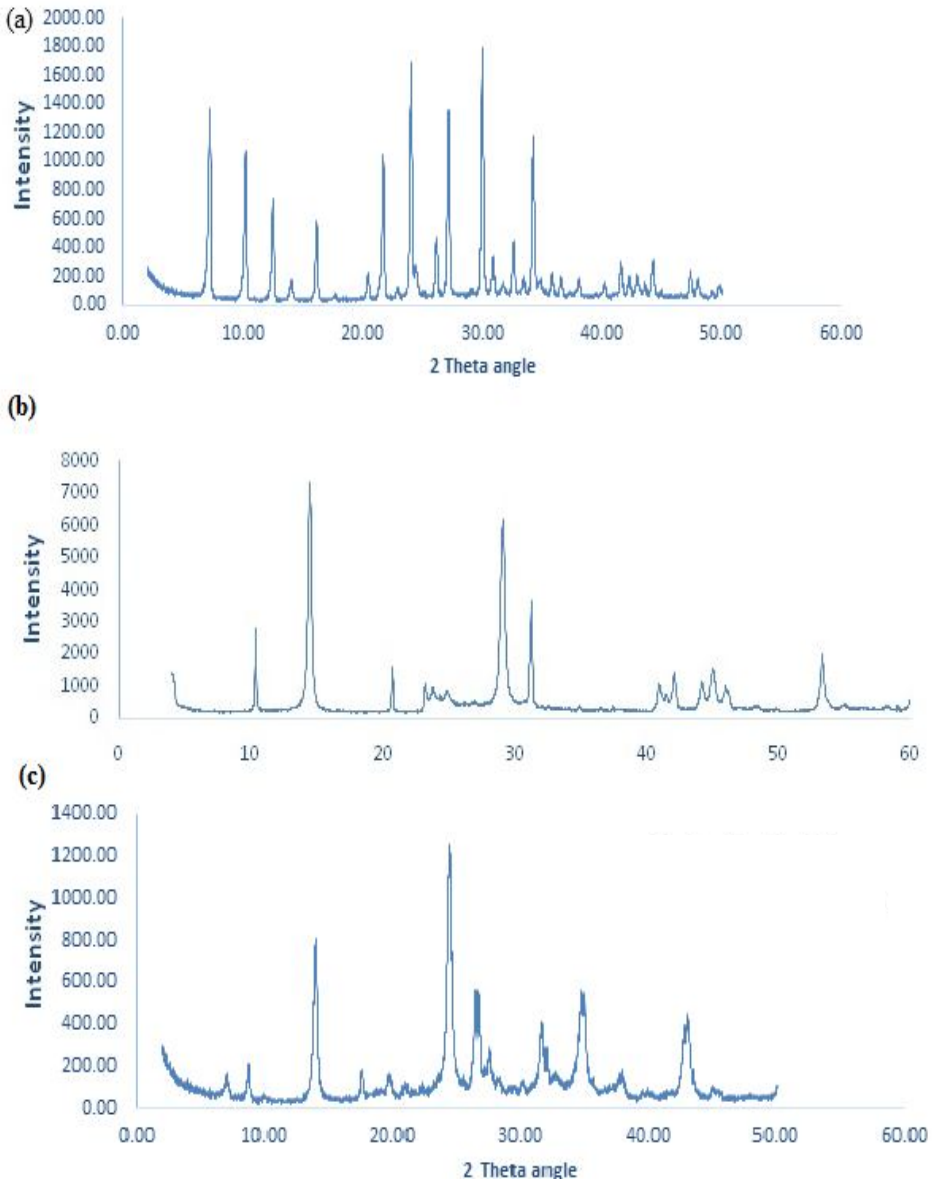
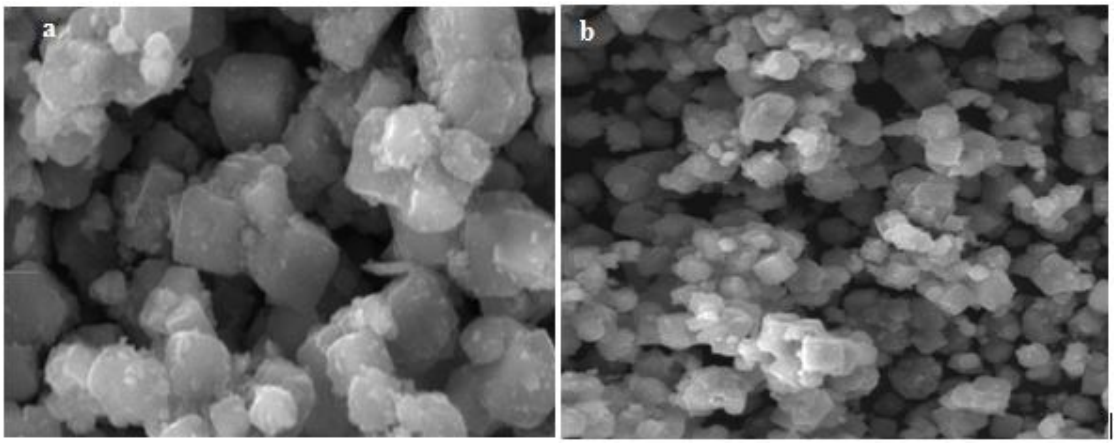


Figure 4.1. XRD pattern for (a) Zeolite 4A (b) Kaolin (c) Metakaolin

Table 4.2: XRF Result of Chemical Composition of Zeolite 4A, Beneficiated Kankara Kaolin and Metakaolin

Composition (wt %)	Zeolites 4A	Beneficiated kaolin	Metakaolin
SiO_2	52.600	51.900	53.67
Al_2O_3	34.000	35.800	38.53
K_2O	2.320	4.01	3.89
CaO	0.439	0.625	0.634
TiO_2	0.120	0.059	0.0488
MnO	0.010	0.123	0.221
Fe_2O_3	0.180	1.789	1.815
CuO	0.049	0.016	0.019
NiO	*nd	0.016	0.021
ZnO	*nd	0.064	0.059
LOI	10.177	6.089	1.010
Total	99.895	100	100

*nd= not detected
LOI = Loss on ignition



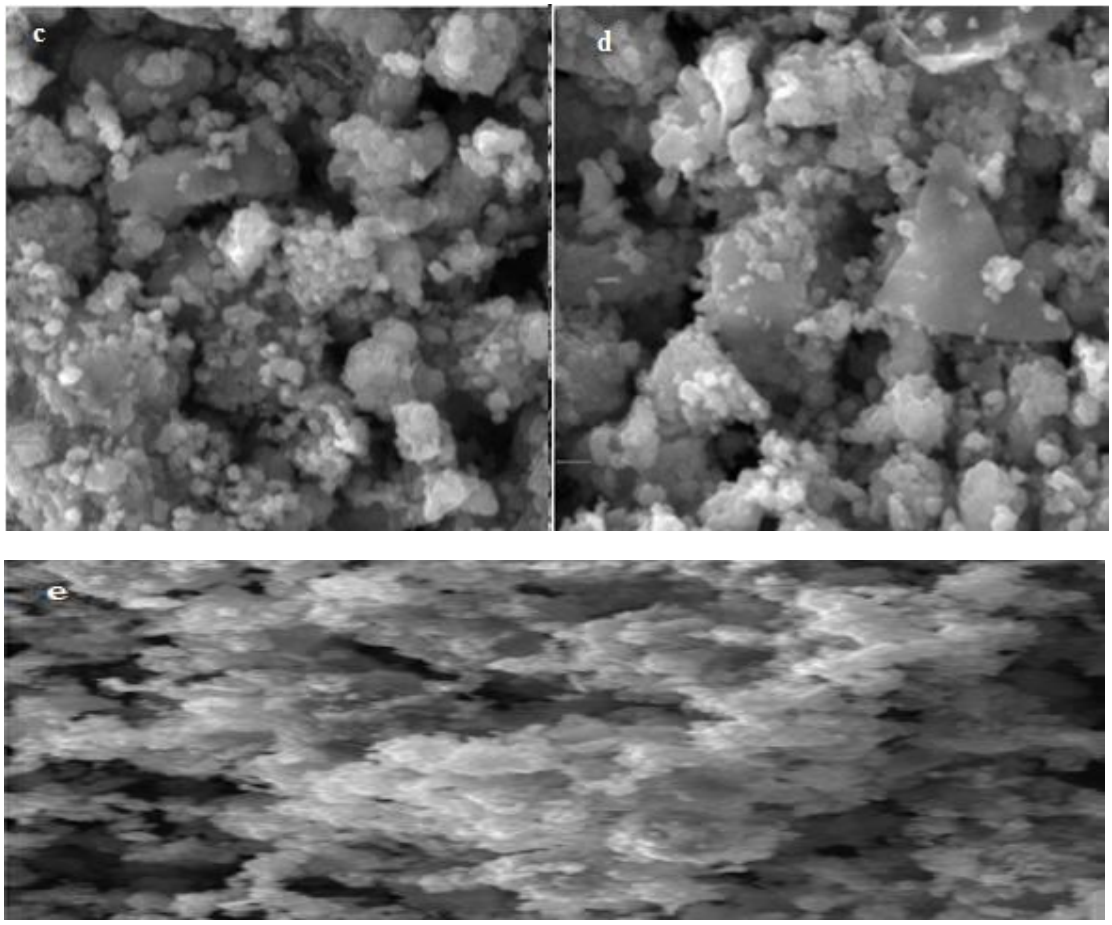


Figure 4.2. SEM images of (a) Matrix 1; (b) Matrix 2; (c) Matrix 3; (d) Matrix 4; (e) Matrix 5

4.2.1 Ion exchange capability of the matrices

Table 4.3 Ion Exchange Capacity for Matrix 1, 2, 3, 4 and 5

Conc. of Solution (ppm)	Ion Exchange Capacities (EC) of the Matrices				
	Matrix 1	Matrix 2	Matrix 3	Matrix 4	Matrix 5
600	28716.7	25005.7	17703.9	18915.7	12765.5
1000	33126.1	34238.6	24200.2	27547.4	16634.7
1400	43087.9	30308.5	29105.7	31097.8	17949.4
2000	60186.2	59127.4	56686.6	56189.6	44442.6

4.3 Heavy Metal Removal from Simulated Wastewater by the Matrices

4.3.1 Effect of pH on heavy metal removal

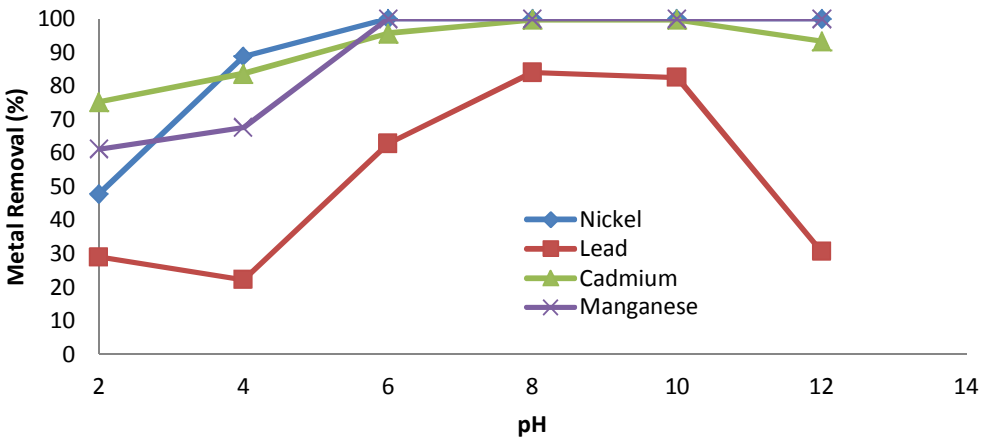


Figure 4.3. Effect of pH on Heavy Metal Removal by Zeolite 4A (Matrix 1)

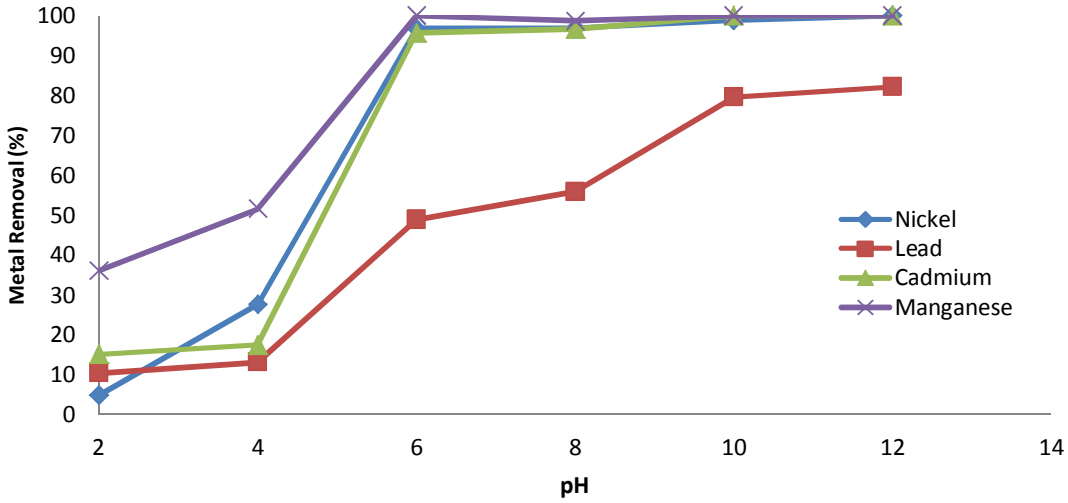


Figure 4.4. Effect of pH on Heavy Metal Removal for Metakaolin (Matrix 5)

4.3.2 Effect of matrix dose on heavy metal removal

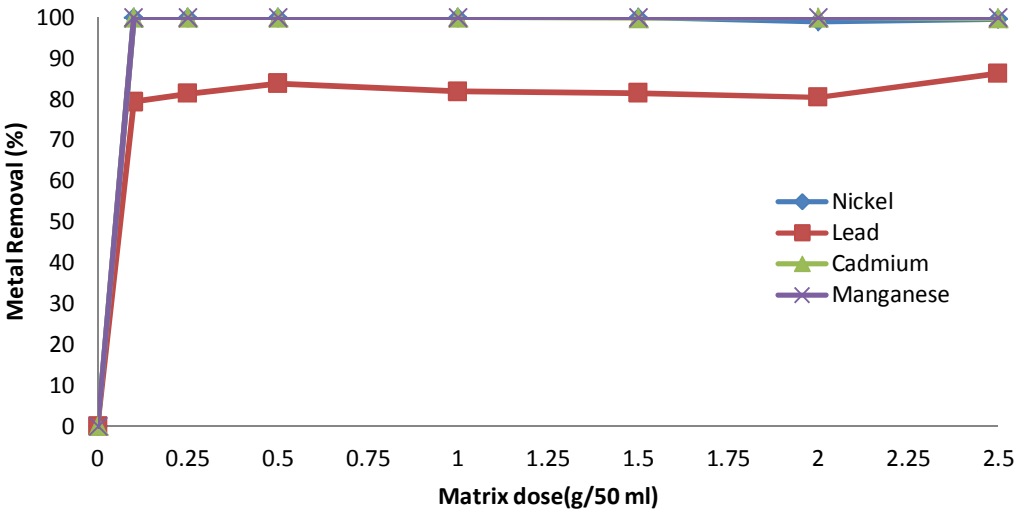


Figure 4.5. Effect of Matrix 1 (100 % Zeolite 4A / 0 % metakaolin) dose on heavy metal removal

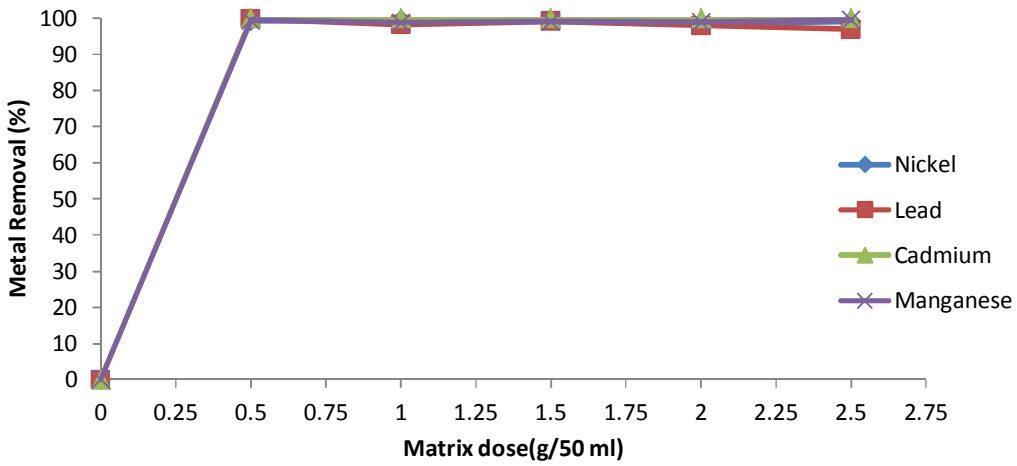


Figure 4.6. Effects of Matrix 2 (75 % Zeolite 4A / 25 % metakaolin) dose on Heavy Metal Removal

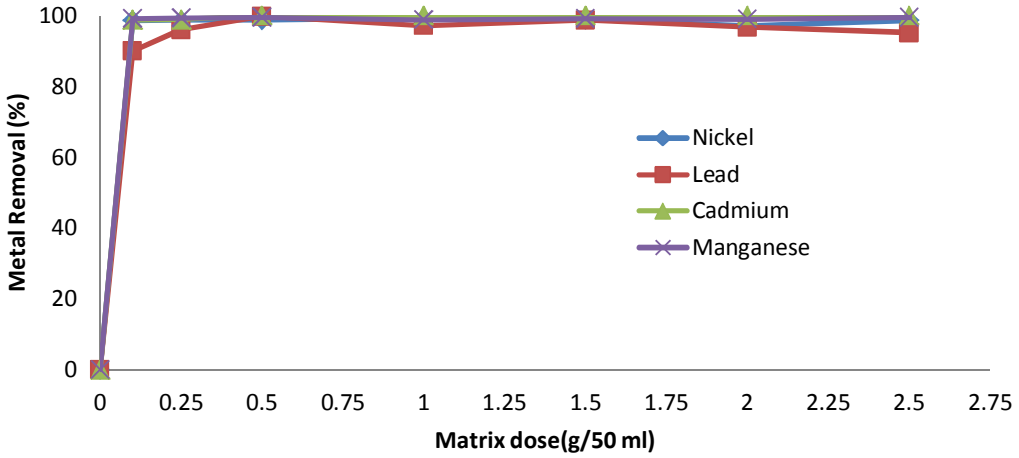


Figure 4.7. Effects of Matrix 3 (50 % Zeolite 4A / 50 % metakaolin) dose on Heavy Metal Removal

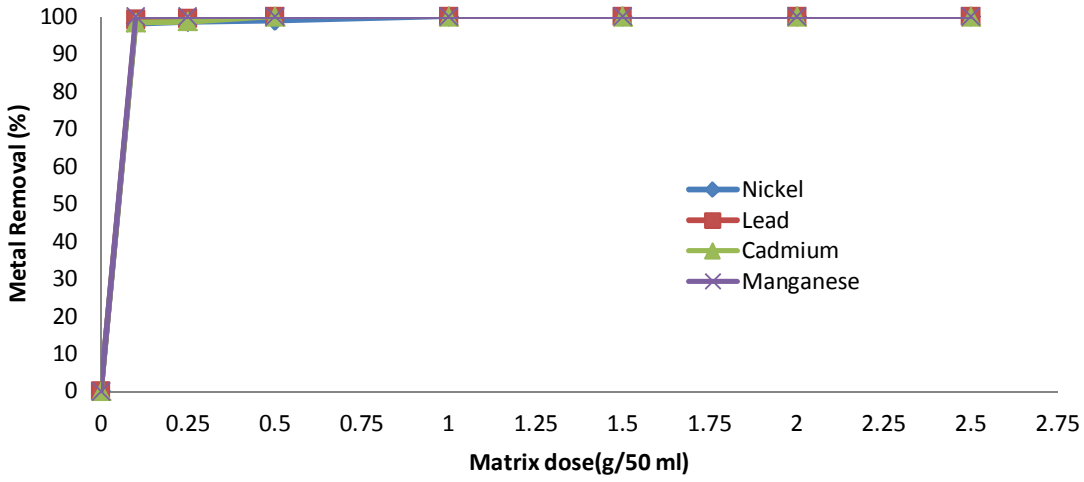


Figure 4.8. Effects of Matrix 4 (25 % Zeolite 4A / 75 % Metakaolin) dose on Heavy Metal Removal

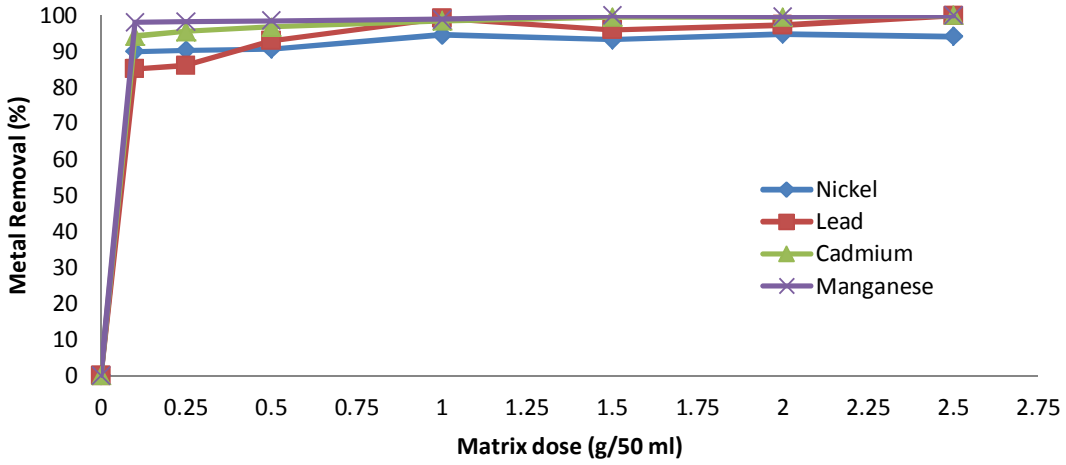


Figure 4.9. Effect of Matrix 5 (0 % Zeolite 4A / 100 % Metakaolin) dose on Heavy Metal Removal

4.3.3 Effect of contact time on heavy metal removal

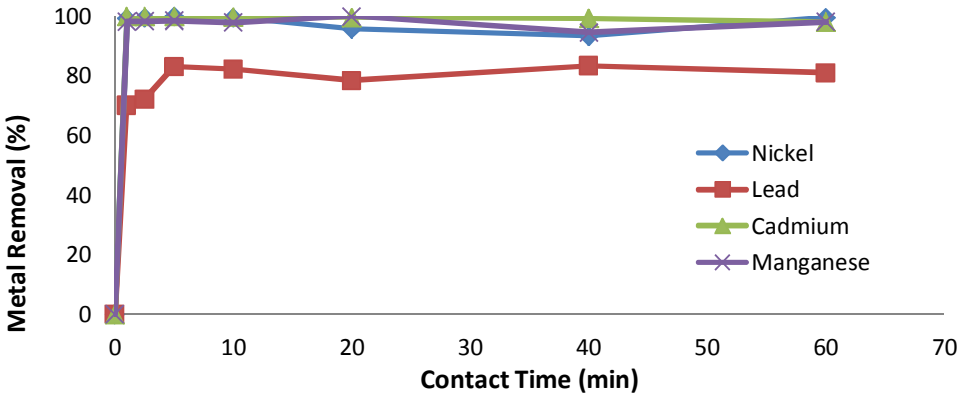


Figure 4.10. Effect of Contact time on Heavy Metal Removal by Matrix 1(100 % Zeolite 4A / 0 % Metakaolin)

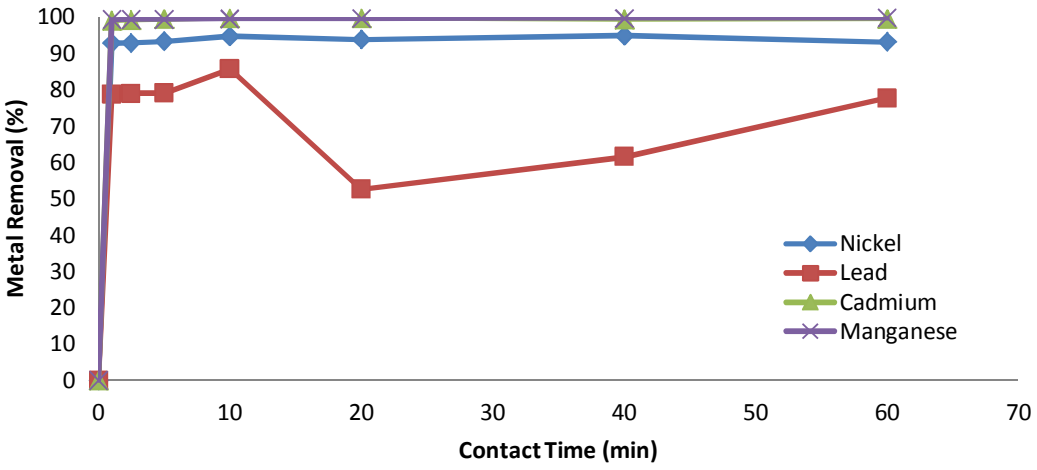


Figure 4.11. Effects of Contact time on Heavy Metal Removal by Matrix 2 (75 % Zeolite 4A / 25 % Metakaolin)

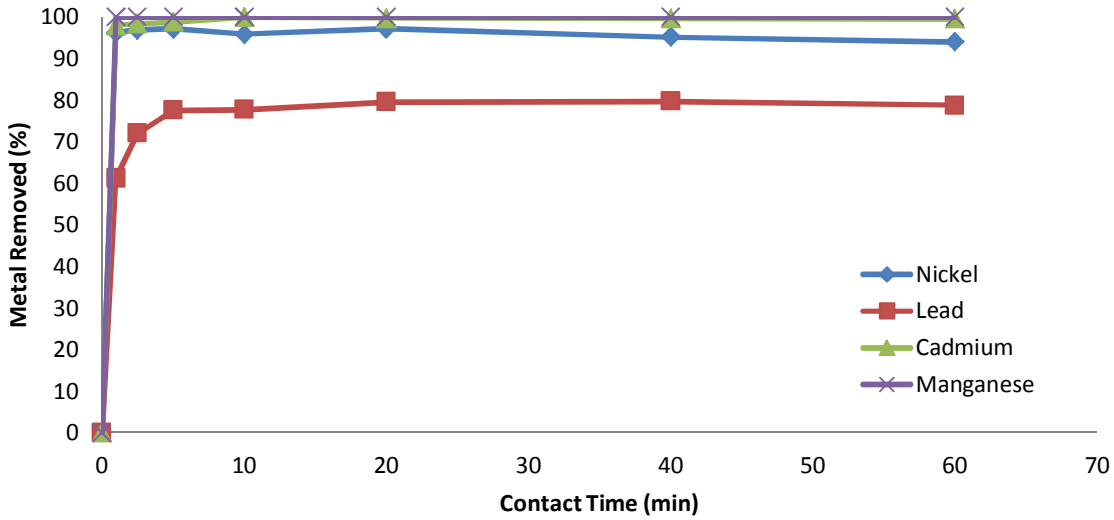


Figure 4.12. Effect of Contact time on Heavy Metal Removal by Matrix 3 (50 % Zeolite 4A / 50 % metakaolin)

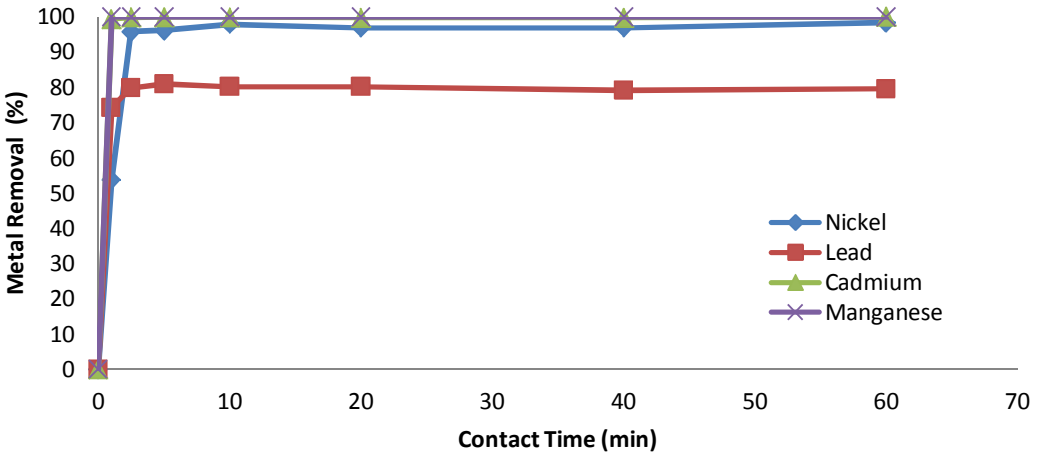


Figure 4.13. Effect of Contact time on Heavy Metal Removal by Matrix 4 (25 % Zeolite 4A / 75 % metakaolin)

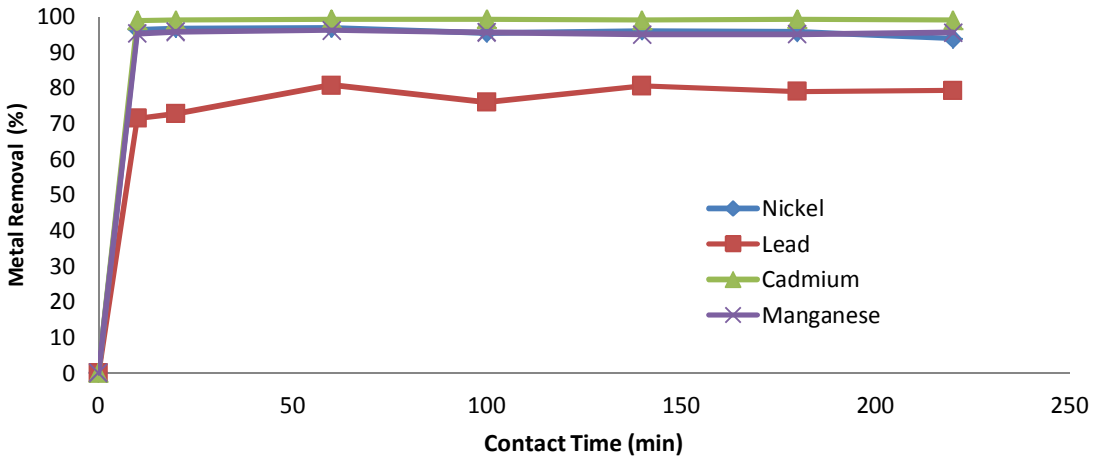


Figure 4.14. Effect of Contact Time on Metal Removal by Matrix 5 (0 % Zeolite 4A / 100 % Metakaolin)

4.3.4 Effect of initial concentration of heavy metals on adsorption

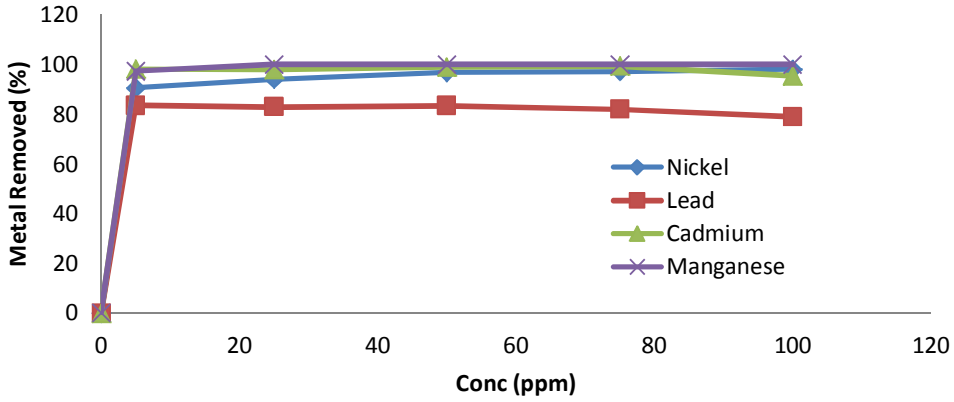


Figure 4.15. Effect of Initial Metal Concentration on Heavy Metal Removal by Zeolite 4A (Matrix 1)

4.4 Determination of Best Matrix and Selectivity

4.4.1 Selection of the best matrix based on adsorption capacity

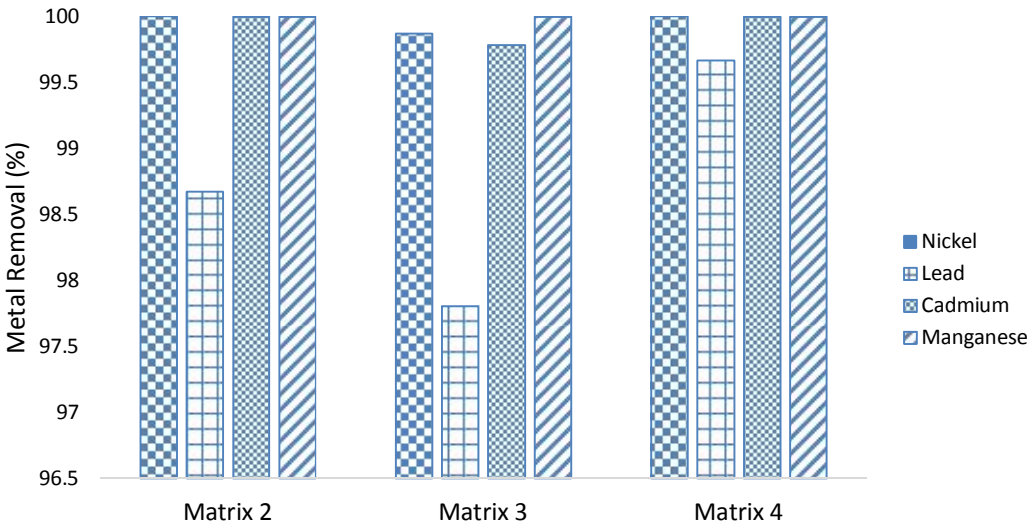


Figure 4.16. Relative Heavy Metal Removal by the Adsorbents

4.4.2 Determination of the selectivity for heavy metals removal

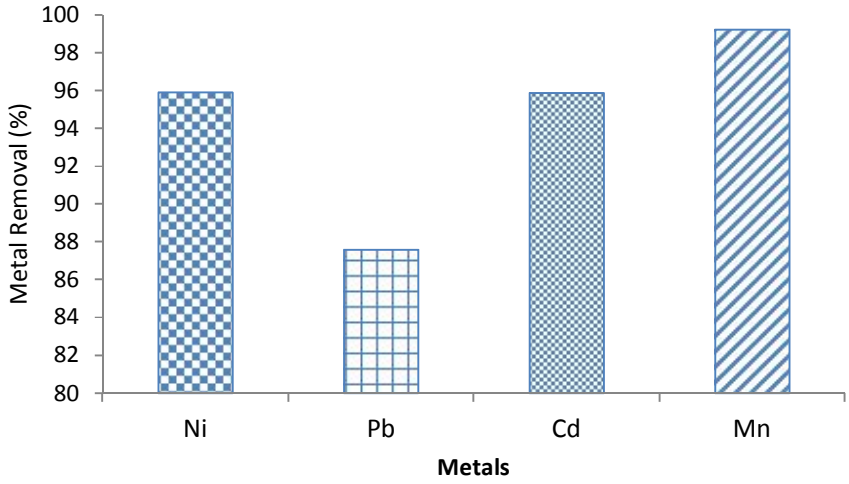


Figure 4.17. Removal order (selectivity) of Heavy Metals by Matrix 4 (25 % Zeolite 4A/75 % Metakaolin) at pH of 8, Matrix dose of 1 g/50 ml and Contact time of 10 minutes.

4.5 Analysis on Interferences of the Individual Heavy Metals in the Simulated Wastewater

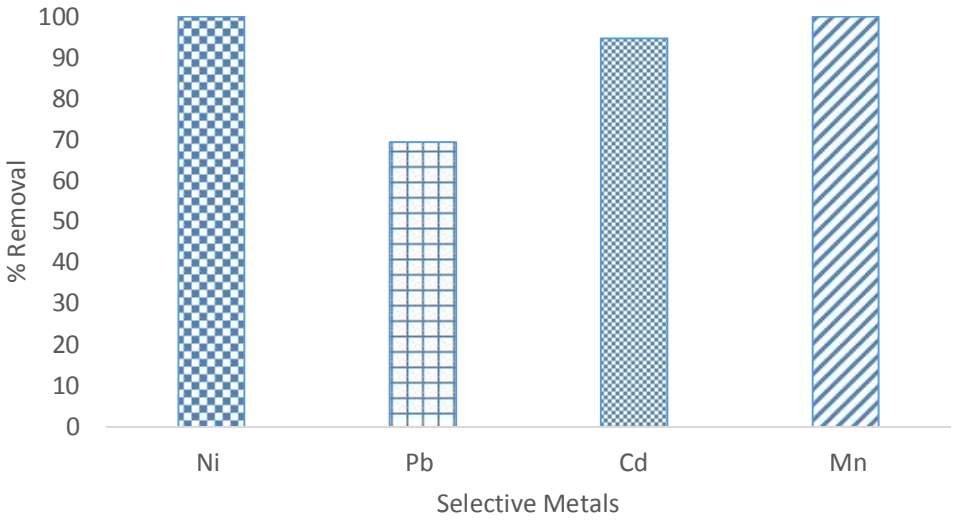


Figure 4.18. Effect of Matrix 4 (25 % Zeolite 4A / 75 % Metakaolin) dose on Single Heavy Metal in Solution at pH; 8, Contact time; 10 minutes and dose; 1 g/50 ml

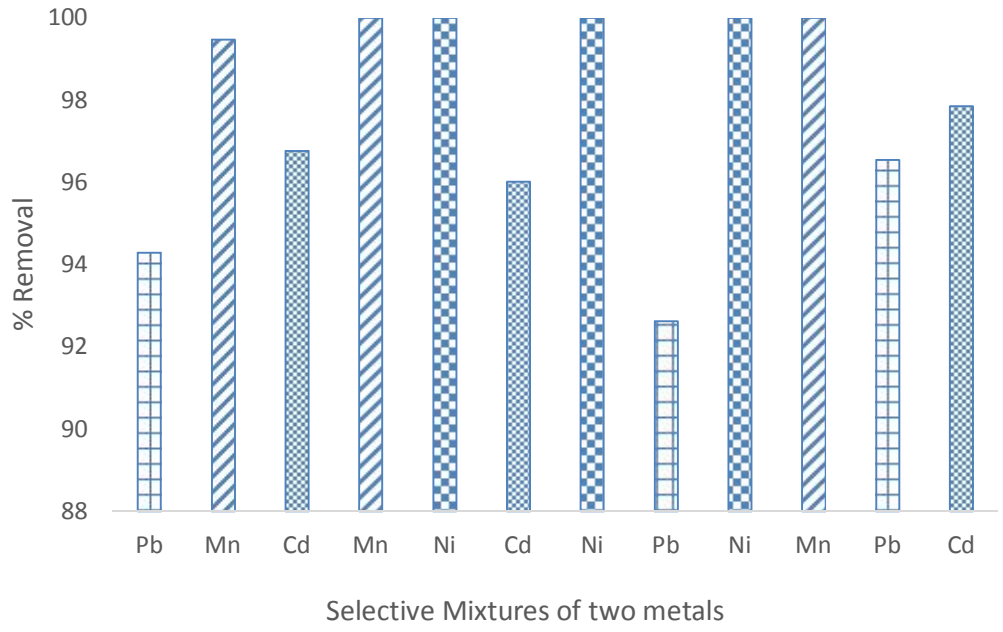


Figure 4.19. Effect of Matrix 4 (25 % Zeolite 4A / 75 % Metakaolin) dose on two Metals in Solution (binary mixture) at *p*H; 8, Contact time; 10 minutes

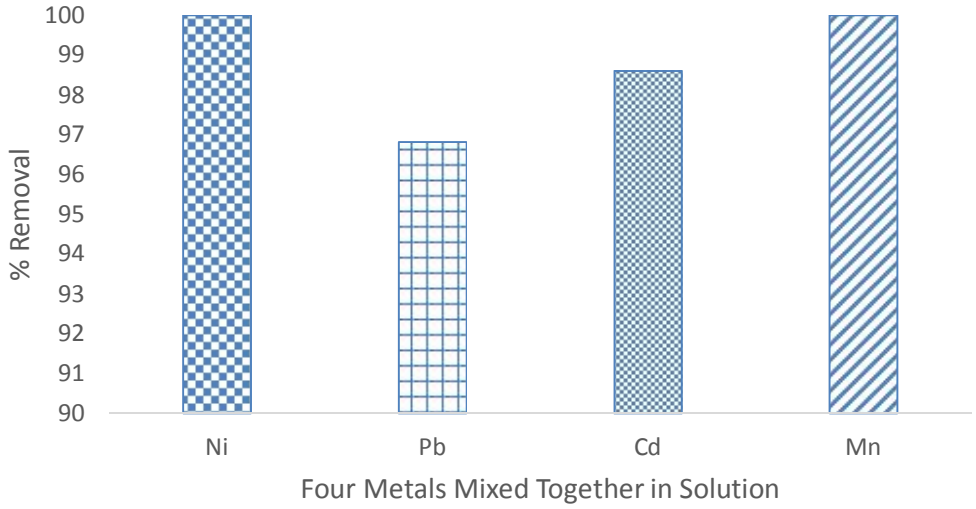


Figure 4.20. Effect of Matrix 4 (25 % Zeolite 4A/75 % Metakaolin) on Four Metals mixed together (composite mixture)

4.6 Characterization of the Best Matrix (Matrix 4)

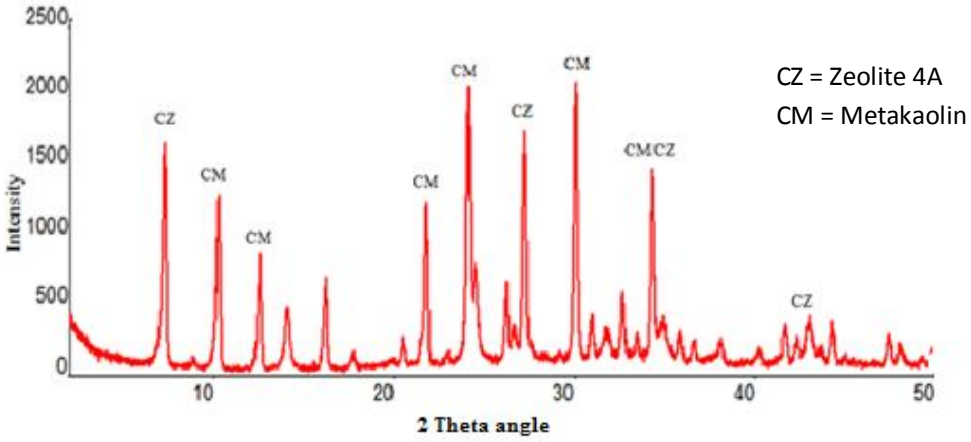


Figure 4.21. XRD Pattern of Matrix 4 (25 % Zeolite 4A /75 % Metakaolin)

4.6.1 Morphology and surface conditions of the Fresh and Spent matrices

.

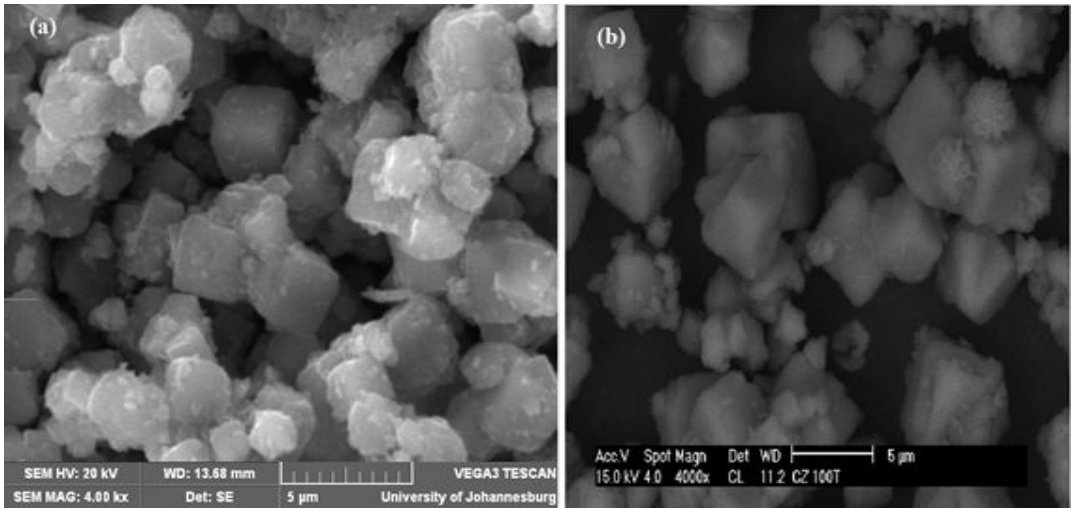


Figure 4.22. SEM images of Matrix 1 (a) Fresh and (b) Spent

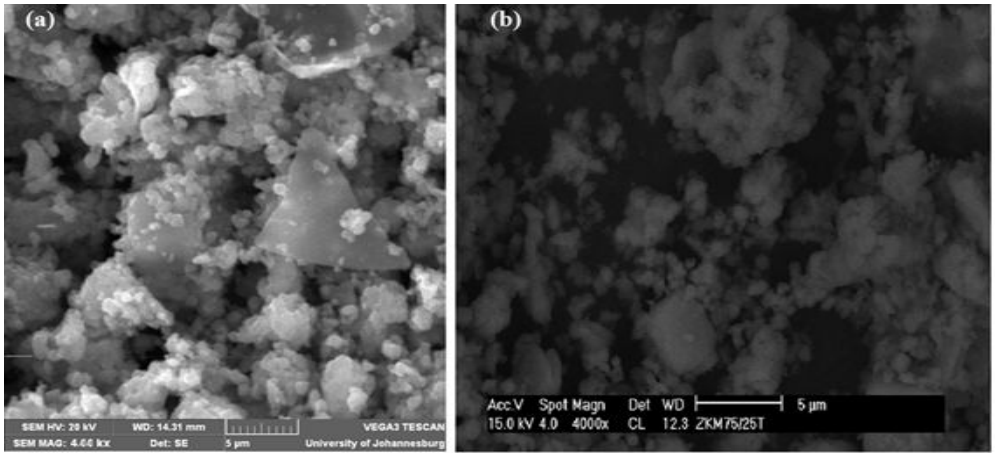


Figure 4.23. (a) SEM images of Matrix 4 (a) Fresh and (b) Spent

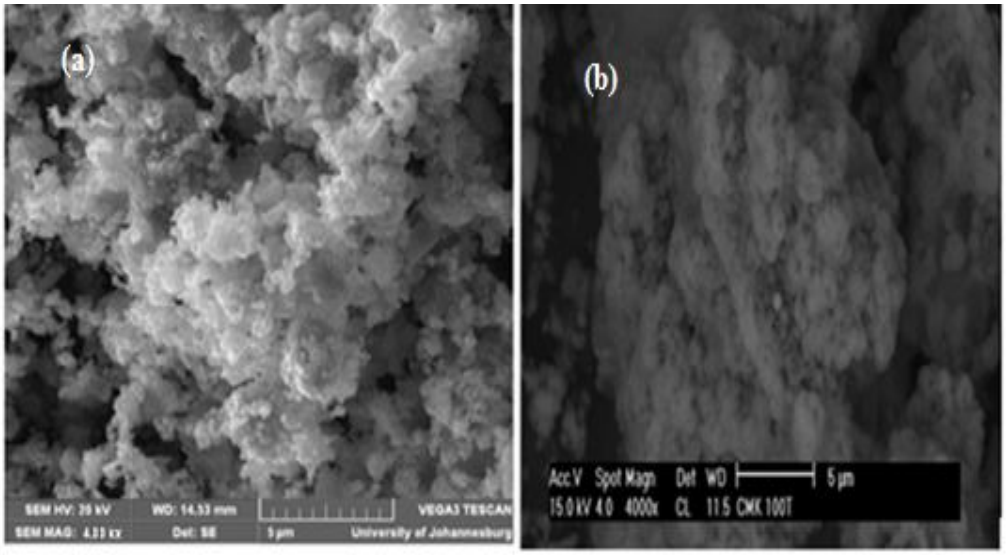


Figure 4.24. SEM images of Matrix 5 (a) Fresh and (b) Spent

Table 4.4. Comparative Coposition of the Matrices Before and After Adsorption (EDX Results)

	Sodium Composition (wt%)	
Matrix	**Before Adsorption**	**After Adsorption**
1	21.3	8.02
4	16.81	11.23
5	7.06	6.87

Legend;
Matrix 1= 100% zeolite 4AA & 0%metakaolin
Matrix 4 = 25% zeolite 4A & 75% metakaolin
Matrix 5 = 0% zeolite 4A & 100% metakaolin

Table 4.5. BET Surface Characteristics of the Adsorbents Matrices

Parameters	Matrix 1		Matrix 4		Matrix 5	
	Before Use	After Use	Before Use	After Use	Before Use	After Use
Surface area (m^2/g)	7.8960	5.7060	3.0945	2.9315	26.4429	6.5112
Cumulative surface area (m^2/g)	8.1940	6.5030	3.2960	3.1860	27.2360	6.8270
Total pore volume of pores(cm^3/g)	0.0442	0.0227	0.0109	0.0100	0.0830	0.0290
Cumulative volume of pores(cm^3/g)	0.0441	0.0223	0.0106	0.0097	0.0849	0.0286
Average pore diameter (nm)	21.5082	13.74280	12.8927	12.2277	12.4664	16.7463

Legend:
Matrix 1 = 100% zeolite 4A & 0% metakaolin
Matrix 4 = 25% zeolite 4A & 75% metakaolin
Matrix 5 = 0% zeolite 4A & 100% metakaolin

4.7 Determination of Heavy Metal Removal from Crude Oil Tank Farm Wastewater

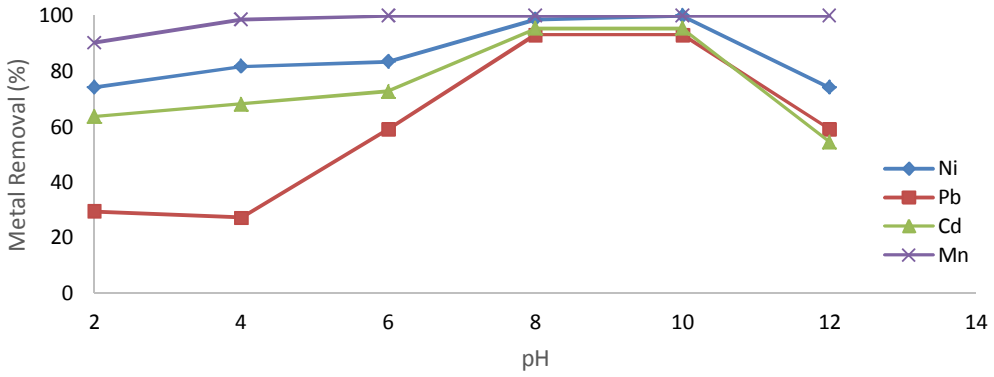


Figure 4.25. Effect of pH on Crude Oil Tank Farm Wastewater Sample at Contact time of 10 minutes, Matrix 4 dose of 1 g/50 ml

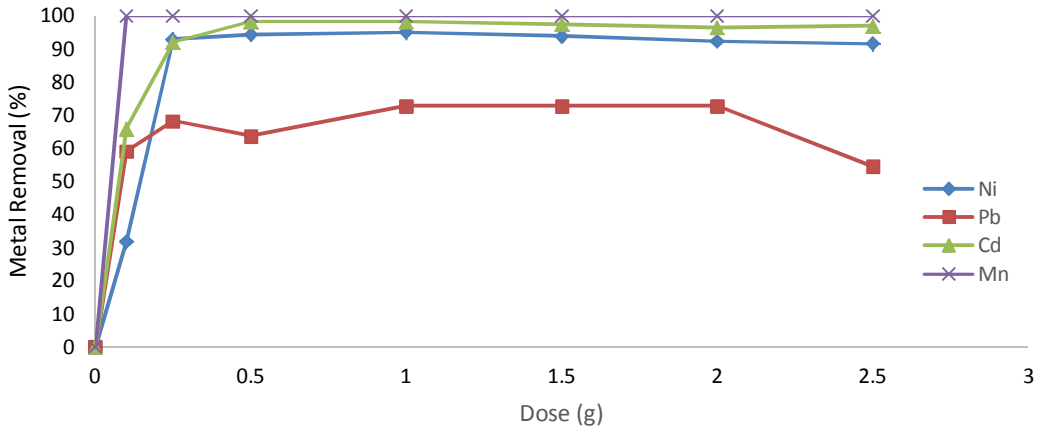


Figure 4.26. Effect of Matrix 4 dose on Crude Oil Tank Farm Wastewater at pH of 8, contact time of 10 minutes)

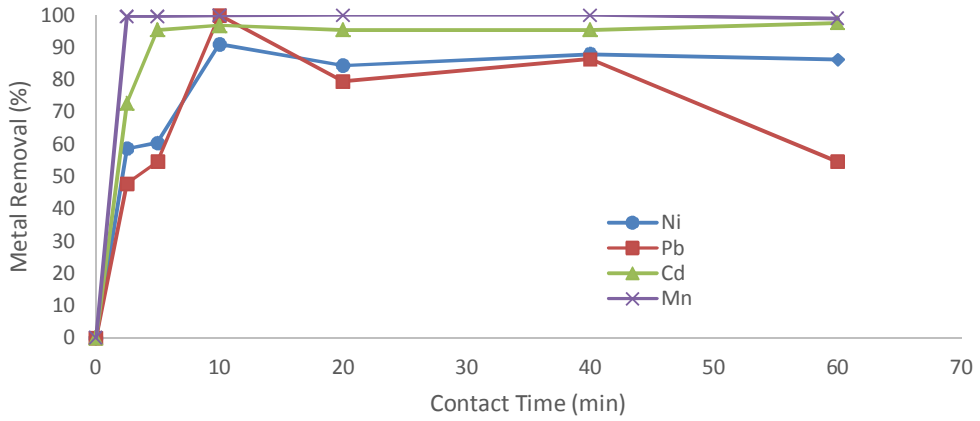


Figure 4.27. Effect of Contact time on Crude Oil Tank Farm Wastewater at pH of 8, Matrix 4 dosage of 1 g/50 ml

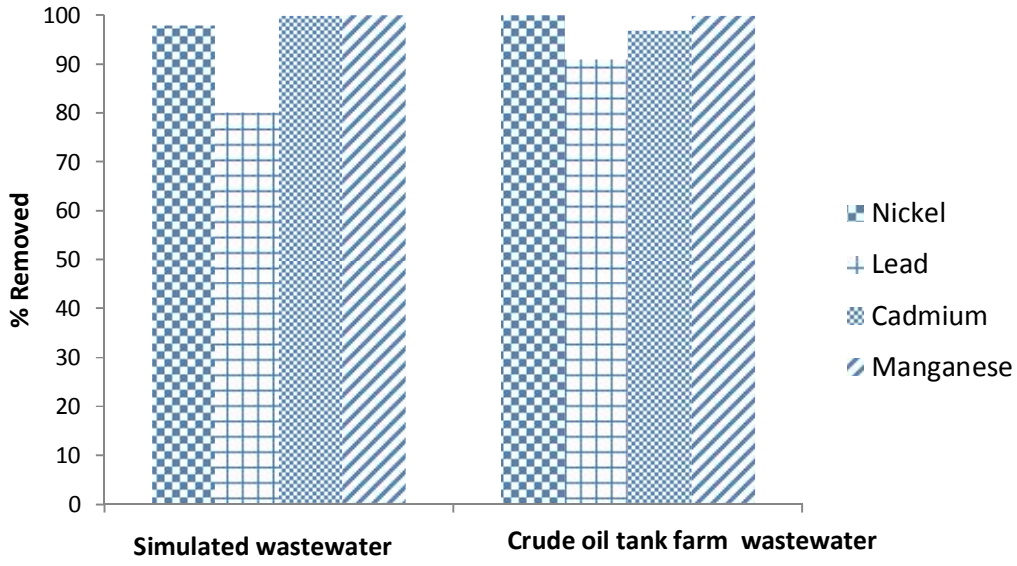


Figure 4.28. Comparison of Effect of Best Matrix on Simulated Wastewater and Crude Oil Tank Farm Wastewater

Table 4.6. Quality of the Untreated and Treated Crude Oil Tank Farm wastewater

Metals	Untreated crude oil tank farm Wastewater	Treated crude oil tank farm wastewater	*Drinking water Quality standard (NESREA)
Ni (mg/l)	0.040	nd	0.0100
Pb(mg/l)	0.225	*0.020	0.0100
Cd(mg/l)	0.022	0.001	0.003
Mn (mg/l)	1.858	0.001	0.200

*Value varies, for USEPA=0.015mg/l

4.8 Adsorption Isotherms and Kinetic

4.8.1 Adsorption isotherms

Note: Graph cannot be plotted for manganese when all the x values are the same (See appendix K1d)

Freundlich Isotherm Plots

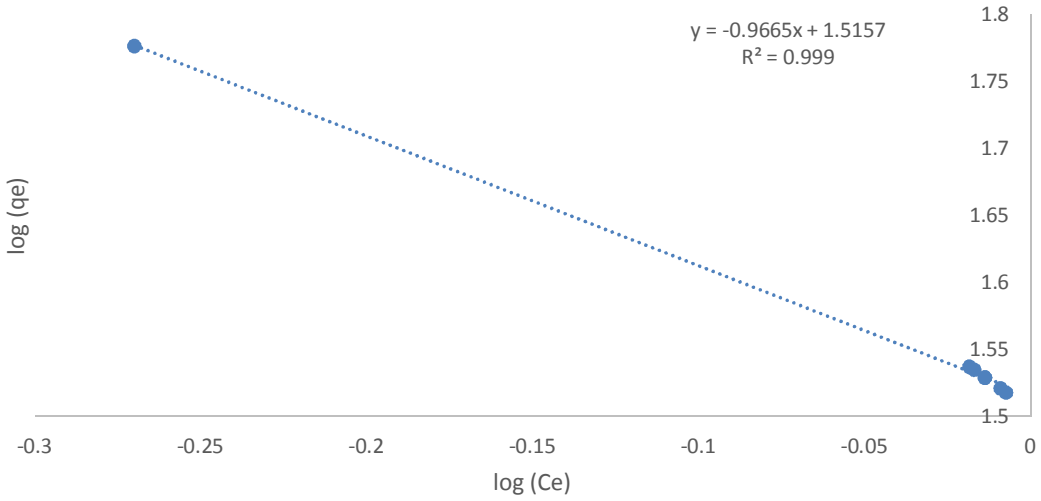


Figure 4.29a. Freundlich plot Ni ions

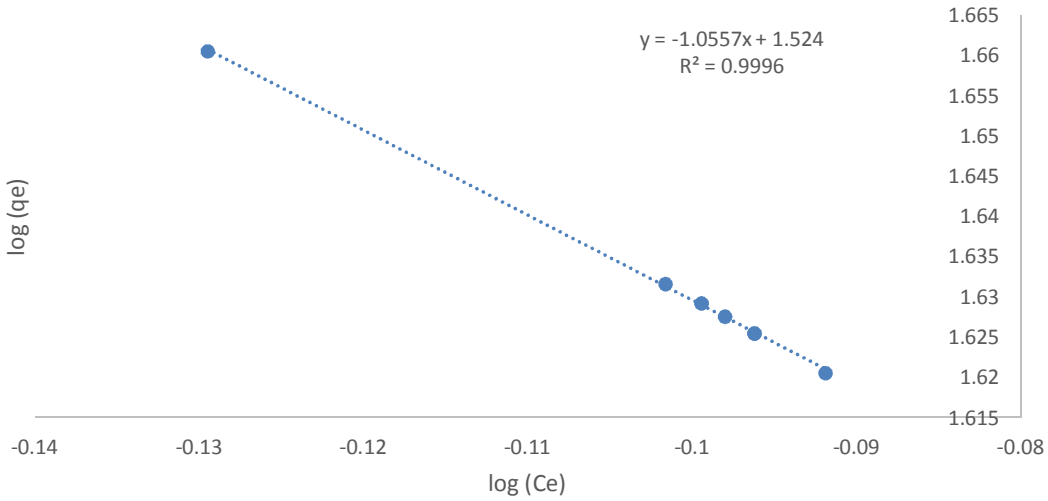


Figure 4.29b. Freundlich plot Pb ions

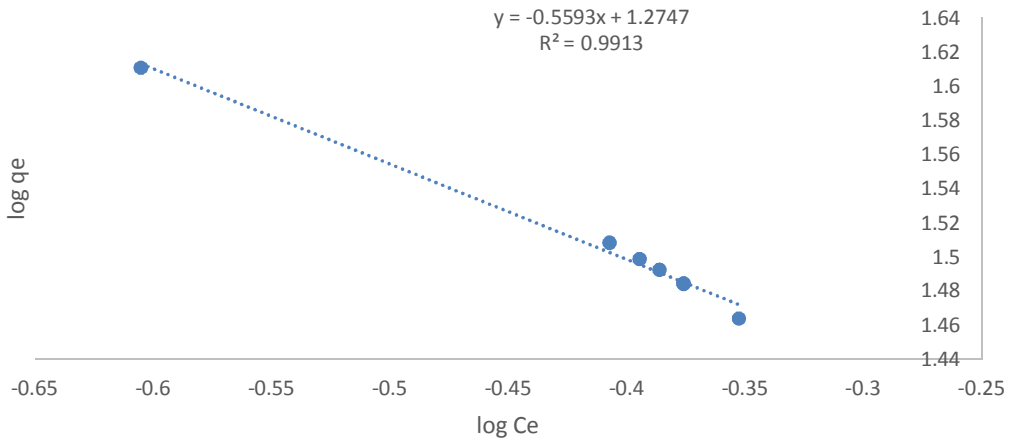


Figure 4.29c. Freundlich plot Cd ions

Langmuir Isotherm Plots

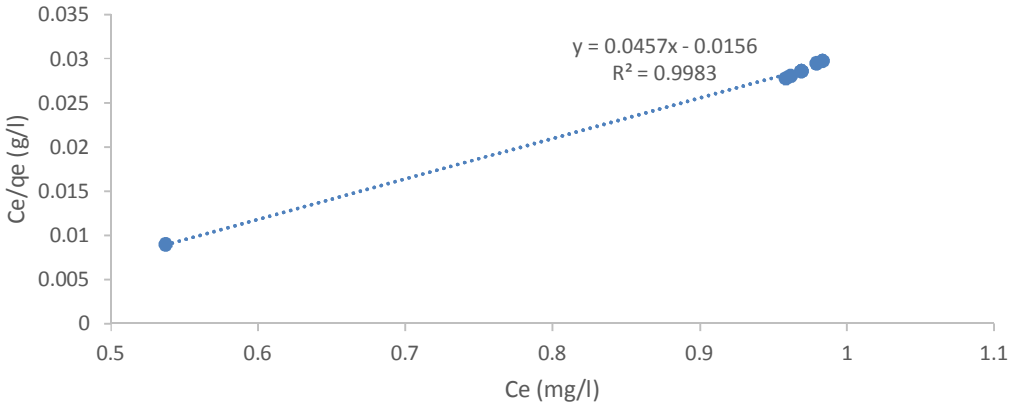


Figure 4.30a. Langmuir Isotherm for Ni ions

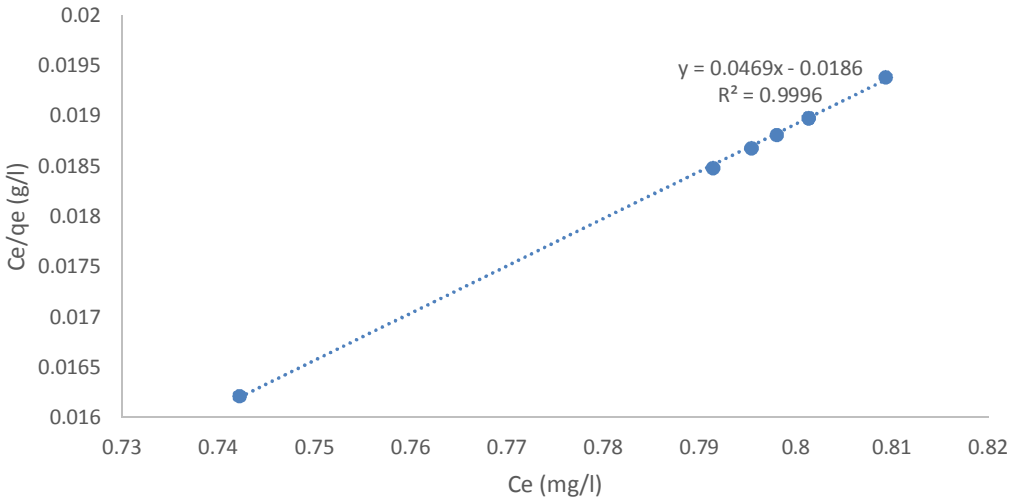


Figure 4.30b. Langmuir Isotherm for Pb ions

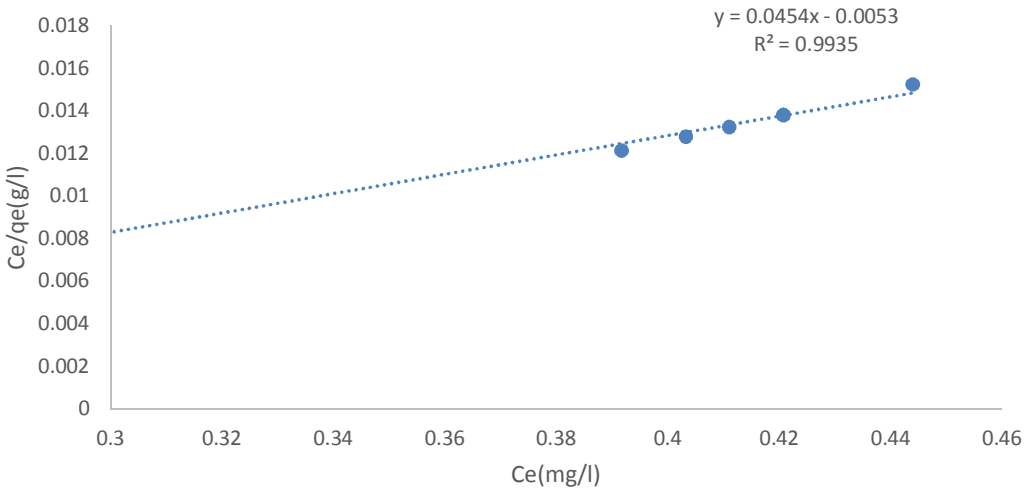


Figure 4.30c. Langmuir Isotherm for Cd ions

Temkin Isotherm Plots

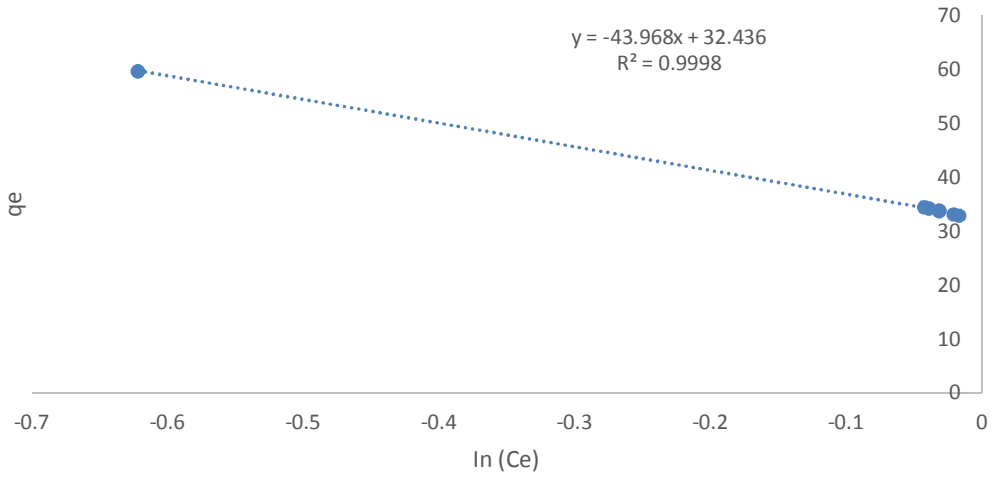


Figure 4.31a. Temkin plot Ni ions

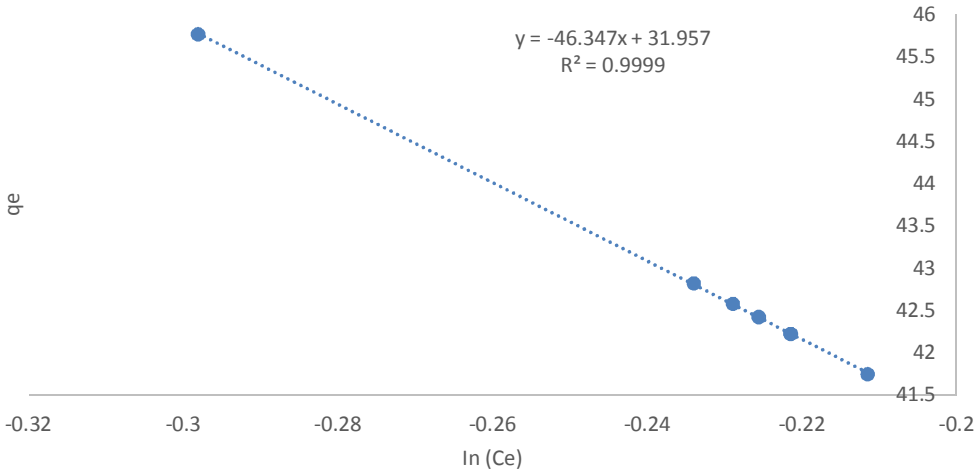


Figure 4.31b. Temkin plot Pb ions

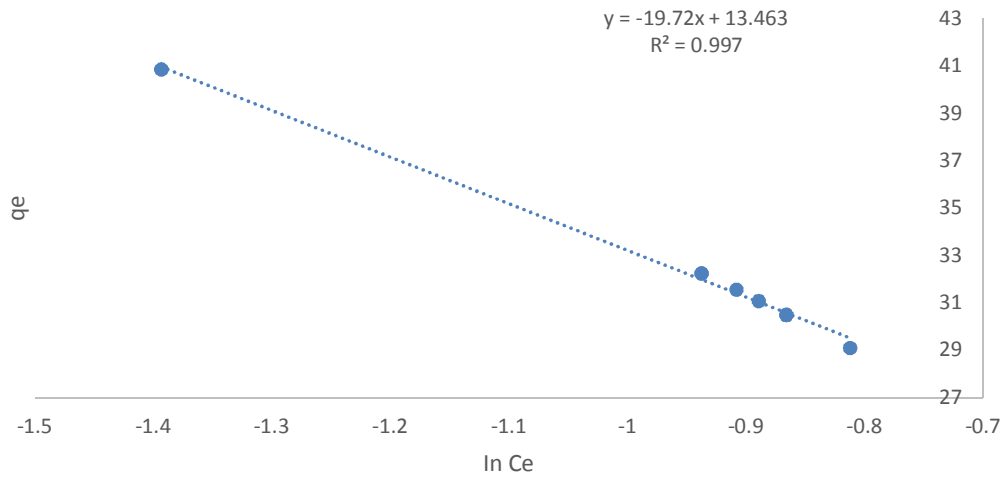


Figure 4.31c. Temkin plot Cd ions

4.8.2 Adsorption kinetic studies

First Order Kinetics

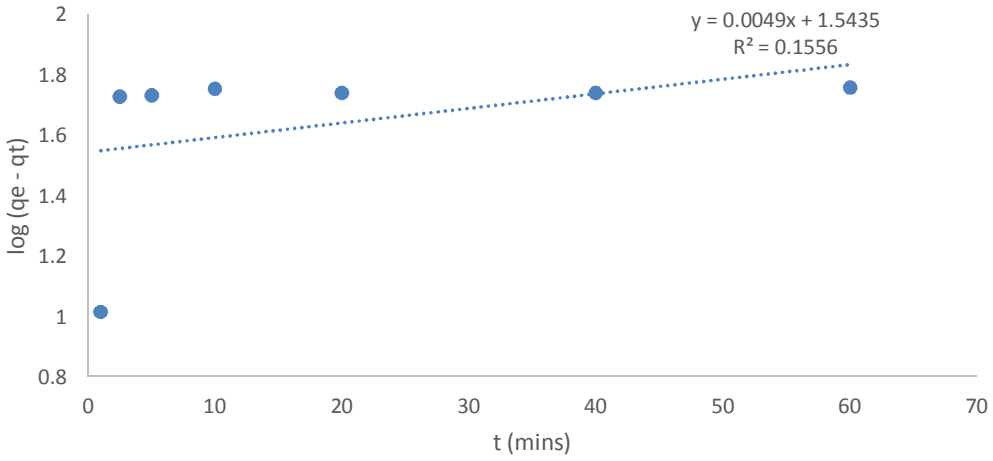


Figure 4.32a. First order kinetics Ni

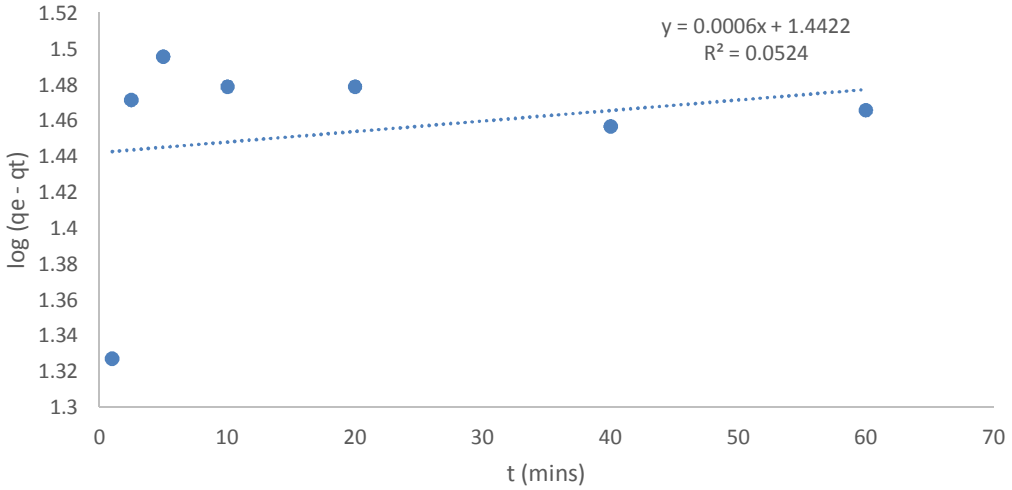


Figure 4.32b. First order kinetics Pb

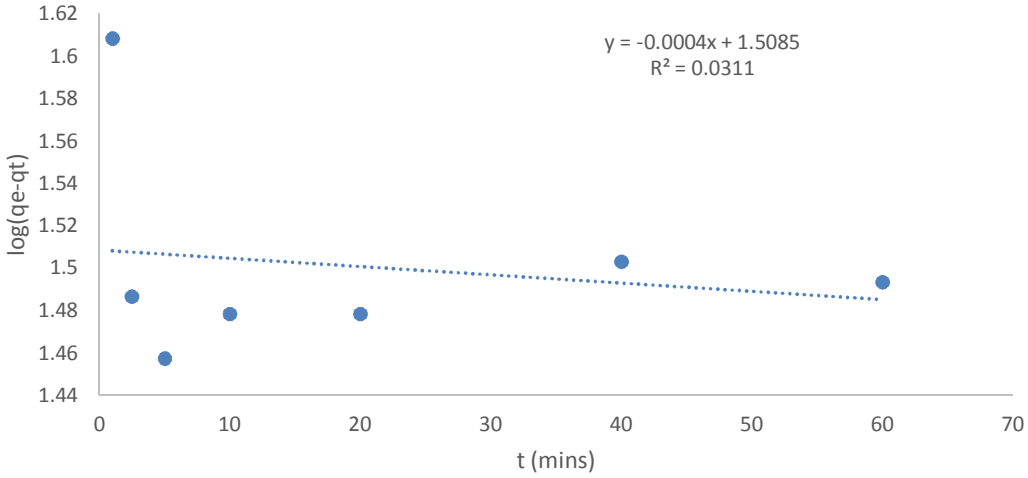


Figure 4.32c. First order kinetics Cd

Second Order Kinetics

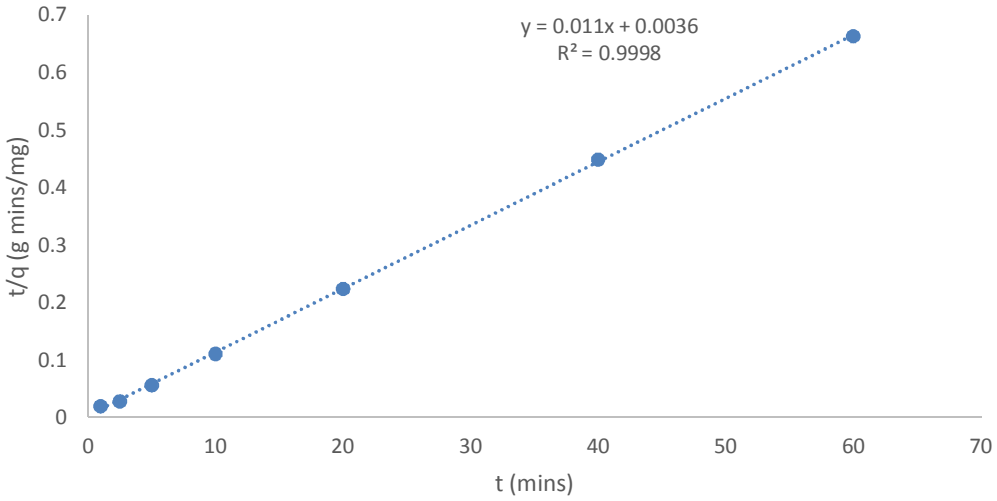


Figure 4.33a. Second order kinetics Ni

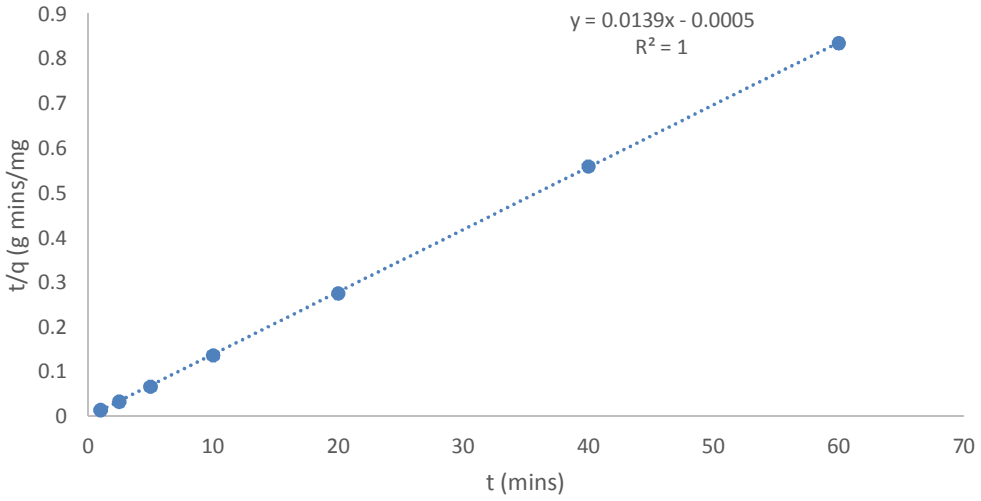


Figure 4.33b. Second order kinetics Pb

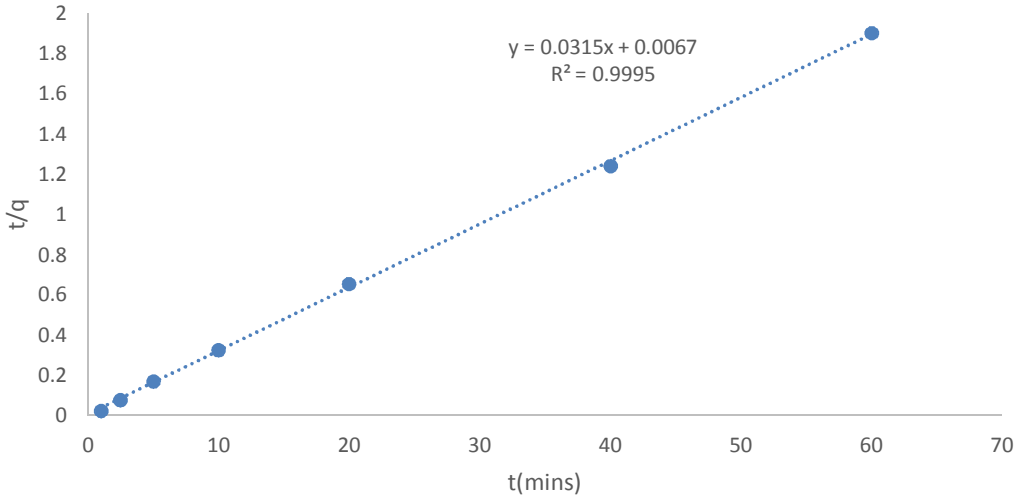


Figure 4.33c. Second order kinetics Cd

Intra Particle

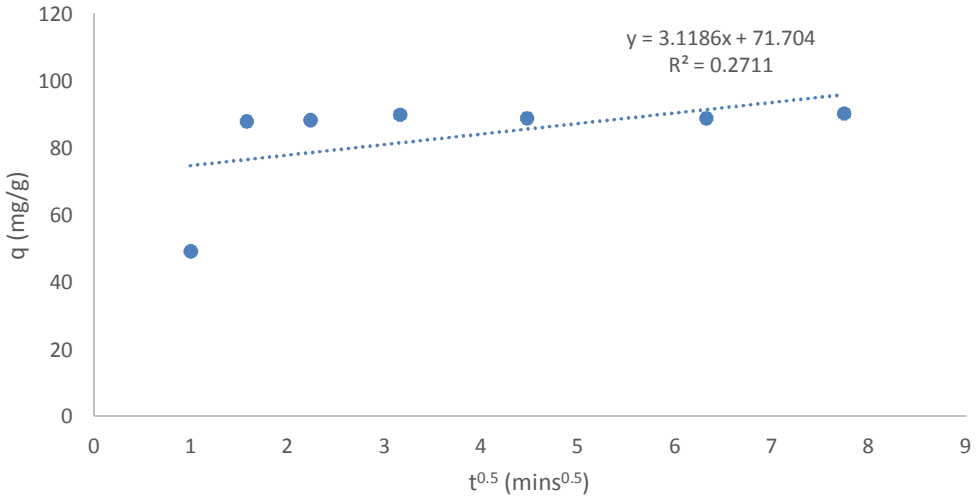


Figure 4.34a. Intra particle Ni

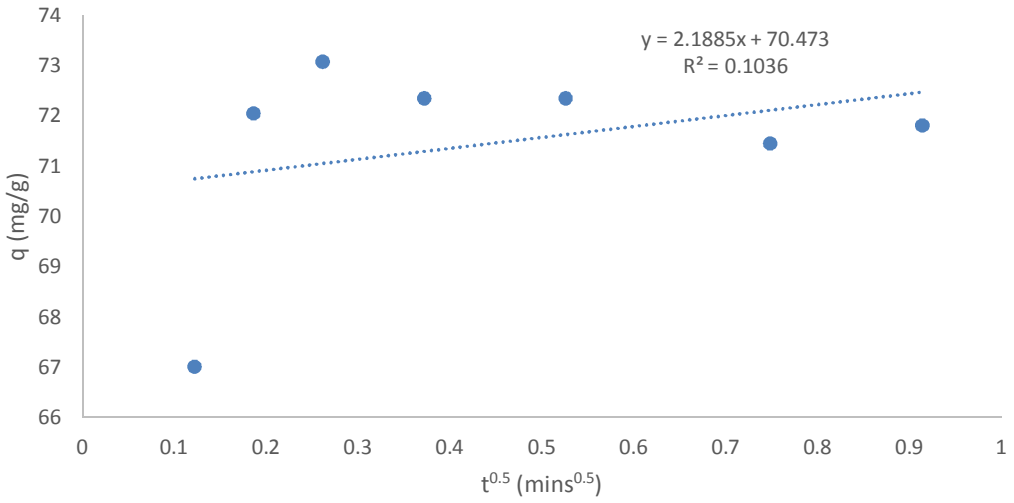


Figure 4.34b. Intra particle Pb

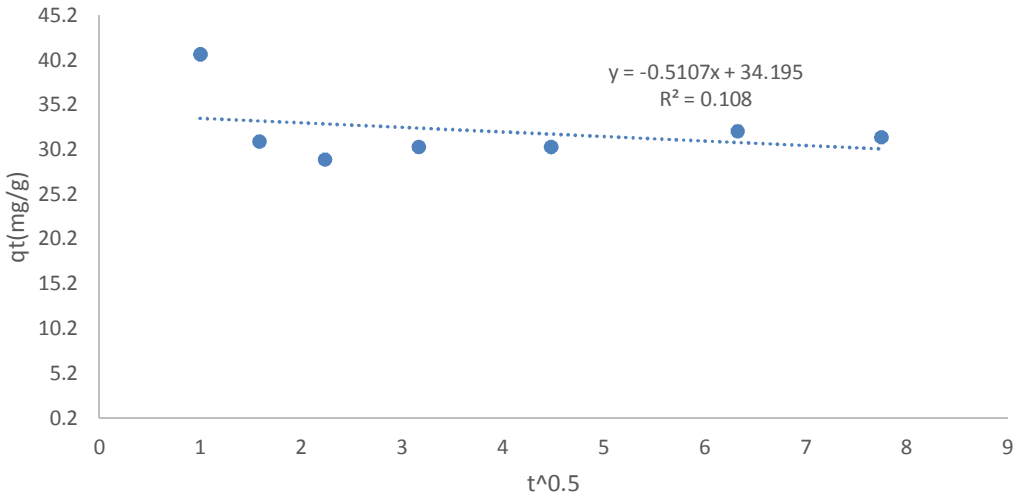


Figure 4.34c. Intra particle Cd

Table 4.7 Parameters for Adsorption Isotherm Models using Matrix 4 for Heavy Metal Removal from Simulated Wastewater

Isotherm	Parameter	Ni(II)	Pb(II)	Cd(II)
Langmuir	q_m	21.88	21.32	22.02
	b	-2.93	-2.52	-8.56
	R^2	0.9983	0.9996	0.9935
Freundlich	K_f	32.787	33.420	18.823
	1/n	0.9665	1.0557	0.5593
	R^2	0.999	0.9996	0.9913
Temkin	K_T	0.182929	0.204401	0.207631
	b_T	-56.7003	-53.7899	-126.42
	R^2	0.9998	0.9999	0.997

Table 4.8 Parameters for Adsorption Kinetic Models using Matrix 4 for Heavy Metal Removal from Simulated Wastewater

Metal Ions	Pseudo First Order Model			Pseudo Second Order Model			Intraparticle Diffusion Model	
	$q_{e,cal}$ mg/g)	k_1 1/min)	R^2	$q_{e,cal}$	k_2	R^2	k_{diff}	R^2
Ni	34.954	0.0112	0.1556	90.90	0.0336	0.9998	3.1186	0.2711
Pb	27.682	0.0013	0.0524	71.94	0.3864	1	2.1885	2.1885
Cd	4.078	0.0009	0.0311	99.25	0.148	0.9991	0.5107	0.1080

4.9 Statistical Analysis of Data using Computer Software

4.9.1 Full factorial analysis

Table 4.9 Factorial Design of Experiments and Percentage Heavy Metal Removal (Response) at the Specified Conditions of Matrix 4 dose, Contact time and pH

RunOrder	CenterPt	Blocks	X_1	X_2	X_3

						y_{Ni}	y_{Pb}	y_{Cd}	y_{Mn}
1	1	1	1.5	20	12	99.6391	99.6105	99.2122	99.9011
2	1	1	0.5	5	4	86.6002	80.1325	79.2324	96.1112
3	1	1	1.5	20	4	91.7811	89.7889	91.5444	97.8883
4	1	1	0.5	20	12	96.6079	99.2105	98.9788	99.4007
5	1	1	0.5	20	4	90.0984	84.7669	90.8772	95.9933
6	1	1	1.5	5	4	93.2219	95.4551	88.7756	98.0046
7	1	1	0.5	20	12	97.3801	99.2444	98.8888	99.3117
8	1	1	1.5	20	4	91.6904	96.1552	91.0006	97.8323
9	1	1	1.5	20	12	98.9944	99.7788	98.8991	99.8899
10	1	1	0.5	5	12	97.0019	99.1778	96.9885	99.4444
11	1	1	0.5	20	4	84.1124	85.0114	84.1113	96.1888
12	1	1	1.5	5	12	99.8811	99.7325	98.9912	99.8859
13	1	1	0.5	5	12	97.0624	98.7987	95.8888	99.6401
14	1	1	1.5	5	12	99.9703	99.4999	99.0418	99.8986
15	1	1	1.5	5	4	90.4316	90.0341	87.8868	96.6443
16	1	1	0.5	5	4	83.8756	81.0818	80.1322	95.6116

Notation:

X_1 = Matrix 4 dose (g/50 ml Simulated wastewater)
X_2 =Contact time (minutes)
X_3 = pH
y_{Ni}= Nickel removal
y_{Pb}= Lead removal
y_{Cd}= Cadmium removal
y_{Mn}= Manganese removal

Full Factorial Model Equations:

$$y_{Ni} = 93.6468 + 2.0544x_1 + 4.6703x_3 \quad (4.1)$$

$$y_{Pb} = 93.592 + 2.664x_1 + 5.789x_3 - 2.391x_1.x_3 \quad (4.2)$$

$$y_{Cd} = 92.528 + 1.891x_1 + 1.661x_2 - 0.74420x_3 - 0.916x_1.x_2 - 1.216x_1.x_3 - 1.027x_2.x_3 \quad (4.3)$$

$$y_{Mn} = 98.2279 + 0.5152 + 1.4436x_3 - 0.2929x_1.x_3 \quad (4.4)$$

Table 4.10. Estimated Effects and Coefficients for yNi, yPb, yCd & yMn (coded units)

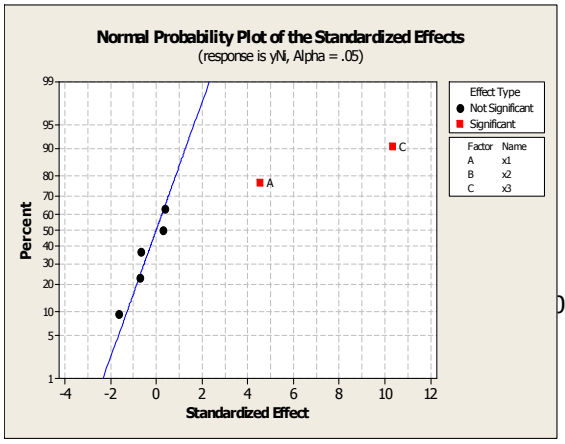
(a) **Nickel** (R^2 = 94.28%; R^2 (adj) = 89.28%)

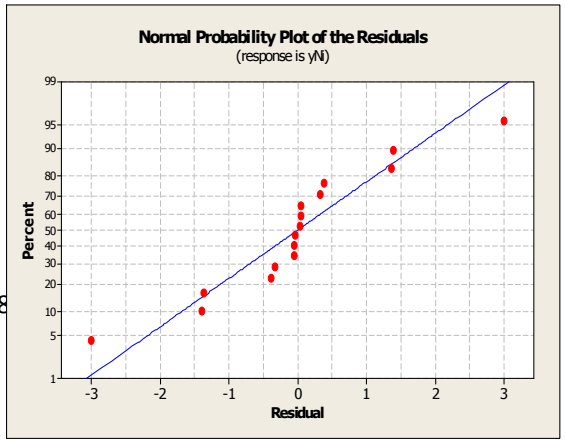
Term	Effect	Coef	SE Coef	T	P
Constant		93.6468	0.4510	207.64	0.000
x1	4.1088	2.0544	0.4510	4.56	0.002
x2	0.2823	0.1412	0.4510	0.31	0.762
x3	9.3407	4.6703	0.4510	10.36	0.000
x1*x2	-0.6323	-0.3162	0.4510	-0.70	0.503

x1*x3	-1.5007	-0.7504	0.4510	-1.66	0.135
x2*x3	-0.6059	-0.3029	0.4510	-0.67	0.521
x1*x2*x3	0.3469	0.1735	0.4510	`0.38	0.711
(b) **Lead**	(R^2 = 95.53%; R^2 (adj) = 91.62%)				
Constant		93.592	0.5270	177.59	0.000
x1	5.329	2.664	0.5270	5.06	0.001
x2	1.207	0.603	0.5270	1.14	0.285
x3	11.578	5.789	0.5270	10.98	0.000
x1*x2	-1.054	-0.527	0.5270	-1.00	0.347
x1*x3	-4.781	-2.391	0.5270	-4.54	0.002
x2*x3	-1.048	-0.524	0.5270	-0.99	0.349
x1*x2*x3	0.973	0.487	0.5270	0.92	0.383
(c) **Cadmium**	(R^2 = 96.62% R^2 (adj) = 93.67)				
Constant		92.528	0.4375	211.51	0.000
x1	3.782	1.891	0.4375	4.32	0.003
x2	3.322	1.661	0.4375	3.80	0.005
x3	11.666	5.833	0.4375	13.33	0.000
x1*x2	-1.832	-0.916	0.4375	-2.09	0.070
x1*x3	-2.432	-1.216	0.4375	-2.78	0.024
x2*x3	-2.055	-1.027	0.4375	-2.35	0.047
x1*x2*x3	0.604	0.302	0.4375	0.69	0.510
(a) **Manganese**	(R^2 = 97.29%; R^2 (adj) = 94.93%)				
Constant		98.2279	0.09244	1062.56	0.000
x1	1.0304	0.5152	0.09244	5.57	0.001
x2	0.1457	0.0728	0.09244	0.79	0.454
x3	2.8873	1.4436	0.09244	15.62	0.000
x1*x2	0.1239	0.0619	0.09244	0.67	0.522
x1*x3	-0.5858	-0.2929	0.09244	-3.17	0.013
x2*x3	-0.2371	-0.1185	0.09244	-1.28	0.236
x1*x2*x3	-0.0292	-0.0146	0.09244	-0.16	0.878

Notation:
Coef = Coefficient
SE Coef = Standard error (Variability associated with an estimated coefficient)
T = T – test (Test the significance of terms or groups of terms in models)
P = P-value of an estimated effect (Probability of observing an effect that is largly purely by chance)

Nickel Factorial Plots





Lead Factorial Plots

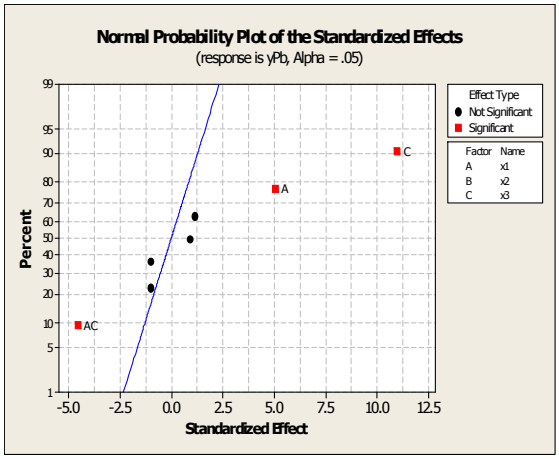


Figure 4.39 Normal Probability Plot of the Standardized effects for Lead

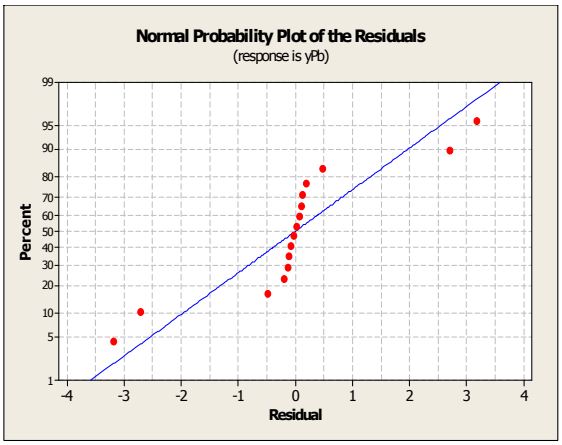


Figure 4.40 Normal Probability of the Residuals for Lead

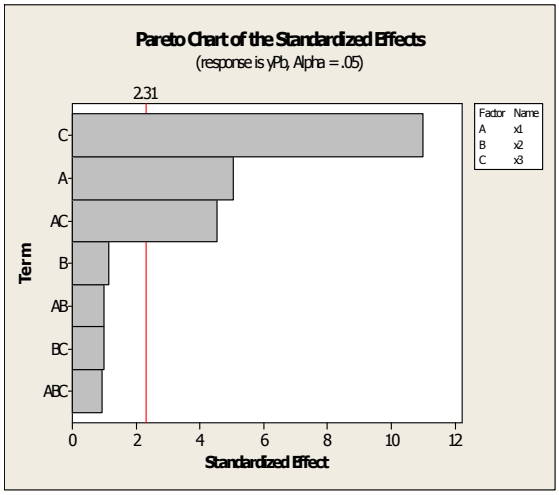


Figure 4.41 Pareto Chart of the Standardized Effects for Lead

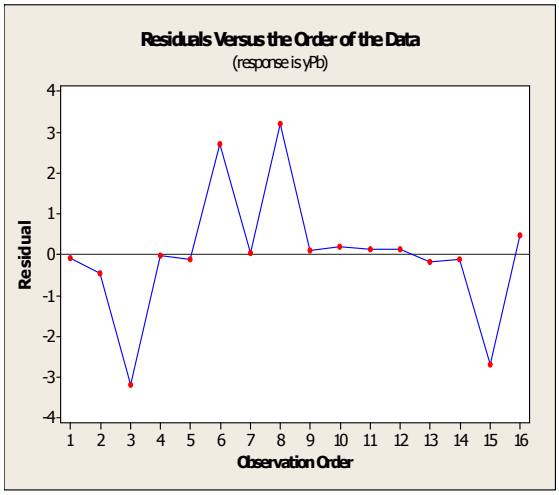


Figure 4.42 Residuals versus the Order of the Data for Lead

Cadmium Factorial Plots

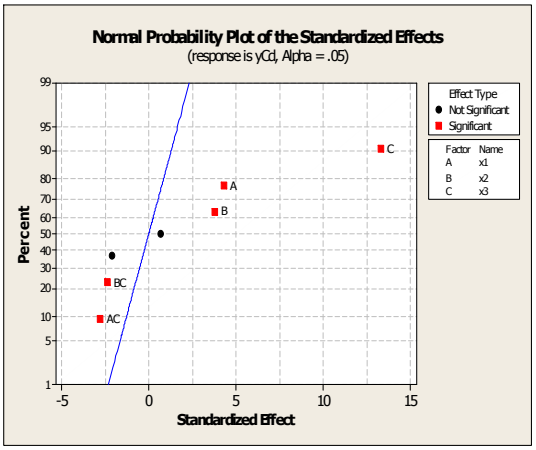


Figure 4.43 Normal Probability Plot of the Standardized Effects for Cadmium

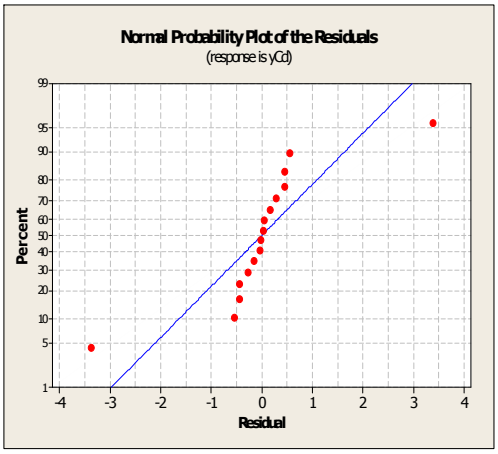


Figure 4.44 Normal Probability of the Residuals for Cadmium

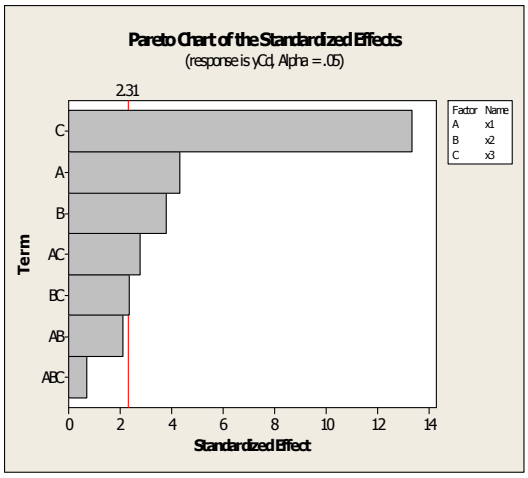


Figure 4.45 Pareto chart of the Standardized Effects for Cadmium

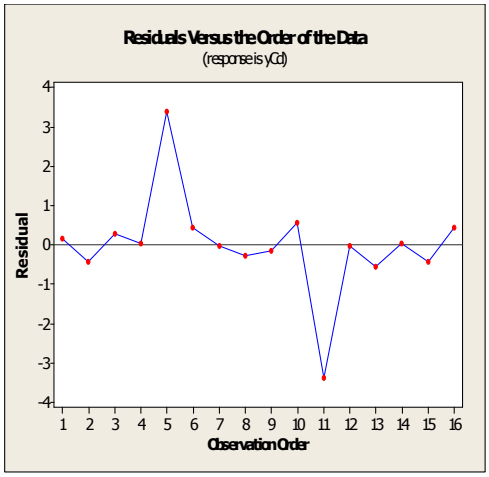


Figure 4.46 Residuals Versus order of the Data for cadmium

Manganese Factorial Plots

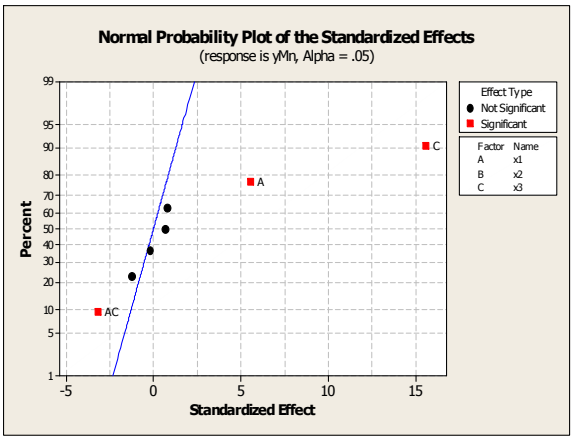


Figure 4. 47 Normal Probability Plot of the Standardized effects for Manganese

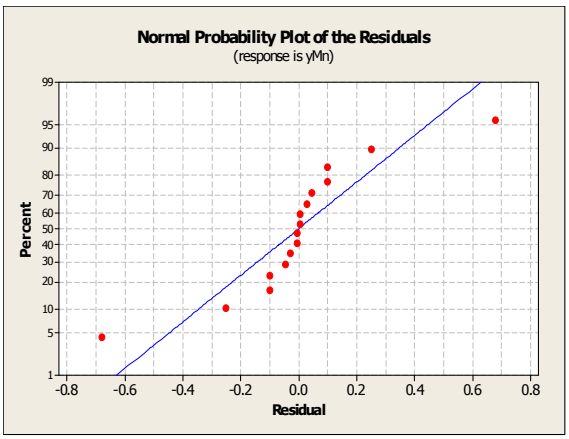


Figure 4.48 Normal probability Plot of the residuals for Manganese

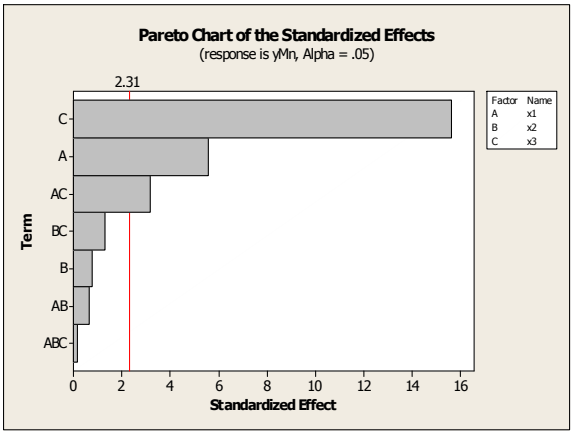


Figure 4.49 Pareto Chart of the Standardized Effects for Manganese

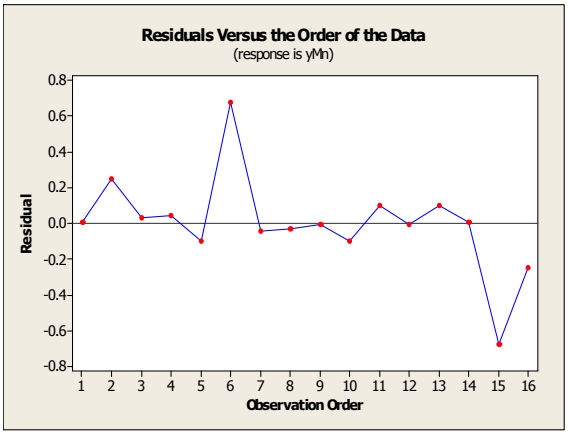


Figure 4.50 Residuals versus the order of the Data for manganese

Table 4.11. Analysis of Variance (coded units)

(a) Nickel

Source	DF	Seq SS	Adj SS	Adj MS	F	P
Main Effects	3	416.843	416.843	138.948	42.69	0.000
2-Way Interactions	3	12.077	12.077	4.026	1.24	0.358
3-Way Interactions	1	0.481	0.481	0.481	0.15	0.711
Residual Error	8	26.036	26.036	3.255		
Pure Error	8	26.036	26.036	3.255		
Total	15	455.438				
(b) Lead						
Main Effects	3	655.650	655.650	218.550	49.18	0.000
2-Way Interactions	3	100.278	100.278	33.426	7.52	0.010
3-Way Interactions	1	3.790	3.790	3.790	0.85	0.383
Residual Error	8	35.553	35.553	4.444		
Pure Error	8	35.553	35.553	4.444		
Total	15	795.272				
(c) Cadmium						
Main Effects	3	645.736	645.736	215.245	70.30	0.000
2-Way Interactions	3	53.964	53.964	17.988	5.87	0.020
3-Way Interactions	1	1.458	1.458	1.458	0.48	0.510
Residual Error	8	24.495	24.495	3.062		
Pure Error	8	24.495	24.495	3.062		
Total	15	725.653				
(d) Manganese						
Main Effects	3	37.6768	37.6768	12.5589	91.85	0.000
2-Way Interactions	3	1.6587	1.6587	0.5529	4.04	0.051
3-Way Interactions	1	0.0034	0.0034	0.0034	0.02	0.878
Residual Error	8	1.0939	1.0939	0.1367		
Pure Error	8	1.0939	1.0939	0.1367		
Total	15	40.4327				

Notation:
DF = Degrees of Freedom
Seq SS = Sequential Sum of Squares
Adj MS= Adjusted Mean Squares

Adj SS = Adjusted Sum of Squares
F = Fischer and associated p values
P = P - value of an estimated effect

Table 4.12. Factorial Statistics for Nickel, Lead, Cadmium and Manganese

	Full Factorial Statistics		
Heavy Metals	R^2	R^2adj	SS
Nickel	0.9428	0.8928	1.80404
Lead	0.9553	0.9162	2.10810
Cadmium	0.9662	0.9367	1.74983
Manganese	0.9729	0.9493	0.36977

4.9.2 Optimisation by Response Surface Method (RSM)

Table 4.13 Design of Experiment (DOE) for Optimisation by Response Surface methodology (RSM) and Percentage heavy metal removal

Std	Run	Block	x_1	x_2	x_3	y_{Ni}	y_{Pb}	y_{Cd}	y_{Mn}
8	1	Block 1	0.5	5	8	97.0224	99.0182	96.7805	99.7180
15	2	Block 1	0.5	5	8	97.7260	98.8118	96.7805	99.7265
4	3	Block 1	1	20	12	98.7006	87.3896	99.6879	99.8327
2	4	Block 1	1	5	12	98.2135	88.4229	97.1419	99.8853
6	5	Block 1	1.5	12.5	4	99.4316	99.5341	98.6037	99.5414
16	6	Block 1	1	12.5	8	97.8343	98.9666	98.8175	99.7443
1	7	Block 1	1.5	20	8	97.5638	99.6905	98.6037	99.9032
11	8	Block 1	0.5	20	8	97.7804	98.6038	99.2443	99.5414
12	9	Block 1	1	5	4	99.0254	99.0182	99.4909	99.5414
9	10	Block 1	1	20	4	99.2964	99.1730	96.2221	99.8938
7	11	Block 1	1	12.5	8	97.7804	98.1396	99.9984	99.9032
17	12	Block 1	1	12.5	8	98.0508	99.4825	99.9984	99.7443
5	13	Block 1	1	12.5	8	98.1591	98.9150	99.9983	99.7443
14	14	Block 1	0.5	12.5	12	98.7005	86.3562	98.4725	99.6917
13	15	Block 1	0.5	12.5	4	98.0508	98.5007	98.4735	99.5413
3	16	Block 1	1	12.5	8	98.1591	98.6038	99.1953	99.6823
10	17	Block 1	1.5	12.5	12	98.3488	90.1286	98.8503	99.7970

Notation:
X_1 = Matrix 4 dose (g/50 ml Simulated wastewater)
X_2 =Contact time (minutes)
X_3 = pH
y_{Ni}= Nickel removal
y_{Pb}= Lead removal
y_{Cd}= Cadmium removal
y_{Mn}= Manganese removal

Table 4.14. Sequential Model Sum of Squares: Response: Ni, Pb, Cd, & Mn Removal

Source	Sum of squares	DF	Mean Square	F Vaue	Prob>F	
(a) Nickel						
Mean	1.640E+005	1	1.640E+005			Suggested
Linear	1.31	3	0.44	1.10	0.3853	
2FI	1.78	3	0.59	1.76	0.2185	
Quadratic	**2.74**	**3**	**0.91**	**10.04**	**0.0063**	**Suggested**
Cubic	0.26	2	0.13	1.73	0.2688	Aliased
Residual	0.38	5	0.075			
Total	1.640E+005	17	9648.75			
(b) Lead						
Mean	1.580E+005	1	1.580E+005			
Linear	241.36	3	80.45	7.98	0.0029	Suggested
2FI	13.22	3	4.41	0.37	0.7739	
Quadratic	**116.39**	**3**	**38.80**	**182.32**	**<0.0001**	**Suggested**
Cubic	0.49	2	0.24	1.22	0.3696	Aliased
Residual	1.00	5	0.20			
Total	1.583E+005	17	9314.36			
(c) Cadmium						
Mean	1.653E+005	1	1.653E+005			Suggested
Linear	2.78	3	0.93	0.59	0.6323	
2FI	12.70	3	4.23	5.51	0.0170	
Quadratic	**5.27**	**3**	**1.76**	**5.10**	**0.0351**	**Suggested**
Cubic	1.16	2	0.58	2.32	0.1942	Aliased
Residual	1.25	5	0.25			
Total	1.653E+005	17	925.17			
(d) Manganese						
Mean	1.691E+005	1	1.691E+005			Suggested
Linear	0.094	3	0.031	2.27	0.1289	
2FI	0.088	3	0.029	3.25	0.0689	
Quadratic	**0.061**	**3**	**0.020**	**4.90**	**0.0384**	**Suggested**
Cubic	2.031E-003	2	1.016E-003	0.19	0.8354	Aliased
Residual	0.027	5	5.446E-003			
Total	1.691E+005	17	9946.35			

Notation: DF = Degrees of Freedom
F = Fischer and associated p values

Table 4.15. The model fit summary

Source	Std. Dev.	R-Squared	R^2(Adj)	R^2 (Pred)	PRESS	
(a) Nickel						
Linear	0.63	0.2020	0.0178	-0.5539	10.04	
2FI	0.58	0.4776	0.1641	-1.2909	14.79	
Quadratic	0.30	0.9015	0.7748		+	Suggested
Cubic	0.27	0.9418	0.8136		+	Aliased
(b) Lead						
Linear	3.18	0.64802	0.5668	0.3481	242.80	Suggested
2FI	3.43	0.68351	0.4936	-0.2573	468.29	
Quadratic	0.46	0.99601	0.9909		+	Suggested
Cubic	0.45	0.99731	0.9914		+	Aliased
(c) Cadmium						
Linear	1.25	0.1198	-0.0833	-0.5883	36.78	
2FI	0.88	0.6683	0.4693	-0.0306	23.86	
Quadratic	0.59	0.8958	0.7619		+	Suggested
Cubic	0.50	0.9459	0.8270		+	Aliased
(d) Manganese						
Linear	0.12	0.3435	0.1920	-0.3327	0.36	
2FI	0.095	0.6675	0.4680	-0.3562	0.37	
Quadratic	0.065	0.8927	0.7548		+	Suggested
Cubic	0.074	0.9002	0.6806		+	Aliased

Notation: Std Dev. = Standard Deviation
R^2 Adj = Adjusted R - squared
R^2 (pred) = Predicted R - squared

Table 4.16. Lack of Fit Tests

Source	SS	DF	MS	F Vaue	Prob>F	
(a) Nickel						
Linear	4.78	8	0.60	7.94	0.0177	
2FI	3.00	5	0.60	7.97	0.0199	
Quadratic	**0.26**	**2**	**0.13**	**1.73**	**0.2688**	**Suggested**
Cubic	0.00	0				Aliased
Pure Error	0.38	5	0.075			
(b) Lead						
Linear	130.10	8	16.26	81.28	<0.0001	
2FI	116.88	5	23.38	116.83	<0.0001	
Quadratic	**0.49**	**2**	**0.24**	**1.22**	**0.3696**	**Suggested**
Cubic	0.00	0				Aliased
Pure Error	1.00	5	0.20			
(c) Cadmium						
Linear	19.13	8	2.39	9.55	0.0118	
2FI	6.43	5	1.29	5.13	0.0484	
Quadratic	**1.16**	**2**	**0.58**	**2.32**	**0.1942**	**Suggested**
Cubic	0.00	0				Aliased
Pure Error	1.25	5	0.25			
(d) Manganese						
Linear	0.15	8	0.019	3.49	0.0925	
2FI	0.063	5	0.013	2.33	0.1872	
Quadratic	**2.031E-003**	**2**	**1.016E-003**	**0.19**	**0.8354**	**Suggested**
Cubic	0.00	0				Aliased
Pure Error	0.027	5	5.446E-003			

Notation: DF = Degrees of Freedom
SS = Sum of Squares
MS= Mean Squares
F = Fischer and associated p values

Model equations for nickel, lead, cadmium and manganese

Final Equations in terms of Actual Factors

$$y_{Ni} = 98.24919 + 4.55040x_1 + 0.071753x_2 - 0.74420x_3 - 0.97818{x_1}^2 - 1.21809E^{-003}{x_2}^2 + 0.055046{x_3}^2 - 0.043846x_1.x_2 - 0.21657x_1.x_3 + 1.80069E^{-003}x_2.x_3 \quad (4.5)$$

$$y_{Pb} = 89.35916 - 3.66843x_1 - 0.055691x_2 + 4.10711x_3 + 2.02752{x_1}^2 + 6.71848E^{-003}{x_2}^2 - 0.35616{x_3}^2 - 0.084979x_1.x_2 + 0.34239x_1.x_3 - 9.90132E^{-003}x_2.x_3 \quad (4.6)$$

$$y_{Cd} = 93.95332 + 6.22434x_1 + 0.22755x_2 + 0.11537x_3 - 1.16835{x_1}^2 - 0.013446{x_2}^2 - 044341{x_3}^2 - 0.26637x_1.x_2 + 0.030956x_1.x_3 + 0.048457x_2.x_3 \quad (4.7)$$

$$y_{Mn} = 99.29425 + 0.42803x_1 - 0.014116x_2 + 0.043608x_3 - 0.51135{x_1}^2 + 3.13442E^{-004}{x_2}^2 + 4.35181E^{-004}{x_3}^2 + 0.042870x_1.x_2 + 0.013159x_1.x_3 - 3.37617E^{-003}x_2.x_3 \quad (4.8)$$

Refined Equations in terms of Actual Factors

$$y_{Ni} = 98.24919 + 0.055046{x_3}^2 - 0.21657x_1.x_3 \quad (4.9)$$

$$y_{Pb} = 89.35916 - 3.66843x_1 + 4.10711x_3 + 2.02752{x_1}^2 - 0.35616{x_3}^2 + 0.34239x_1.x_3 \quad (4.10)$$

$$y_{Cd} = 93.95332 - 0.013446{x_2}^2 - 0.26637x_1.x_2 + 0.048457x_2.x_3 \quad (4.11)$$

$$y_{Mn} = 99.29425 - 0.014116x_2 + 0.043608x_3 + 0.042870x_1.x_2 - 3.37617E^{-003}x_2.x_3 \quad (4.12)$$

Where,

$y_{Ni} = Nickel\ Removal$
$y_{Pb} = Lead\ Removal$
$y_{Cd} = Cadmium\ Removal$
$y_{Mn} = Manganese\ Removal$

$x_1 = Matrix\ 4\ dose$
$x_2 = B = Contact\ time$
$x_3 = C = pH$

Table 4.17. ANOVA of Response Surface Quadratic Model for Ni, Pb, Cd and Mn

(a) Nickel

Source	SS	DF	MS	F Value	Prob> F	
Model	5.83	9	0.0179	7.12	0.0085	Significant
A	*0.14*	*1*	*0.14*	*1.51*	*0.2586*	
B	*0.044*	*1*	*0.044*	*0.49*	*0.5077*	
C	*0.42*	*1*	*0.42*	*4.66*	*0.0678*	
A^2	*0.21*	*1*	*0.21*	*2.26*	*0.1766*	
B^2	*0.016*	*1*	*0.016*	*0.18*	*0.6863*	
C^2	*2.66*	*1*	*2.66*	*29.30*	*0.0010*	
AB	*0.058*	*1*	*0.058*	*0.64*	*0.4499*	
AC	*0.75*	*1*	*0.75*	*8.25*	*0.0239*	
BC	*0.012*	*1*	*0.012*	*0.13*	*0.7307*	
Residual	*0.64*	*7*	*0.091*			
Lack of Fit	*0.26*	*2*	*0.13*	*1.73*	*0.2688*	*not significant*
Pure Error	*0.38*	*5*	*0.075*			
Cor Total	6.46	16				
Std Dev	0.30					
AdeqPrecision	9.421					

(b) Lead

Source	SS	DF	MS	F Value	Prob> F	
Model	370.97	9	41.22	193.70	<0.0001	significant
A	*5.96*	*1*	*5.96*	*28.01*	*0.0011*	
B	*0.85*	*1*	*0.85*	*3.99*	*0.0859*	
C	*241.21*	*1*	*241.21*	*1133.53*	*<0.0001*	
A^2	*0.88*	*1*	*0.88*	*4.15*	*0.0811*	
B^2	*0.49*	*1*	*0.49*	*2.31*	*0.1727*	
C^2	*111.56*	*1*	*111.56*	*524.26*	*<0.0001*	
AB	*0.22*	*1*	*0.22*	*1.03*	*0.3444*	
AC	*1.88*	*1*	*1.88*	*8.81*	*0.0208*	
BC	*0.35*	*1*	*0.35*	*1.66*	*0.2387*	
Residual	*1.49*	*7*	*0.21*			
Lack of Fit	*0.49*	*2*	*0.24*	*1.22*	*0.3696*	*significant*
Pure Error	*1.00*	*5*	*0.20*			
Cor Total	372.46	16				
Std Dev	0.46					
AdeqPrecision	38.461					

(c) Cadmium

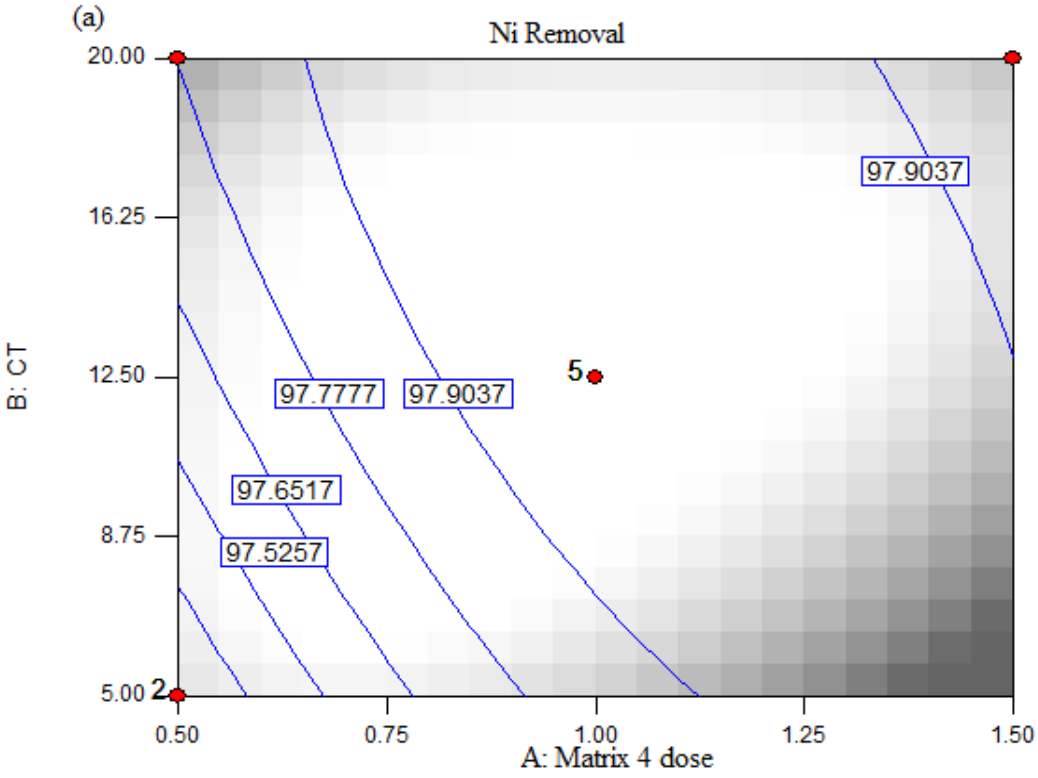
Source	SS	DF	MS	F Value	Prob> F	
Model	20.74	9	2.30	6.69	0.0101	Significant
A	*0.91*	*1*	*0.91*	*2.64*	*0.1484*	

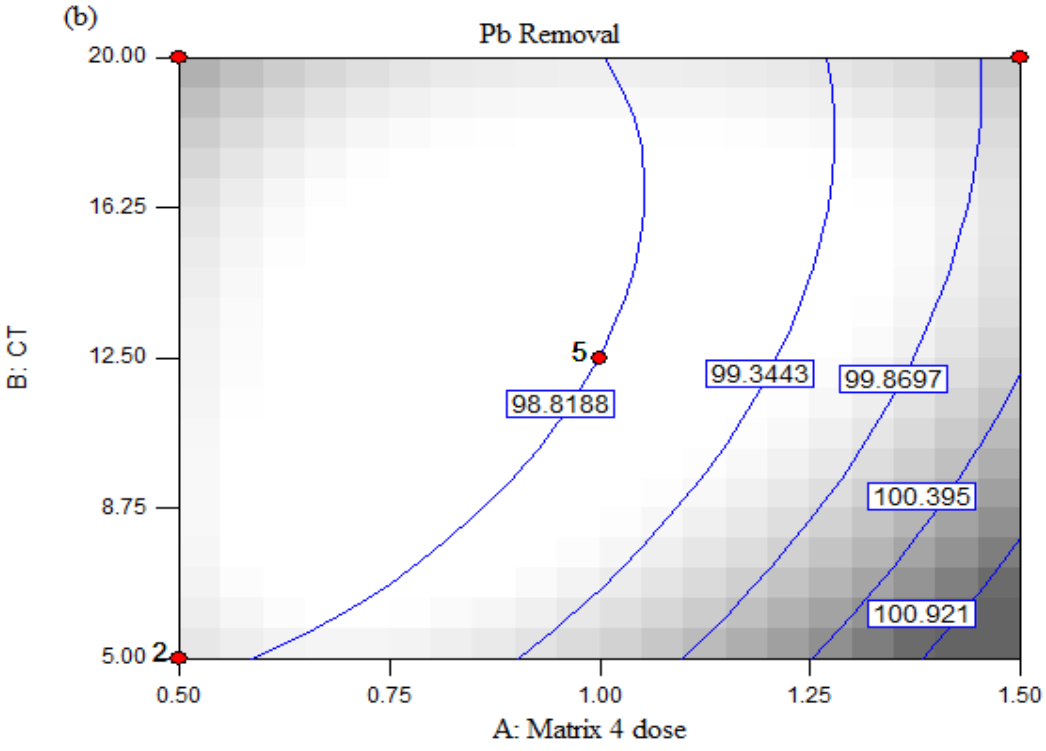
B	*0.051*	*1*	*0.051*	*0.15*	*0.7128*	
C	*0.23*	*1*	*0.23*	*0.67*	*0.4389*	
A^2	*0.29*	*1*	*0.29*	*0.85*	*0.3870*	
B^2	*2.26*	*1*	*1.97*	*5.70*	*0.0483*	
C^2	*1.97*	*1*	*1.73*	*5.02*	*0.0601*	
AB	*1.73*	*1*	*2.15*	*6.24*	*0.0411*	
AC	*2.15*	*1*	*0.015*	*0.045*	*0.8389*	
BC	*0.015*	*1*	*8.45*	*24.53*	*0.0017*	
Residual	*8.45*	*7*	*0.34*			
Lack of Fit	*1.16*	*2*	*0.58*	*2.32*	*0.1942*	*not significant*
Pure Error	*1.25*	*5*	*0.25*			
Cor Total	23.15	16				
Std Dev	0.59					
AdeqPrecision	7.215					

(d) Manganese

Source	SS	DF	MS	F Value	Prob> F	
Model	0.24	9	0.027	6.47	0.0111	significant
A	*3.026E-003*	*1*	*3.026E-003*	*0.72*	*0.4230*	
B	*0.029*	*1*	*0.029*	*6.92*	*0.0339*	
C	*0.059*	*1*	*0.059*	*14.19*	*0.0070*	
A^2	*0.056*	*1*	*0.056*	*13.43*	*0.0080*	
B^2	*1.068E-003*	*1*	*1.068E-003*	*0.26*	*06288*	
C^2	*1.666E-004*	*1*	*1.666E-004*	*0.040*	*0.8475*	
AB	*0.056*	*1*	*0.056*	*13.32*	*0.0082*	
AC	*2.770E-003*	*1*	*2.770E-003*	*0.66*	*0.4424*	
BC	*0.041*	*1*	*0.041*	*9.82*	*0.0165*	
Residual	*0.029*	*7*	*4.180E-003*			
Lack of Fit	*2.031E-003*	*2*	*1.016E-003*	*0.19*	*0.8354*	*not significant*
Pure Error	*0.027*	*5*	*5.446E-003*			
Cor Total	0.27	16				
Std Dev	0.065					
AdeqPrecision	7.669					

Where, DF = Degrees of Freedom
SS = Sum of Squares
MS= Mean Squares
F = Fischer and associated p values
$y_{Ni} = Nickel\ Removal$
$y_{Mn} = Manganese\ Removal$
$x_1 = A = Matrix\ 4\ dose$
$x_2 = B = Contact\ time$
$x_3 = C = pH$
$y_{Pb} = Lead\ Removal$
$y_{Cd} = Cadmium\ Removal$


(a)
Ni Removal
20.00
16.25
12.50
8.75
5.00
B: CT
0.50
0.75
1.00
1.25
1.50
A: Matrix 4 dose
97.9037
97.7777
97.9037
97.6517
97.5257
5
2


(b)
Pb Removal
20.00
16.25
12.50
8.75
5.00
B: CT
0.50
0.75
1.00
1.25
1.50
A: Matrix 4 dose
98.8188
99.3443
99.8697
100.395
100.921
5
2

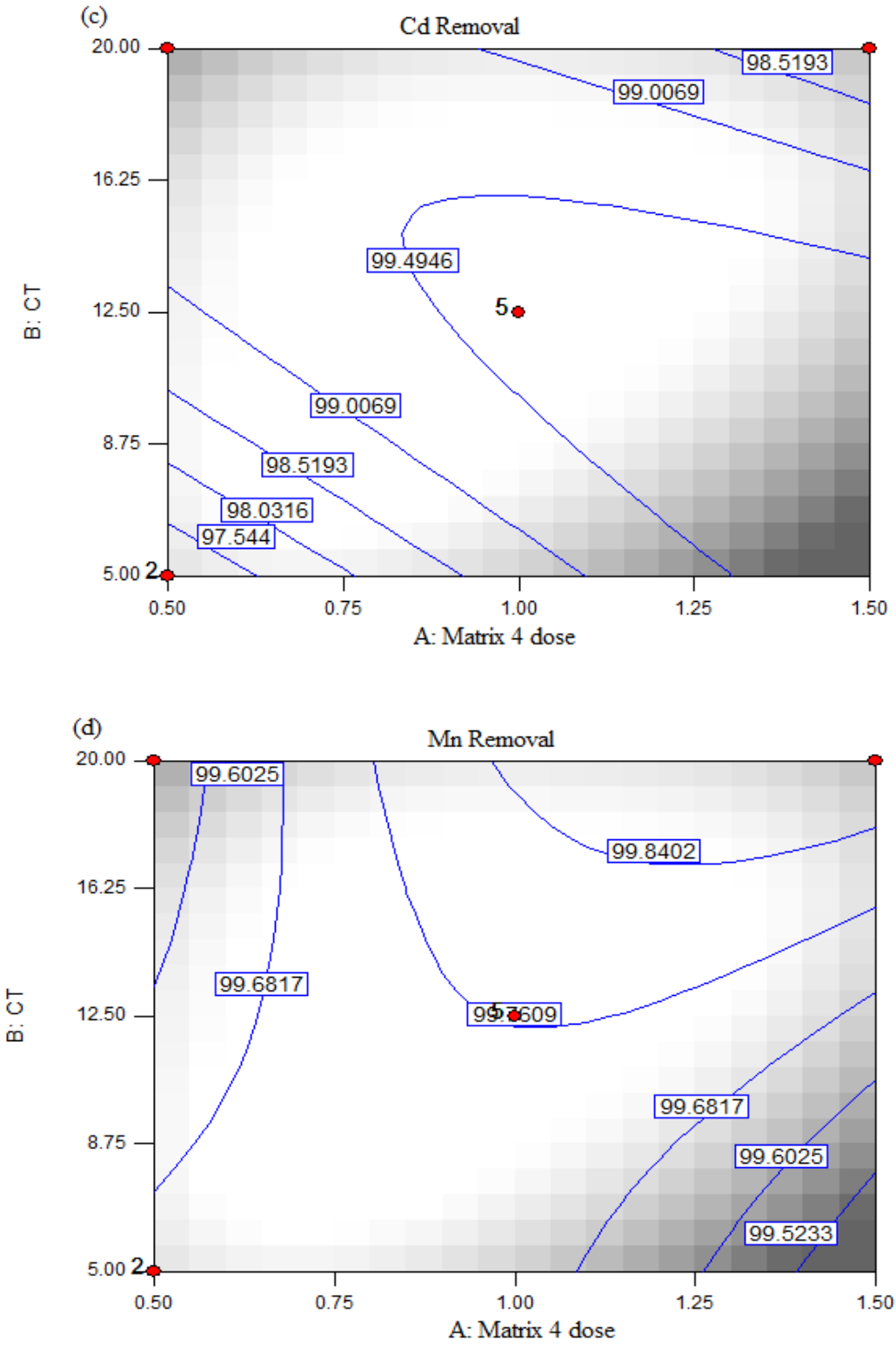


Figure. 4.51. The contour diagram for (a) Nickel (b) Lead (c) Cadmium and (d) Manganese

Table 4.18 Diagnostic case statistics for Nickel, Lead, Cadmium and Manganese

(a) Nickel

Standard Order	Actual Value	Predicted Value	Residual
1	98.70	98.72	-0.021
2	97.73	97.27	0.45
3	99..43	99.45	-0.021
4	97.56	97.76	-0.20
5	98.35	98.13	0.22
6	97.02	97.27	-0.25
7	98.21	98.44	-0.22
8	97.83	98.00	-0.16
9	98.16	98.00	0.16
10	98.05	98.00	0.054
11	97.78	97.78	0.000
12	99.03	99.00	0.021
13	98.05	98.27	-0.22
14	97.78	98.00	-0.22
15	98.16	98.00	0.16
16	99.30	99.07	0.22
17	98.70	98.68	0.021

(b) Lead

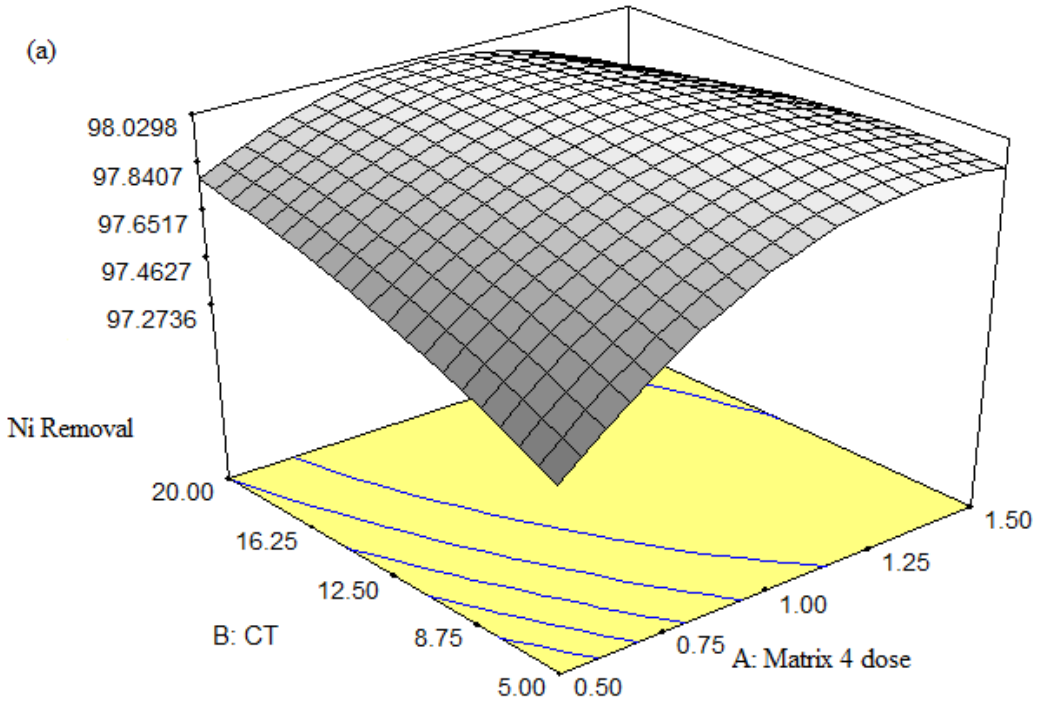
Standard Order	Actual Value	Predicted Value	Residual
1	87.39	87.32	0.066
2	98.81	98.75	0.067
3	99.53	99.47	0.066
4	99.69	100.03	-0.340
5	90.13	89.86	0.270
6	99..02	98.75	0.270
7	88.42	88.70	-0.270
8	98.97	98.82	0.150
9	98.60	98.82	-0.220
10	99.48	98.82	0.660
11	98.60	98.60	0.000
12	99.02	99.08	-0.066
13	98.50	98.77	-0.270
14	98.14	98.82	-0.068
15	98.92	98.82	0.094
16	99.17	98.90	0.270
17	86.36	86.42	0.660

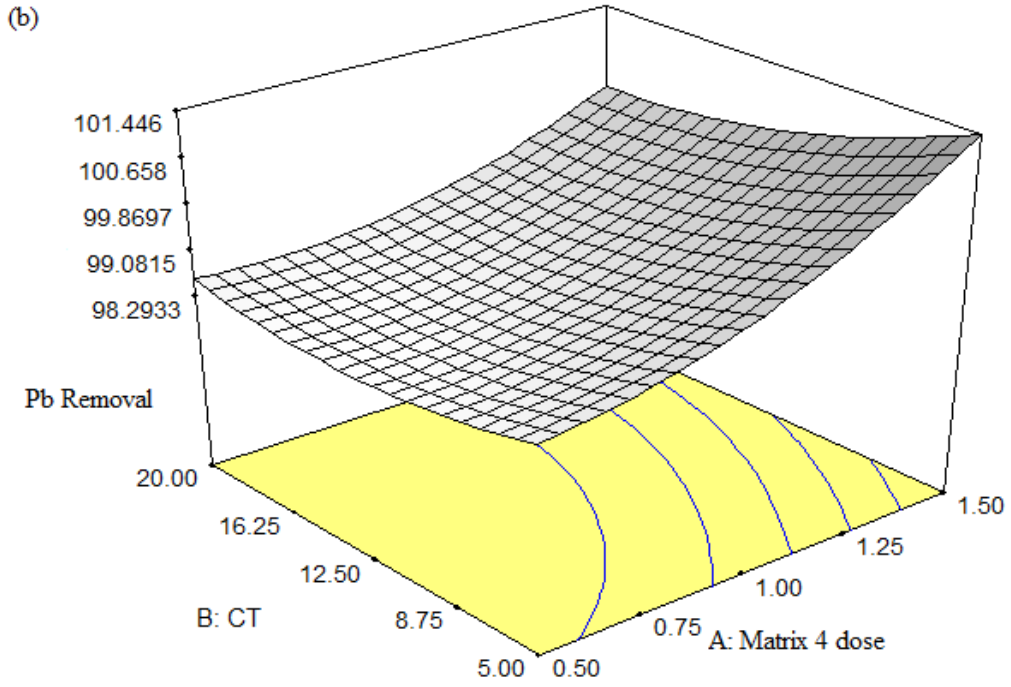
(c) Cadmium

Standard Order	Actual Value	Predicted Value	Residual
1	99.69	99.85	-0.17
2	96.78	97.06	-0.28
3	98.60	98.77	-0.17
4	98.60	98.05	0.55
5	98.85	99.24	-0.38
6	96.78	97.06	-0.28
7	97.14	96.76	0.38
8	98.82	99.60	-0.78
9	99.20	99.60	-0.41
10	100.00	99.60	0.40
11	99.24	99.24	0.000
12	99.49	99.32	0.17
13	98.47	98.09	0.38
14	100.00	99.60	0.40
15	100.00	99.60	0.40
16	96.22	96.61	-0.38
17	98.47	98.31	0.17

(d) Manganese

Standard Order	Actual Value	Predicted Value	Residual
1	99.83	99.84	-0.012
2	99.73	99.72	7.348E-003
3	99.54	99.55	-0.012
4	99.90	99.91	-6.196E-003
5	99.80	99.78	0.018
6	99.72	99.72	-1.152E-003
7	99.89	99.90	-0.018
8	99.74	99.76	-0.019
9	99.68	99.76	-0.081
10	99.74	99.76	-0.019
11	99.54	99.54	0.000
12	99.54	99.53	0.012
13	99.54	99.56	-0.018
14	99.90	99.76	0.14
15	99.74	99.76	-0.019
16	99.89	99.88	0.018
17	99.69	99.68	0.012


(a)
98.0298
97.8407
97.6517
97.4627
97.2736
Ni Removal
20.00
16.25
12.50
8.75
5.00
B: CT
0.50
0.75
1.00
1.25
1.50
A: Matrix 4 dose


(b)
101.446
100.658
99.8697
99.0815
98.2933
Pb Removal
20.00
16.25
12.50
8.75
5.00
B: CT
0.50
0.75
1.00
1.25
1.50
A: Matrix 4 dose

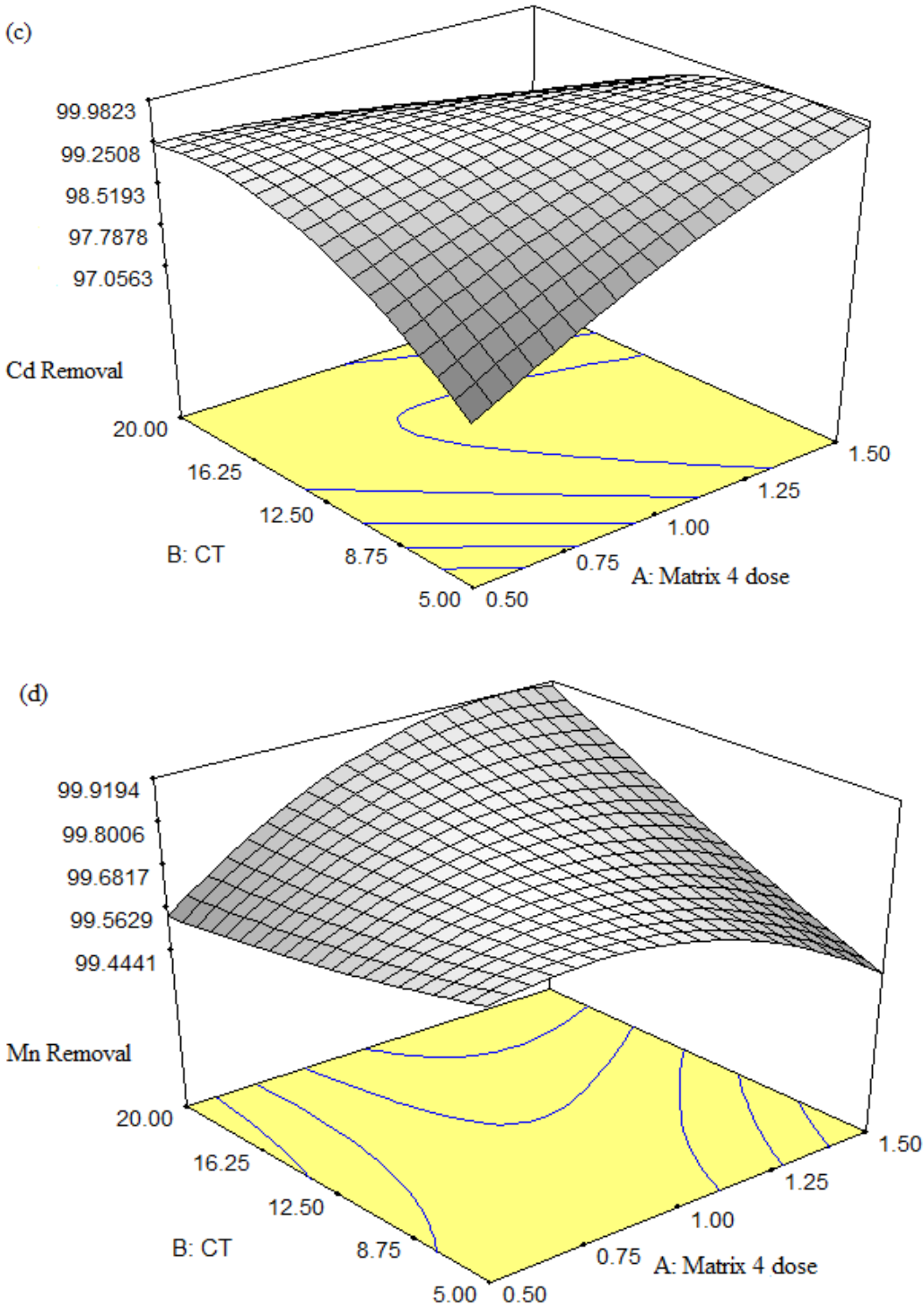


Figure 4.52 Three- dimentional Response Surface Plots for (a) nickel (b) lead (c) cadmium and (d) manganese

Table 4.19. The optimized RSM values

Name	Goal	Lower Limit	Upper Limit	Lower Weight	Upper Weight	Importance
Matrix 4 dose	maximize	0.5	1.5	1	1	3
Cont. time	maximize	5	20	1	1	3
pH	maximize	4	12	1	1	3
Ni Rmd	maximize	97.0224	99.4316	1	1	3
Pb Rmd	maximize	86.3561	99.6905	1	1	3
Cd Rmd	maximize	96.2221	99.9984	1	1	3
Mn	maximize	99.5413	99.9032	1	1	5

No.	Matrix 4 dose	Cont. time	pH	Ni Rmd	Pb Rmd	Cd Rmd	Mn Rmd	Desirability	
1	1.28	20.00	10.35	97.9908	94.234	99.239	99.9186	0.757	Selected
2	1.26	20.00	10.37	98.0194	94.1081	99.2856	99.9156	0.757	

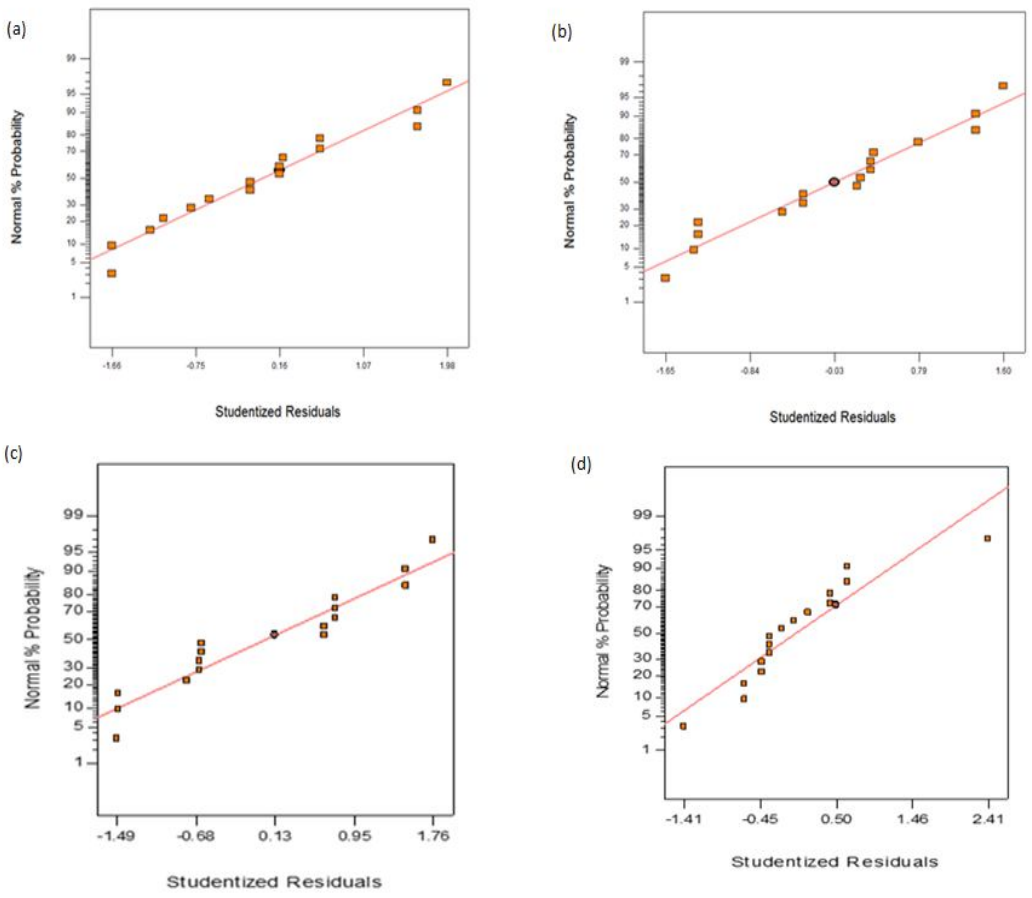


Figure. 4.53. Residual plot for (a) nickel (b) lead (c) cadmium and (d) manganese

CHAPTER FIVE

DISCUSSION OF RESULTS

5.1 Determination of Level of Heavy Metals in Crude Oil Tank Farm Wastewater

Table 4.1 shows the contaminant level of the crude oil tank farm wastewater discharged into the environment from a typical petroleum refinery. It can be seen from Table 4.1 that the difference in contaminant level before and after treatment by the refinery is negligible suggesting that the heavy metals are not adequately handled by the refineries. The pollution loading were ultimately high when compared with the regulatory standards in Tables 2.4 and 4.6.

5.2 Characteristics of the Adsorbents

5.2.1 Composition and structure of adsorbents

The chemical composition of the adsorbents from XRF results in Table 4.2 presents the weight percent of Zeolite 4A, beneficiated Kaolin and metakaolin that were employed in this work. The relative increase in the weight percent of silicon and aluminium oxides when kaolin was calcined was due to thermal decomposition of raw kaolin which eliminated the hydroxyl ions and undersirable volatile matter. Table 4.2 also revealed a loss of ignition (LOI) of 10.1777 wt % for Zeolite 4A which agreed with the literature values of (650 oC ± 10 oC, 3 hrs) < 12 % (http://www.weiku.com/quality-products) and a decrease in loss of ignition (LOI) for Kaolin to metakaolin, calcined at 750 ^{o}C for 3 hrs.Thus LOI for silicate minerals are within the range of 1 – 10 wt % (http://www.xrf.ethz.ch/xrf-forms.html). This can be attributed to the expurgence of water molecules. This compares favorably with findings of Hazard (2010), Ajayi (2012) and Carlos and Liz (2011). The Si/Al ratio of beneficiated kaolin fall within the

expected range, moreso when the geographical location and geological formation type and the process of beneficiation adopted are considered (Janjira, 2002, Ahmed, 1986, Ajayi, 2012). The elemental analysis conducted on the beneficiated kaolin, metakaolin and Zeolite 4A indicated the presence of impurities in kaolin, these findings are supported by XRD patterns presented in Figures 4.1(a-c). The Si/Al ratio clearly indicates the effect of these impurities, as also observed by Adel *et al.,* (2010).

Figures 4.1 (a-c) presents the XRD patterns for Zeolite 4A, kaolin and metakaolin. The XRD-pattern obtained in Figure 4.1a indicates a crystallite Zeolite 4A type. The commercial Zeolite 4A matched the characteristic peaks of the standard pattern at 2 theta values of 7.2, 10.3, 12.6, 21.8, 26.2, 32.6, and 34.3 as reported by Treacy and Higgins (2001). This means that the purchased commercial Zeolite 4A from UOP Honeywell Company USA was well refined. The X-ray diffraction analysis indicates the degree of crystallinity of the commercial Zeolites 4A sample indicating that the crystallite size is within the literature range (moderate crystallite size), thus high values indicate crystallization defects and lower value produces octahedral geometry (Adel *et al.,* 2010*)*.

Impurites and suspended solids were removed on beneficiation of Kankara kaolin. The beneficiated kaolin was calcined at 750 ^{o}C for 3 hours converting it to metakaolin. During this process, the kaolinite structure was destroyed yielding a more reactive and more amorphous metakaolin. The peaks for the kaolinite disappeared but some phases were relatively passive to the thermal treatment. This could aslo be attributed to the removal of the hydroxyl ions and rearrangement of the structure as depicted in Figure 4.1b & c. Thus the intensity of inherent impurities reduces drastically with thermal treatment. These observations were similar to those reported by Belver *et al.* (2002), Ajayi (2012) and Aderemi (2004).

An analysis of the peaks indicated a sharp peak with intensity at 2 theta = 12.335^{o} and d = 7.154 Å for Kankara Kaolin in Figure. 4.1b which was the main peak used for literature identification of Kankara Kaolin (Kovo, 2010). The XRD-patterns obtained for the metakaolin in Figure 4.1c showed a sharp peak with intensity at 2theta = 24.437 and d =3.6395Å different from that of kaolin which showed a difference in pattern as a result of the aforementioned thermal decomposition due to calcination processes as also observed by Ugal (2010).

From previous studies, this depicts a high quality metakaolin Tarek (2010), Min-qin Jiang (2010), Ajayi (2012) and Carlos and Liz (2011), suggesting a successful transformation of crystallinite phase of kaolin into a more amorphous phase called metakaolin.

The SEM pictures of Matrix 1, 2, 3, 4 and 5 presented in Figures 4.2 a - e showed the blends of cubic shape of Zeolite 4A and amorphous metakaolin in the respective ratios, indicaing homogeneity of the matrices

5.2.2 Ion Exchange Capability of the Matrices

Table 4.3 presents the ion exchange capacity for the five matrices. This was done to determine the effectiveness of the conditioning process. It was observed that the ion exchange capacities increased with increase in solution concentration for the matrices for Matrix 2 that showed a decrease for 1400 ppm concentration of the solution. This probably could be due to experimental blocks. However the result showed an improved sodium based matrices with high ionic sites, in line with Janjira's previous claim (Janjira, 2002). Comparing matrices 1 to 5 in this same order at 2000 ppm solution concentration in Table 4.3, it was observed that there was decrease in the exchange

capacities. This could be as a result of the Zeolite 4A - metakaolin compostions. This was confirmed by the results from Janjira (2002).

5.3 Heavy Metal Removal from Simulated Wastewater by the Matrices

This section presents discussions on the metals' adsorption from the simulated wastewater by application of the five matrices to estabublish the best Matrix and best conditions.

5.3.1 Effect of pH on Heavy Metal Removal

Figures 4.3 and 4.4 indicate an increased removal from pH of 4 to 10. Thereafter, the metal removal dropped to 10 % for lead as shown in Figure 4.3. No significant metal removal was observed after the pH of 10 as indicated Figure 4.4. This then implies that metal removal was significant within the pH range of 8 to 10. This might be due to the concept of point of zero charge (pzc) which is the pH at which a solid exhibit zero net charge on the surface when submerged in an electrolyte. Thus there could be possible precipitation of hydroxyl ions and the possible formation of complexes which might clog the pores leading to partial destruction of the structure at pH above 10 (above pzc). This agrees to the findings reported by Inglezakis (2000). At lower pH (below pzc), the acidic simulated wastewater donates more proton, hence, the reduced heavy metals removal at pH 2 and 4 in Figure 4.4 could probably be as a result of competitions between the hydrogen and the metal ions for the exchage sites. The pH range of 8 to 10 was obtained for nickel, cadmium, manganese and 12 for lead as depicted in Figure 4.4. The mechanism of adsorption at the surface reflects the nature of the physiochemical interaction of the metal ions (present in the solution) and the adsorbent's active sites, which is also in agreement with Hui's report (Hui, 2005).

5.3.2 Effect of matrix dose on heavy metal removal

Figures 4.5 to 4.9 present the removal of Ni, Pb, Cd and Mn ions as a function of adsorbent dose at a sample pH of 8 and maximium contact time of 60 minutes (Selverj *et al.*, 2003). It was observed that increasing Matrix 1 adsorbent dosage, lead to increased percentage removal for almost all the metal ions at 0.25 g/50 ml except for lead as depicted in Figure 4.5, whose relative ionic radius is large compared to Ni, Cd and Mn as indicated in Table 2.3. It was also observed that the removal efficiency increases up to the optimal dosage of 0.5 g/50 ml for Matrix 2, 3, 4 and 1 g/50 ml for Matrix 5 beyond which increase in Matrix dose has no significant change in the removal efficiency of the heavy metals as shown in Figures 4.6, 4.7, 4.8 and 4.9. It is apparent that the percentage removal of heavy metals increases rapidly with increase in the dosage of the matrices due to the greater availability of the exchangeable sites and surface area (Edison *et al.,* 2011)

5.3.3 Effect of contact time on heavy metal removal

Figures 4.10 to 4.14 show the effects of contact time on the removal of nickel, lead, cadmium and manganese ions by matrices 1 to 5. The time to attain maximum nickel, cadmium and manganese metals removal with Matices 1 and 3 appear to be 5 minutes (Figures 4.10 and 4.12), 10 minutes with Matrices 2 and 4 as indicated in Figure 4.11 and 4.13. Then 60 minutes with Matrix 5 shown in Figures 4.14. This could probably be attributed to the available active sites, pore volumes and surface area of the different matrices. There was an observed drop in lead ion removal at contact time of 20 minutes for the five matrices which is well pronounced in Figure 4.11. This could be attributed to the properties of lead. The relative ionic radius of lead is high compared to other metals as depicted in Table 2.3. This implied that the bond existing between the

adsorbate and adsorbent is a weak bond probably vander-Waals bond. Upon continuous agitation, there is every possibility that desorption could occur thereby creating more active sites. Adsorption of lead increased after 20 minutes probably because of the unoccupied sites. This therefore assumed a heterogenous coverage which is depended on available sites.

The longer contact time of 60 minutes for Matrix 5 in Figure 4.14 could be attributed to the fact that the amorphous metakaolin is not structurally as rigid as Zeolites 4A, as such there could be the possibility of compacted layers as it comes in contact with simulated wastewater thereby hindering immediate diffusion into the pores. It is then evident from the results that contact required to attain maximium metal removal is dependent on the initial concentration of heavy metals in the wastewater and the type of adsorbent used as reported by (Taha *et al.*, 2010).

5.3.4 Effect of initial concentration of heavy metals on adsorption

Figure 4.15 presents the effect of initial concentration on the removal of nickel, lead, cadmium and manganese ions by Matrix 5. There was increase in the removal of the four metals at 55 ppm. Further increase in initial concentration resulted no significant effect on heavy metals removal which conformed to an observation made earlier by Inglezakis (2000). Nickel ion removal recorded a sharp drop with 100 ppm solution. This implies that the percentage removal decrease with increase in initial heavy metal concentration. This could be attributed to the fact that, at lower initial metal concentration, sufficient adsorption sites are available for adsorption. Then at higher concentration, the metal ions are relatively high against the available adsorption sites. This agree with the observation made by Ajay *et al*. (2005). The difference in percentage metals removal of different metal ions at the same conditions (adsorbent dose, contact time, pH and initial concentration) may be attributed to the difference in

chemical affinity and ion exchange capacities (Ajay *et al*. 2005, Inglezakis, 2000 and Ismail, 2013). The minimal removal of lead compared to the three other metals could be attributed to the large relative ionic radius as shown in Table 2.3.

5.4 Determination of Best Matrix and its Selectivity

5.4.1 Selection of the best matrix based on adsorption capacity

Figure 4.16 presents the metal removal capacities for three matrices (blends of Zeolite 4A and metakaolin). The three matrices are blends of Zeolite 4A and metakaolin treated at the same conditions of initial concentration, contact time of 10 minutes and at pH of 8. The Matrix 2, Matrix 3 and Matrix 4 showed high removal (nearly 100 %) of all the metals except lead as shown in Figure 4.16. Comparing Matrices 2, 3, 4 based on lead removal, Matrix 4 was considered as the best because it almost attained aggregate removal of all the metals under consideration and contained the least proportion of the expensive Zeolite 4A.

5.4.2 Determination of the selectivity for metal removal

The effect of Matrix 4 on heavy metal removal is shown in Figure 4.17. As indicated in Figure 4.17, removal order of the metal by Matrix 4 is Mn^{2+}> Cd^{2+}> Ni^{2+}.>Pb^{2+}.

Lead has the highest relative ionic radius among the selected heavy metals as presented in Table 2.3. As such it is loosely bonded with low effective ionization energy, so adsorption of lead would be minimal when compared to other metals under consideration. Furthermore, because the mechanism is physical adsorption, a weak van der Waal bond could be expected which under constant vigorous agitation could lead to desorption of the loosely bonded metals. This probably could further be attributed to the affinity of the metals to the adsorbent and the effective properties they present arising from their relative placement in the Periodic Table.

5.5 Analysis on Interferences of the Individual Heavy Metals in the Simulated Wastewater

Figures 4.18 to 4.20 were used to determine the interactive effect of metal salts. Steric effects could arise from the fact that each metal occupies a certain space. Since all the metals were brought together for preparation of the simulated wastewater as described in Section 3.2.2, there could be overlapping electron clouds affecting ionic shape and reactivity (www.chem.swin.edu.au). These were checked by adopting an experimental design whereby the dosing was done first indently (i.e. selectively), next dosing with two at a time and ultimately all together. The various known concentrations were then carefully analyzed using AAS. Ni and Mn ion were completely removed, followed by Cd and then Pb as shown in Figure 4.18. Figure 4.19 showed the same trend for Ni and Mn irrespective of the variations of the solution composition. Figure 4.20 showed a removal order as observered in Figure 4.17 for heavy metal selectivity. This implied that there is no interference of the metals as they were in solution and there is no steric hindrance or resistance which could have been as a result of steric effects. Incases, where there are complexes of metals in wastwater, pretreatments like chemical digestion could be carried out, to release the metals to their free ionic form (Mudi, 2011).

5.6 Characterization of the Best Matrix (Matrix 4)

The XRD of the best matrix (Matrix 4) is presented in Figure 4.21.The various peaks of Zeolite 4A and metakaolin were indicated in Figure 4.21, which shows a blend of Zeolite 4A and metakaolin in the ratio of 25 to 75 % respectively. The cubic shaped Zeolite 4A and amorphous structured metakaolin were evenly distributed at the various 2 theta positions. The crystalline structure of Zeolite 4A were identified by sharp peaks with specific 2 theta angle while the amorphous metakaolin were equally identified by diffuse peaks distributed in a wide 2 theta range.

5.6.1 Morphology and surface conditions of the matrices

Figures 4.22(a) & (b) present the SEM results of Matrix 1 before and after metals' adsorption respectively. Figures 4.22(b) presents the SEM image of a cloudy phase of spent Matrix 1 showing that the metals have been deposited on the surfaces.

The SEM image of the corresponding spent Matrix 4 shown in Figure 4.23(b) indicates deposition of heavy metals in the lattices of the Zeolite 4A - metakaolin matrix. This could further be observed in the corrresponding EDX results in Table 4.4. The drop in the weight percent of sodium oxide could be attributed to its ion being exchanged with the heavy metals in the simulated wastewater.

The results of XRD pattern in Figure 4.21 as supported by SEM images of Matrix 5 (100 % metakaolin) before and after metals' adsorption presented in Figure 4.24 (a) and (b) show phase transformation of kaolinite into amorphous metakaolin. The diffused peaks show clustered amorphous phase of metakaolin obtained by decomposition by the reaction such as:

$$2Al_2SiO_5(OH)_4 \rightarrow 2Al_2SiO_7 + 4H_2O \qquad \text{(Ugal } \textit{et al.,}\text{ 2010)}$$

Generally the SEM images of spent Matrices 1, 4 and 5 shown in Figures 4.22(b), 4.23(b) and 4.24(b) respectively indicate the deposition of heavy metals in the pores of the matrices. The pictorial view was further supported by the BET results in Table 4.5 which indicated the difference in the surface area and pore volumes of Matrix 1, 4 and 5 before and after metals' ion exchange depicting the sites occupied by the deposited heavy metals. The magnitude of the pore volume occupied suggests a hetero-layer coverage as would be subsequently explained by the isotherm and kinetic models in Section 4.8.

The heavy metal ion exchange capabilty of the matrices depends on the Si/Al ratios (Adel *et al.,* 2010). Ratios greater than 1.15, could lead to the intra-ionic Na–Na repulsive forces resulting in displacement of the ions by itself from the sodalite units, so Si/Al ratio close to 1 improves ion exchange ability for the matrices (Adel *et al*., 2010).

The EDX results in Table 4.4 depicted other consituents of the matrices. This quantified the mineral phases and some associated elements before and after metals' adsorption showing the inherent impurities present and indicates the Si/Al ratios which promotes ion exchange abilities of the matrices. Siddhesh *et al.* (2004) observed that the improved ion exchange performance of zeolites is related to the Si/Al ratio.

The EDX results in Table 4.4 indicate a marked reduction in sodium (weight %) from 21.31 to 8.02, 16.81 to 11.23 and 7.06 to 6.87 for Matrix 1, 4 and 5 respectively. This is possible indicator that the deposited heavy metals within the pores of matrices 1, 4 and 5 as shown in Figures 4.22, 4.23 and 4.24 were actively exchanged by the sodium ions in their pores. This could explain the reduction in the surface areas of the adsorbent matrices as presented by BET result in Table 4.5.

Table 4.5 presents the BET results showing the external area, surface area, the pore size, pore distribution and pore volumes. All these control transport phenomena and selectivity as reported by Kovo (2011).

The differences in pore volume and surface area in Matrix 1, Matrix 4 and Matrix 5 before and after use indicate the amount of the metals deposited on the surfaces of the matrices as depicted in Figures 4.22, 4.23 and 4.24 in the SEM images and possibly the quantity taken into the pore volume and the surface area occupied by these metals. The calcined Kaolin (irrespective of its source and treatment) had specific surface area ranging from 8.5 to 10.6 m^2/g as reported by Ajayi (2012), thus the high surface area of

Matrix 5 is inappropriate. This could probably be attributed to its muddled layer due to its irregular structure. But the marked reduction is an evidence that metals were deposited on the surfaces. The reduction in surface areas after metals' adsorption could likely be attributed to aggregation of particles when water molecules were removed. The increase in average pore diameter of Matrix 5 from 12.4664 to 16.7463 could also be attributed to its irregular pore size (lack of molecular sieve effect) as such metals gained high accessibility to the pores in Matrix 5 resulting to adsorption of other molecules. But the EDX result in Table 4.4 indicates the actual concentration of the heavy metal ions exchanged with sodium ions. These agrees with the observations made by Adel (2010).

5.7 Determination of Heavy Metal Removal from Crude Oil Tank Farm Wastewater

The crude oil tank farm wastewater was analysed at the best experimental treatment conditions of 1 g of Matrix 4 in 50 ml crude oil tank farm wastewater at 10 minutes contact time and pH of 8. The results shown in Figures 4.25, 4.26 and 4.27 for crude oil tank farm wastewater followed the same trend as in Figures 4.3, 4.8 and 4.13 for simulated wastewater. They showed very high removal for nickel, cadmium and manganese. The relatively low lead removal could be attributed to the aforementioned effective properties they present arising from their relative placement in the Periodic Table – the relative weak strength of the ionic charge of lead arising from its bigger radius than others (Table 2.3), may account for this phenomenon.

Figure 4.28 presents the comparison of heavy metal removal results obtained for the laboratory simulated wastewater and the real crude oil tank farm wastewater. The aforementioned samples were subjected to the same treatment at the same conditions of

Matrix 4 dose of 1 g/50 ml, pH of 8 and contact time of 10 minutes. Thus Matrix 4 is able to remove the following ions as shown in Figure 4.28:

Nickel (Ni) – 100%

Manganese (Mn) – 100 %

Cadmium (Cd) – 90 - 99 %

Lead (Pb) – 80 – 90 %

The only discrepancy here is lead, and this could be attributed to the aforementioned properties (Table 2.3).

The concentrations before and after treatment for the crude oil tank farm wastewater presented in Table 4.6 indicate that the heavy metals were removed even far beyond the threshold limits of NESREA. This signifies the appropriateness of the selected matrix and conditions for heavy metal removal.

5.8 Adsorption Isotherms and Kinetic Studies

5.8.1 Adsorption isotherms studies

Figures 4.29 (a-c), 4.30 (a-c) and 4.31 (a-c) present the plots of Freundlich, Langmuir and Temkin's adsorption isotherm models for nickel, lead and cadmium. The removal of metals for the various contact times for manganese are rapid due to it's affinity to the matrix, thus graph cannot be plotted where all the x values are the same. The values of the constants and correlation coefficient (R^2) shown in Table 4.7, confirmed that adsorption of the heavy metals on Matrix 4 were best fitted to Freundlich (Figure 4.29a-c), Langmuir (Figure 4.30a-c) and Temkin (Figure 4.31a-c) isotherm models, with higher values of correlation coefficient (R^2) for nickel, lead, cadmium respectively

indicating that adsorption is onto heterogeneous surface with decrease in adsorption energy due to adsorbent–adsorbate interaction as also reported by Ismail *et al*. (2013). This is in agreement with Freundlich assumption which states that adsorption is dependent on available sites. Ions continue to pile on the active sites until saturation is attained. At this point, the driving force approaches zero. The slope between 0 and 1 presented in Table 4.7 for Freundlich is a measure of adsorption intensity or surface heterogeneity, becoming more heterogeneous as its value approaches zero (Mohammad *et al.*, 2010). $1/n > 1$ indicates a favourable adsorption condition. Thus the plot of log q_e versus log C_e in Figure 4.29 gave a straight line with slope 1/n greater than 1. K_F was calculated from the intercept value. The values of linear regression correlation (R^2) are tabulated in Table 4.7.

The high value correlation coefficient of determination for Langmiur isotherm in Figure 30 indicates that the model is significant to the process. Langmuir assumption was based on the fact that all active sites have equal potentials, as such adsorption is unto a monolayer coverage. The correlation and calculated parameters are also shown in Tables 4.7.

The Temkin isotherm model presented in Figure 4.31 (a-c) is a good fit for the process. As aforementioned, this presents the adsorbate-adsorbent interaction during the adsorption process. The correlation coefficient of determination R^2 shown in Table 4.7 suited the process. Energy of adsorption decreases linearly with the adsorption process indicating multi-layer coverage as described by Freundlich isotherm in Figure 4.29. The negative values for b (constant, related to heat of adsorption) in Table 4.7 is an indication of physical adsorption process as well as exothermic process as also described by Xiaolin *et al.* (2012). Suggesting that the selected heavy metals has high affinity with the Matrix as such less binding energy was required.

5.8.2 Adsorption kinetics

Three models were considered, the pseudo-first-order kinetic model, pseudo-second-order kinetic model and the intra-particle diffusion model as shown in Figures 4.32 (a-c), 4.33 (a-c) and 4.34 (a-c). The R^2 for the pseudo-first-order model does not fit the process as indicated in Table 4.8, this according to Lagergren, (1989) assumed that the rate of solid uptake with time is directly proportional to the difference in the equilibrium concentration and the amount of solute uptake with time (Silvio and Jorge, 2009).

The correlation coefficients for pseudo-second-order kinetic model in Figures 4.33 (a-c) were all approximately equal to 1 as shown in Table 4.8 with high predicted adsorption capacity (q_e) in Table 4.8 which are close to the experimental values. This was based on adsorbate-adsorbent interaction as comfirmed by Ho and Mckay (1998). It is assumed that adsorption capacity is proportional to the active sites occupied by the adsorbent, thus the values of R^2 clearly depicts a high adsorbate–adsorbent interaction for all the metals indicating that the process is of the pseudo-second-order kinetic model. This also supports Freundlich description of adsorbate-adsorbent interaction indicated in Figure 4.29 (a-c). This process is said to be achieved through exchange of electrons btween the adsorbent and adsorbate until equilibrium was attained thus adsorption is onto heterogeneous surface as reported by Xiaolin *et al* (2012).

Intra-particle Diffusion Model

Intra-particle diffusion model in Figure 4.34 showed a very low coefficient of determination (Table 4.8). Thus, this diffusion model explains the transport of the metals from the solution phase to the surface of the adsorbent (Aleksandra *et al.,* 2013), as such, this does not fit the process as it covers only the external transport.

5.9 Statistical Analysis of Data using Computer Software

5.9.1 Full factorial analysis

A MINITAB version 14.0 software was used to carry out a full factorial analysis to evaluate the three factors at a time and in two replicates as presented in Table 4.9. For each run in Table 4.9, the percentage heavy metal removal from the simulated wastewater sample was measured. The heavy metal profile indicates the efficiency of heavy metal removal from the simulated wastewater and the responses in the experimental design.

Equations 4.1 to 4.4 were generated from the factorial analysis using the data in Table 4.9. The significant coefficients were substituted into the model equations based on the values of P less than 0.05 as depicted in Table 4.10.

It is a known fact that a good standard by which to evaluate a model is to look at p-values as presented in Table 4.10. The "p" – values of 5 % are normally used for chemical industries and if all terms have p-values less than the level "α" appropriated for the experiment, it is certain to have a good model (Montgomery, 2005). In this research, $\alpha = 0.05$ was chosen.

The p-value for each term in the model is less than 0.05 except for X_2 and $X_1 X_2 X_3$ for almost all the metals, indicating a good model for further exploration and validation. This model is considerably simpler and fits the data reasonably well.

The models in Equation 4.1, 4.2, 4.3and 4.4 were further checked by using the residual plots as shown in Figures 4.36, 4.38, 4.40, 4.42, 4.44, 4.46, 4.48 and 4.50. The fitted values were the results predicted by the model. These residuals are the actual response data minus the predicted response. A randomly distributed residual plot is an indicator of adequacy of a model as also reported by Daaniya (2012) thus the residuals were

randomly distributed and did not follow a particular trend signifying the models are statistically appropriate.

Active effects, are effects that are significant or important as shown in Figures 4.35, 4.39, 4.43 and 4.47. In these normal plot of the effects, points that do not fit the line well usually signal active effects.Thus active effects are larger and further from the fitted line than inactive effects therefore, inactive effects tend to be smaller and centred on zero, the mean of all the effects. The normal probability plot labels effects that are lower than the level. The normal probability plot of the standard effects shown in Figures 4.35, 4.39, 4.43 and 4.47 indicates that all other terms in the model are significant and active except the X_2.

A Pareto chart in Figures 4.37, 4.41, 4.45 and 4.49 is another useful tool that was used to determine the effects that were active. The Pareto chart uses the same α as the normal plot to determine the significance of effects, terms in the model except X_2 and X_2X_3 were significant ($\alpha = 0.05$).

To calculate main effects, Minitab subtracts the mean response at the low or first level of the factor from the mean response at the high or second level of the factor. Tables 4.10, 4.11 and 4.12 summarized the findings: An interaction plot shows the impact that changing the settings of one factor has on another factor. Because an interaction can magnify or diminish main effects, evaluating interactions is extremely important.

The p-value for each term in the model is less than 0.05 as shown in Table 4.10 except for for contact time and other terms interacting with it denoted as two-way interaction and three-way interaction as presented in Table 4.11 and Table 4.12 depicts the model fit based on the values of correlation coefficient. This indicates that X_1 and X_3 have bigger main effect on the dependent variables than X_2. Thus X_2 (contact time) produces a

relatively small effect as it changes from the reference point due to saturation of the active sites within a short period of time.

5.9.2 Optimisation by Response Surface Method (RSM)

A factorial analysis could indicate the significant factors and their interactive effects on the response. And could also give an idea of the optmal conditions for maximium output but response surface method (RSM) by DESIGN EXPERT version 6.0.8 would give a more precise and specific optimal values that will achieve the desired response/target (maximium removal of the heavy metals from the simulated wastewater) (Sumen, 2013). Table 4.13 presents a sequence of designed experiments that will be used to obtain optimal response. A total of 17 adsorption experimental runs as detailed in Table 4.13 were carried out in a batch process, employing detailed conditions designed by response surface methodology (Box – Behnken design) and the respective responses were obtained in percentages (y_{Ni}, y_{Pb}, y_{Cd} and y_{Mn}).

Tables 4.14 (a – d), present the highest order polynomial where the terms are significant. For each source of terms (linear, quadratic and cubic), the probability ("PROB > F") was examined to see if it falls below 0.05, the quadratic model looks best – these terms are significant, but adding the cubic other terms will not significantly improve the fit.

The fit summary in Table 4.15 shows that quadratic model is the suggested selected model with R^2 of 0.9015 and adjusted R^2 of 0.7748 for nickel, the same trend applied for lead, cadmium and manganese. This value is higher than -0.5539 and -1.2901 values respectively obtained for linear and two factor interaction (2FI) model. This shows that adding the quadratic (squared) terms to the mean, block, linear and two factor interaction terms already in the model is significant. Lead, cadmium and manganese

followed the same trend with R^2 0.9960, 0.8958, 0.8927 and adjusted R^2 of 0.9909, 0.7619, 0.7548 respectively.

The word lack of fit refers to the fact that the simple linear regression model may not adequately fit the data. If the sum of squares (SS) for lack of fit is small, there is evidence that the simple regression model is more appropriate to explain the relationship of the parameter (Prasad, 2002, Yi *et al.*, 2011). The "Lack of Fit Tests" shown in Table 4.16 compares the residual error to the "Pure Error" from replicated design points. In this case, the linear model definitely can be ruled out, because it's Prob > F falls below 0.05. The "Lack of Fit F-value" of 1.73, 1.22, 2.32 and 0.19 for nickel, lead, cadmium and manganese in Table 4.16 implied that the lack of fit is not significant relative to the pure error. There were 26.88, 36.96, 19.42 and 83.54 % chance that a "Lack of Fit F-value" this large could occur due to noise. Non-significant lack of fit is good so the model was proven to fit.

The "Model Summary Statistics" Table 4.15 lists other statistics useful in comparing models. The quadratic model comes out best with Equations 4.5, 4.6, 4.7 and 4.8. It exhibits low standard deviation ("Std. Dev.") values of 0.30, 0.46, 0.59 and 0.065, high "R-Squared" value of 0.9015 for Ni and 0.9960 for Pb, 0.8958 for cadmium and 0.8927 for manganese.

Values of "Prob > F" less than 0.0500 indicate model terms were significant. In this case C^2 , and AC for nickel, A, C, C^2, AC for lead, B^2, AB, BC for cadmium and B, C, A^2, AB, BC for manganese are significant model terms. Values greater than 0.1000 indicate the model terms are not significant. If there are many insignificant model terms (not counting those required to support hierarchy), model reduction could improve the

model thus applying the concept led to the generation of refined Equations 4.9, 4.10, 4.11 and 4.12.

Adequate precision measures the signal to noise ratio. A ratio greater than 4 is desirable (Myers and Montgomery, 2002). The ratio of 9.421, 38.461, 7.215 and 7.669 for nickel, lead, cadmium and manganese respectively indicate an adequate signal.

The ANOVA presented in Table 4.17 confirms the adequacy of the quadratic model (the Model Prob>F is less than 0.05). The Model F-value of 7.12, 193.70, 6.69 and 6.47 for nickel, lead, cadmium and manganese implies the models are significant. There is only a 0.85, 0.01, 1.01 and 1.11 % chance for nickel, lead, cadmium and manganese respectively, that the "Model F-Value" this large could occur due to noise.Values of "Prob > F" less than 0.0500 indicated model terms are significant..

The contour plots shown in Figures 4.51 (a to d) and the three- dimensional response surface plots presented in Figure 4.52 (a – d) are for Ni, Pb, Cd, and Mn removal as a function of contact time and Matrix 4 dose at a mid-level slice of pH. This slice includes five center points as indicated by the dot at the middle of the contour plot. By replicating center points, a very good power of prediction at the middle of experimental region could be obtained.

The important diagnostic tool presented in Table 4.18, which was used was for the normal probability plot of the standardized residuals. The data points from the plot were approximately linear, which showed that the quadratic model developed a good representation of the process.

Figures 4.53 (a-d) show the plots of the predicted versus actual experimental values for nickel, lead, cadmium and manganese showing that the actual values are distributed relatively near the straight line. This also indicates a close range between the

experimental values to the calculated values as presented in Table 4.18. These indicate that the models are adequate for predicting the efficiency within the range of the variables studied as was also observed by Prasad (2002). Thus the optimal conditions for maximum removal of the heavy metals as shown in Table 4.19 are the Matrix 4 dose of 1.28 g/50 ml, contact time of 20 minutes and pH of 10.35.

CHAPTER SIX

CONCLUSION AND RECOMMENDATIONS

6.1 Conclusion

The analysis of the wastewater drained from the crude oil tanks of Kaduna Refining and Petrochemical Company (KRPC) in Kaduna is highly toxic; as such, the conventional treatments by the petroleum refineries does not cater for the toxic inorganic heavy metals contained in the effluent.

Adsorption and ion exchange of Zeolite 4A–metakaolin matrices obtained by blending commercial Zeolite 4A and calcined Kankara Kaolin was efficient for aggregate removal of the four heavy metals (Ni, Pb, Cd and Mn) from the crude oil tank farm wastewater. The results of cation exchange capacity (CEC) study proved that that a sodium base matrices were achieved after the pre – treatment (calcination and conditioning) processes. Well-defined mathematical models were established for the process. The correlation coefficient (R^2) for the models showed that the actual data fitted well with the predicted data from the models and the values of R^2 for adsorption isotherm showed that the experimental data fitted well with the Freundlich, Langmuir and Temkin isotherms which implied a multi – layer adsorption, with adsorption energy decreasing linearly with surface area coverage due to adsorbent–adsorbate interactions. The factorial experimental design with MINITAB 14 software was a useful tool for the screening process and it indicated that the interactive effect of the variables on the response is highly significant. The R^2 depicts that the model equations are good representation of the experimental data. The residual plot showed randomly distributed points indicating that the models are good representation of the experiment. The optimal

conditions for the maximium removal of the heavy metals are as follows: Matrix 4 dose is 1.0 g/50 ml, contact time of 20 minutes and pH of 10.

6.2 Recommendations

Based on the extent of work covered on this dissertation, the following recommendations and suggestions were made:

1. The produced water from the main oilfields should be used to test the generated models.
2. The study should be extended to cover the engineering design and fabrication of an adsorption unit based on the generated models and conditions.
3. The adsorption column study for the process should be undertaken.
4. There is the need need to upgrade the structure of locally available kaolin in terms of rigidity.
5. Adequate awareness should be created on the need to exploit the local kaolin for industrial applications.
6. The laid – down environmental regulatory polices should be enforced strictly to monitor wastewaters discharge to the environments.

6.2.1 Contributions to knowledge

1. The development of adsorbent for aggregate removal of some specified heavy metals.
2. Development of models for adsorption processes.
3. The use of experimental data to relate adsorption properties of the heavy metals in the Periodic Table.

REFERENCES

APHA-AWWA-WPCE (1980). *Standard Methods for the Examination of Water and Wastewater,* 15th ed. APHA Washington, U.S.A.

Adel, A. I., Mohameda, R., Ibrahima, I. A., Kinib, G. & Koopman, B. (2010). Synthesis, Optimization and Characterization of Zeolite and its Ion-exchange Properties. *Physicochemical and Engineering Aspects*, 366, 80–87.

Adefila, S. S., Ajayi, O. A., Atta, A., Aderemi, B. O., Ahmed, A. S. & Ityokumbul, M. T. (2012). Synthesis of Zeolite ZSM3 from Faujasite: Effects of Post–synthesis Ageing and Insitu Seeding. *Chemical and Process Engineering Research*, 3, 29-39.

Adefila, S. S. (2013). Production of Zeolites from Local Minerals for Petroleum Refining Processes. *A Public Lecture on Raw Materials as Ingredient to National Development*, Association of Professional Women Engineers (APWEN), Kaduna Chapter, Nigeria, 25 June, 2013.

Adefila S. S, Aderemi B. O, Ajayi O. A. & Baderin D. A. (2003). Comparative Surface Area Determination Using Water Adsorption Method. *Nigerian Journal of Engineering*, 11(2), 88- 95.

Aderemi, B. O (2000). *Development of Zeolite Cracking Catalyst from Local Raw Materials*. (Doctoral dissertation, Ahmadu Bello University Zaria, Nigeria).

Aderemi, B. O (2004). Preliminary Studies on Synthesis of Zeolites from Local Clay. *Nigeria Journal of Scientific Research*, 4(2), 7-12.

Aderogba, K. A (2011). Significance of Kaduna River to Kaduna Refinery and Petrochemical Complex. Some Checks and Balances. *International Multidisciplinary Journal*, 5(5), 83-98. doi:http://dx.doi.org/10.4314/afrrev.v5i5.8

Ahmed, K. S. & Onaji, P. B. (1986). The Effects of Beneficiation on the Properties of some Nigerian Clay. *Journal of Nigerian Society of Chemical Engineering,* 6(2), 119-129.

Ajay, K.M, Mishra G. K., Rai, P. K., Chitra, R. & Nagar, P. N. (2005). Removal of Heavy Metal Ions from Aqueous Solutions using Carbon Aerogel as an Adsorbent. *Journal of Hazardous Materials*, 122(1-2), 161-70. doi: 10.1016/j.jhazmat.2005.03.024

Ajayi, O. A. (2012). *Development of Large Pore Zeolite from Kankara and Elefun Kaolinite*. Chemical Engineering Dept, Ahmadu Bello University Zaria, Nigeria.

Ajayi, O.A. & Adefila S.S. (2012). Comparative Study of Chemical and Biological Methods of Beneficiation of Kankara Kaolin. *International Journal of Scientific and Technology Research*, 1(8), 13-18.

Akor, (2009, March 2). Environmental Pollution Deepens in Niger Delta, Says Expert. *The Tide Online*, pp. 9.

Aleksandra, R. N., Sava, J. V. & Dušan, G. A. (2013). Modification of Chitosan by Zeolite A and Adsorption of Bezactive Orange 16 from Aqueous Solution. *Composites Part B Engineering*, 53, 145–151. doi: 10.1016/j.compositesb.2013.04.053

Atta, A.Y., Ajayi O.A. & Adefila S.S. (2008). Synthesis of Faujasite Zeolite from Kankara Kaolin Clay. *Journal of Applied Sciences Research,* 1017–1021.

Babel, S. & Kurniawan, T. A. (2004). Cr (VI) Removal from Synthetic Wastewater using Coconut Shell Charcoal and Commercial Activated Carbon Modified with Oxidizing Agent and/or Chitosan. *Chemosphere*, 54(7), 951-67.

Badmus, M. A. O, Audu, T. O. K. & Anyata B. U. (2006). Removal of Heavy Metal from Industrial Wastewater Using Hydrogen Peroxide. *Journal of Biotechnology*, 6(3), 238-242.

Bailey, S.W (1980). *Structures of Layer Silicates.* In: Brindley GW & Brown G. (Ed) Crystals Structures of Clay Minerals and their X-ray Identification. London, Mineralogical Society, 1–123 (Monograph No.5).

Bamidele, A. (2011). *Exporting from Nigeria; Product Profile: Kaolin* (www.linkedin.com/in/bayemibo .info@3timpex.com)

Bamidele, A. (2012). *Global Trade Finance Survey Nigeria* (www.linkedin.com/in/bayemibo.info@3timpex.com)

Barakat, M. A. (2011). New Trend in Removing Heavy Metals from Industrial Wastewater. *Arabian Journal of Chemistry*, 4(4), 361–377. doi: 10.1016/j.arabjc.2010.07.019

Bashir, A. A. (2008). *Liquid Effluent Treatment and Environmental and Control in KRPC.* Kaduna Refinery and Petrochemical Company, Kaduna, Nigeria.

Bashir, Y. S. (2011). *The Effect of Modification Techniques on the Performance of Zeolite Y Catalysts.* (Master's Thesis, The University of Manchester, UK). Retrieved from https://www.escholar.manchester.ac.uk/uk-ac-man-scw:133717

Bell, R.G. (2001). *Zeolites*. [Online]Available at http://www.bza.org/zeolites.html. [Accessed 1 May 2010].

Belver, C., Munoz, M. A. B. & Vincente, M.A. (2002). Chemical Activation of a Kaolinite under Acid and Alkaline Conditions. *Chemical Material*, 14, 2033-2043.

BET – *Instrument Guid. User Manual and Final Review of Micrometrics* - Coulter Model SA-3100 Surface Area Analyzer. Technical Reference PN 4237215A, 1994.

Bongeard, D., Geidel E., & Smirnor K.S. (2000). *Vibrational Spectra and Structure of Kaolinite: A Computer Simulation Study*. International Zeolite Association, Elsevier. B. (104), 9210-9217.

Boparai, H. K. (2010). Kinetics and Thermodynamics of Cadmium Ion Removal by Adsorption onto Nano Zerovalent Iron Particles. *Journal of Hazardous Materials*, 186, 458–465. doi:10.1016/j.jhazmat.2010.11.029.

Brindley, G.W. & Nakahira, M. (1957). Kinetics of Dehydroxylation. *Journal American Ceramic Society*, (40), N10, 346–350, 311-314.

Brindley, G.W. & Nakahira, M. (1959). The Kaolinite-Mullite Reaction Series: II, Metakaolin. *Journal American Ceramic Society*, (42) N7, 314 – 318.

Brindley, G.W. & Nakahira, M. (1959). The Kaolinite-Mullite Reaction Series: A Survey of Outstanding Problems. *Journal American Ceramic. Society,* (42) N7, 311–314.

Brunauer, S., Emmett, P. & Teller, E. (1938). Adsorption of Gases in Multimolecular Layers. *Journal American. Chemical Society*, 60 (2), 309-319.

Brunauer, S., Deming, S., Deming, W. & Teller, E. (1940). On a Theory of the Vander Waals Adsorption of Gases. *Journal American Chemical Society*, 62 (7), 1723-1730.

Carlos, A. R. & Liz, Y. V (2011). Application of Illite- and Kaolinite-Rich Clays in the Synthesis of Zeolites for Wastewater Treatment. *Earth and Environmental Sciences*, 363-371. doi: 10.5772/25895

Chandra, P., Sahu, J., Mohanty, C., Raj, B. & Meikap, B. (2007). Column Performance of Granular Activated Carbon Packed Bed for Pb(II) Removal. *Journal of Hazardous Materials,* 156(1-3), 596-603. doi:10.1016/j.jhazmat.2007.12.097.

Chiyoda Chemical Engineering & Construction Co. (1980). *Operational manual for Wastewater Treatment. (WWT) Unit.*

Chngombe, P., Saha, B. & Wakeman, R.J. (2006). Sorption of Atrazine on Conventional and Surface Modified Activated Carbons. *Journal Colloid Interface Science,* 302, 408–416.

Cullity, B. D. (2012). *Elements of X-Ray Diffraction*. 101-102. [Online]Available at http:www.researchgate.net.

Daaniya, R. (2012). *Kinetic Modelling of Methanol Synthesis from carbon Monoxide, Carbondioxide, and Hydrogen over a Cu/ZnO/Cr_2O_3 Catalyst. (*Master's Thesis, Faculty of the Department of Chemical and Materials Engineering, San José State University).

Database of Zeolite Structures. (2002). http://www.zeolites.ch/zeolites/StdAtlas.htm

Delloyd, Analchem Resources, (2000). Sourced from Pye Unicam *Atomic absorption Data Book* (1979).

Do, D.D. (1998). *Adsorption Analysis: Equilibria and Kinetics.* Imperial College Press, London.

EC Safety Data Sheet (91/155/EEC) (2006) GREEN STUFF® *Universal Absorbent Concentrate Oil and chemical binder Product information*, Dipl.-Ing. M. Fischer.

Eccles, H. (1999). Treatment of Metal – contaminated Wastes. Why Select a Biological Process. *Trends Biotechnology*, 17(12), 462-5.

Edison, M., John, K., Freeman, N., Mansoor, M., & Antoine, F. M-B. (2011). Cu (II) Removal from Synthetic Wastewater by Ion Exchange Process. *Proceedings of the World Congress on Engineering and Computer Science*, vol. II WCECS, San Francisco, USA.

EDX Analysis and WDX Analysis [Website]. Available from: http://www.siliconfareast.com/edxwdx.htm [Accessed: 8 January 2011].

El–Nafaty, U.A. & Jibril, B. Y. (2008). *Use of Zeolitic Material for the Treatment of Contaminants in Water and Soil*. (Master's Thesis, Tafawa Balewa University, Bauchi Nigeria), 8-12

Feijen, E.J.P., Martens, J.A. & Jacobs, P.A. (1994). *Zeolite and their Mechanism of Synthesis, Zeolites and Related Microporous Materials*. Elsevier Science B. V. (84), 3-18.

FEPA Green Book, (1991) *Guidelines &standards for Environmental Pollution Control in Nigeria*. Decree 1988 No.58.

Fernández, Y., Marañón, E., Castrillón, L. & Vázquez, I. (2005). Removal of Cd and Zn from Inorganic Industrial Waste Leachate by Ion Exchange. *Journal of Hazardous Materials*, 126(1-3), 169–175. doi: 10.1016/j.jhazmat.2005.06.016

Frank, D.D. (2009). *Growth of Pentenary Chalcopyite Thin Films and Characterization of Photovoltaic Devices from these Firms*. Physics Department, University of Johannesburg, South Africa, 11.

Gregg S. J. & Sing, K. S. W. (1982). *Adsorption, Surface Area and Porosity* (2nd ed.). New York: Academic Press.

Grim, R.E. (1968). *Clay mineralogy, structure of clay mineral*. New York: McGraw-Hill Book Co, 57-66.

Gokhale, S.V., Jyoti, K. K. & Lele, S. S. (2009). Modelling of Chromium (VI) Biosorption by Immobilized Spirulina Platensis in Packed Column. *Journal of Hazardous Materials,* 170(2-3), 735-43. doi: 10.1016/j.jhazmat.2009.05.005

Guggenheim, S., Koval, P.V., Muller, G., Neiva, A.M.R, Radoslovich, E.W., Robert, J.L., Sassi, F.P., Takeda H., Weiss Z. & Wones DR (1998). *Nomenclature of Micas*. Clays and Clay Minerals, 46, 586–595.

Hazard, J. M. (2010). The Adsorption Behaviour of Zeolite A and X from Local Egyptian Clay. *Journal of Hazard Material*, 182(1-3), 842-7. doi: 10.1016/j.jhazmat.2010.06.118

Ho, Y.S. & McKay, G. (1998). Adsorption of Dye from Aqueous Solution by Peat. *Chemical Engineering Journal*, 70(2), 115–124.

Hsien, L.I., Yu-Chung, K. & Jia-Ming, C. (2006). Factorial Experimental Design for Recovering Heavy Metals from Sludge with Ion-Exchange Resin. *Journal of Hazardous Materials,* 549–559.

Hui, K. S., Chao, C. Y. H. & Kot, S. C (2005). Removal of Mixed Heavy Metal ions in Wastewater by Zeolite 4A and Residual Products from recycled Coal fly ash. *Journal of Hazardous Materials*, B127, 89-101.

Inductively Coupled Plasma (ICP) Excitation Source [Website]. Available from: http://elchem.kaist.ac.kr/vt/chem-ed/spec/atomic/emission/icp.htm (Accessed: 12 January 2013)

Inelo, B. A. (2010). *Wastewater Treatment Plant Performance and Environmental Management in KRPC*.

Inglezakis, V. J., Hadjiandreou, K. J., Loizidou, M. D. & Grigoropoulou, H. P. (2001). Pre-treatment of Natural Clinoptilolite in a Laboratory-scale Ion-Exchange Packed Bed. *Water Research*, 35(9), 2161-2166.

Inglezakis, V. J., Lemonidou, M. & Grigoropoulou, H. P. (2001). Liquid Holdup and Flow Dispersion in Zeolite Packed Beds. *Journal of Colloid and Interface Science*, 234(2), 434-441.

Inglezakis, V. J., Lemonidou, M. & Grigoropoulou, H. P. (2002). Equilibrium and Kinetic Ion Exchange Studies of Pb^{2+}, Cr^{3+}, Fe^{3+} and Cu^{2+} on Natural Clinoptilolite. *Water Research*, (36), 2784-2792.

Inglezakis, V. J. & Grigoropoulou, H. (2004). Effects of Operating Conditions on the Removal of Heavy Metals by Zeolite in Fixed Bed Reactors. *Journal of Colloid and Interface Science,* 275 (2), 570-576.

Ismail, M.A., Eltayeb, M.A.Z. & Abdel, M.S.A. (2013). *Elimination of Heavy Metals from Aqueous Solutions using Zeolite LTA Synthesized from Sudanese Clay.* Available online at: www.isca.in

Jacque, L. & Barboza, M. (2008). *Energy Specialist at National Petroleum Agency of Brazil.* (www.eolss.net/sample-chapters/c08/E6)

Janjira, W. (2002). *Synthesis and Kinetic Study of Zeolite Na-A from Thai kaolin* (Master's Thesis, University of Technology Academic).

Jelena, P., Siecko, S., Bernd, F. & Zeljko, K. (2007). Selective Removal of Heavy Metals from Metal-bearing Wastewater in a Cascade Line Reactor. *Environmental Science* and *Pollution Research,* 14(7), 518-22.

Kovo, A.S. (2011). *Development of Zeolites and Zeolite Membranes from Ahoko Nigerian Kaolin.* (Master's Thesis, University of Manchester, Faculty of Engineering and Physical Sciences School of Chemical Engineering and Analytical Science), 160-194.

Kurniawan, T.A., Chan, G. Y. S, Lo, W. H., & Babel, S. (2006). Physcio-Chemical Treatment Techniques for Wastewater Laden with Heavy Metals. *Chemical Engineering Journal,* 118(1-2), 83-98.

Langmuir, (1918). The Adsorption of Gases on Plane Surfaces of Glass Mica and Platinum. *Journal of the American Chemical Society*, 40(9), 1361-1403.

Lagergren, S. (1989). Zur Theorie der Sogenannten Adsorption Gelöster Stoff. Kungliga Svenska Vetenskapas akademiens, Handlingar, 24(4), 1–39.

Lars, J. (2011). British Medical Bulletin. Department of Epidemiology and Public Health, Imperial College London. *Oxford Journal*, 68, 167-182.

Lawrence, C. E, Garbor, S. O., Idowu, O. A. & Bawa, S. G. (2013). Kinetics of Adsorption of Nickel Ion on Kankara Kaolinite. *Leonardo Electronic Journal of Practices and Technologies,* 22, 83-92.

Leung, W. C, Wong, M. F, Chua, H. & Leung, C. K (2000). Removal and Recovery of Heavy Metals by Bacteria Isolated from Activated Sludge Treating Industrial Effluents and Municipal Wastewater. *Water Science & Technology*, 41(12), 233–240.

Li, L. X, Dong, J. H and Nenoff, T. M. (2007). *Transport of Water and Alkali Metal Ions through MFI Zeolite Membranes during Reverse Osmosis*. Separation and Purification Technology, 53(1), 42–48.

Li, Q., Creaser, D. & Sterte, J. (1999). The Nucleation Period for TPA-silicalite-1 Crystallization Determined by a Two-Stage Varying-Temperature Synthesis. *Journal Microporous Mesoporous Material*, 31(1), 141-150.

Liu, F. F., Jiang, C. H. & Xia, X. L. (2011). Effect on Performance of Gasoline Engine about Intake Valve Closing Angle. *Journal of Nanchang University (Engineering and Technology)*, 66-68.

Manager *Data Management–CP&S:* email: *adamu.mhya@nnpcgroup.com* NNPC ASB 2011 – 1st Edition.

Martin, T.D., Martin, E.R., & Long, S.E. (1989). Sample Preparation Procedure for Spectrochemical Determination of Total Recoverable Elements. *Technology Applications, Inc*., Method 2002, Revision 1.1

Mckay, G. (1984). The Adsorption of Basic Dye onto Silica from Aqueous-solution Solid
Diffusion Model. *Chemical Engineering Science*, 39, 131–136.

Metcalf & Eddy (2003). *Wastewater Engineering: Treatment, Disposal, Reuse*. 4. Ed. [S.l.] 1819.

Ming-qin, J., Xiao-ying, J., Xiao-Qiao, L. & Zu-liang, C. (2010). Adsorption of Pb, Cd, Ni and Cu onto Naturally Kaolinite Clay. *Desalination*, 252, 33–39.

Mohammed, J.K., Bashir, H.A.A., Mohd, S.Y. & Mohd., N.A. (2010). Application of Response Surface Methodology (RSM) for Optimization of Ammoniacal Nitrogen Removal from Semi-Aerobic Landfill Leachate Using Ion Exchange Resin. *Desalination*, 254, 154–161.

Mohammed, M. N. & Nwaedozie, J. M. (2011). Application of Marine Biomass for the Removal of Metals from Industrial Wastewater. *Human Resource Management Academic Research Society*.

Mohammad, N. J. (2011). *The Preparation and Characterization of Mesoporous*. Faculty of Engineering and Physical Sciences Films for Electrochemical Applications School of Chemistry.

Montgomery, D. C. (2005). *Design and Analysis of Experiments,* 6^{th} edition, John Wiley, New York.

MRL, Materials Research Laboratory (2011), *Introduction to X-ray Diffraction* [Website]. Available from http://www.mrl.ucsb.edu/mrl/centralfacilities/xray/xray- basics/index.html#.

Mudi, K. Y. (2010). *Modeling of Heavy Metal Removal from Wastewater by Phytoxtraction*. (Master's Thesis, Federal University of Technology, Minna).

Myers, R. H. & Montgomery, D. C. (2002). *Response Surface Methodology. Process and Product Optimization using Designed Experiments*. 2nd Edition. John Wiley and sons New York.

Myzaurah, H., Zaini, U, Mohamed, M., Gustaf, N., Tony, H. & Nurfarhain, M. R., (2013). Optimization of Parameters Affecting Adsorption of Nickel (II), Zinc (II), Lead (II) on Dowex 50W Resin using a Response Surface Methodology Approach. *Journal of Environmental Science and Technology*, 6, 106 – 118.

NESREA (2010). *National Environmental Standard and Regulation Enforcement Agency*. Nigeria.

NNPC Kaduna Refinery Operational Manual (1980) for Wastewater Treatment Unit No. 63. Chiyoda Chemical Eng'g and Construction Co. Ltd.

New Logic Research. (2003) (www.vsep.com/pdf/desaltercasestudy)

Nermen, N. M., George, F. N. & Wan W. K (2010) Removal of Heavy Metals from Wastewater by Adsorption and Membrane Processes. *World Academy of Science and Technology,* 4, 532-537.

Nhapi, I., Banadda, N., Murenzi, R., Sekomo, C. B. & Wali, U. G. (2011*)*. Removal of Heavy Metals from Industrial Wastewater Using Rice Husks. *Environmental Engineering Journal,* 4, 170-180.

Nweke, C. O. & Okpokwasili, G. C. (2011). Inhibition of β-Galactosidase and α-Glucosidase Synthesis in Petroleum Refinery Effluent Bacteria by Zinc and Cadmium. *Journal of Environmental Chemistry and Ecotoxicology*, 3(3), 68-74.

Obidiaku, M.C. (2003). *Boiler Feed Water Treatment in KRPC*. (COMDP 028)

Ojha, K., Pradhan, N.C. & Samanta, A.N. (2004). Zeolite from Fly Ash: Synthesis and Characterization. *Indian Academy of Sciences, Bulletin Material. Sciences*, 27(6), 555-564.

Oledibe, M. C. (2011). *Remediation of a Simulated Petroleum Polluted Water using Pulverized Use-Water-Sachet (Polyethylene) as Sorbent*. (Master's Thesis, Federal University of Technology Minna, Nigeria).

Onwuka, S. C. (2004). *Wastewater Treatment in Kaduna Refinery and Petrochemical Company,* Kaduna, Nigeria.

Osuji, L.C. & Uwakwe, A.A (2006). Petroleum Industry Effluents and Other Oxygen-Demanding Wastes in Niger Delta, Nigeria. *Chemistry & Biodiversity*, 3(7), 705-717.

Ozge, C., Devrim, B. & Semra, U. (2010). Batch and Column Studies on Heavy Metal Removal Using a Local Zeolite Tuff. *Desalination*, 259(1-3), 17-21. doi: 10.1016/j.desal.2010.04.047.

Palesa, P. D., Edison, M. & Zimba, J. (2011). A Study of South African Natural Zeolites Properties and Applications. *Proceedings of the World Congress on Engineering and Computer Science,* vol II.

Prasad, S., Picchlah, S. & Manickam, M. (2012). Optimization of operating Parameters using Response Surface Methodology for Activated Carbon Prepared from Mango Kernal. *Sustainable Environment. Research*, 22(1), 1-7.

QPI (2012). *NNPC Quarterly Report*. [Online] Available at http://www.nnpcgroup.com/Portals/0/NNPC_Files/Quarterly/29.%202012%20First%20Quarter%20QPI.pdf [Accessed 1 May 2010].

Rasheed, M.M. (2001). Agricultural Products and By-products as a Low Cost Technology for Wastewater Treatment in Developing Countries, Natural Materials for Removal of Toxic Heavy Metals from Wastewater. *Scientific Research and Essay*, 1(2), 033-037.

Remco Engineering, Ion Exchange Chemistry and Operation. Water Systems and Control. www.remco.com/ix.thm. Retrieved 17/7/2009.

Rieder, M., Cavazzini, G., D'yakonov, Y. S., Frank-Kamenetskii, V. A., Gottardi, G., Guggenheim, S., Koval, P. V., Muller, G., Neiva, AMR, Radoslovich, E.W., Robert, J. L., Sassi, F.P., Ttakeda, H., Weiss, Z. & Wones, D.R. (1998) *Nomenclature of Micas*. Clays Clay Miner, 46, 586 – 595.

Saifuddi, M, & Kumaran, P. (2005) Removal of Heavy Metal from Industrial Wastewater using Chitosan Coated Oil Palm Shell Charcoal. *Environmental Biotechnology*, 8. doi: 10.2225/vol8-issue1-fulltext-7.

Sample Preparation Procedure for Spectrochemical Determination of Total Recoverable Elements Revision 2.8 Emmc Version T.D. Martin, E.R. Martin, and S.E. Long (*Technology Applications, Inc.*) Method 2002, Revision 1.1 (1989)

Sameer, A., Nabil, A. & Fawzi, B. (2002). Packed-Bed Sorption of Copper Using Spent Animal Bones: Factorial Experimental Design, Desorption and Column Regeneration. *Advances in Environmental Research*, 6(3), 221-227.

Scanning Electron Microscope [Website]. Available from: http://www.gmu.edu/departments/SRIF/tutorial/sem/sem.htm (Accessed: 8 January 2011).

Scott Wilson, (1998). NPDES's Produced Water Permitting Requirements by USEPA *United States Environmental Protection Agency (USEPA) Region 6.*

Selvaraj, R., Younghun, K., Cheol, K. J., Kyunghee, C. & Jongheop, Y. (2003). Batch Adsorptive Removal of Copper Ions in Aqueous Solutions by Ion Exchange Resins. *Korean Journal of Chemical Engineering*, 21(1), 187-194.

Settle, T., Mollock, G. N., Hinchman, R. R. & Negri, M, C. (1998*). Engineering the Use of Green Plant to Reduce Produced Water Volume*. Society of Petroleum Engineers. Inc. Devon Energy Corporation, Oklahoma City. doi: 10.2118/39763-MS

Siddhesh, S. & Robert, G. F, (2004). Use of Synthetic Zeolites for Arsenate Removal from Pollutant Water. *Water Research*, 38, 3197–3204.

Silvio, R. T. & Jorge, R. (2008). Removal of Mn^{2+} Ions by Adsorption onto Natural and Activated Chilean Zeolites. *Minerals Engineering*, 22(4), 336–343. doi: 10.1016/j.mineng.2008.09.007

Standard Organization of Nigeria (2007). *Nigerian Standard for Drinking Water Quality*. Retrieved from http://www.unicef.org/nigeria/ng_publications_Nigerian_Standard_for_Drinking_Water_Quality.pdf

Standard Analytical Procedures for Water Analysis (1999). *Standard Methods*, 19th Edition.

Surinder, S., Lokesh, K. V., Sambi, S. S. & Sharma, S. K, (2008). Adsorption Behaviour of Ni (II) from Water onto Zeolite X: Kinetics and Equilibrium Studies. *Proceedings of the World Congress on Engineering and Computer Science,* San Francisco, USA.

Sumen, D. (2013). *Optimization of Reactive Black 5 removal by adsorption process using Box -Behnken Design*, 1-8.

Surface Area Measurement [Website]. Available from: http://www.refiningonline.com/engelhardkb/crep/TCR2_10.htm [Accessed: 15 January 2011]

Taha, A. W., Dakroury, A. M., El-Sayed, G. O., & El-Salam, S. A. (2010). Assessment Removal of Heavy Metals Ions from Wastewater by Cement Kiln Dust**.** *Journal of American Science,* 6(12), 911-917.

Tarek, S., Jamil, H.S., Ibrahim, I.H., Abd, E. & El-Wakeel, S.T. (2010). Application of Zeolite prepared from Egyptian Kaolin for removal of heavy metals at Optimum Conditions. *Desalination*, 258, 1-.25.

Treacy, M. M. & Higgins, J.B. (2001). *Collection of Simulated XRD Powder Patterns for Zeolites*. 4th Edition. Amsterdam-London-Paris: Elsevier Publishing Co.

Ugal, J. R., Hassan, K. H. & Ali, I. H. (2010). Preparation of Type 4A Zeolite from Iraq Kaolin*: Characterization and Properties Measurement*, 142 -146.

Umudi, E.Q. (2011). Analysis of Produced Water from Four Communities in Delta State (Niger Delta). *Journal of Physical Sciences and Innovation*, 3, 1-6.

Uwakwe, A. A. (2006). Application of Simple Chemistry. *Chemistry & Biodiversity*, 3(7), 705-717.

Velde, B. (1992). *Clay mineral structure, Introduction of Clay Minerals*. 1st ed.-New York: Chapman & Hall.

Worrall, W.E. (1986). *Clays and ceramic raw materials*. Elsevier Applied Science Publishers, 2nd Edition.

Warren, B.E. (1990). *X-ray diffraction*. USA: Courier Dover Publications, 1990.

WHO (2007). *Guidelines for drinking water quality.*http://www.lanntech.com//

applications/drinking/standard/who-drinking-waterstandard.htro.

X-ray Diffraction Techniques [Website]. Available from: http://www.doitpoms.ac.uk/tlplib/xray-diffraction/printall.phpUniversity of Cambridge [Accessed: 7 January 2011].

Xiaolin, Y., Shengrui, T., Maofa, G., Lingyan, W., Junchao, Z., Changyan, C. & Weiguo, S. (2012). Adsorption of Heavy Metal Ions from Aqueous Solution by Carboxylated Cellulose Nanocrystals. *Journal of Environmental Sciences,* 25(5), 933–943. doi: 10.1016/S1001-0742(12)60145-4

Yang, C.H. (1998). Statistical Mechanical Study on the Freundlich Isotherm Equation. *Journal of Colloid and Interface Science*, 208, 379–387.

Yiye, O. B (2006) *Waste Management and Environmental Control in KRPC.*

Yi L., Yian, Z. & Aiqin, W. (2011). Fast Removal of Ammonium Ion Using a Hydrogel Optimized with Response Surface Methodology. *Chemical Engineering Journal*, 171, 1201–1208.

Zaida, N. & Piakong, (2011). Removal of Metals by Indigenous aquatic Plants from Simulated Wastewater. *Proceedings of the 3rd CUTSE International Conference Miri, Sarawak*, Malaysia.

Zeolites [Website]. Available from: *http://www.bza.org/Zeolites.html* [Accessed: 26 December 2010].

Zeolites [Website]. Available from: *http://www.tobiasweisenberger.de/5Zeolites.html* [Accessed: 28 December 2010].

www.ladco.org/reports/control/whitepappers/petroleum (Retrieved February, 2011)

www.ipieca.org

http://www.personal.utusa.edu/geoffery-price/zeolite/ita.htm

www.decimpinti.com/DEC/TEXT/ENGLISH/dec.zeolite.uk.html

http://www.molelarsieve.org/zeolitemolecularsieve.htm

http://farriconsulting.blogspot.com/2010/07/kaolin-deposits-in-nigeria-08.html

http://www.lenntech.com/periodic/elements/htm

http://www.scanning-electron-microscopy

http://www.chemistry-of-zeolite-and-related-porous-materials-synthesis-and-structure

http://www.foramfera.com/index/investment-opportunities-in-nigeria-deposites-mining-in-nigeria-the-opportunities

http://www.researchgate.net/publication/kinetics-and-thermodynamics-of-cadmium-ion-removal

http://www.weiku.com/quality-products

http://www.xrf.ethz.ch/xrf-forms.html

Publications from the Work

1) Nwafulugo, F. U., Adefila, S. S., Olawale, A. S., Ajayi, O. A. (2014). Application of Response Surface Methodology (RSM) for Optimization of Removal of Nickel and Lead from Petroleum Wastewater. *International Research Journal of Engineering Science, Technology and Innovation*, 3(1), 8-16.

2) Nwafulugo, F. U., Adefila, S. S., Olawale, A. S. and Ajayi, O. A. (2014). Determination of Best Blend of Zeolite 4A-metakaolin Matrices for Heavy Metal Removal from Synthetic Wastewater. *International Journal of Chemistry and Material Science,* 2(2), 18-27.

3) Nwafulugo, F. U., Adefila, S. S., Olawale, A. S., Ajayi, O. A. (2014). Environmental Impact and Removability of Selected Heavy Metals from Petroleum Wastewater Using Zeolite 4A–Metakaolin Matrices. *Journal of Environmental Science and Water Resources*, 3(6), 132-143.

4) Nwafulugo, F. U., Adefila, S. S., Olawale, A. S. (2014). Studies of Interactive Effects of some Variables on Removal of Nickel from Petroleum Wastewater by Factorial Analysis. *Journal of Petroleum and Gas Exploration Research,* 4(2), 17-23.

5) Nwafulugo, F. U., Adefila, S. S., Olawale, A. S., Ajayi, A. O., Usman, J.G. (2014). Mathematical Model for Removal of Nickel from Petroleum Waste Water. *Global Advanced Research Journal of Engineering, Technology and Innovation,* 3(2), 27-33.

APPENDICES

APPENDIX A

The Petroleum Industry

Table A1 Quantity of crude extracted from reserves

S/N	Producing Nation	10^3bbl/d (2006)	10^3bbl/d (2007)	10^3bbl/d (2008)	10^3bbl/d (2009)	Present Share
1	Saudi Arabia (OPEC)	10,665	10,234	10,782	9,760	11.8%
2	Russia[1]	9,677	9,876	9,789	9,934	12.0%
3	United States [1]	8,331	8,481	8,514	9,141	11.1%
4	Iran (OPEC)	4,148	4,043	4,174	4,177	5.1%
5	China	3,846	3,901	3,973	3,996	4.8%
6	Canada [2]	3,288	3,358	3,350	3,294	4.0%
7	Mexico[1]	3,707	3,501	3,185	3,001	3.6%
8	United Arab Emirates (OPEC)	2,945	2,948	3,046	2,795	3.4%
9	Kuwait (OPEC)	2,675	2,613	2,742	2,496	3.0%
10	Venezuela (OPEC) [1]	2,803	2,667	2,643	2,471	3.0%
11	Norway[1]	2,786	2,565	2,466	2,350	2.8%
12	Brazil	2,166	2,279	2,401	2,577	3.1%
13	Iraq (OPEC) [3]	2,008	2,094	2,385	2,400	2.9%
14	Algeria (OPEC)	2,122	2,173	2,179	2,126	2.6%
15	Nigeria (OPEC)	2,443	2,352	2,169	2,211	2.7%
16	Angola (OPEC)	1,435	1,769	2,014	1,948	2.4%
17	Libya (OPEC)	1,809	1,845	1,875	1,789	2.2%
18	United Kingdom	1,689	1,690	1,584	1,422	1.7%
19	Kazakhstan	1,388	1,445	1,429	1,540	1.9%
20	Qatar (OPEC)	1,141	1,136	1,207	1,213	1.5%
21	Indonesia	1,102	1,044	1,051	1,023	1.2%
22	India	854	881	884	877	1.1%
23	Azerbaijan	648	850	875	1,012	1.2%
24	Argentina	802	791	792	794	1.0%
25	Oman	743	714	761	816	1.0%
26	Malaysia	729	703	727	693	0.8%
27	Egypt	667	664	631	678	0.8%
28	Colombia	544	543	601	686	0.8%
29	Australia	552	595	586	588	0.7%
30	Ecuador (OPEC)	536	512	505	485	0.6%
31	Sudan	380	466	480	486	0.6%
32	Syria	449	446	426	400	0.5%
33	Equatorial Guinea	386	400	359	346	0.4%
34	Thailand	334	349	361	339	0.4%
35	Vietnam	362	352	314	346	0.4%
36	Yemen	377	361	300	287	0.3%
37	Denmark	344	314	289	262	0.3%
38	Gabon	237	244	248	242	0.3%
39	South Africa	204	199	195	192	0.2%
40	Turkmenistan	No data	180	189	198	0.2%

Source: U.S. Energy Information Administration

Table A2. An Overview of the Permissible Limits of some Metals with the health Impacts.

Metals	WHO	*Drinking water Quality standard	**Maximum Permitted Limit	Health Impact
Ni (mg/l)	0.010	0.100	0.020	Possible carcinogenic
Cd(mg/l)	0.003	0.003	0.003	Toxic to the kidney
Mn (mg/l)	0.040	0.200	0.200	Neurological disorder
Pb (mg/l)	0.010	0.200	0.010	Cancer

*Values from National Environmental Standards and Regulations Enforcement Agency (NESREA, 2010). **The Maximum Permitted Limit. (SON, 2007).

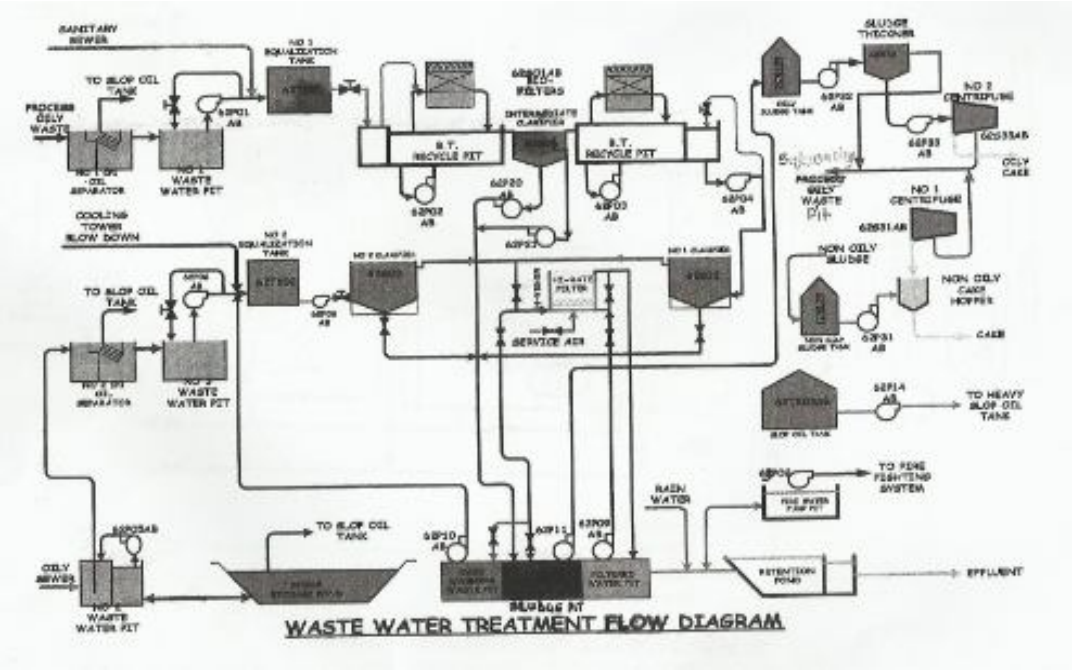


Figure A1. Wastewater Treatment Flow Diagram (KRPC) (NNPC Kaduna Refinery Operational Manual, 1980, Inelo, 2010).

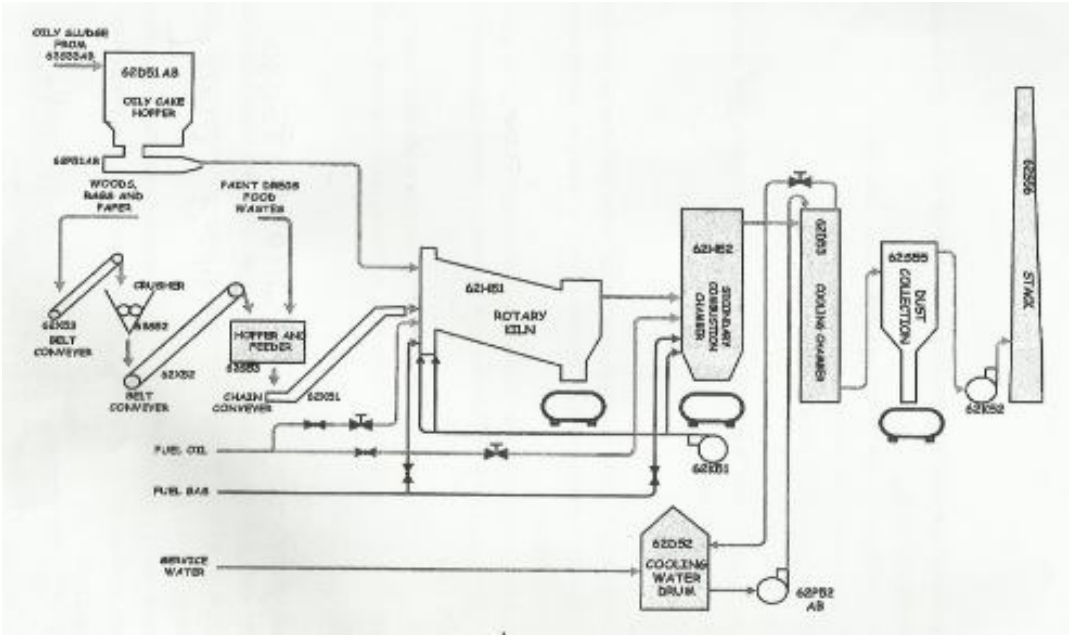


Figure A2. Sludge Incinerator Diagram (NNPC Kaduna Refinery Operational Manual, 1980, Inelo, 2010).

APPENDIX B

Calibration Curves for Matrix 1 (100% zeolite 4A/ 0% metakaolin)

Table B1. Absorbance – Concentration for Ni

Ni (ppm)	Abs
0	0
4	0.08
8	0.16
12	0.23

Table B2. Absorbance – Concentration for Pb

Pb (ppm)	Abs
0	0
3	0.03
5	0.05
7	0.075

Table B3. Absorbance – Concentration for Cd

Cd (ppm)	Abs
0	0
0.6	0.1
1.8	0.28
2.4	0.37

Table B4. Absorbance – Concentration for Mn

Mn (ppm)	Abs
0	0
1	0.012
2	0.022
3	0.032

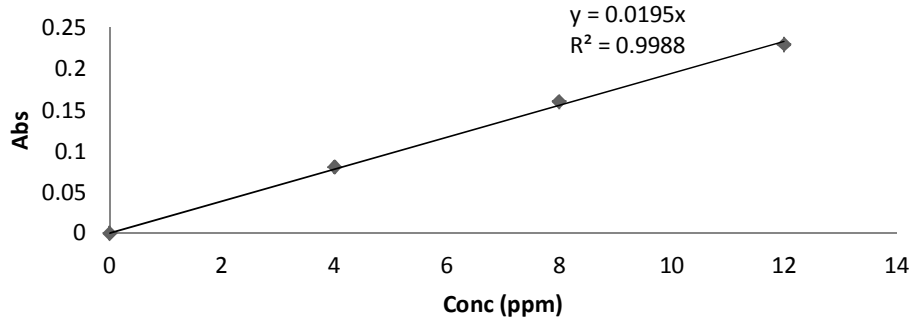


Figure B1. Absorbance - Concentration calibration curve for Ni

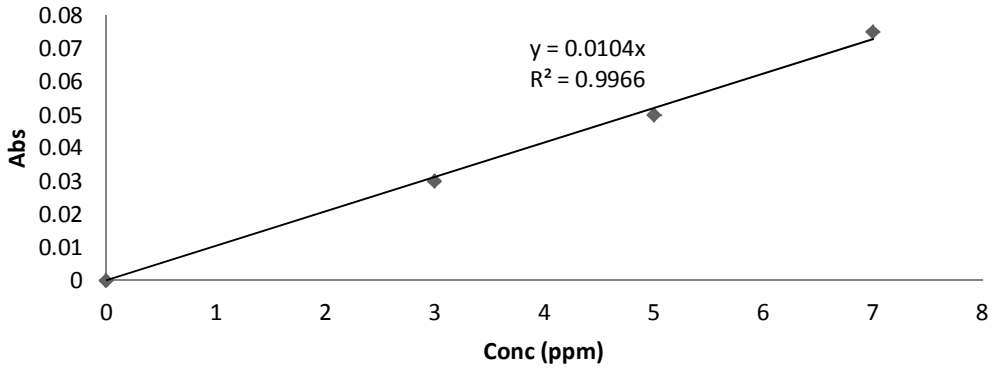


Figure B2. Absorbance - Concentration Calibration curve for Pb

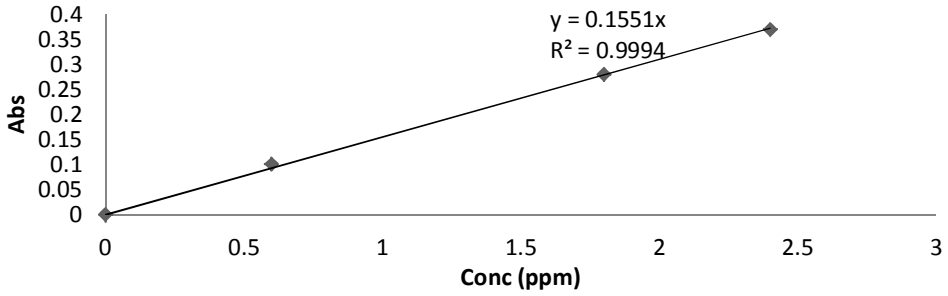


Figure B3. Absorbance - Concentration Calibration curve for Cd

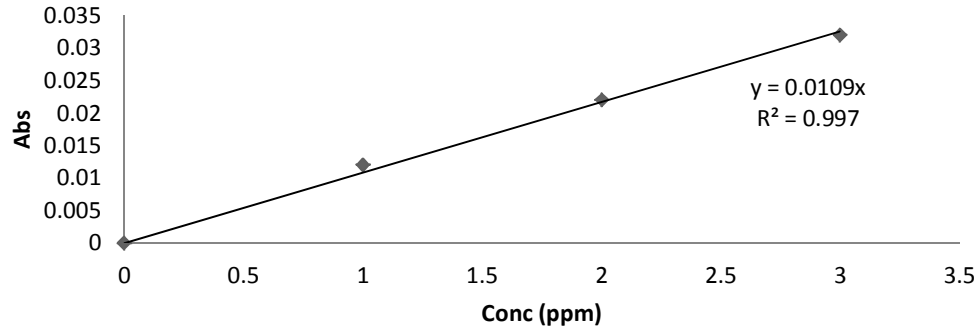


Figure B4. Absorbance - Concentration curve for Mn

Table B5: Effect of Contact time Matrix 1 (zeolite 4 A) on Heavy Metal Removal

Cont time (min)	Ni in soln (mg/l)	%Ni uptake	Pb in soln (mg/l)	%Pb uptake	Cd in soln (mg/l)	%Cd uptake	Mn in soln (mg/l)	%Mn uptake
0	1.533	0	1.505	0	0.929	0	4.89	0
1	0.009	99.41292	0.0451	97.00332	0.0015	99.83854	0.091	98.13906
2.5	0.007	99.54338	0.42	72.09302	0.0014	99.8493	0.087	98.22086
5	0	100	0.256	82.99003	0.001	99.89236	0.076	98.44581
10	0.006	99.60861	0.268	82.19269	0.002	99.78471	0.105	97.85276
20	0.066	95.69472	0.325	78.40532	0.004	99.56943	0	100
40	0.103	93.28115	0.251	83.32226	0.007	99.2465	0.269	94.49898
60	0.007	99.54338	0.286	80.99668	0.018	98.06243	0.093	98.09816

Table B6: Effect of pH on Heavy Metal Removal using Matrix 1

pH	Ni in soln	%Ni uptake	Pb in soln	%Pb uptake	Cd in soln	%Cd uptake	Mn in soln	%Mn uptake
2	0.802	47.68428	1.07	28.90365	0.23	75.2422	1.902	61.10429
4	0.173	88.71494	1.171	22.19269	0.152	83.63832	1.587	67.54601
6	0	100	0.561	62.72425	0.04	95.69429	0	100
8	0	100	0.241	83.98671	0.003	99.67707	0	100
10	0	100	0.264	82.45847	0.003	99.67707	0	100
12	0	100	1.044	30.63123	0.062	93.32616	0	100

Table B7: Effect of Initial Concentration on Heavy Metal Removal using Matrix 1

Initial conc(ppm)	NI in soln	%Ni uptake	Pb in soln	%%Pb uptake	Cd in soln	%Cd uptake	Mn in soln	%Mn uptake
0	1.533	0	1.505	0	0.929	0	4.89	0
5	0.146	90.47619	0.249	83.45515	0.017	98.17008	0.13	97.34151
25	0.091	94.06393	0.258	82.85714	0.02	97.84715	0	100
50	0.049	96.80365	0.251	83.32226	0.009	99.03122	0	100
75	0.044	97.12981	0.272	81.92691	0.006	99.35414	0	100
100	1.031	32.74625	0.318	78.87043	0.042	95.47901	0	100

Table B8: Effect ofMatrix 1 Dose on Heavy Metal Removal

Zeolite dose(g)	Ni in soln	%Ni uptake	Pb in soln	%Pb uptake	Cd in soln	%Cd uptake	Mn in soln	%Mn uptake
0	1.533	0	1.505	0	0.929	0	4.89	0
0.1	0	100	0.31	79.40199	0	100	0	100
0.25	0	100	0.28	81.39535	0	100	0	100
0.5	0	100	0.242	83.92027	0	100	0	100
1	0	100	0.272	81.92691	0	100	0	100
1.5	0	100	0.278	81.52824	0.001	99.89236	0	100
2	0.014	99.08676	0.293	80.53156	0	100	0	100
2.5	0.005	99.67384	0.206	86.31229	0.002	99.78471	0	100

APPENDIX C

Calibration Curve for Matrix 5 (0% zeolite 4A/100% metakaolin)

Table C1: Absorbance – Concentration for Cd

Cd (ppm)	Abs
0	0
0.6	0.0604
1.2	0.1252
1.8	0.1872
2.4	0.2628
3	0.3294

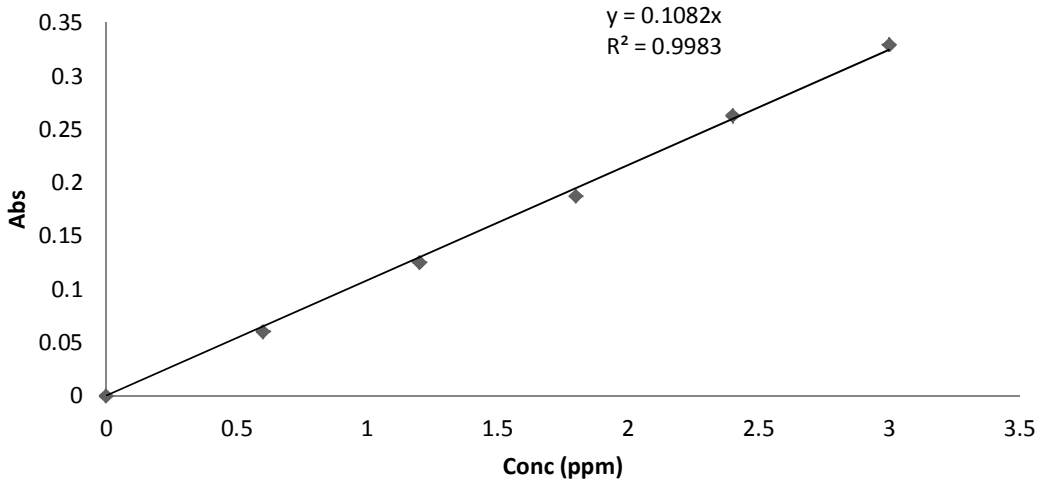


Figure C1. Absorbance - Concentration Calibration Curve for Cd

Table C2: Absorbance – Concentration for Pb

Pb (ppm)	Abs
0	0.0006
3	0.0203
5	0.0389
7	0.0542
9	0.0721

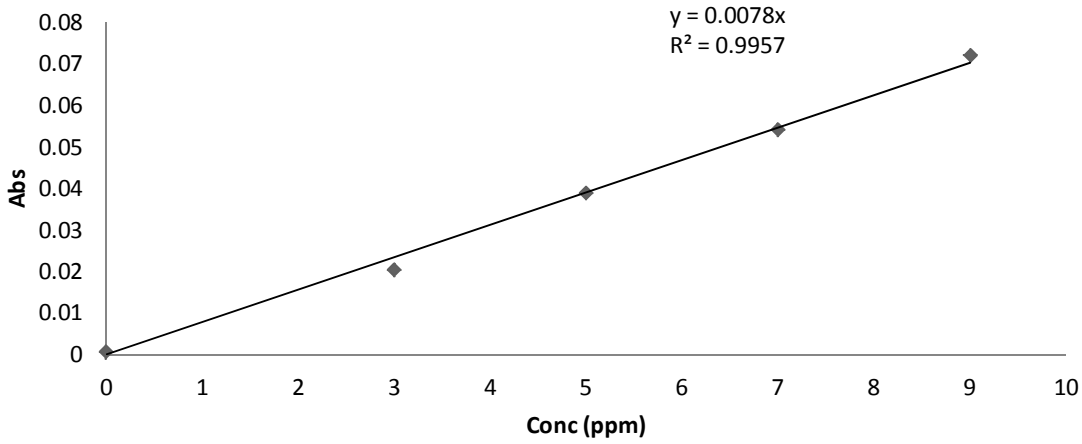


Figure C2. Absorbance - Concentration Calibration Curve for Pb

Table C3: Absorbance – Concentration for Ni

Ni (ppm)	Abs
0	0
4	0.06
8	0.12
12	0.16
16	0.2

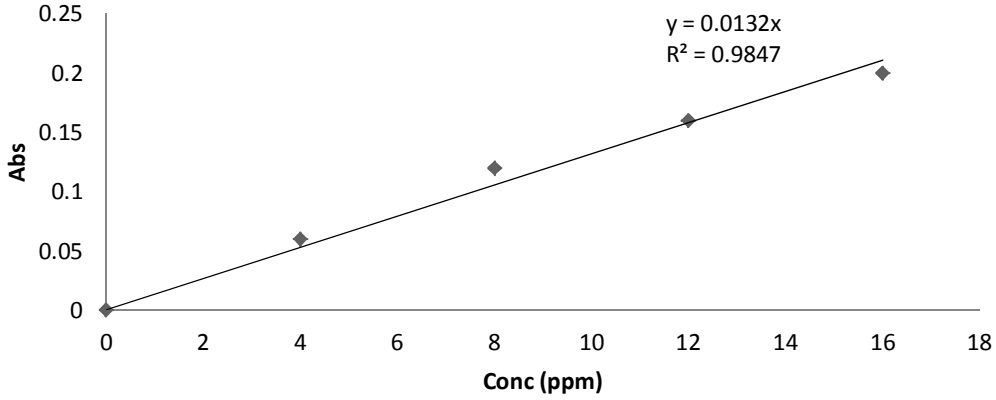


Figure C3. Absorbance - Concentration Calibration Curve for Ni

Table C4: Absorbance – Concentration for Mn

Mn (ppm)	Abs
0	0
1	0.006
2	0.017
3	0.028
4	0.036

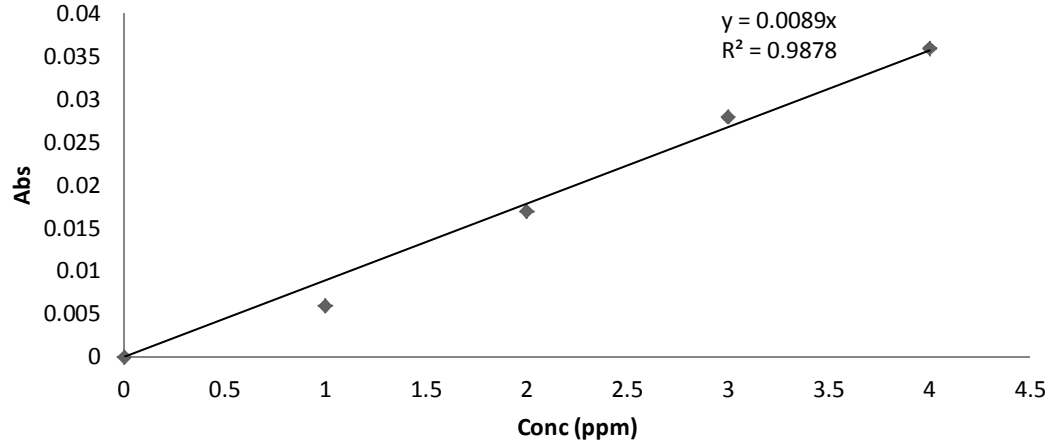


Figure C4. Absorbance - Concentration Calibration Curve for Mn

Table C5: Effect of Matrix 5 (Pure metakaolin) Dose on Heavy Metal Removal

Ad dose	Ni in soln	%Ni Rmd	Pb in Soln	% Pb Rmd	Cd in Soln	%Cd Rmd	Mn in Soln	%MnRRmd
0	1.533	0	1.505	0	0.929	0	4.89	0
0.1	0.154	89.95434	0.224	85.11628	0.054	94.1873	0.093	98.09816
0.25	0.149	90.2805	0.21	86.04651	0.041	95.58665	0.088	98.20041
0.5	0.143	90.67189	0.106	92.95681	0.03	96.77072	0.073	98.50716
1	0.084	94.52055	0.013	99.13621	0.014	98.493	0.053	98.91616
1.5	0.104	93.21592	0.061	95.94684	0.005	99.46179	0	100
2	0.08	94.78147	0.041	97.27575	0.005	99.46179	0.013	99.73415
2.5	0.09	94.12916	0.002	99.86711	0	100	0	100

Table C6: Effect of Contact Time on Metal Removal using Matrix 5

Cont Time(min)	Ni in Soln	% Ni Rmd	Pb in Soln	% Pb Rmd	Cd in Soln	% Cd Rmd	Mn in Soln	% Mn Rmd
0	1.533	0	1.505	0	0.929	0	4.89	0
10	0.055	96.41226	0.43	71.42857	0.01	98.92357	0.231	95.27607
20	0.05	96.73842	0.41	72.75748	0.009	99.03122	0.21	95.70552
60	0.047	96.93412	0.289	80.79734	0.007	99.2465	0.187	96.17587
100	0.07	95.43379	0.361	76.01329	0.007	99.2465	0.216	95.58282
140	0.06	96.08611	0.293	80.53156	0.009	99.03122	0.244	95.01022
180	0.066	95.69472	0.316	79.00332	0.007	99.2465	0.24	95.09202
220	0.095	93.803	0.312	79.2691	0.009	99.03122	0.219	95.52147

Table C7: Effect of pH on Metal Removal using Matrix 5

pH	Ni in Soln	% Ni Rmd	Pb in soln	% Pb Rmd	Cd in soln	% Cd Rmd	Mn in Soln	% MnRmd
2	1.459	4.827136	1.348	10.43189	0.789	15.06997	3.123	36.13497
4	1.11	27.59295	1.307	13.15615	0.767	17.43811	2.369	51.55419
6	0.05	96.73842	0.77	48.83721	0.04	95.69429	0	100
8	0.048	96.86888	0.664	55.88044	0.031	96.66308	0.063	98.71166
10	0.017	98.89106	0.307	79.60133	0	100	0	100
12	0	100	0.268	82.19269	0	100	0	100

APPENDIX D

Effect of Contact Time on Matrix 2, 3 & 4

Table D1: Absorbance – Concentration for Ni

Ni (ppm)	Abs
0	0
4	0.09
8	0.17
12	0.22

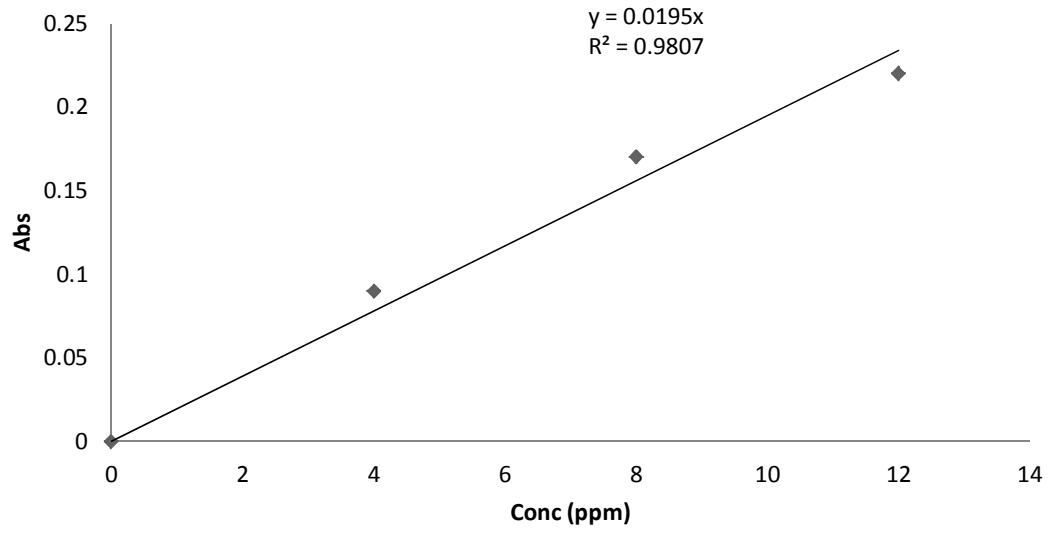


Figure D1. Absorbance - Concentration Calibration Curve for Ni

Table D2: Absorbance – Concentration for Pb

Pb (ppm)	Abs
0	0
1	0.02
3	0.04
5	0.06

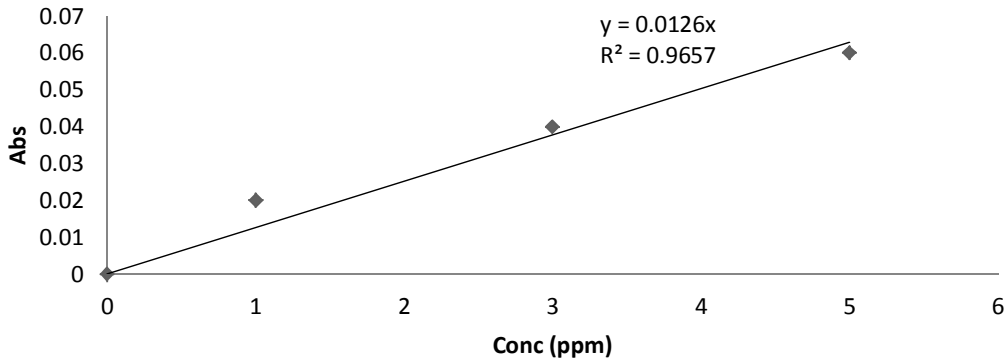


Figure D2. Absorbance - Concentration Calibration Curve for Pb

Table D3: Absorbance – Concentration for Cd

Cd (ppm)	Abs
0	0

0.6	0.08
1.2	0.16
1.8	0.24

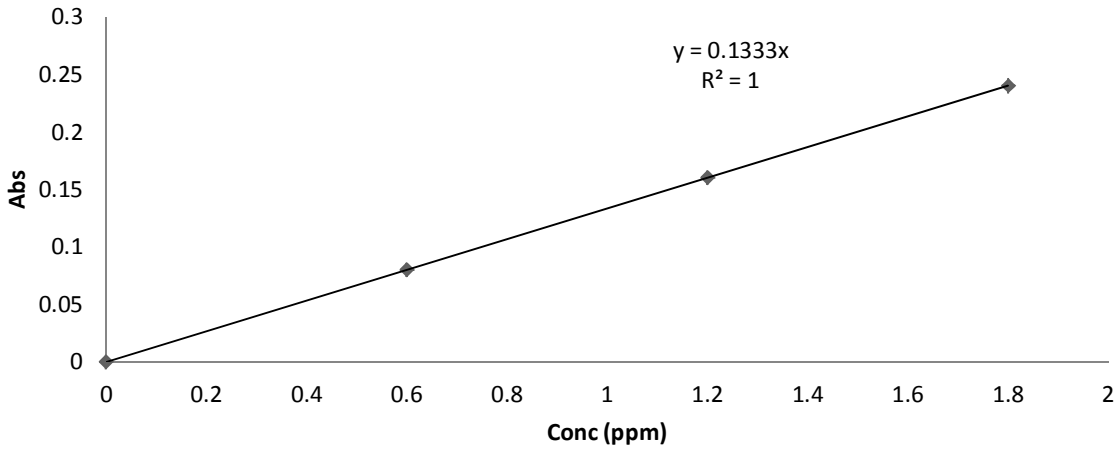


Figure D3. Absorbance - Concentration Calibration Curve for Cd

Table D4. Absorbance – Concentration for Mn

Mn (ppm)	**Abs**
0	0
1	0.01
2	0.02
3	0.03

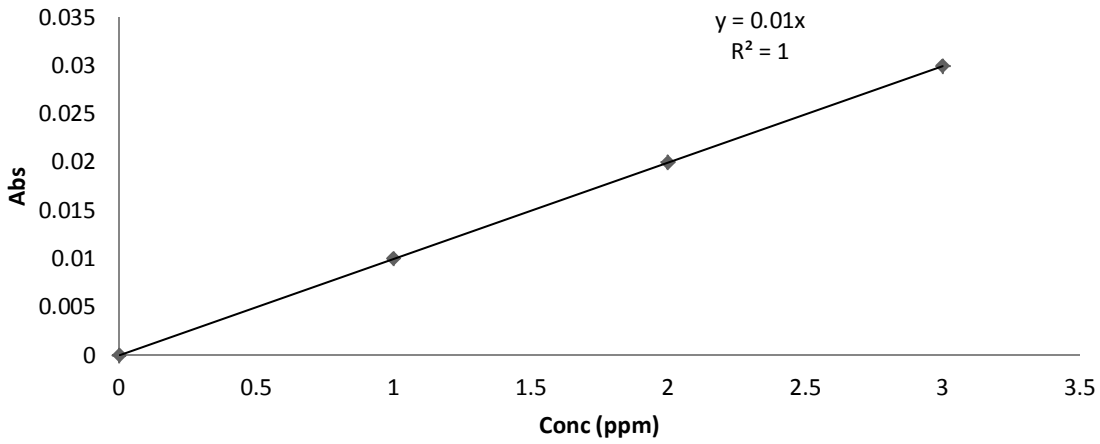


Figure D4. Absorbance - Concentration Calibration Curve for Mn

Table D5: Effects of contact time on Matrix 2 (75% zeolite 4A/ 25%metakaolin)

Contact time (mins)	Ni in soln(ppm)	% Ni uptake	Pb in soln	% Pb uptake	Cd in slon	% Cd uptake	Mn in soln	% Mn uptake
0	1.533	0	1.505	0	0.929	0	4.89	0
1	0.11	92.82453	0.318	78.87043	0.009	99.03122	0.034	99.3047
2.5	0.109	92.88976	0.316	79.00332	0.007	99.2465	0.03	99.3865
5	0.102	93.34638	0.315	79.06977	0.005	99.46179	0.032	99.3456
10	0.081	94.71624	0.215	85.71429	0.003	99.67707	0.024	99.5092
20	0.095	93.803	0.714	52.55814	0.003	99.67707	0.018	99.6319
40	0.078	94.91194	0.579	61.52824	0.006	99.35414	0.014	99.7137
60	0.105	93.15068	0.336	77.67442	0.004	99.56943	0.011	99.77505

Table D6: Effects of Contact time on Matrix 3 (50% zeolite 4A /50% metakaolin)

Contact time(mins)	Ni in soln	% Ni uptake	Pb in soln	% Pb uptake	Cd in soln	% Cd uptake	Mn in soln	%Mn uptake
0	1.533	0	1.505	0	0.929	0	4.89	0
1	0.057	96.2818	0.583	61.26246	0.018	98.06243	0	100
2.5	0.048	96.86888	0.42	72.09302	0.015	98.38536	0	100
5	0.043	97.19504	0.338	77.54153	0.011	98.81593	0	100

10	0.064	95.82518	0.336	77.67442	0	100	0	100
20	0.043	97.19504	0.307	79.60133	0.002	99.78471	0	100
40	0.074	95.17286	0.305	79.73422	0.003	99.67707	0	100
60	0.091	94.06393	0.319	78.80399	0.004	99.56943	0	100

Table D7: Effect of Contact time on Matrix 4 (25% zeolite 4A/75% metakaolin)

Contact time (mins)	Ni in soln	% Ni uptake	Pb in soln	%Pb uptake	Cd in soln	% Cd uptake	Mn in soln	% Mn uptake
0	1.533	0	1.505	0	0.929	0	4.89	0
1	0.71	53.68558	0.388	74.21927	0.006	99.35414	0	100
2.5	0.064	95.82518	0.304	79.80066	0.002	99.78471	0	100
5	0.059	96.15134	0.287	80.93023	0.001	99.89236	0	100
10	0.032	97.91259	0.299	80.13289	0.001	99.89236	0	100
20	0.048	96.86888	0.299	80.13289	0.003	99.67707	0	100
40	0.048	96.86888	0.314	79.13621	0.003	99.67707	0	100
60	0.026	98.30398	0.308	79.53488	0	100	0	100

APPENDIX E

Effect of Adsorbent Dose on Matrix 2, 3 and 4

Table E1: Absorbance – Concentration for Ni

Ni (ppm)	Abs
0	0
4	0.09
8	0.17
12	0.25

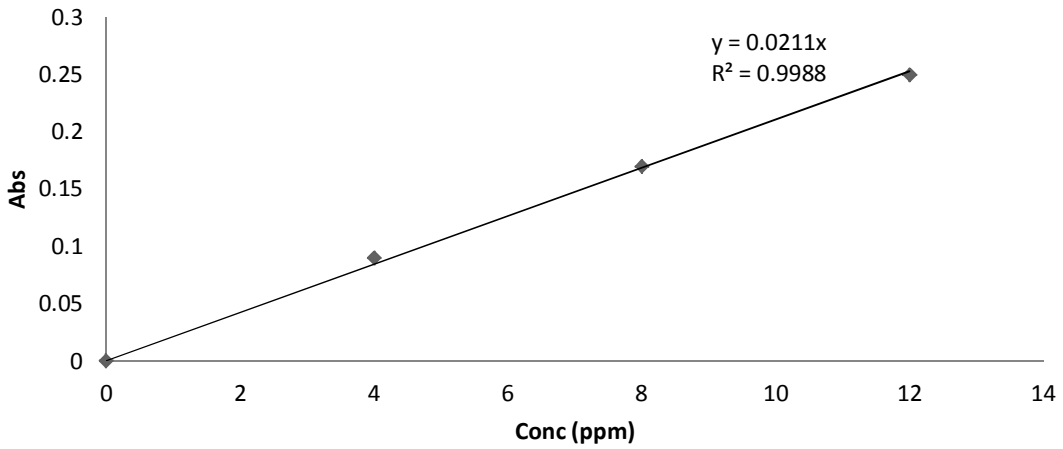


Figure E1. Absorbance - Concentration Calibration Curve for Ni

Table E2: Absorbance – Concentration for Pb

Pb (ppm)	Abs
0	0
3	0.04
5	0.06
7	0.08

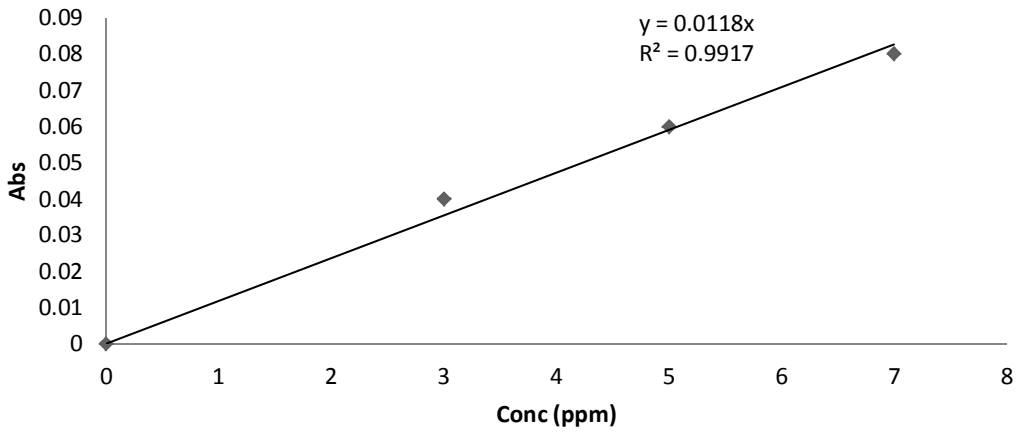


Figure E2. Absorbance - Concentration Calibration Curve for Pb

Table E3. Absorbance – Concentration for Cd

Cd (ppm)	Abs
0	0
0.6	0.08
1.2	0.16
1.8	0.25

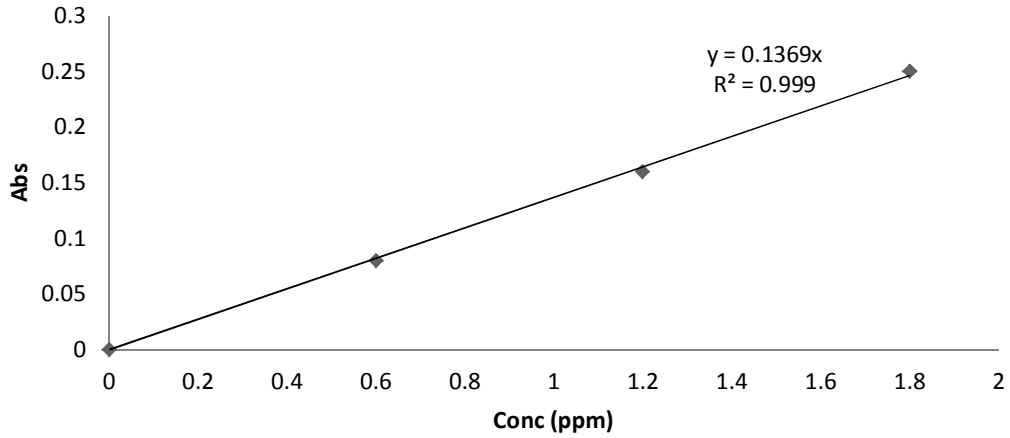


Figure E3. Absorbance - Concentration Calibration Curve for Cd

Table E4. Absorbance – Concentration for Mn

Mn (ppm)	Abs
0	0
1	0.015
2	0.028
3	0.045

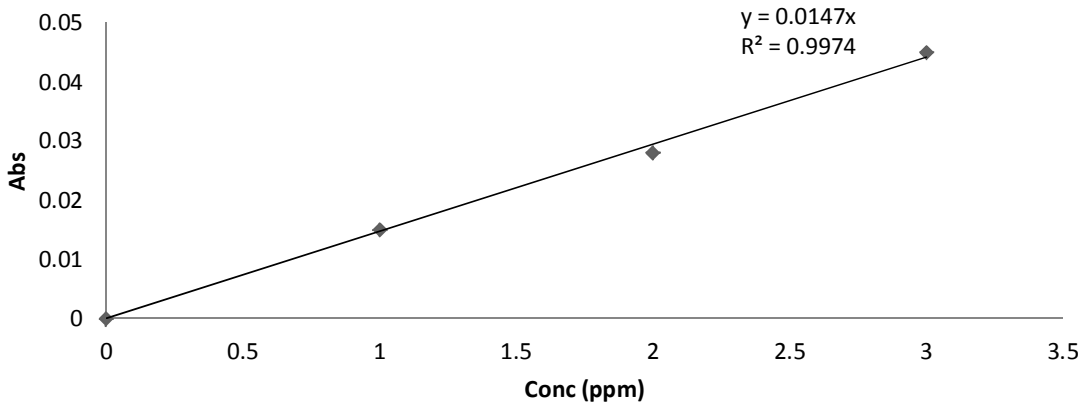


Figure E4. Absorbance - Concentration Calibration Curve for Mn

Table E5 Effects of adsorbent dose on the Matrix 2 (75%Zeolite 4A and 25% Metakaolin)

Adsorbent dose(g)	Ni in soln	% Ni uptake	Pb in soln	% Pb uptake	Cd in soln	% Cd uptake	Mn in soln	% Mn uptake
0	1.533	0	1.505	0	0.929	0	4.89	0
0.1	0.012	99.21722	0.021	98.60465	0.009	99.03122	0.003	99.93865
0.25	0.031	97.97782	0.01	99.33555	0.007	99.2465	0.001	99.97955
0.5	0.019	98.7606	0.004	99.73422	0	100	0.025	99.48875
1	0.012	99.21722	0.043	97.14286	0	100	0.057	98.83436
1.5	0.017	98.89106	0.019	98.73754	0	100	0.039	99.20245

2	0.044	97.12981	0.049	96.74419	0	100	0.047	99.03885
2.5	0.02	98.69537	0.073	95.1495	0	100	0.022	99.5501

Table E6 Effects of adsorbent dose on the Matrix 3 (50% zeolite 4A and 50% metakaolin)

Adsorbent dose(g)	Ni in soln	% Ni uptake	Pb in soln	% Pb uptake	Cd in soln	% Cd uptake	Mn in soln	% Mn uptake
0	1.533	0	1.505	0	0.929	0	4.89	0
		98.6953		89.9667		98.8159		
0.1	0.02	7	0.151	8	0.011	3	0.042	99.1411
				96.0132		98.9235		
0.25	0.019	98.7606	0.06	9	0.01	7	0.034	99.3047
				99.7342				99.4887
0.5	0.019	98.7606	0.004	2	0	100	0.025	5
		99.2172		97.1428				98.8343
1	0.012	2	0.043	6	0	100	0.057	6
		98.8910		98.7375				99.2024
1.5	0.017	6	0.019	4	0	100	0.039	5
		97.1298		96.7441				99.0388
2	0.044	1	0.049	9	0	100	0.047	5
		98.6953						
2.5	0.02	7	0.073	95.1495	0	100	0.022	99.5501

Table E7: Effects of adsorbent dose on Blend 3 (25% zeolite 4A and 25% metakaolin)

Adsorbent dose(g)	Ni in soln	% Ni uptake	Pb in soln	% Pb uptake	Cd in soln	% Cd uptake	Mn in soln	% Mn uptake
0	1.533	0	1.505	0	0.929	0	4.89	0
0.1	0.029	98.10828	0.014	99.06977	0.015	98.38536	0	100
0.25	0.022	98.56491	0.009	99.40199	0.013	98.60065	0	100
0.5	0.018	98.82583	0.0003	99.98007	0	100	0	100
1	0	100	0.0002	99.98671	0	100	0	100
1.5	0	100	0.0007	99.95349	0	100	0	100
2	0	100	0.0002	99.98671	0	100	0	100
2.5	0	100	0.0007	99.95349	0	100	0	100

APPENDIX F

DETERMINATION OF OPTIMUM BLEND

Table F1: Determination of the Best Matrix

Class of Matrix	Ni in soln	% Ni uptake	Pb in soln	% Pb uptake	Cd in soln	% Cd uptake	Mn in soln	% Mn uptake
2	0	100	0.02	98.6711	0	100	0	100
3	0.002	99.86954	0.033	97.8073	0.002	99.7847	0	100
4	0	100	0.005	99.6678	0	100	0	100

APPENDIX G

ELEMENTAL ANALYSIS OF THE CRUDE OIL TANK FARM WASTEWATER

Table G1: Elemental Analysis of the untreated wastewater

Raw water	Ni	Pb	Cd	Mn
Sample 1	0.044	0.225	0.022	1.858
Sample 2	0.04	0.225	0.022	1.823
STD NESREA	0.02	0.01	0.003	0.2

Table G2: Effect of Matrix 4 dose on wastewater at pH of 8, contact time of 10mins and shaking time of 10rpm (maximum speed)

Dose (g)150ml	Ni	Pb	Cd	Mn
0.1	31.81818	65.77778	59.09091	100
0.25	92.95455	92	68.18182	100
0.5	94.31818	98.22222	63.63636	100
1	95	98.22222	72.72727	100
1.5	93.86364	97.33333	72.72727	100
2	92.27273	96.44444	72.72727	100
2.5	91.59091	96.88889	54.54545	100

Table G3: Effect of pH on wastewater sample at contact time of 10mins, Matrix 4 dose of 1g/50ml and shaking speed of 10rpm (maximum speed)

pH	Ni	Pb	Cd	Mn
2	29.54545	74.22222	63.63636	90.31216
4	27.27273	81.77778	68.18182	98.65447
6	59.09091	83.55556	72.72727	100
8	93.18182	98.66667	95.45455	100
10	93.18182	100	95.45455	100
12	59.09091	74.22222	54.54545	100

TableG4: Effect of contact time on wastewater at pH of 8, contact time of 10mins and shaking time of 10 rpm (maximum speed).

Time (mins)	Ni	Pb	Cd	Mn
2.5	47.72727	58.66667	72.72727	99.67707
5	54.54545	60.44444	95.45455	99.62325
10	100	91.11111	96.81818	99.94618
20	79.54545	84.44444	95.45455	100
40	86.36364	88	95.45455	100
60	54.54545	86.22222	97.72727	98.9774

APPENDIX H

TREATMENT OF SIMULATED WASTEWATER WITH SELECTIVE METALS

Table H1. % removal of the metals at the optimal conditions

Metal in soln	B/f trtment	A/ft trtmnt	% removal
Ni	1.533	0.587	61.70907
Pb	1.505	0.823	45.31561
Cd	0.929	0.286	69.21421
Mn	4.89	0.127	97.40286

Table H2. Effect of Matrix 4 dose on selective metals at pH: 8, CT; 10mins and dose; 1g/50ml

Dose(g/50ml)	Ni	Pb	Cd	Mn
untreated	4.89	4.89	4.89	4.89
Treated	0	1.49786	0.2579	0
% Removal	100	69.36892	94.72597	100

Table H3. Effect of Matrix 4 dose on selective mixtures of two metals at pH; 8, CT; 10 mins

Metals	Pb	Mn	Cd	Mn	Ni	Cd	Ni	Pb	Ni	Mn	Pb	Cd
Untreated	4.89	4.89	4.89	4.89	4.89	4.89	4.89	4.89	4.89	4.8	4.89	4.89
Treated	0.279	0.026	0.158	0	0	0.195	0	0.361	0	0	0.169	0.105
% Removal	94.29	99.47	96.77	100	100	96.01	100	92.62	100	100	96.54	97.85

Table H4. Effect of Matrix 4 on all Ni, Pb, Cd and Mn mixed together

Dose (g)	Ni	Pb	Cd	Mn
untreated	4.89	4.89	4.89	4.89
Treated	0	0.15596	0.06843	0
% Removal	100	96.81063	98.60065	100

Table H5. Effect of Matrix 4 on heavy metal removal Ni, Pb, Cd and Mn

Metals in solution	Before Treatment	After Treatment	% Removal
Ni	1.533	0.587	61.70907
Pb	1.505	0.823	45.31561
Cd	0.929	0.286	69.21421
Mn	4.89	0.127	97.40286

APPENDIX I

ELEMENTAL ANALYSIS OF THE CRUDE OIL TANK FARM WASTEWATER

Table I1. Elemental Analysis of the untreated crude oil tank farm Wastewater

Raw water	Ni	Pb	Cd	Mn
Sample 1	0.044	0.225	0.022	1.858
Sample 2	0.04	0.225	0.022	1.823
STD NESREA	0.02	0.01	0.003	0.2

Table I2. Effect of Matrix 4 dose on wastewater at pH of 8, contact time of 10mins and shaking time of 10rpm (maximum speed)

Dose (g)150ml	Ni	Pb	Cd	Mn
0	0	0	0	0
0.1	31.81818	59.09091	65.77778	100
0.25	92.95455	68.18182	92	100
0.5	94.31818	63.63636	98.22222	100
1	95	72.72727	98.22222	100
1.5	93.86364	72.72727	97.33333	100
2	92.27273	72.72727	96.44444	100
2.5	91.59091	54.54545	96.88889	100

Table I3. Effect of pH on Wastewater Sample at Contact time of 10mins, Matrix 4 dose of 1g/50ml and shaking speed of 10rpm (maximum speed)

*p*H	Ni	Pb	Cd	Mn
2	74.22222	29.54545	63.63636	90.31216
4	81.77778	27.27273	68.18182	98.65447
6	83.55556	59.09091	72.72727	100
8	98.66667	93.18182	95.45455	100
10	100	93.18182	95.45455	100
12	74.22222	59.09091	54.54545	100

Table I4. Effect of Contact time on wastewater at pH of 8, contact time of 10mins and shaking time of 10 rpm (maximum speed).

Time (mins)	Ni	Pb	Cd	Mn
0	0	0	0	0
2.5	58.66667	47.72727	72.72727	99.67707
5	60.44444	54.54545	95.45455	99.62325
10	91.11111	100	96.81818	99.94618
20	84.44444	79.54545	95.45455	100
40	88	86.36364	95.45455	100
60	86.22222	54.54545	97.72727	98.9774

APPENDIX J

RESULTS FOR ION EXCHANGE CAPABILITY

Table J1. Matrix 1(100% zeolite 4A/0% metakaolin)

Conc (ppm)	K in solution	Standard	K Removed
600	145.795	432.962	66.3261441
1000	379.962	711.223	46.5762496
1400	398.691	829.57	51.9400412
2000	790.274	1392.136	43.2329887

Table J2. Matrix 5 (0% zeolite 4A/100%metakaolin)

Conc (ppm)	K in solution	Standard	K Removed
600		432.962	100
1000	544.876	711.223	23.3888668
1400	650.076	829.57	21.6369927
2000	947.71	1392.136	31.9240362

TableJ3. Matrix 2 (75% zeolite 4A/25% metakaolin)

Conc (ppm)	K in solution	Standard	K Removed
600	182.905	432.962	57.7549531
1000	368.837	711.223	48.1404567
1400	526.485	829.57	36.5351929
2000	800.862	1392.136	42.4724309

Table J4. Matrix 3 (50% zeolite 4A and 50% metakaolin)

Conc (ppm)	K in solution	Standard	K Removed
600	255.923	432.962	40.8901936
1000	469.22	711.223	34.026318
1400	538.513	829.57	35.0852851
2000	825.27	1392.136	40.7191539

Table J5. Matrix 4 (25% zeolite 4A/75% metakaolin)

Conc (ppm)	K in solution	Standard	K Removed
600	243.805	432.962	43.6890535
1000	435.749	711.223	38.7324369
1400	518.592	829.57	37.4866497
2000	830.24	1392.136	40.3621485

APPENDIX K

ADSORPTION ISOTHERMS / KINETICS STUDIES

The uptake of metal ion at any time, *t* was calculated as:

$$Ce = (co - Ct)/Co$$

The adsorption capacity of a sorbent is calculated as;

$$qe = (Co - Ce)V/M$$

Where

*C*0: is the initial adsorbate concentration (mg/l)

V: the Volume of the solution in the flask, (50 ml of simulated wastewater))

Ct: the adsorbate concentration (mg/l) after time *t*

M: is the mass of the Matrix 4 (sorbent) (g) used in the experiment. (1 g of Matrix 4)

At equilibrium conditions, *qt* and *Ct* are replaced by *q*e and *C*e, respectively.

Table K 1 Freundlich, Langmuir, Temkin Isotherm Models (tables from excel sheet)

(a)

Langmuir		Ni Co=1.533			
t (mins)	Ni in soln(ppm)	Ce	qe	Ce plot	Ce/qe
1	0.71	0.537052	59.75691	0.537052	0.008987
2.5	0.064	0.958447	34.47315	0.958447	0.027803
5	0.059	0.961709	34.27746	0.961709	0.028057
10	0.032	0.979322	33.2207	0.979322	0.029479
20	0.048	0.968885	33.84693	0.968885	0.028625
40	0.048	0.968885	33.84693	0.968885	0.028625
60	0.026	0.983235	32.98587	0.983235	0.029808

(b)	Pb Co=1.505			
t	Ct	qe	Ce	Ce/qe
1	0.388	45.76844	0.742193	0.016216
2.5	0.304	42.4196	0.798007	0.018812
5	0.287	41.74186	0.809302	0.019388
10	0.299	42.22027	0.801329	0.01898
20	0.299	42.22027	0.801329	0.01898
40	0.314	42.81827	0.791362	0.018482
60	0.308	42.57907	0.795349	0.018679

(c)	Cd Co=0.929			
t	Ct	qe	Ce	Ce/qe
1	0.6984	40.84657	0.248224	0.006077
2.5	0.5472	31.08123	0.41098	0.013223
5	0.5166	29.10491	0.443918	0.015252
10	0.5382	30.49996	0.420667	0.013792
20	0.5382	30.49996	0.420667	0.013792
40	0.5652	32.24377	0.391604	0.012145
60	0.5544	31.54624	0.403229	0.012782

(d)

	Mn Co=4.89			
t	Ct	qe	Ce	Ce/qe
1	0	233.4	1	0.004284
2.5	0	233.4	1	0.004284
5	0	233.4	1	0.004284
10	0	233.4	1	0.004284
20	0	233.4	1	0.004284
40	0	233.4	1	0.004284
60	0	233.4	1	0.004284

Table K2 FREUNDLICH

FREUNDLICH

(a)	Ni Co=1.533					
t (mins)	Ni in soln(ppm)	Ce	qe	Ce plot	log Ce	log qe
1	0.71	0.537052	59.75691	0.537052	-0.26998	-1.776388
2.5	0.064	0.958447	34.47315	0.958447	-0.01843	-1.537481
5	0.059	0.961709	34.27746	0.961709	-0.01696	-1.535009
10	0.032	0.979322	33.2207	0.979322	-0.00907	-1.521409
20	0.048	0.968885	33.84693	0.968885	-0.01373	-1.529519
40	0.048	0.968885	33.84693	0.968885	-0.01373	-1.529519
60	0.026	0.983235	32.98587	0.983235	-0.00734	1.518328

(b)	Pb Co=1.505				
t	Ct	qe	Ce	log Ce	log qe
1	0.388	45.76844	0.742193	-0.12948	-1.660566
2.5	0.304	42.4196	0.798007	-0.09799	-1.627567
5	0.287	41.74186	0.809302	-0.09189	-1.620572
10	0.299	42.22027	0.801329	-0.09619	-1.625521
20	0.299	42.22027	0.801329	-0.09619	-1.625521
40	0.314	42.81827	0.791362	-0.10162	-1.631629
60	0.308	42.57907	0.795349	-0.09944	-1.629196

(c)	Cd Co=0.929			
t	log Ce	log qe	InCe	qe
1	-0.60516	1.611156	-1.39342	-40.84657
2.5	-0.38618	1.492498	-0.88921	-31.08123
5	-0.3527	1.463966	-0.81211	-29.10491
10	-0.37606	1.484299	-0.86591	-30.49996
20	-0.37606	1.484299	-0.86591	-30.49996
40	-0.40715	1.508446	-0.9375	-32.24377
60	-0.39445	1.498948	-0.90825	-31.54624

Table K 3 TEMKIN

(a)	Ni Co=1.533					
t (mins)	Ni in soln(ppm)	Ce	qe	Ce plot	In Ce	qe plot
1	0.71	0.537052	59.75691	0.537052	-0.62166	59.75691
2.5	0.064	0.958447	34.47315	0.958447	-0.04244	34.47315
5	0.059	0.961709	34.27746	0.961709	-0.03904	34.27746
10	0.032	0.979322	33.2207	0.979322	-0.0209	33.2207
20	0.048	0.968885	33.84693	0.968885	-0.03161	33.84693
40	0.048	0.968885	33.84693	0.968885	-0.03161	33.84693
60	0.026	0.983235	32.98587	0.983235	-0.01691	32.98587

(b)	Pb Co=1.505				
t	Ct	qe	Ce	In Ce	qe plot
1	0.388	45.76844	0.742193	-0.29815	45.76844
2.5	0.304	42.4196	0.798007	-0.22564	42.4196
5	0.287	41.74186	0.809302	-0.21158	41.74186
10	0.299	42.22027	0.801329	-0.22148	42.22027
20	0.299	42.22027	0.801329	-0.22148	42.22027
40	0.314	42.81827	0.791362	-0.234	42.81827
60	0.308	42.57907	0.795349	-0.22897	42.57907

(c)	Cd Co=0.929			
t	log Ce	log qe	InCe	qe
1	-0.60516	-1.611156	-1.39342	40.84657
2.5	-0.38618	-1.492498	-0.88921	31.08123
5	-0.3527	-1.463966	-0.81211	29.10491
10	-0.37606	-1.484299	-0.86591	30.49996
20	-0.37606	-1.484299	-0.86591	30.49996
40	-0.40715	-1.508446	-0.9375	32.24377
60	-0.39445	-1.498948	-0.90825	31.54624

Table K4 KINETICS

(a) Ni ions kinetic data evaluation table

t (mins)	Ni in soln(ppm)	qe-qt	abs (qe-qt)	log(qe-qt)	t/q	t^0.5	q
1	0.71	10.37691	10.37691	1.01606805	0.020251	1	49.38
2.5	0.064	53.6668	53.6668493	1.7297061	0.028364	1.581139	88.14
5	0.059	54.1625	54.162544	1.73369906	0.056536	2.236068	88.44
10	0.032	56.8393	56.8392955	1.75464869	0.111037	3.162278	90.06
20	0.048	55.2531	55.2530724	1.74235643	0.224467	4.472136	89.1
40	0.048	55.2531	55.2530724	1.74235643	0.448934	6.324555	89.1
60	0.026	57.4341	57.4341292	1.75917004	0.66357	7.745967	90.42

(b) Pb ions kinetic data evaluation table

t	Ct	qe-qt	t plot	log(qe-qt)	t/q	t^0.5	q
1	0.388	21.25156	1	1.327391	0.014921	0.122151	67.02
2.5	0.304	29.6404	2.5	1.471884	0.034693	0.186261	72.06
5	0.287	31.33814	5	1.496073	0.068418	0.261569	73.08
10	0.299	30.13973	10	1.479139	0.138198	0.37175	72.36
20	0.299	30.13973	20	1.479139	0.276396	0.525734	72.36
40	0.314	28.64173	40	1.456999	0.559754	0.748167	71.46
60	0.308	29.24093	60	1.465991	0.835422	0.914014	71.82

(C) Cd ions kinetic data evaluation table

t	qt	qe-qt	t	log(qe-qt)
1	0.248224	40.59834	1	1.608508
2.5	0.41098	30.67025	2.5	1.486717
5	0.443918	28.66099	5	1.457291
10	0.420667	30.07929	10	1.478268
20	0.420667	30.07929	20	1.478268
40	0.391604	31.85216	40	1.503139
60	0.403229	31.14301	60	1.493361

APPENDIX L

OPTIMIZATION STUDIES

FULL FACTORIAL ANALYSIS

Table L1. Parameters Blend dose, Contact time, pH and Ni, Pb, Cd, Mn Removed (%)

RunOrder	CenterPt	Blocks	x1	x2	x3	yNi	yPb	yCd	yMn
1	1	1	1.5	20	12	99.6391	99.6105	99.2122	99.9011
2	1	1	0.5	5	4	86.6002	80.1325	79.2324	96.1112
3	1	1	1.5	20	4	91.7811	89.7889	91.5444	97.8883
4	1	1	0.5	20	12	96.6079	99.2105	98.9788	99.4007
5	1	1	0.5	20	4	90.0984	84.7669	90.8772	95.9933
6	1	1	1.5	5	4	93.2219	95.4551	88.7756	98.0046
7	1	1	0.5	20	12	97.3801	99.2444	98.8888	99.3117
8	1	1	1.5	20	4	91.6904	96.1552	91.0006	97.8323
9	1	1	1.5	20	12	98.9944	99.7788	98.8991	99.8899
10	1	1	0.5	5	12	97.0019	99.1778	96.9885	99.4444
11	1	1	0.5	20	4	84.1124	85.0114	84.1113	96.1888
12	1	1	1.5	5	12	99.8811	99.7325	98.9912	99.8859
13	1	1	0.5	5	12	97.0624	98.7987	95.8888	99.6401
14	1	1	1.5	5	12	99.9703	99.4999	99.0418	99.8986
15	1	1	1.5	5	4	90.4316	90.0341	87.8868	96.6443
16	1	1	0.5	5	4	83.8756	81.0818	80.1322	95.6116

Notation;
X1; Matrix 4 dose
X2; Contact time
X3; pH
yNi; Percentage nickel removed
yPb. Percentage lead removed
yCd. Percentage cadmium removed
yMn. Percentage manganese removed

Nickel Factorial Plot

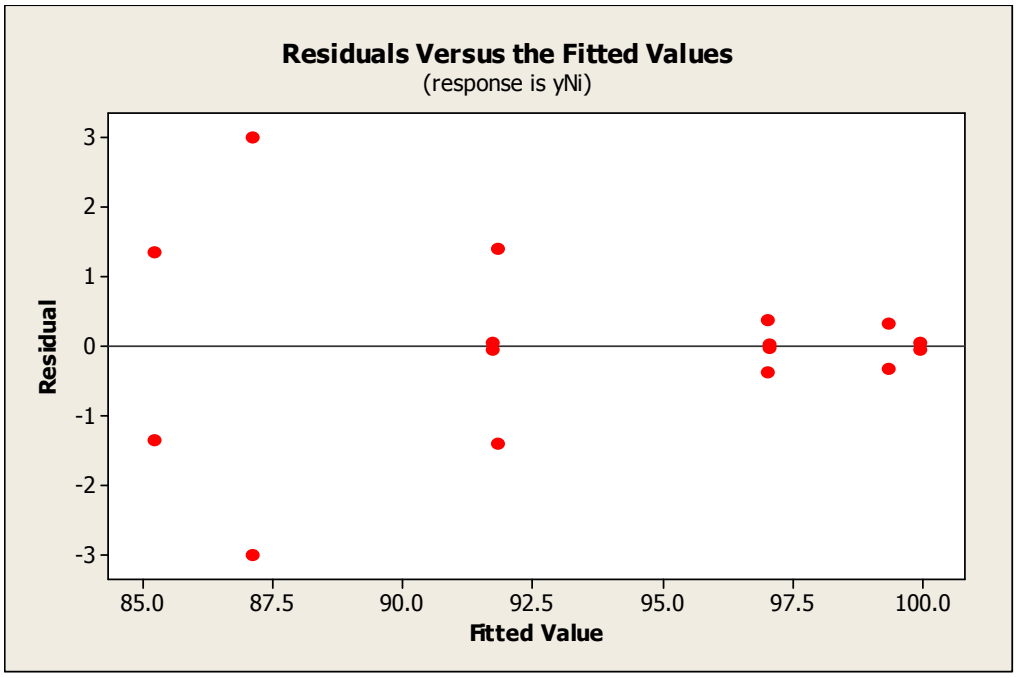


Figure L1 Residuals Versus the Fitted values

Full Factorial Design

```
Factors:    3   Base Design:          3, 8
Runs:      16   Replicates:             2
Blocks:     1   Center pts (total):     0

All terms are free from aliasing.
```

Factorial Fit: yNi versus x1, x2, x3

Table L2 Estimated Effects and Coefficients for yNi (coded units)

Term	Effect	Coef	SE Coef	T	P
Constant		93.6468	0.4510	207.64	0.000
x1	4.1088	2.0544	0.4510	4.56	0.002
x2	0.2823	0.1412	0.4510	0.31	0.762
x3	9.3407	4.6703	0.4510	10.36	0.000
x1*x2	-0.6323	-0.3162	0.4510	-0.70	0.503
x1*x3	-1.5007	-0.7504	0.4510	-1.66	0.135
x2*x3	-0.6059	-0.3029	0.4510	-0.67	0.521
x1*x2*x3	0.3469	0.1735	0.4510	0.38	0.711

```
S = 1.80404   R-Sq = 94.28%   R-Sq(adj) = 89.28%
```

Table L3 Analysis of Variance for yNi (coded units)

Source	DF	Seq SS	Adj SS	Adj MS	F	P
Main Effects	3	416.843	416.843	138.948	42.69	0.000
2-Way Interactions	3	12.077	12.077	4.026	1.24	0.358
3-Way Interactions	1	0.481	0.481	0.481	0.15	0.711
Residual Error	8	26.036	26.036	3.255		
Pure Error	8	26.036	26.036	3.255		
Total	15	455.438				

Table L4 Estimated Coefficients for yNi using data in uncoded units

Term	Coef
Constant	73.7404
x1	9.32058
x2	0.276431
x3	1.81354
x1*x2	-0.176824
x1*x3	-0.519729
x2*x3	-0.0216621
x1*x2*x3	0.0115639

Effects Plot for yNi

Effects Pareto for yNi

Alias Structure
I
x1
x2
x3
x1*x2
x1*x3
x2*x3
x1*x2*x3

LEAD FACTORIAL PLOT

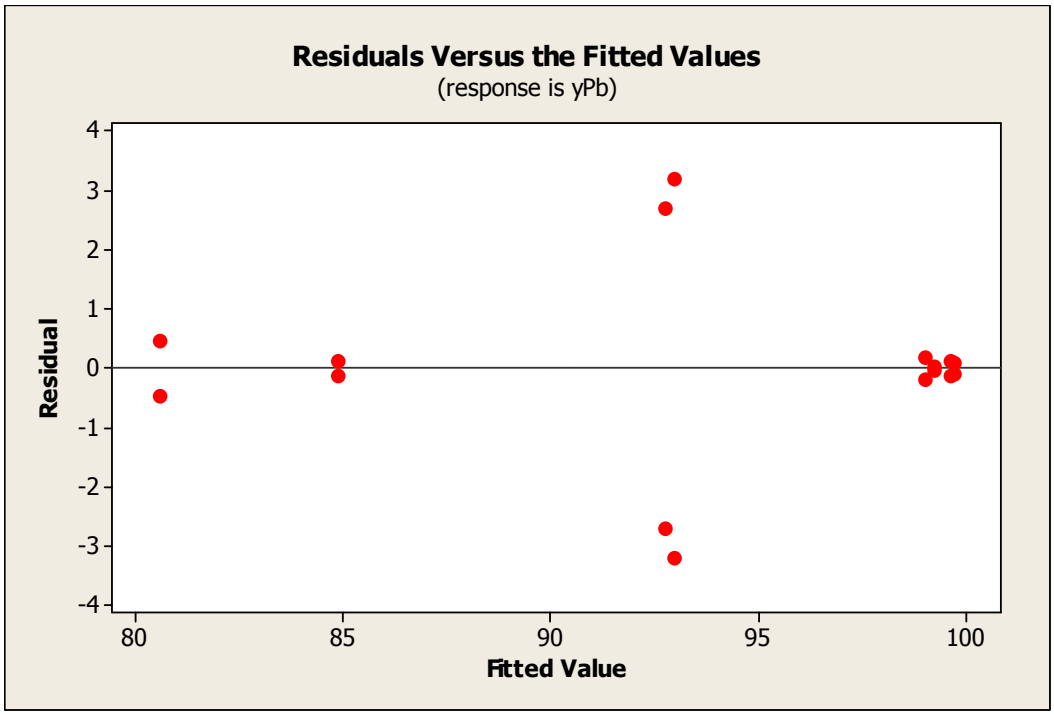


Figure L2 Residuals versus the Fitted Values for Lead

Factorial Fit: yPb versus x1, x2, x3

Table 5 Estimated Effects and Coefficients for yPb (coded units)

Term	Effect	Coef	SE Coef	T	P
Constant		93.592	0.5270	177.59	0.000
x1	5.329	2.664	0.5270	5.06	0.001
x2	1.207	0.603	0.5270	1.14	0.285
x3	11.578	5.789	0.5270	10.98	0.000
x1*x2	-1.054	-0.527	0.5270	-1.00	0.347
x1*x3	-4.781	-2.391	0.5270	-4.54	0.002
x2*x3	-1.048	-0.524	0.5270	-0.99	0.349
x1*x2*x3	0.973	0.487	0.5270	0.92	0.383

S = 2.10810 R-Sq = 95.53% R-Sq(adj) = 91.62%

Table L6 Analysis of Variance for yPb (coded units)

Source	DF	Seq SS	Adj SS	Adj MS	F	P
Main Effects	3	655.650	655.650	218.550	49.18	0.000
2-Way Interactions	3	100.278	100.278	33.426	7.52	0.010
3-Way Interactions	1	3.790	3.790	3.790	0.85	0.383
Residual Error	8	35.553	35.553	4.444		
Pure Error	8	35.553	35.553	4.444		
Total	15	795.272				

Table L7 Estimated Coefficients for yPb using data in uncoded units

Term	Coef
Constant	59.3691
x1	19.8927
x2	0.620275
x3	3.26655
x1*x2	-0.400097
x1*x3	-1.60093
x2*x3	-0.0499142
x1*x2*x3	0.0324483

Effects Plot for yPb

Effects Pareto for yPb

Alias Structure
I
x1
x2
x3
x1*x2
x1*x3
x2*x3
x1*x2*x3

Cadmium FACTORIAL PLOT

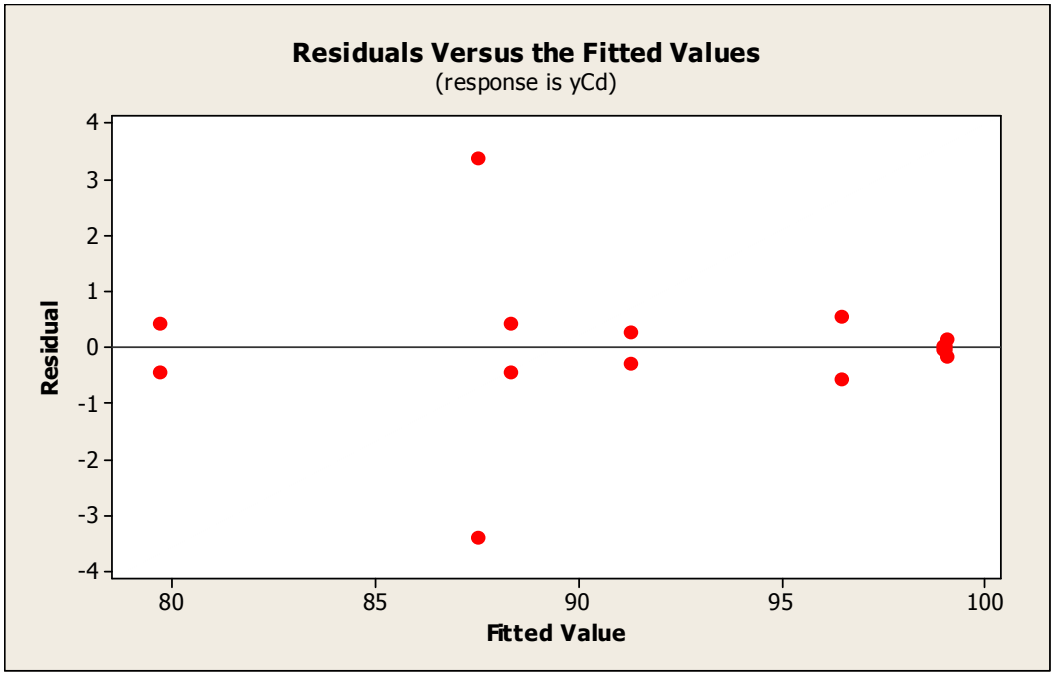


Figure L3 residuals Versus the Fitted Values

Factorial Fit: yCd versus x1, x2, x3

Table L8 Estimated Effects and Coefficients for yCd (coded units)

Term	Effect	Coef	SE Coef	T	P
Constant		92.528	0.4375	211.51	0.000
x1	3.782	1.891	0.4375	4.32	0.003
x2	3.322	1.661	0.4375	3.80	0.005
x3	11.666	5.833	0.4375	13.33	0.000
x1*x2	-1.832	-0.916	0.4375	-2.09	0.070
x1*x3	-2.432	-1.216	0.4375	-2.78	0.024
x2*x3	-2.055	-1.027	0.4375	-2.35	0.047
x1*x2*x3	0.604	0.302	0.4375	0.69	0.510

S = 1.74983 R-Sq = 96.62% R-Sq(adj) = 93.67%

Table L9 Analysis of Variance for yCd (coded units)

Source	DF	Seq SS	Adj SS	Adj MS	F	P
Main Effects	3	645.736	645.736	215.245	70.30	0.000
2-Way Interactions	3	53.964	53.964	17.988	5.87	0.020
3-Way Interactions	1	1.458	1.458	1.458	0.48	0.510
Residual Error	8	24.495	24.495	3.062		
Pure Error	8	24.495	24.495	3.062		
Total	15	725.653				

Table L10 Estimated Coefficients for yCd using data in uncoded units

Term	Coef
Constant	60.9588
x1	13.7104
x2	0.900624
x3	2.74583
x1*x2	-0.405199
x1*x3	-0.859496
x2*x3	-0.0543681
x1*x2*x3	0.0201223

Effects Plot for yCd

Effects Pareto for yCd

Alias Structure
I
x1
x2
x3
x1*x2
x1*x3
x2*x3
x1*x2*x3

MANGANESE FACTORIAL PLOT

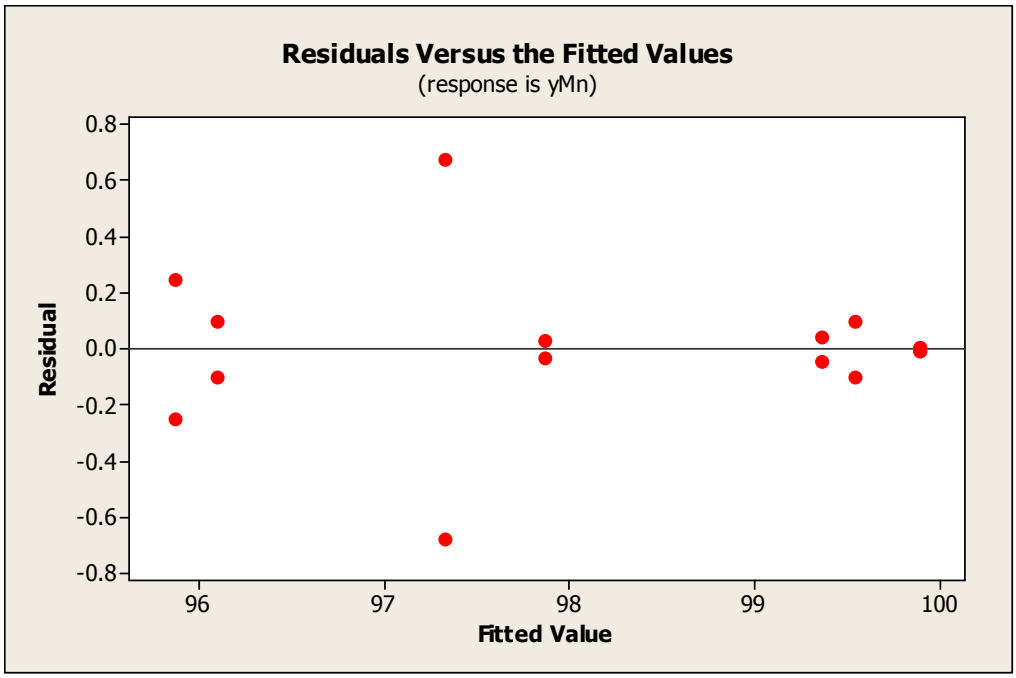


Figure L4 Residuals versus Fitted Values for Manganese

Factorial Fit: yMn versus x1, x2, x3

Table L11 Estimated Effects and Coefficients for yMn (coded units)

Term	Effect	Coef	SE Coef	T	P
Constant		98.2279	0.09244	1062.56	0.000
x1	1.0304	0.5152	0.09244	5.57	0.001
x2	0.1457	0.0728	0.09244	0.79	0.454
x3	2.8873	1.4436	0.09244	15.62	0.000
x1*x2	0.1239	0.0619	0.09244	0.67	0.522
x1*x3	-0.5858	-0.2929	0.09244	-3.17	0.013
x2*x3	-0.2371	-0.1185	0.09244	-1.28	0.236
x1*x2*x3	-0.0292	-0.0146	0.09244	-0.16	0.878

S = 0.369777 R-Sq = 97.29% R-Sq(adj) = 94.93%

Table L12 Analysis of Variance for yMn (coded units)

Source	DF	Seq SS	Adj SS	Adj MS	F	P
Main Effects	3	37.6768	37.6768	12.5589	91.85	0.000
2-Way Interactions	3	1.6587	1.6587	0.5529	4.04	0.051
3-Way Interactions	1	0.0034	0.0034	0.0034	0.02	0.878
Residual Error	8	1.0939	1.0939	0.1367		
Pure Error	8	1.0939	1.0939	0.1367		
Total	15	40.4327				

Table L13 Estimated Coefficients for yMn using data in uncoded units

Term	Coef
Constant	92.9261
x1	1.89808
x2	0.0170138
x3	0.544564
x1*x2	0.0243073
x1*x3	-0.134265
x2*x3	-0.00297742
x1*x2*x3	-0.00097392

Effects Plot for yMn

Effects Pareto for yMn

Alias Structure
I
x1
x2
x3
x1*x2
x1*x3
x2*x3
x1*x2*x3

APPENDIX M

RESPONSE SURFACE METHODOLOGY (RSM)

Table M1. Experimental results for RSM at three parameters under consideration; matrix 4 dose (0.5 - 1.5), pH; (4 - 12) and contact time; (5 - 20 mins)

RUN	BLOCK	Matrix 4 dose g/50ml	Cont. Time(MnS)	*p*H	%NiRmd	%Pb Rmd	%Cd Rmd	%Mn Rmd
1	1	0.5	5	8	97.02236	99.01819	96.7805	99.71801
2	1	0.5	5	8	97.72598	98.81184	95.92649	99.72651
3	1	1	20	12	98.70056	87.38955	99.68792	99.83268
4	1	1	5	12	98.21352	88.42294	97.14193	99.88534
5	1	1.5	12.5	4	99.43162	99.53406	98.60368	99.9295
6	1	1	12.5	8	97.83427	98.9666	98.81745	99.74434
7	1	1.5	20	8	97.5638	99.69048	98.60368	99.90317
8	1	0.5	20	8	97.78037	98.60383	99.24428	99.80635
9	1	1	5	4	99.02542	99.01819	99.4909	99.54135
10	1	1	20	4	99.29638	99.17295	96.22212	99.89383
11	1	1	12.5	8	97.78037	98.13955	96.79696	99.90317
12	1	1	12.5	8	98.05084	99.48247	91.09726	99.74434
13	1	1	12.5	8	98.15913	98.91502	99.99825	99.92101
14	1	0.5	12.5	12	98.70056	86.35615	98.47248	99.69168
15	1	0.5	12.5	4	98.05084	98.50066	95.15433	99.69168
16	1	1	12.5	8	98.15913	98.60383	99.1953	99.68234
17	1	1.5	12.5	12	98.34875	90.12863	98.85033	99.797

(1) NICKEL

Table M2 Design Summary

Study Type	Response Surface			**Experiments**	17
Initial Design	Box Behnken			**Blocks**	No Blocks
Design Model	Quadratic				
Response	**Name**	**Units**	**Obs**	**Minimum**	**Maximum**
Trans	**Model**				
Y1	Ni Rmd	%	17	97.02	99.43
None	Quadratic				
Y2	Pb Rmd	%	17	86.36	99.69
None	Quadratic				
Y3	Cd Rmd	%	17	91.10	100.00
None	Mean				
Y4	Mn	%	17	99.54	99.93
None	2FI				

Factor	**Name**	**Units**	**Type**	**Low Actual**	**High Actual**	
Low Coded	**High Coded**					
A	Matrix 4 dose	g/50ml	Numeric	0.50	1.50	-
1.000	1.000					
B	Cont. time	mins	Numeric	5.00	20.00	-
1.000	1.000					
C	pH		Numeric	4.00	12.00	-
1.000	1.000					

Response: Ni Rmd

***** WARNING: The Cubic Model is Aliased! *****

Table M3 **Sequential Model Sum of Squares**

Source	Sum of Squares	DF	Mean Square	F Value	Prob > F	
Mean	1.640E+005	1	1.640E+005			Suggested
Linear	1.31	3	0.44	1.10	0.3853	
2FI	1.78	3	0.59	1.76	0.2185	
Quadratic	2.74	3	0.91	10.04	0.0063	Suggested
Cubic	0.26	2	0.13	1.73	0.2688	Aliased
Residual	0.38	5	0.075			
Total	1.640E+005	17	9648.75			

"Sequential Model Sum of Squares": Select the highest order polynomial where the additional terms are significant and the model is not aliased.

Table M4 **Lack of Fit Tests**

Source	Sum of Squares	DF	Mean Square	F Value	Prob > F	
Linear	4.78	8	0.60	7.94	0.0177	
2FI	3.00	5	0.60	7.97	0.0199	
Quadratic	0.26	2	0.13	1.73	0.2688	Suggested
Cubic	0.000	0				Aliased
Pure Error	0.38	5	0.075			

"Lack of Fit Tests": Want the selected model to have insignificant lack-of-fit.

Table M5 **Model Summary Statistics**

Source	Std. Dev.	R-Squared	Adjusted R-Squared	Predicted R-Squared	PRESS	
Linear	0.63	0.2020	0.0179	-0.5539	10.04	
2FI	0.58	0.4776	0.1641	-1.2901	14.80	
Quadratic	0.30	0.9015	0.7748		+	Suggested
Cubic	0.27	0.9418	0.8136		+	Aliased

+ Case(s) with leverage of 1.0000: PRESS statistic not defined

"Model Summary Statistics": Focus on the model maximizing the "Adjusted R-Squared"
and the "Predicted R-Squared".

Response: Ni Removal

Table M6 **ANOVA for Response Surface Quadratic Model**

Analysis of variance table [Partial sum of squares]

Source	Sum of Squares	DF	Mean Square	F Value	Prob > F	
Model	5.83	9	0.65	7.12	0.0085	significant
A	*0.14*	*1*	*0.14*	*1.51*	*0.2586*	
B	*0.044*	*1*	*0.044*	*0.49*	*0.5077*	
C	*0.42*	*1*	*0.42*	*4.66*	*0.0678*	
A^2	*0.21*	*1*	*0.21*	*2.26*	*0.1766*	
B^2	*0.016*	*1*	*0.016*	*0.18*	*0.6863*	
C^2	*2.66*	*1*	*2.66*	*29.30*	*0.0010*	
AB	*0.058*	*1*	*0.058*	*0.64*	*0.4499*	
AC	*0.75*	*1*	*0.75*	*8.25*	*0.0239*	
BC	*0.012*	*1*	*0.012*	*0.13*	*0.7307*	
Residual	0.64	7	0.091			
Lack of Fit	*0.26*	*2*	*0.13*	*1.73*	*0.2688*	*not significan*
Pure Error	*0.38*	*5*	*0.075*			
Cor Total	6.46	16				

Std. Dev.	0.30	R-Squared	0.9015
Mean	98.23	Adj R-Squared	0.7748
C.V.	0.31	Pred R-Squared	N/A
PRESS	N/A	Adeq Precision	9.421

Case(s) with leverage of 1.0000: Pred R-Squared and PRESS statistic not defined

Table M7 Precision" measures

Factor	Coefficient Estimate	DF	Standard Error	95% CI Low	95% CI High	VIF
Intercept	98.00	1	0.13	97.68	98.32	
A-Matrix 4 dose	0.16	1	0.13	-0.14	0.46	1.39
B-Cont. time	0.089	1	0.13	-0.21	0.39	1.43
C-pH	-0.23	1	0.11	-0.48	0.022	1.00
A^2	-0.24	1	0.16	-0.63	0.14	1.23
B^2	-0.069	1	0.16	-0.45	0.32	1.23
C^2	0.88	1	0.16	0.50	1.27	1.23
AB	-0.16	1	0.21	-0.65	0.32	1.75
AC	-0.43	1	0.15	-0.79	-0.077	1.00
BC	0.054	1	0.15	-0.30	0.41	1.00

Table M8 **Final Equation in Terms of Coded Factors:**

Ni Rmd	=
+98.00	
+0.16	* A
+0.089	* B
-0.23	* C
-0.24	* A^2
-0.069	* B^2
+0.88	* C^2
-0.16	* A * B
-0.43	* A * C
+0.054	* B * C

Table M9 **Final Equation in Terms of Actual Factors:**

Ni Rmd	=
+98.24919	

+4.55040 * Matrix 4 dose
+0.071753 * Cont. time
-0.74420 * pH
-0.97818 * Matrix 4 dose^2
-1.21809E-003 * Cont. time^2
+0.055046 * pH^2
-0.043847 * Matrix 4 dose * Cont. time
-0.21657 * Matrix 4 dose * pH
+1.80069E-003 * Cont. time * pH

Table M 10 Diagnostics Case Statistics

Standard Order	Actual Value	Predicted Value	Residual	Leverage	Student Residual	Cook's Distance	Outlier	Run Order
1	98.70	98.72	-0.021	0.804	-0.159	0.010	-0.148	3
2	97.73	97.27	0.45	0.429	1.984	0.295	2.777	2
3	99.43	99.45	-0.021	0.804	-0.159	0.010	-0.148	5
4	97.56	97.76	-0.20	0.714	-1.247	0.389	-1.310	7
5	98.35	98.13	0.22	0.804	1.664	1.132	1.981	17
6	97.02	97.27	-0.25	0.429	-1.102	0.091	-1.122	1
7	98.21	98.44	-0.22	0.804	-1.664	1.132	-1.981	4
8	97.83	98.00	-0.16	0.200	-0.602	0.009	-0.573	6
9	98.16	98.00	0.16	0.200	0.602	0.009	0.572	16
10	98.05	98.00	0.054	0.200	0.201	0.001	0.186	12
11	97.78	97.78	0.000	1.000				8
12	99.03	99.00	0.021	0.804	0.159	0.010	0.148	9
13	98.05	98.27	-0.22	0.804	-1.664	1.132	-1.981	15
14	97.78	98.00	-0.22	0.200	-0.802	0.016	-0.779	11
15	98.16	98.00	0.16	0.200	0.602	0.009	0.572	13
16	99.30	99.07	0.22	0.804	1.664	1.132	1.981	10
17	98.70	98.68	0.021	0.804	0.159	0.010	0.148	14

Case(s) with leverage of 1.0000: Student Residuals, Cooks Distance & Outlier T undefined.

(2) LEAD

Response: Pb Rmd
***** WARNING: The Cubic Model is Aliased! *****

Table M11 **Sequential Model Sum of Squares**

Source	Sum of Squares	DF	Mean Square	F Value	Prob > F	
Mean	1.580E+005	1	1.580E+005			
Linear	241.36	3	80.45	7.98	0.0029	Suggested
2FI	13.22	3	4.41	0.37	0.7739	
Quadratic	116.39	3	38.80	182.32	< 0.0001	Suggested
Cubic	0.49	2	0.24	1.22	0.3696	Aliased
Residual	1.00	5	0.20			
Total	1.583E+005	17	9314.36			

"Sequential Model Sum of Squares": Select the highest order polynomial where the additional terms are significant and the model is not aliased.

Table M12 **Lack of Fit Tests**

Source	Sum of Squares	DF	Mean Square	F Value	Prob > F	
Linear	130.10	8	16.26	81.28	< 0.0001	Suggested
2FI	116.88	5	23.38	116.83	< 0.0001	
Quadratic	0.49	2	0.24	1.22	0.3696	Suggested
Cubic	0.000	0				Aliased
Pure Error	1.00	5	0.20			

"Lack of Fit Tests": Want the selected model to have insignificant lack-of-fit.

Table M13 **Model Summary Statistics**

Source	Std. Dev.	R-Squared	Adjusted R-Squared	Predicted R-Squared	PRESS	
Linear	3.18	0.6480	0.5668	0.3481	242.80	Suggested
2FI	3.43	0.6835	0.4936	-0.2573	468.29	
Quadratic	0.46	0.9960	0.9909		+	Suggested
Cubic	0.45	0.9973	0.9914		+	Aliased

+ Case(s) with leverage of 1.0000: PRESS statistic not defined

"Model Summary Statistics": Focus on the model maximizing the "Adjusted R-Squared" and the "Predicted R-Squared".

Response: Pb Rmd

Table M14 ANOVA for Response Surface Quadratic Model

Analysis of variance table [Partial sum of squares]

Source	Sum of Squares	DF	Mean Square	F Value	Prob > F	
Model	370.97	9	41.22	193.70	< 0.0001	significant
A	*5.96*	*1*	*5.96*	*28.01*	*0.0011*	
B	*0.85*	*1*	*0.85*	*3.99*	*0.0859*	
C	*241.21*	*1*	*241.21*	*1133.53*	*< 0.0001*	
A^2	*0.88*	*1*	*0.88*	*4.15*	*0.0811*	
B^2	*0.49*	*1*	*0.49*	*2.31*	*0.1727*	
C^2	*111.56*	*1*	*111.56*	*524.26*	*< 0.0001*	
AB	*0.22*	*1*	*0.22*	*1.03*	*0.3444*	
AC	*1.88*	*1*	*1.88*	*8.81*	*0.0208*	
BC	*0.35*	*1*	*0.35*	*1.66*	*0.2387*	
Residual	1.49	7	0.21			
Lack of Fit	*0.49*	*2*	*0.24*	*1.22*	*0.3696*	*not significan*
Pure Error	*1.00*	*5*	*0.20*			
Cor Total	372.46	16				

Std. Dev.	0.46	R-Squared	0.9960
Mean	96.40	Adj R-Squared	0.9909
C.V.	0.48	Pred R-Squared	N/A
PRESS	N/A	Adeq Precision	38.461

Case(s) with leverage of 1.0000: Pred R-Squared and PRESS statistic not defined

Table M15 Precision" measures

Factor	Coefficient Estimate	DF	Standard Error	95% CI Low	95% CI High	VIF
Intercept	98.82	1	0.21	98.33	99.31	
A-Matrix 4 dose	1.03	1	0.19	0.57	1.49	1.39
B-Cont. time	-0.39	1	0.19	-0.85	0.072	1.43
C-pH	-5.49	1	0.16	-5.88	-5.11	1.00
A^2	0.51	1	0.25	-0.082	1.10	1.23
B^2	0.38	1	0.25	-0.21	0.97	1.23
C^2	-5.70	1	0.25	-6.29	-5.11	1.23
AB	-0.32	1	0.31	-1.06	0.42	1.75
AC	0.68	1	0.23	0.14	1.23	1.00
BC	-0.30	1	0.23	-0.84	0.25	1.00

Table M16 **Final Equation in Terms of Coded Factors:**

Pb Rmd =

+98.82	
+1.03	* A
-0.39	* B
-5.49	* C
+0.51	* A^2
+0.38	* B^2
-5.70	* C^2
-0.32	* A * B
+0.68	* A * C
-0.30	* B * C

Table M17 **Final Equation in Terms of Actual Factors:**

Pb Rmd	=
+89.35916	
-3.66843	* Matrix 4 dose
-0.055691	* Cont. time
+4.10711	* pH
+2.02752	* Matrix 4 $dose^2$
+6.71848E-003	* Cont. $time^2$
-0.35616	* pH^2
-0.084979	* Matrix 4 dose * Cont. time
+0.34239	* Matrix 4 dose * pH
-9.90132E-003	* Cont. time * pH

Table M18 Diagnostics Case Statistics

Standard Order	Actual Value	Predicted Value	Residual	Leverage	Student Residual	Cook's Distance	Outlier	Run Order
1	87.39	87.32	0.066	0.804	0.324	0.043	0.302	3
2	98.81	98.75	0.067	0.429	0.191	0.003	0.177	2
3	99.53	99.47	0.066	0.804	0.324	0.043	0.302	5
4	99.69	100.03	-0.34	0.714	-1.377	0.474	-1.493	7
5	90.13	89.86	0.27	0.804	1.337	0.731	1.434	17
6	99.02	98.75	0.27	0.429	0.783	0.046	0.759	1
7	88.42	88.70	-0.27	0.804	-1.337	0.731	-1.434	4
8	98.97	98.82	0.15	0.200	0.352	0.003	0.329	6
9	98.60	98.82	-0.22	0.200	-0.528	0.007	-0.498	16
10	99.48	98.82	0.66	0.200	1.602	0.064	1.864	12
11	98.60	98.60	0.000	1.000				8
12	99.02	99.08	-0.066	0.804	-0.324	0.043	-0.302	9
13	98.50	98.77	-0.27	0.804	-1.337	0.731	-1.434	15
14	98.14	98.82	-0.68	0.200	-1.653	0.068	-1.960	11
15	98.92	98.82	0.094	0.200	0.227	0.001	0.211	13
16	99.17	98.90	0.27	0.804	1.337	0.731	1.434	10
17	86.36	86.42	-0.066	0.804	-0.324	0.043	-0.302	14

(3) CADMIUM

Table M19 **Sequential Model Sum of Squares**

Source	Sum of Squares	DF	Mean Square	F Value	Prob > F	
Mean	1.653E+005	1	1.653E+005			Suggested
Linear	2.78	3	0.93	0.59	0.6323	
2FI	12.70	3	4.23	5.51	0.0170	
Quadratic	5.27	3	1.76	5.10	0.0351	Suggested
Cubic	1.16	2	0.58	2.32	0.1942	Aliased
Residual	1.25	5	0.25			
Total	1.653E+005	17	9725.17			

"Sequential Model Sum of Squares": Select the highest order polynomial where the additional terms are significant and the model is not aliased.

Table M20 **Lack of Fit Tests**

Source	Sum of Squares	DF	Mean Square	F Value	Prob > F	
Linear	19.13	8	2.39	9.55	0.0118	
2FI	6.43	5	1.29	5.13	0.0484	
Quadratic	1.16	2	0.58	2.32	0.1942	Suggested
Cubic	0.000	0				Aliased
Pure Error	1.25	5	0.25			

"Lack of Fit Tests": Want the selected model to have insignificant lack-of-fit.

Table M21 **Model Summary Statistics**

Source	Std. Dev.	R-Squared	Adjusted R-Squared	Predicted R-Squared	PRESS	
Linear	1.25	0.1198	-0.0833	-0.5883	36.78	
2FI	0.88	0.6683	0.4693	-0.0306	23.86	
Quadratic	0.59	0.8958	0.7619		+	Suggested
Cubic	0.50	0.9459	0.8270		+	Aliased

+ Case(s) with leverage of 1.0000: PRESS statistic not defined

"Model Summary Statistics": Focus on the model maximizing the "Adjusted R-Squared"
and the "Predicted R-Squared".

Table M22 **Analysis of variance table [Partial sum of squares]**

Source	Sum of Squares	DF	Mean Square	F Value	Prob > F	
Model	20.74	9	2.30	6.69	0.0101	significant
A	*0.91*	*1*	*0.91*	*2.64*	*0.1484*	
B	*0.051*	*1*	*0.051*	*0.15*	*0.7128*	
C	*0.23*	*1*	*0.23*	*0.67*	*0.4389*	
A^2	*0.29*	*1*	*0.29*	*0.85*	*0.3870*	
B^2	*1.97*	*1*	*1.97*	*5.70*	*0.0483*	
C^2	*1.73*	*1*	*1.73*	*5.02*	*0.0601*	
AB	*2.15*	*1*	*2.15*	*6.24*	*0.0411*	
AC	*0.015*	*1*	*0.015*	*0.045*	*0.8389*	
BC	*8.45*	*1*	*8.45*	*24.53*	*0.0017*	
Residual	2.41	7	0.34			
Lack of Fit	*1.16*	*2*	*0.58*	*2.32*	*0.1942*	*not significan*
Pure Error	*1.25*	*5*	*0.25*			
Cor Total	23.15	16				

Std. Dev.	0.59	R-Squared	0.8958
Mean	98.61	Adj R-Squared	0.7619
C.V.	0.60	Pred R-Squared	N/A
PRESS	N/A	Adeq Precision	7.215

Case(s) with leverage of 1.0000: Pred R-Squared and PRESS statistic not defined

Table M23 Precision" measures

Factor	Coefficient Estimate	DF	Standard Error	95% CI Low	95% CI High	VIF
Intercept	99.60	1	0.26	98.98	100.22	
A-Blend3 dose	0.40	1	0.25	-0.18	0.99	1.39
B-CT	0.095	1	0.25	-0.49	0.68	1.43
C-pH	0.17	1	0.21	-0.32	0.66	1.00
A^2	-0.29	1	0.32	-1.04	0.46	1.23
B^2	-0.76	1	0.32	-1.51	-7.513E-003	1.23
C^2	-0.71	1	0.32	-1.46	0.039	1.23
AB	-1.00	1	0.40	-1.94	-0.053	1.75
AC	0.062	1	0.29	-0.63	0.76	1.00
BC	1.45	1	0.29	0.76	2.15	1.00

Tale M24 **Final Equation in Terms of Coded Factors:**

Response 3	=
+99.60	
+0.40	* A
+0.095	* B
+0.17	* C
-0.29	* A^2
-0.76	* B^2
-0.71	* C^2
-1.00	* A * B
+0.062	* A * C
+1.45	* B * C

Table M25 **Final Equation in Terms of Actual Factors:**

Response 3 =
+93.95332
+6.22434 * Blend3 dose
+0.22755 * CT
+0.11537 * pH
-1.16835 * Blend3 dose^2
-0.013446 * CT^2
-0.044341 * pH^2
-0.26637 * Blend3 dose * CT
+0.030956 * Blend3 dose * pH
+0.048457 * CT * pH

Table M26. Diagnostics Case Statistics
Diagnostics Case Statistics

Standard Order	Actual Value	Predicted Value	Residual	Leverage	Student Residual	Cook's Distance	Outlier	Run Order
1	99.69	99.85	-0.17	0.804	-0.642	0.168	-0.612	3
2	96.78	97.06	-0.28	0.429	-0.622	0.029	-0.592	2
3	98.60	98.77	-0.17	0.804	-0.642	0.168	-0.612	5

4	98.60	98.05	0.55	0.714	1.758	0.773	2.178	7
5	98.85	99.24	-0.38	0.804	-1.479	0.894	-1.651	17
6	96.78	97.06	-0.28	0.429	-0.622	0.029	-0.592	1
7	97.14	96.76	0.38	0.804	1.479	0.894	1.651	4
8	98.82	99.60	-0.78	0.200	-1.493	0.056	-1.675	6
9	99.20	99.60	-0.41	0.200	-0.774	0.015	-0.749	16
10	100.00	99.60	0.40	0.200	0.756	0.014	0.730	12
11	99.24	99.24	0.000	1.000				8
12	99.49	99.32	0.17	0.804	0.642	0.168	0.612	9
13	98.47	98.09	0.38	0.804	1.479	0.894	1.651	15
14	100.00	99.60	0.40	0.200	0.756	0.014	0.730	11
15	100.00	99.60	0.40	0.200	0.756	0.014	0.730	13
16	96.22	96.61	-0.38	0.804	-1.479	0.894	-1.651	10
17	98.47	98.31	0.17	0.804	0.642	0.168	0.612	14

Case(s) with leverage of 1.0000: Student Residuals, Cooks Distance & Outlier T undefined.

4) MANGANESE

Table M27 Sequential Model Sum of Squares

Source	Sum of Squares	DF	Mean Square	F Value	Prob > F	
Mean	1.691E+005	1	1.691E+005			Suggested
Linear	0.094	3	0.031	2.27	0.1289	
2FI	0.088	3	0.029	3.25	0.0685	
Quadratic	0.061	3	0.020	4.90	0.0384	Suggested
Cubic	2.031E-003	2	1.016E-003	0.19	0.8354	Aliased
Residual	0.027	5	5.446E-003			

Total	1.691E+005	17	9946.35		

Table M28 **Lack of Fit Tests**

Source	Sum of Squares	DF	Mean Square	F Value	Prob > F	
Linear	0.15	8	0.019	3.49	0.0925	
2FI	0.063	5	0.013	2.33	0.1872	
Quadratic	2.031E-003	2	1.016E-003	0.19	0.8354	Suggested
Cubic	0.000	0				Aliased
Pure Error	0.027	5	5.446E-003			

"Lack of Fit Tests": Want the selected model to have insignificant lack-of-fit.

Table M29 **Model Summary Statistics**

Source	Std. Dev.	R-Squared	Adjusted R-Squared	Predicted R-Squared	PRESS	
Linear	0.12	0.3435	0.1920	-0.3327	0.36	
2FI	0.095	0.6675	0.4680	-0.3562	0.37	
Quadratic	0.065	0.8927	0.7548		+	Suggested
Cubic	0.074	0.9002	0.6806		+	Aliased

+ Case(s) with leverage of 1.0000: PRESS statistic not defined

Table M30. ANOVA for Response Surface Quadratic Model

Analysis of variance table [Partial sum of squares]

Source	Sum of Squares	DF	Mean Square	F Value	Prob > F	
Model	0.24	9	0.027	6.47	0.0111	significant
A	*3.026E-003*	*1*	*3.026E-003*	*0.72*	*0.4230*	
B	*0.029*	*1*	*0.029*	*6.92*	*0.0339*	
C	*0.059*	*1*	*0.059*	*14.19*	*0.0070*	
A²	*0.056*	*1*	*0.056*	*13.43*	*0.0080*	
B²	*1.068E-003*	*1*	*1.068E-003*	*0.26*	*0.6288*	
C²	*1.666E-004*	*1*	*1.666E-004*	*0.040*	*0.8475*	
AB	*0.056*	*1*	*0.056*	*13.32*	*0.0082*	
AC	*2.770E-003*	*1*	*2.770E-003*	*0.66*	*0.4424*	
BC	*0.041*	*1*	*0.041*	*9.82*	*0.0165*	
Residual	0.029	7	4.180E-003			
Lack of Fit	*2.031E-003*	*2*	*1.016E-003*	*0.19*	*0.8354*	*not significan*
Pure Error	*0.027*	*5*	*5.446E-003*			
Cor Total	0.27	16				

Std. Dev.	0.065	R-Squared	0.8927
Mean	99.73	Adj R-Squared	0.7548

C.V.	0.065	Pred R-Squared	N/A
PRESS	N/A	Adeq Precision	7.669

Case(s) with leverage of 1.0000: Pred R-Squared and PRESS statistic not defined

Table M31 **Precision" measures**

Factor	Coefficient Estimate	DF	Standard Error	95% CI Low	95% CI High	VIF
Intercept	99.76	1	0.029	99.70	99.83	
A-Blend3 dose	0.023	1	0.027	-0.041	0.088	1.39
B-CT	0.072	1	0.027	7.250E-003	0.14	1.43
C-pH	0.086	1	0.023	0.032	0.14	1.00
A^2	-0.13	1	0.035	-0.21	-0.045	1.23
B^2	0.018	1	0.035	-0.065	0.10	1.23
C^2	6.963E-003	1	0.035	-0.076	0.089	1.23
AB	0.16	1	0.044	0.057	0.26	1.75
AC	0.026	1	0.032	-0.050	0.10	1.00
BC	-0.10	1	0.032	-0.18	-0.025	1.00

Table M32 **Final Equation in Terms of Coded Factors:**

Response 4	=
+99.76	
+0.023	* A
+0.072	* B
+0.086	* C

-0.13	* A^2
+0.018	* B^2
+6.963E-003	* C^2
+0.16	* A * B
+0.026	* A * C
-0.10	* B * C

Table M33 **Final Equation in Terms of Actual Factors:**

Response 4	=
+99.29425	
+0.42803	* Blend3 dose
-0.014116	* CT
+0.043608	* pH
-0.51135	* Blend3 $dose^2$
+3.13442E-004	* CT^2
+4.35181E-004	* pH^2
+0.042870	* Blend3 dose * CT
+0.013159	* Blend3 dose * pH
-3.37617E-003	* CT * pH

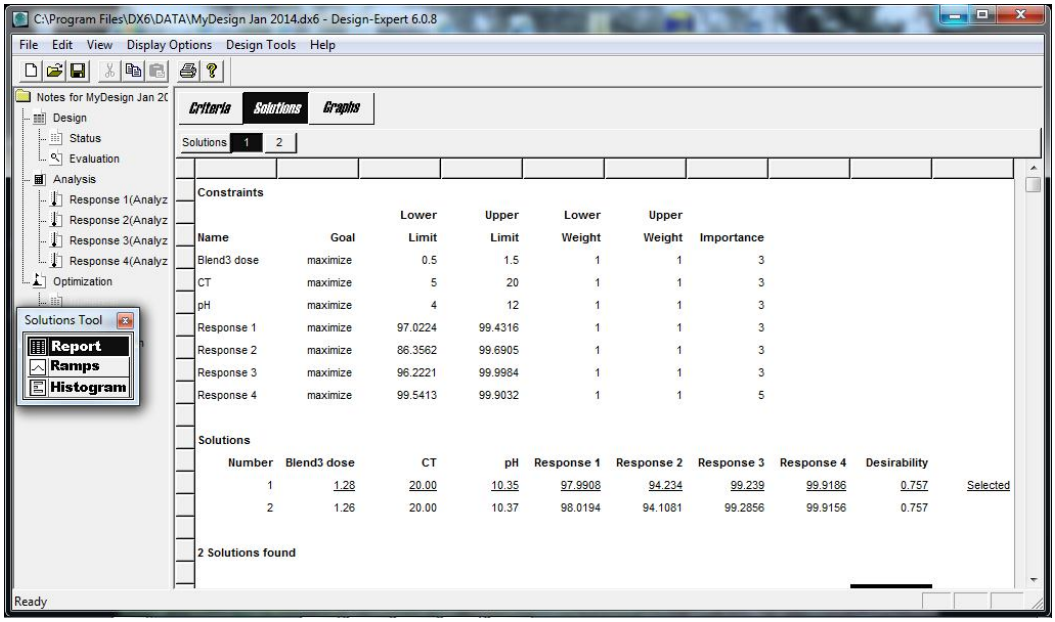
Table M34. Diagnostics Case Statistics

Standard Order	Actual Value	Predicted Value	Residual	Leverage	student Residual	Cook' Distance	Run order
1	99.83	99.84	-0.012	0.804	-0.429	0.075	-0.403
2	99.73	99.72	7.348E-003	0.429	0.150	0.002	0.139
3	99.54	99.55	-0.012	0.804	-0.429	0.075	-0.403
4	99.90	99.91	-6.196E-003	0.714	-0.179	0.008	-0.166
5	99.80	99.78	0.018	0.804	0.645	0.170	0.616
6	99.72	99.72	-1.152E-003	0.429	-0.024	0.000	-0.022
7	99.89	99.90	-0.018	0.804	-0.645	0.170	-0.616
8	99.74	99.76	-0.019	0.200	-0.335	0.003	-0.313
9	99.68	99.76	-0.081	0.200	-1.407	0.049	-1.538
10	99.74	99.76	-0.019	0.200	-0.335	0.003	-0.313
11	99.54	99.54	0.000	1.000			
12	99.54	99.53	0.012	0.804	0.429	0.075	0.403
13	99.54	99.56	-0.018	0.804	-0.645	0.170	-0.616
14	99.90	99.76	0.14	0.200	2.412	0.145	5.428 *
15	99.74	99.76	-0.019	0.200	-0.335	0.003	-0.313
16	99.89	99.88	0.018	0.804	0.645	0.170	0.616
17	99.69	99.68	0.012	0.804	0.429	0.075	0.403

Case(s) with leverage of 1.0000: Student Residuals, Cooks Distance & Outlier T undefined.

* Case(s) with |Outlier T| > 3.50

Table M35. Optimized values by RSM


C:\Program Files\DX6\DATA\MyDesign Jan 2014.dx6 - Design-Expert 6.0.8
File Edit View Display Options Design Tools Help
Notes for MyDesign Jan 2(
Design
Status
Evaluation
Analysis
Response 1(Analyz
Response 2(Analyz
Response 3(Analyz
Response 4(Analyz
Optimization
Solutions Tool
Report
Ramps
Histogram
Criteria
Solutions
Graphs
Solutions 1 2
Constraints
Name Goal Lower Limit Upper Limit Lower Weight Upper Weight Importance
Blend3 dose maximize 0.5 1.5 1 1 3
CT maximize 5 20 1 1 3
pH maximize 4 12 1 1 3
Response 1 maximize 97.0224 99.4316 1 1 3
Response 2 maximize 86.3562 99.6905 1 1 3
Response 3 maximize 96.2221 99.9984 1 1 3
Response 4 maximize 99.5413 99.9032 1 1 5
Solutions
Number Blend3 dose CT pH Response 1 Response 2 Response 3 Response 4 Desirability
1 1.28 20.00 10.35 97.9908 94.234 99.239 99.9186 0.757 Selected
2 1.26 20.00 10.37 98.0194 94.1081 99.2856 99.9156 0.757
2 Solutions found
Ready

APPENDIX N

Characterization of Zeolite 4A, Metakaolin and Zeolite 4A-metakaolin Matrix

XRD Analysis Results for CZ100

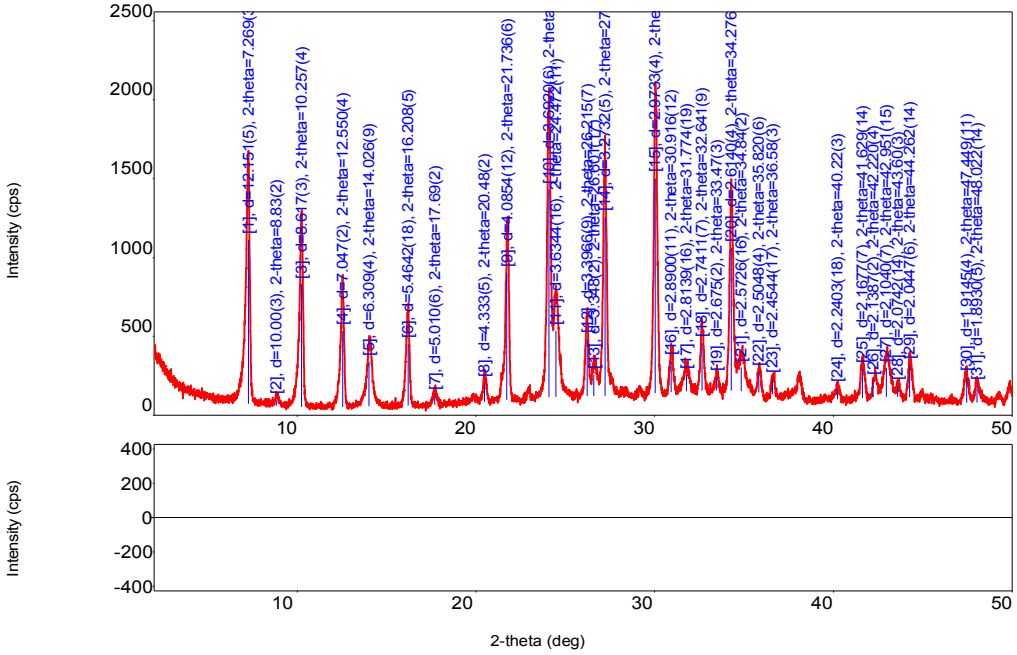


Figure N1. Measurement profile for CZ100 diffraction

Table N1. Peak list for CZ100

No.	2-theta(deg)	d(ang.)	Height(cps)	FWHM(deg)	Int. I(cps deg)	Int. W(deg)	Size(ang.)
1	7.269(3)	12.151(5)	1039(42)	0.228(3)	321(3)	0.309(15)	365(6)
2	8.83(2)	10.00(3)	35(8)	0.21(3)	9.7(14)	0.27(10)	394(57)
3	10.257(4)	8.617(3)	778(36)	0.225(3)	217(2)	0.278(16)	370(6)
4	12.550(4)	7.047(2)	482(28)	0.234(4)	127.9(19)	0.27(2)	357(6)
5	14.026(9)	6.309(4)	284(22)	0.308(1	119(2)	0.42(4)	271(9)
6	16.208(5)	5.4642(18	391(26)	0.226(4)	94.9(18)	0.24(2)	370(7)
7	17.69(2)	5.010(6)	58(10)	0.244(1	15.1(13)	0.26(7)	345(24)
8	20.48(2)	4.333(5)	118(14)	0.19(2)	28(2)	0.24(5)	443(49)
9	21.736(6)	4.0854(12	804(37)	0.181(7)	191(3)	0.238(15)	466(18)
10	24.084(4)	3.6920(6)	1316(47)	0.204(4)	324(7)	0.246(14)	415(7)
11	24.472(11	3.6344(16	419(26)	0.354(1	180(6)	0.43(4)	240(10)
12	26.215(7)	3.3966(9)	362(25)	0.188(7)	84(2)	0.23(2)	454(16)
13	26.601(17	3.348(2)	135(15)	0.34(3)	62(4)	0.46(8)	252(19)
14	27.222(4)	3.2732(5)	1129(43)	0.187(4)	260(5)	0.230(13)	457(11)
15	30.030(4)	2.9733(4)	1362(48)	0.209(3)	314(3)	0.231(10)	412(5)
16	30.916(12	2.8900(11	195(18)	0.200(9)	41.6(15)	0.21(3)	431(18)
17	31.774(19	2.8139(16	103(13)	0.354(1	38.8(16)	0.38(6)	243(11)
18	32.641(9)	2.7411(7)	303(22)	0.196(6)	63.4(19)	0.21(2)	440(14)
19	33.47(3)	2.675(2)	82(12)	0.18(2)	16.0(17)	0.19(5)	474(52)
20	34.276(5)	2.6140(4)	905(39)	0.205(4)	200(7)	0.221(17)	423(8)
21	34.84(2)	2.5726(16	150(16)	0.57(4)	91(5)	0.61(10)	154(11)
22	35.820(6)	2.5048(4)	131(15)	0.159(1	22.5(19)	0.17(3)	547(59)
23	36.58(3)	2.4544(17	97(13)	0.16(2)	16.0(19)	0.17(4)	562(80)
24	40.22(3)	2.2403(18	69(11)	0.19(4)	17.8(15)	0.26(6)	465(96)
25	41.629(14	2.1677(7)	185(18)	0.215(1	42.4(17)	0.23(3)	413(20)
26	42.220(4)	2.1387(2)	108(13)	0.215(1	25.2(19)	0.23(5)	414(33)
27	42.951(15	2.1040(7)	183(17)	0.403(1	83(3)	0.45(6)	221(8)
28	43.60(3)	2.0742(14	66(10)	0.19(3)	14.3(16)	0.22(6)	469(77)
29	44.262(14	2.0447(6)	202(18)	0.189(1	40.6(18)	0.20(3)	474(28)
30	47.449(11	1.9145(4)	159(16)	0.209(1	41.3(15)	0.26(4)	434(27)
31	48.022(14	1.8930(5)	105(13)	0.201(1	28.8(15)	0.28(5)	451(40)

Analysis Results FOR CMK100

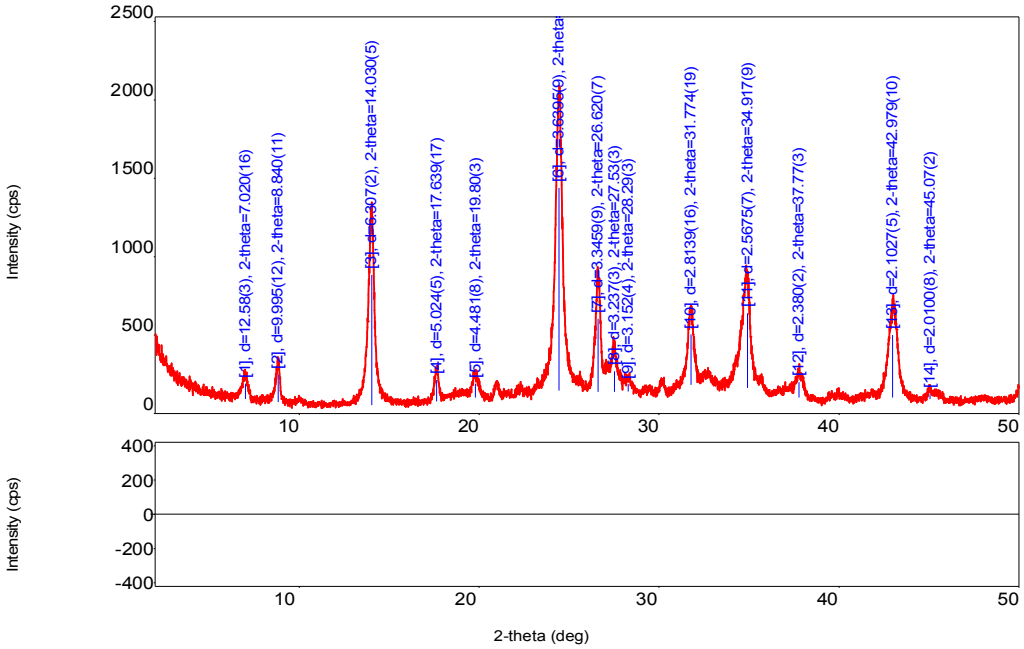


Figure N2. Figure L1. Measurement profile for CMK100 diffraction

Table N2 Peak list for CMK100

No	2-theta(deg)	d(ang.)	Height(cps)	FWHM(deg)	Int. I(cps deg)	Int. W(deg)	Size(ang.)
1	7.020(16)	12.58(3)	98(13)	0.379(14)	40.3(19)	0.41(7)	219(8)
2	8.840(11)	9.995(12)	174(17)	0.249(11)	60.2(16)	0.35(4)	334(15)
3	14.030(5)	6.307(2)	831(37)	0.354(5)	416(3)	0.50(3)	236(3)
4	17.639(17	5.024(5)	135(15)	0.267(18)	46.6(19)	0.35(5)	315(21)
5	19.80(3)	4.481(8)	90(12)	0.44(5)	59(4)	0.66(13)	192(21)
6	24.437(6)	3.6395(9)	1294(46)	0.406(6)	737(5)	0.57(2)	209(3)
7	26.620(7)	3.3459(9)	465(28)	0.312(6)	156(4)	0.34(3)	274(6)
8	27.53(3)	3.237(3)	132(15)	0.70(4)	99(9)	0.75(15)	122(7)
9	28.29(3)	3.152(4)	48(9)	0.9(2)	44(9)	0.9(4)	100(24)
10	31.774(19	2.8139(16	322(23)	0.373(19)	154(4)	0.48(5)	232(12)
11	34.917(9)	2.5675(7)	477(28)	0.523(13)	323(5)	0.68(5)	166(4)
12	37.77(3)	2.380(2)	99(13)	0.48(4)	72(3)	0.73(13)	181(17)
13	42.979(10	2.1027(5)	398(26)	0.560(8)	268(3)	0.67(5)	159(2)
14	45.07(2)	2.0100(8)	31(7)	0.60(6)	19(2)	0.6(2)	151(14)

Analysis Results FOR ZMK75/25

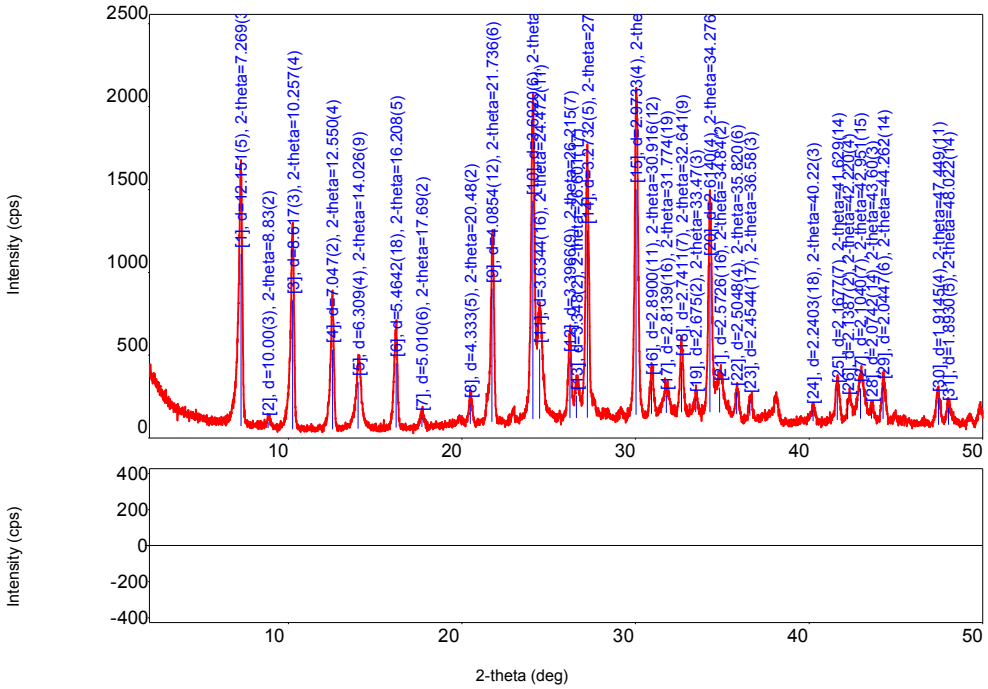


Figure N3. Measurement profile for ZMK75/25 diffraction

No.	2-theta(deg)	d(ang.)	Height(cps)	FWHM(deg)	Int. I(cps deg)	Int. W(deg)	Size(ang.)
1	7.269(3)	12.151(5)	1039(42)	0.228(3)	321(3)	0.309(15)	365(6)
2	8.83(2)	10.00(3)	35(8)	0.21(3)	9.7(14)	0.27(10)	394(57)
3	10.257(4)	8.617(3)	778(36)	0.225(3)	217(2)	0.278(16)	370(6)
4	12.550(4)	7.047(2)	482(28)	0.234(4)	127.9(19)	0.27(2)	357(6)
5	14.026(9)	6.309(4)	284(22)	0.308(10)	119(2)	0.42(4)	271(9)
6	16.208(5)	5.4642(18	391(26)	0.226(4)	94.9(18)	0.24(2)	370(7)
7	17.69(2)	5.010(6)	58(10)	0.244(17)	15.1(13)	0.26(7)	345(24)
8	20.48(2)	4.333(5)	118(14)	0.19(2)	28(2)	0.24(5)	443(49)
9	21.736(6)	4.0854(12	804(37)	0.181(7)	191(3)	0.238(15)	466(18)
10	24.084(4)	3.6920(6)	1316(47)	0.204(4)	324(7)	0.246(14)	415(7)
11	24.472(11	3.6344(16	419(26)	0.354(15)	180(6)	0.43(4)	240(10)
12	26.215(7)	3.3966(9)	362(25)	0.188(7)	84(2)	0.23(2)	454(16)
13	26.601(17	3.348(2)	135(15)	0.34(3)	62(4)	0.46(8)	252(19)
14	27.222(4)	3.2732(5)	1129(43)	0.187(4)	260(5)	0.230(13)	457(11)
15	30.030(4)	2.9733(4)	1362(48)	0.209(3)	314(3)	0.231(10)	412(5)
16	30.916(12	2.8900(11	195(18)	0.200(9)	41.6(15)	0.21(3)	431(18)
17	31.774(19	2.8139(16	103(13)	0.354(17)	38.8(16)	0.38(6)	243(11)
18	32.641(9)	2.7411(7)	303(22)	0.196(6)	63.4(19)	0.21(2)	440(14)
19	33.47(3)	2.675(2)	82(12)	0.18(2)	16.0(17)	0.19(5)	474(52)
20	34.276(5)	2.6140(4)	905(39)	0.205(4)	200(7)	0.221(17)	423(8)
21	34.84(2)	2.5726(16	150(16)	0.57(4)	91(5)	0.61(10)	154(11)
22	35.820(6)	2.5048(4)	131(15)	0.159(17)	22.5(19)	0.17(3)	547(59)
23	36.58(3)	2.4544(17	97(13)	0.16(2)	16.0(19)	0.17(4)	562(80)
24	40.22(3)	2.2403(18	69(11)	0.19(4)	17.8(15)	0.26(6)	465(96)
25	41.629(14	2.1677(7)	185(18)	0.215(10)	42.4(17)	0.23(3)	413(20)
26	42.220(4)	2.1387(2)	108(13)	0.215(17)	25.2(19)	0.23(5)	414(33)
27	42.951(15	2.1040(7)	183(17)	0.403(14)	83(3)	0.45(6)	221(8)
28	43.60(3)	2.0742(14	66(10)	0.19(3)	14.3(16)	0.22(6)	469(77)
29	44.262(14	2.0447(6)	202(18)	0.189(11)	40.6(18)	0.20(3)	474(28)
30	47.449(11	1.9145(4)	159(16)	0.209(13)	41.3(15)	0.26(4)	434(27)
31	48.022(14	1.8930(5)	105(13)	0.201(18)	28.8(15)	0.28(5)	451(40)

Table N3. Peak list for ZMK75/25

Table N4 Qualitative Analysis for Zeolite 4A and Metakaolin

Zeolite 4A		Metakaolin	
Phase name	**Content (%)**	**Phase name**	**Content (%)**
Zeolite A, Dodecasodium tecto-dodecaalumododecasilicate dehydrate	99.6	Sodalite (Na, NO_2), octasodium tecto-hexaalumohexasilicate	93.644112
octasodium hexakis (alumosilicate) dicyanide	0.403	Cesium Thulium Telluride	6.355888
Unknown	0.000e+00	Unknown	0.000e+00
		Sodalite (Na, NO_2),01-073-5668@ octasodium tecto-Cesium Thulium Telluride	

Table N5 Crystallite Size for Zeolites 4A and Metakaolin

Zeolite 4A			Metakaolin		
Phase name	**Crystallite size (nm)**	**Strain (%)**	**Phase name**	**Crystallite size (nm)**	**Strain (%)**
Zeolite A, Dodecasodium tecto-dodecaalumododecasilicate dehydrate	34.17	0.21	Sodalite (Na, NO2), octasodium tecto-hexaalumohexasilicate bisnitrate(III),		
octasodium hexakis(alumosilicate) dicyanide	28.456	0.198	sodalite nitrate	14.832	0.43
			Cesium Thulium Telluride	16.368	0.34

BET RESULTS

CMK100 BET SUMMARY

Full Report Set

ASAP 2020 V4.00 (V4.00 H) Unit 1 Serial #: 1665

Adsorptive: N2

Sample Mass: 0.1997 g
Warm Free Space: 16.7447 cm³
Measured
Cold Free Space: 48.1414 cm³
Equilibration Interval: 10 s
Ambient Temperature: 22.00 °C
Low Pressure Dose: None
Automatic Degas: Yes

Summary Report Surface Area

Single point surface area at P/Po = 0.300062937: 6.0608 m²/g

BET Surface Area: 6.5112 m²/g

t-Plot External Surface Area: 8.3520 m²/g

BJH Adsorption cumulative surface area of pores between 17.000 Å and 3000.000 Å diameter: 6.827 m²/g

BJH Desorption cumulative surface area of pores between 17.000 Å and 3000.000 Å diameter: 6.8816 m²/g

Pore Volume

Single point adsorption total pore volume of pores less than 3199.599 Å diameter at P/Po = 0.993935663: 0.029028 cm³/g

t-Plot micropore volume: -0.001111 cm³/g

BJH Adsorption cumulative volume of pore between 17.000 Å and 3000.000 Å diameter: 0.028583 cm³/g

BJH Desorption cumulative volume of pores between 17.000 Å and 3000.000 Å diameter: 0.028555 cm³/g

Summary on Pore Size

Adsorption average pore width (4V/A by BET): 178.3285 Å

BJH Adsorption average pore diameter (4V/A): 167.463 Å

BJH Desorption average pore diameter (4V/A): 165.978 Å

Full Report Set

ASAP 2020 V4.00 (V4.00 H) Unit 1 Serial #: 1665

Thermal Correction: No
Sample Mass: 0.1997 g
Warm Free Space: 16.7447 cm³
Measured
Cold Free Space: 48.1414 cm³
Equilibration Interval: 10 s
Ambient Temperature: 22.00 °C
Low Pressure Dose: None
Automatic Degas: Yes

BET Surface Area Report

BET Surface Area: 6.5112 ± 0.0506 m²/g
Slope: 0.645770 ± 0.005119 g/cm³ STP
Y-Intercept: 0.022798 ± 0.000895 g/cm³ STP
C: 29.325950
Qm: 1.4957 cm³/g STP
Correlation Coefficient: 0.9997488
Molecular Cross-Sectional Area: 0.1620 nm²

Table N4 BET Surface Area Plot Data for CMK100

Relative Pressure (P/Po)	Quantity Adsorbed (cm³/g STP)	1/[Q(Po/P - 1)]
0.068762106	1.1306	0.065313
0.080047663	1.1820	0.073614
0.100141164	1.2711	0.087549
0.120233880	1.3500	0.101231
0.140100338	1.4221	0.114566
0.160185042	1.4963	0.127475
0.180078696	1.5716	0.139751
0.200063161	1.6403	0.152474
0.250080320	1.8168	0.183556

0.300062937 1.9

CZ100 BET SUMMARY

Full Report Set

ASAP 2020 V4.00 (V4.00 H) Unit 1 Serial #: 1665

Adsorptive: N2

Thermal Correction: No
Sample Mass: 0.1874 g
Warm Free Space: 16.4998 cm³
Measured
Cold Free Space: 49.2496 cm³
Equilibration Interval: 10 s
Ambient Temperature: 22.00 °C
Low Pressure Dose: None
Automatic Degas: Yes

Summary Report Surface Area

Single point surface area at P/Po = 0.300251464: 2.6076 m²/g

BET Surface Area: 2.9315 m²/g

t-Plot External Surface Area: 4.2483 m²/g

BJH Adsorption cumulative surface area of pores between 17.000 Å and 3000.000 Å diameter: 3.186 m²/g

BJH Desorption cumulative surface area of pores between 17.000 Å and 3000.000 Å diameter: 3.4687 m²/g

Pore Volume

Single point adsorption total pore volume of pores less than 4209.155 Å diameter at P/Po = 0.995402916: 0.010001 cm³/g

t-Plot micropore volume: -0.000802 cm³/g

BJH Adsorption cumulative volume of pores between 17.000 Å and 3000.000 Å diameter: 0.009739 cm³/g

BJH Desorption cumulative volume of pores between 17.000 Å and 3000.000 Å diameter: 0.009736 cm³/g

Pore Size

Adsorption average pore width (4V/A by BET): 136.4657 Å

BJH Adsorption average pore diameter (4V/A): 122.277 Å

BJH Desorption average pore diameter (4V/A): 112.271 Å

Full Report Set

ASAP 2020 V4.00 (V4.00 H) Unit 1 Serial #: 1665
Adsorptive: N2

Thermal Correction: No
Sample Mass: 0.1874 g Warm Free Space: 16.4998 cm³
Measured
Cold Free Space: 49.2496 cm³ Equilibration Interval: 10 s
Ambient Temperature: 22.00 °C Low Pressure Dose: None
Automatic Degas: Yes

BET Surface Area Report

BET Surface Area: 2.9315 ± 0.0426 m²/g
Slope: 1.399981 ± 0.021248 g/cm³ STP
Y-Intercept: 0.084998 ± 0.003719 g/cm³ STP
C: 17.470788
Qm: 0.6734 cm³/g STP
Correlation Coefficient: 0.9990799
Molecular Cross-Sectional Area: 0.1620 nm²

Table N5 BET Surface Area Plot Data CZ100

Relative Pressure (P/Po)	Quantity Adsorbed (cm³/g STP)	1/[Q(Po/P - 1)]

0.068933415	0.4256	0.173940
0.080144591	0.4534	0.192170
0.100324625	0.4887	0.228162
0.120284027	0.5306	0.257705
0.140161828	0.5709	0.285542
0.160326105	0.6135	0.311253
0.180315896	0.6438	0.341717
0.200177277	0.6808	0.367609
0.250151818	0.7721	0.432098
0.300251464	0.8560	0.501251

ZMK75/25 BET SUMMARY

Full Report Set

ASAP 2020 V4.00 (V4.00 H) Unit 1 Serial #: 1665

Adsorptive: N2

Thermal Correction: No
Sample Mass: 0.2389 g
Warm Free Space: 16.9309 cm³
Measured
Cold Free Space: 47.1959 cm³
Equilibration Interval: 10 s
Ambient Temperature: 22.00 °C
Low Pressure Dose: None
Automatic Degas: Yes

Summary Report Surface Area

Single point surface area at P/Po = 0.300013613: 5.1860 m²/g

BET Surface Area: 5.7060 m²/g

t-Plot External Surface Area: 7.9366 m²/g

BJH Adsorption cumulative surface area of pores between 17.000 Å and 3000.000 Å diameter: 6.503 m²/g

BJH Desorption cumulative surface area of pores between 17.000 Å and 3000.000 Å diameter: 7.0946 m²/g

SUMMARY on Pore Volume

Single point adsorption total pore volume of pores less than 3054.573 Å diameter at P/Po = 0.993644480: 0.022690 cm³/g

t-Plot micropore volume: -0.001343 cm³/g

BJH Adsorption cumulative volume of pores between 17.000 Å and 3000.000 Å diameter: 0.022341 cm³/g

BJH Desorption cumulative volume of pores between 17.000 Å and 3000.000 Å diameter: 0.022297 cm³/g

Summary on Pore Size

Adsorption average pore width (4V/A by BET): 159.0603 Å

BJH Adsorption average pore diameter (4V/A): 137.428 Å

BJH Desorption average pore diameter (4V/A): 125.709 Å

Full Report Set

ASAP 2020 V4.00 (V4.00 H) Unit 1 Serial #: 1665

Adsorptive: N2

Thermal Correction: No
Sample Mass: 0.2389 g Warm Free Space: 16.9309 cm³
Measured
Cold Free Space: 47.1959 cm³ Equilibration Interval: 10 s
Ambient Temperature: 22.00 °C Low Pressure Dose: None
Automatic Degas: Yes

BET Surface Area Report

BET Surface Area: 5.7060 ± 0.0686 m²/g
Slope: 0.727184 ± 0.009031 g/cm³ STP
Y-Intercept: 0.035726 ± 0.001579 g/cm³ STP
C: 21.354239
Qm: 1.3108 cm³/g STP
Correlation Coefficient: 0.9993836
Molecular Cross-Sectional Area: 0.1620 nm²

Table N6 BET Surface Area Plot Data for ZMK75/25

Relative Pressure (P/Po)	Quantity Adsorbed (cm^3/g STP)	1/[Q(Po/P - 1)]

0.068636957	0.9006	0.081829
0.080143993	0.9396	0.092722
0.100013792	1.0177	0.109198
0.120229345	1.0948	0.124832
0.140083851	1.1683	0.139442
0.160017989	1.2393	0.153722
0.180101972	1.3072	0.168045
0.199967017	1.3750	0.181785
0.250015150	1.5378	0.216781
0.300013613	1.7019	0.251838

CZ100T RESULT SUMMARY

Full Report Set

ASAP 2020 V4.00 (V4.00 H) Unit 1 Serial #: 1665 Page 1

Sample: 000-300 C
Operator:
Submitter:
File: C:\2020\DATA\MUSYOKA\000-300.SMP

Started: 2013/06/22 9:40:59AM Analysis Adsorptive: N2
Completed: 2013/06/22 2:18:42PM Analysis Bath Temp.: -197.363 °C
Report Time: 2013/07/09 11:18:58AM Thermal Correction: No
Sample Mass: 0.2047 g Warm Free Space: 16.8812 cm^3
Measured
Cold Free Space: 50.1563 cm^3 Equilibration Interval: 10 s
Ambient Temperature: 22.00 °C Low Pressure Dose: None
Automatic Degas: Yes

Summary Report

Surface Area

Single point surface area at P/Po = 0.300147306: 2.7545 m²/g

BET Surface Area: 3.0945 m²/g

t-Plot External Surface Area: 4.4632 m²/g

BJH Adsorption cumulative surface area of pores between 17.000 Å and 3000.000 Å diameter: 3.296 m²/g

BJH Desorption cumulative surface area of pores between 17.000 Å and 3000.000 Å diameter: 3.2446 m²/g

Pore Volume

Single point adsorption total pore volume of pores less than 4099.722 Å diameter at P/Po = 0.995279041: 0.010924 cm³/g

t-Plot micropore volume: -0.000839 cm³/g

BJH Adsorption cumulative volume of pores between 17.000 Å and 3000.000 Å diameter: 0.010624 cm³/g

BJH Desorption cumulative volume of pores between 17.000 Å and 3000.000 Å diameter: 0.010464 cm³/g

Pore Size

Adsorption average pore width (4V/A by BET): 141.2053 Å

BJH Adsorption average pore diameter (4V/A): 128.927 Å

BJH Desorption average pore diameter (4V/A): 129.000 Å

Full Report Set

ASAP 2020 V4.00 (V4.00 H) Unit 1 Serial #: 1665

Adsorptive: N2

Thermal Correction: No
Sample Mass: 0.2047 g
Warm Free Space: 16.8812 cm³
Measured
Cold Free Space: 50.1563 cm³
Equilibration Interval: 10 s
Ambient Temperature: 22.00 °C
Low Pressure Dose: None
Automatic Degas: Yes

BET Surface Area Report

BET Surface Area: 3.0945 ± 0.0362 m²/g
Slope: 1.325767 ± 0.016222 g/cm³ STP
Y-Intercept: 0.081004 ± 0.002839 g/cm³ STP
C: 17.366601
Qm: 0.7108 cm³/g STP
Correlation Coefficient: 0.9994017
Molecular Cross-Sectional Area: 0.1620 nm²

Table N7 BET Surface Area Plot Data for CZ100T

Relative Pressure (P/Po)	Quantity Adsorbed (cm³/g STP)	1/[Q(Po/P - 1)]

0.068931462	0.4458	0.166085
0.080203143	0.4716	0.184908
0.100223033	0.5186	0.214790
0.120211635	0.5645	0.242034
0.140161505	0.6026	0.270528
0.160206871	0.6422	0.297075
0.180251963	0.6820	0.322434
0.200186635	0.7198	0.347706
0.250194410	0.8093	0.412314
0.300147306	0.9041	0.474352

CMK100T RESULT SUMMARY

Full Report Set

ASAP 2020 V4.00 (V4.00 H) Unit 1 Serial #: 1665

Analysis Adsorptive: N2

Thermal Correction: No
Sample Mass: 0.2454 g
Warm Free Space: 16.6637 cm³
Measured
Cold Free Space: 50.1216 cm³
Equilibration Interval: 10 s
Ambient Temperature: 22.00 °C
Low Pressure Dose: None
Automatic Degas: Yes

Summary Report Surface Area

Single point surface area at P/Po = 0.300886592: 26.0901 m²/g

BET Surface Area: 26.4429 m²/g

t-Plot Micropore Area: 4.5637 m²/g

t-Plot External Surface Area: 21.8793 m²/g

BJH Adsorption cumulative surface area of pores between 17.000 Å and 3000.000 Å diameter: 27.236 m²/g

BJH Desorption cumulative surface area of pores between 17.000 Å and 3000.000 Å diameter: 29.1636 m²/g

Summary on Pore Volume

Single point adsorption total pore volume of pores less than 4790.193 Å diameter at P/Po = 0.995965210: 0.082960 cm^3/g

t-Plot micropore volume: 0.002333 cm^3/g

BJH Adsorption cumulative volume of pores between 17.000 Å and 3000.000 Å diameter: 0.084883 cm^3/g

BJH Desorption cumulative volume of pores between 17.000 Å and 3000.000 Å diameter: 0.084360 cm^3/g

Summary on Pore Size

Adsorption average pore width (4V/A by BET): 125.4931 Å

BJH Adsorption average pore diameter (4V/A): 124.664 Å

BJH Desorption average pore diameter (4V/A): 115.706 Å

Full Report Set

ASAP 2020 V4.00 (V4.00 H) Unit 1 Serial #: 1665

Sample: 000-296 A
Operator:
Submitter:
File: C:\2020\DATA\MUSYOKA\000-296.SMP

Started: 2013/06/20 8:48:10AM Analysis Adsorptive: N2
Completed: 2013/06/20 1:57:29PM Analysis Bath Temp.: -197.348 °C
Report Time: 2013/07/09 11:19:37AM Thermal Correction: No
Sample Mass: 0.2454 g Warm Free Space: 16.6637 cm^3
Measured
Cold Free Space: 50.1216 cm^3 Equilibration Interval: 10 s
Ambient Temperature: 22.00 °C Low Pressure Dose: None
Automatic Degas: Yes

BET Surface Area Report

BET Surface Area: 26.4429 ± 0.2797 m²/g
Slope: 0.164650 ± 0.001716 g/cm³ STP
Y-Intercept: -0.000023 ± 0.000300 g/cm³ STP
C: -7029.735735
Qm: 6.0744 cm³/g STP
Correlation Coefficient: 0.9995660
Molecular Cross-Sectional Area: 0.1620 nm²

Table N8 BET Surface Area Plot Data for CMK100T

Relative Pressure (P/Po)	Quantity Adsorbed (cm³/g STP)	1/[Q(Po/P - 1)]

0.067203081	6.3018	0.011432
0.079910851	6.4675	0.013429
0.100224449	6.7151	0.016588
0.120330317	6.9308	0.019737
0.140174534	7.1308	0.022862
0.160245366	7.3265	0.026046
0.180344533	7.5121	0.029289
0.200398380	7.6955	0.032567
0.249752263	8.1264	0.040964
0.300886592	8.5727	0.050204

ZMK75/25 T RESULT SUMMARY

Full Report Set

ASAP 2020 V4.00 (V4.00 H) Unit 1 Serial #: 1665

Adsorptive: N2

Thermal Correction: No
Sample Mass: 0.2206 g
Warm Free Space: 16.5898 cm³
Measured
Cold Free Space: 49.1137 cm³
Equilibration Interval: 10 s
Ambient Temperature: 22.00 °C
Low Pressure Dose: None
Automatic Degas: Yes
Summary Report Surface Area

Single point surface area at P/Po = 0.300286676: 7.6073 m²/g

BET Surface Area: 7.8960 m²/g

t-Plot External Surface Area: 8.4417 m²/g

BJH Adsorption cumulative surface area of pores between 17.000 Å and 3000.000 Å diameter: 8.194 m²/g

BJH Desorption cumulative surface area of pores between 17.000 Å and 3000.000 Å diameter: 9.0318 m²/g

Pore Volume

Single point adsorption total pore volume of pores less than 3324.714 Å diameter at P/Po = 0.994166290: 0.044210 cm³/g

t-Plot micropore volume: -0.000363 cm³/g

BJH Adsorption cumulative volume of pores between 17.000 Å and 3000.000 Å diameter: 0.044061 cm³/g

BJH Desorption cumulative volume of pores between 17.000 Å and 3000.000 Å diameter: 0.044151 cm³/g

Q1d Summary on Pore Size

Adsorption average pore width (4V/A by BET): 223.9641 Å

BJH Adsorption average pore diameter (4V/A): 215.082 Å

BJH Desorption average pore diameter (4V/A): 195.537 Å

Full Report Set

ASAP 2020 V4.00 (V4.00 H) Unit 1 Serial #: 1665 Page 1

Adsorptive: N2

Thermal Correction: No
Sample Mass: 0.2206 g
Warm Free Space: 16.5898 cm³
Measured
Cold Free Space: 49.1137 cm³
Equilibration Interval: 10 s
Ambient Temperature: 22.00 °C
Low Pressure Dose: None
Automatic Degas: Yes

BET Surface Area Report

BET Surface Area: 7.8960 ± 0.0238 m²/g
Slope: 0.543239 ± 0.001639 g/cm³ STP
Y-Intercept: 0.008081 ± 0.000287 g/cm³ STP
C: 68.224736
Qm: 1.8138 cm³/g STP
Correlation Coefficient: 0.9999636
Molecular Cross-Sectional Area: 0.1620 nm²

Table N9 BET Surface Area Plot Data for ZMK75/25T

Relative Pressure (P/Po)	Quantity Adsorbed (cm³/g STP)	1/[Q(Po/P - 1)]
0.068610827	1.6294	0.045211
0.080232187	1.6851	0.051767
0.100264054	1.7723	0.062877
0.120059374	1.8563	0.073500
0.140289756	1.9325	0.084441
0.160236160	2.0092	0.094968
0.180184033	2.0816	0.105583
0.200081588	2.1457	0.116570
0.249964433	2.3248	0.143352
0.300286676	2.4975	0.171836

Appendix O

SEM Micrographs of the Matrices

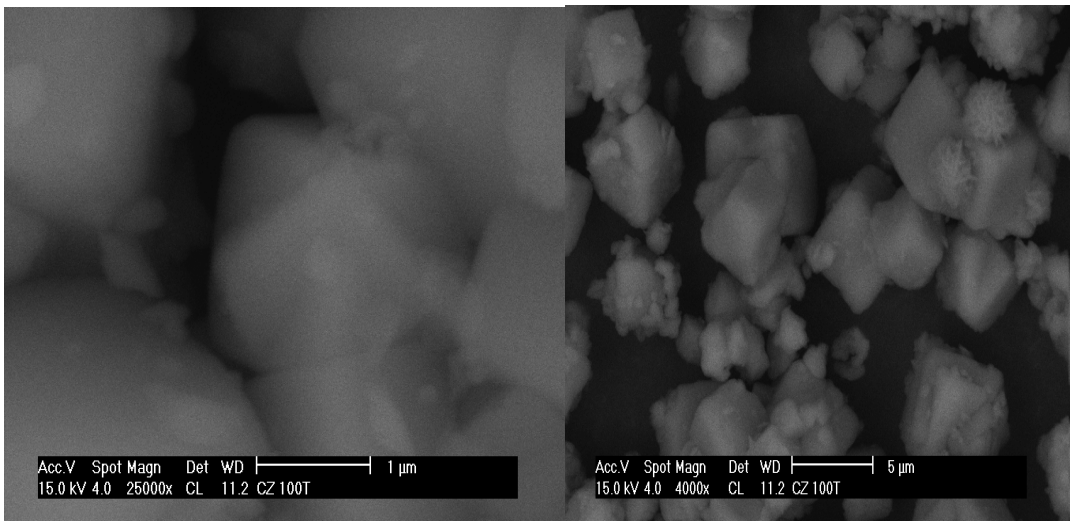


Figure O1. SEM Images of Matrix 1 at Different Magnifications

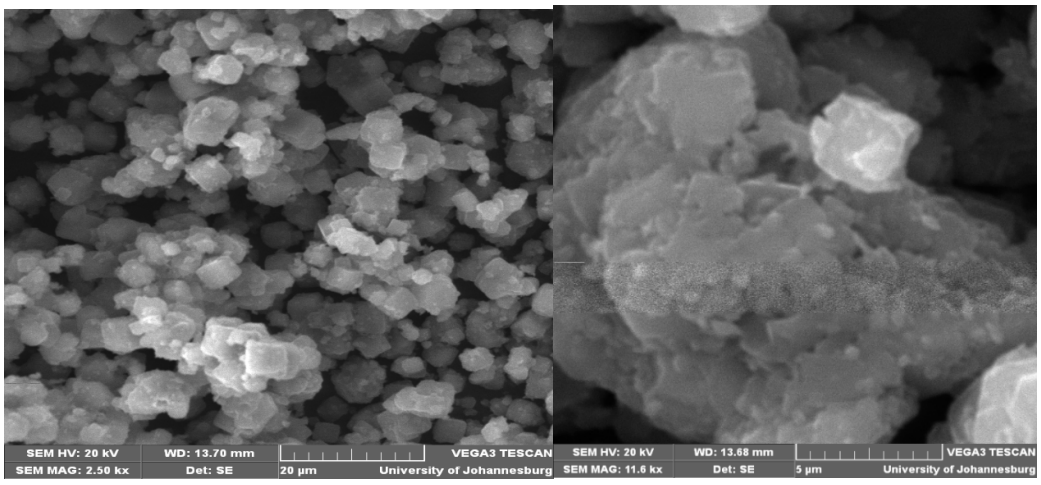


Figure O2. SEM Images of Matrix 2 at Different Magnifications

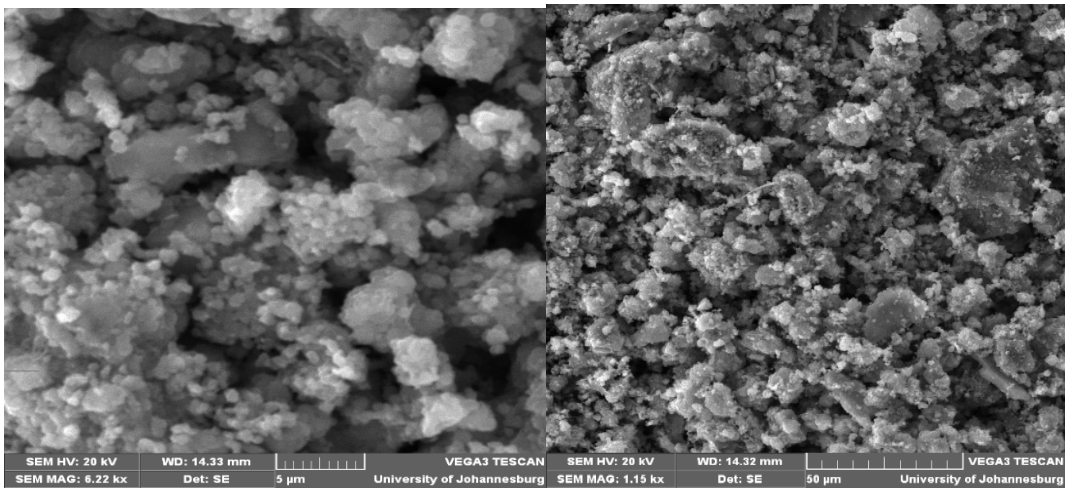


Figure O3. SEM Images of Matrix 3 at Different Magnifications

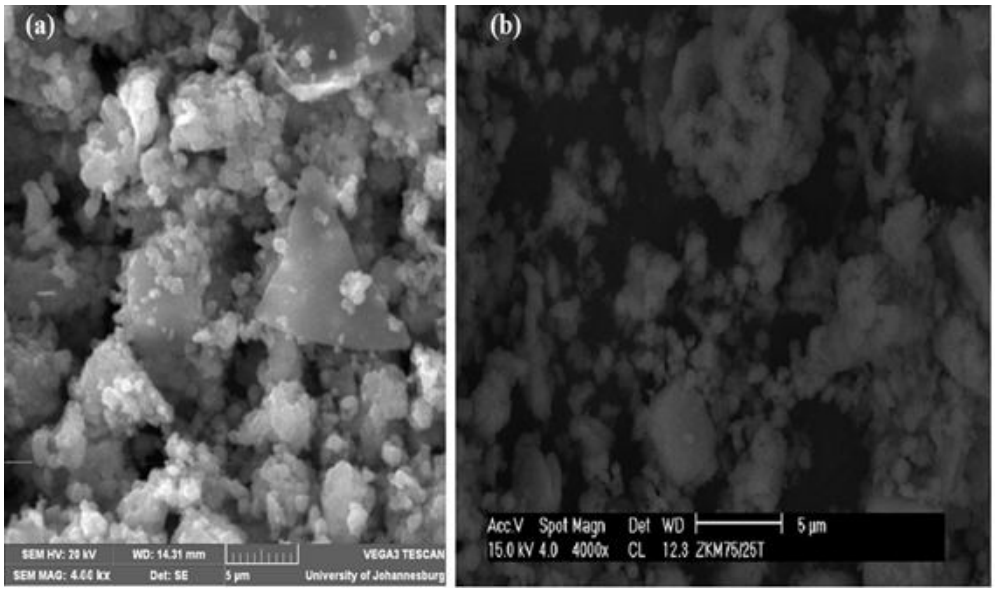


Figure O4. SEM Images of Matrx 4 at Different Magnifications

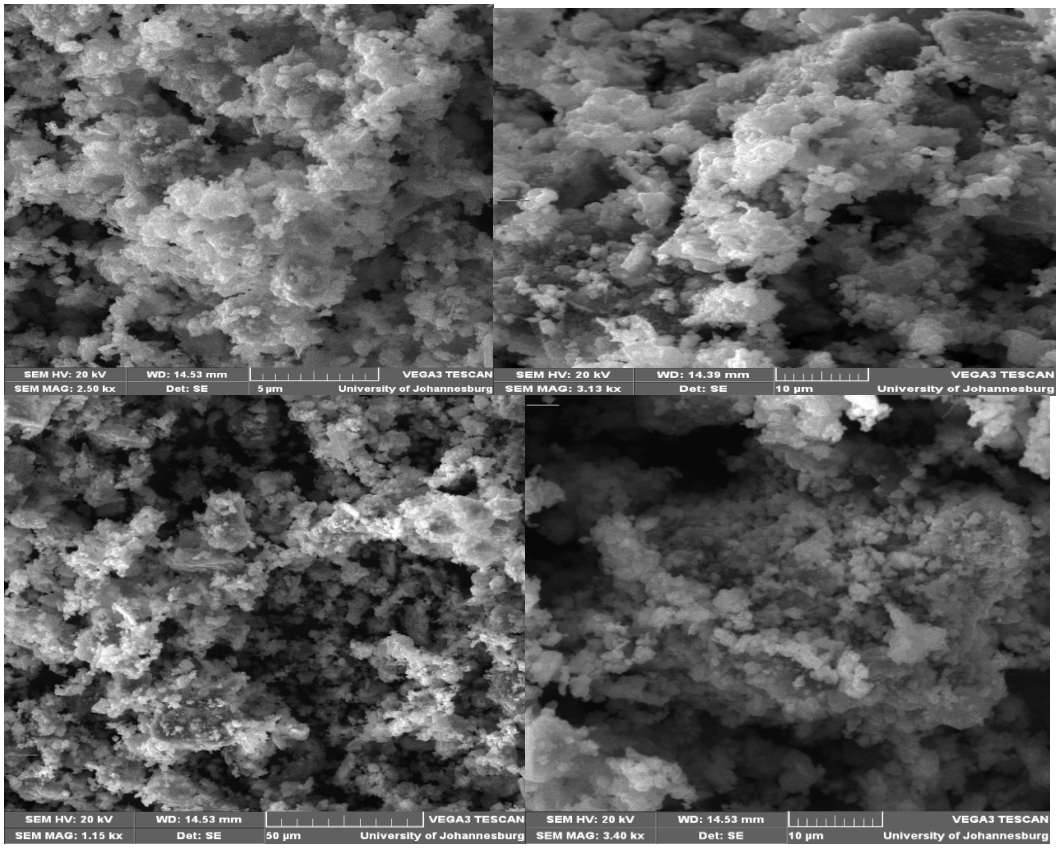


Figure O5. SEM Images of Matrix 5 at Different Magnifications